NBS Special Publication 711

The Investigation of Fundamental Interactions with Cold Neutrons

G.L. Greene, Editor
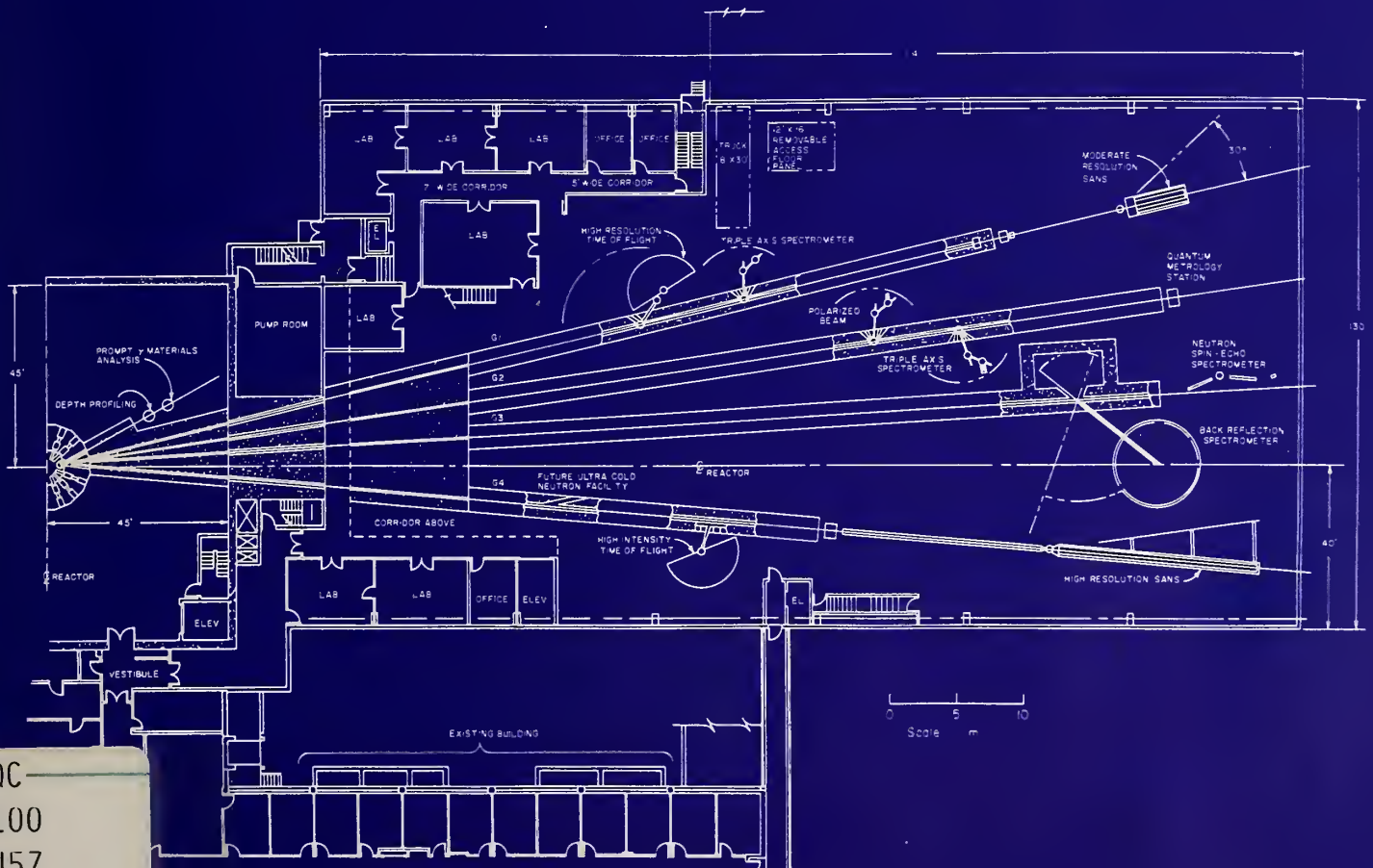
*T*he National Bureau of Standards[1] was established by an act of Congress on March 3, 1901. The Bureau's overall goal is to strengthen and advance the nation's science and technology and facilitate their effective application for public benefit. To this end, the Bureau conducts research and provides: (1) a basis for the nation's physical measurement system, (2) scientific and technological services for industry and government, (3) a technical basis for equity in trade, and (4) technical services to promote public safety. The Bureau's technical work is performed by the National Measurement Laboratory, the National Engineering Laboratory, the Institute for Computer Sciences and Technology, and the Institute for Materials Science and Engineering.

The National Measurement Laboratory

Provides the national system of physical and chemical measurement; coordinates the system with measurement systems of other nations and furnishes essential services leading to accurate and uniform physical and chemical measurement throughout the Nation's scientific community, industry, and commerce; provides advisory and research services to other Government agencies; conducts physical and chemical research; develops, produces, and distributes Standard Reference Materials; and provides calibration services. The Laboratory consists of the following centers:

- Basic Standards[2]
- Radiation Research
- Chemical Physics
- Analytical Chemistry

The National Engineering Laboratory

Provides technology and technical services to the public and private sectors to address national needs and to solve national problems; conducts research in engineering and applied science in support of these efforts; builds and maintains competence in the necessary disciplines required to carry out this research and technical service; develops engineering data and measurement capabilities; provides engineering measurement traceability services; develops test methods and proposes engineering standards and code changes; develops and proposes new engineering practices; and develops and improves mechanisms to transfer results of its research to the ultimate user. The Laboratory consists of the following centers:

- Applied Mathematics
- Electronics and Electrical Engineering[2]
- Manufacturing Engineering
- Building Technology
- Fire Research
- Chemical Engineering[2]

The Institute for Computer Sciences and Technology

Conducts research and provides scientific and technical services to aid Federal agencies in the selection, acquisition, application, and use of computer technology to improve effectiveness and economy in Government operations in accordance with Public Law 89-306 (40 U.S.C. 759), relevant Executive Orders, and other directives; carries out this mission by managing the Federal Information Processing Standards Program, developing Federal ADP standards guidelines, and managing Federal participation in ADP voluntary standardization activities; provides scientific and technological advisory services and assistance to Federal agencies; and provides the technical foundation for computer-related policies of the Federal Government. The Institute consists of the following centers:

- Programming Science and Technology
- Computer Systems Engineering

The Institute for Materials Science and Engineering

Conducts research and provides measurements, data, standards, reference materials, quantitative understanding and other technical information fundamental to the processing, structure, properties and performance of materials; addresses the scientific basis for new advanced materials technologies; plans research around cross-country scientific themes such as nondestructive evaluation and phase diagram development; oversees Bureau-wide technical programs in nuclear reactor radiation research and nondestructive evaluation; and broadly disseminates generic technical information resulting from its programs. The Institute consists of the following Divisions:

- Ceramics
- Fracture and Deformation [3]
- Polymers
- Metallurgy
- Reactor Radiation

[1]Headquarters and Laboratories at Gaithersburg, MD, unless otherwise noted; mailing address Gaithersburg, MD 20899.
[2]Some divisions within the center are located at Boulder, CO 80303.
[3]Located at Boulder, CO, with some elements at Gaithersburg, MD.

NBS Special Publication 711

The Investigation of Fundamental Interactions with Cold Neutrons

Proceedings of a Workshop

G.L. Greene, Editor
Center for Basic Standards
National Measurement
  Laboratory
National Bureau of Standards
Gaithersburg, MD 20899

Table of Contents

Preface

The National Bureau of Standards currently operates a 20 MW research
reactor on its campus in Gaithersburg, Maryland. By early 1986 a
cryogenic moderator will be installed in the reactor core providing cold
neutron fluxes which will be comparable to the most intense sources in the
world. In order to fully benefit from this source, the National Bureau
of Standards plans to establish, at this reactor, a National Cold Neutron
Facility. This facility will consist of a large neutron guide hall as
well as a wide variety of specialized instrumentation. The major thrust
of the scientific effort at this facility will be in the area of materials
research and condensed matter studies. However, as has been amply
demonstrated at the only existing large cold neutron facility, the
Institut Max von Laue-Paul Langevin in Grenoble, France, the research at
such a facility is by no means limited to such areas.

In the last decade a rather rich interdisciplinary effort has developed in
which cold neutron beams have been used as tools in the investigation of
fundamental interactions. This work draws on the techniques of particle
physics, nuclear physics, atomic physics and optics. The results of such
work have implications in the theory of the weak interaction, nuclear
theory, and astrophysics as well as shedding light on the nature (and
violation) of a variety of invariance laws and symmetry principles.

In order to provide guidance in the development of such a research effort
at the new National Cold Neutron Facility, the Department of Energy and
the National Bureau of Standards sponsored, on 14-15 November 1985, a
workshop on "The Investigation of Fundamental Interactions with Cold
Neutrons". This workshop brought together more than 50 participants from
23 institutions in the U.S., Canada and Europe. The twenty-five papers
that were presented comprise these proceedings. These contributions not
only provide a review of recent work in this field but also describe a
variety of future experiments in varying states of preparation. Taken
together these papers describe a vital, exciting scientific endeavor which
can be expected to provide significant results for many years to come.

The organization of this workshop would not have been possible without the
efforts of many individuals. In particular, Dr. Richard Deslattes, of the
National Bureau of Standards, was involved in all phases of the workshop
planning and provided invaluable guidance during its early phases. Ms.
Kathy Stang, of the National Measurement Laboratory, provided extensive
help in the details of the planning. In any affair of this nature, it is
ultimately only the participants themselves who can make a successful
workshop. As such I am very grateful to all who gave presentations and
were involved in the ensuing discussions.

G. L. Greene

PARTICLE PROPERTIES OF THE NEUTRON

Norman F. Ramsey
Lyman Physics Laboratory
Harvard University
Cambridge, MA 02138

Particle properties of the neutron and experiments which have determined these properties are reviewed. Properties discussed include mass, electric charge, magnetic monopole, electric and magnetic dipole moments, neutron mean life for beta decay, ratio of axial vector coupling constants for the weak interaction, electric and magnetic polarizability, period for $n\bar{n}$ oscillations and various quantized properties such as spin, statistics and isospin.

1. Introduction

At the 1982 meeting in Cambridge, England, celebrating the fiftieth anniversary of the discovery of the neutron, I was asked to talk on the Particle Properties of the Neutron (Ramsey 1982). In this meeting, I have been asked to talk on the same subject but to bring the results I reported then up to date by incorporating new measurements since that time.

In the first fifty years following the discovery of the neutron many of the properties of the neutron were measured to quite high precision. It is therefore not surprising that for most of these properties there has been little or no change since my last report. On the other hand, there have been some significant changes.

2. Neutron Mass

Neutron mass measurements go back to the very beginning: Chadwick's (1932) original discovery of the neutron was essentially a mass measurement. Chadwick studied the recoils of H, Li, Be, B, C and N atoms from the objects that were produced when α-particles bombarded Be and he showed that his observations were mutually compatible only if the new neutral object producing the recoils had a mass approximately equal to that of the proton. Chadwick (1932, 1933) also showed that a similar mass was obtained by applying the conservation laws to the production processes.

Chadwick and Goldhaber (1934, 1935) soon discovered the photodisintegration of the deuteron which permitted an accurate determination of the binding energy of the deuteron from the energy of the gamma rays and the energy of the photo-protons. From the binding energy of the neutron and the difference in mass spectroscopic measurements on H_2^+ and D^+, the neutron mass could be accurately determined. Subsequently there have been many improvements in the measurements, particularly by measuring the energy of the photons emitted when slow neutrons are captured by hydrogen. A particularly effective experiment of the latter nature was that of Knowles (1962). The present official value for the mass of the neutron comes from a least squares combination both of various measurements on the deuteron (Mattauch 1965) and on the fundamental constants

affecting all mass scales (Cohen, et al. 1973) and Particle Data Group 1982).
The interaction between different varieties of measurements in the determina-
tion of most fundamental constants is now so great that the values are set by
agreement in an international committee (Cohen et al. 1973) and ordinarily re-
tain those values until the next readjustment of the constants, which is
scheduled to take place within another year. The present official values
(Cohen, et al. 1973 and Particle Data Group 1984) for the rest mass of the
neutron in different units are

$$m_n = 1.008665012(37) \text{ u} \qquad (0.037 \text{ ppm})$$
$$= 1.6749543(86) \times 10^{-27} \text{ kg} \qquad (5.1 \text{ ppm}) \qquad (1)$$
$$= 939.5731(27) \text{ MeV} \qquad (2.9 \text{ ppm})$$

where the first numbers in parentheses are the standard deviation uncertain-
ties in the last digits of the quoted value, u is the atomic mass unit and
ppm is parts per million. The marked variation in uncertainties from
0.037 ppm on the atomic mass scale to 5.1 ppm on the kg scale show that the
limiting error in determining the mass of the neutron in kg is not the nuclear
physics determination of the deuteron binding energy but the value for the
Avogadro constant.

Although the present official values for the neutron mass are those given in
Eq. (1), there have been improvements in such measurements since these numbers
were officially set. The improvements have come in part from new measurements
of the γ-rays emitted when neutrons are captured by γ-rays (Greenwood, Helmer,
Gehrke and Chrein 1979 and Vylor et al. 1978) and in part from a new γ-ray
energy scale determined by Kessler, Deslattes, Henins and Sanders 1978 and
Greene, et al. 1985) have measured the deuteron binding energy by a direct,
absolute measurement of the np capture gamma wavelength in terms of the meter.
Preliminary analysis of this measurement suggests the new value 1.008664919(14)
u (0.011 ppm). Further improvement in m_n will require improved mass spectro-
scopic data since such data provides the dominant source of error. A new
evaluation of the fundamental constants incorporating these measurements is
anticipated soon (Taylor 1982). Until the new evaluation is published I
recommend the continued use of the official values in Eq. (1), unless the
differences are really significant for the purpose at hand; in that case,
however, the new value must be used with great care to be certain that the
quantities with which it is compared are consistently determined.

3. Neutron Electric Charge

There have been a series of limits set on the electric charge of the free
neutron by Shapiro and Estulin (1956), by Shull, Billman and Wedgewood (1967)
and most recently by Gähler, Kalus and Mampe (1982) at the Institute Laue-
Langevin (ILL) at Grenoble. The experiment of Gähler et al. used a focussed
beam of 200 m/s neutrons which passed for 10 meters thrugh an electric field
of 5.9 kV/mm. The experimenters found that the charge q_n of the neutron was

$$q_n = - (1.5 \pm 2.2) \times 10^{-20} \text{ e} \qquad (2)$$

where e is the charge of the proton. The authors are planning a new experi-

ment using using focussing mirrors instead of a lens and a higher flux
(Gähler, et al. 1984).   This experiment was more sensitive than any of the
previous neutron experiments. However, there are experiments reviewed by
Dylla and King (1973) which measure a related quantity -- the charge on a
neutral molecule such as SF_6 and show

$$q_{SF_6} = (0 \pm 4.3) \times 10^{-21} \text{ cm.} \qquad (3)$$

4. Neutron Magnetic Monopole

There has been extensive discussion (Dirac 1948 and Cabrera 1982) of the
possibility of there being free magnetic monopoles. In the theories of Dirac
(1948) and others, magnetic monopoles -- if they exist at all -- are ordinari-
ly multiples of $e/2\alpha$ in Gaussian units.

The first experimental limit on the neutron magnetic monopole for the neutron
was set by Ramsey (1982) in his report at the conference celebrating the
fiftieth anniversary of the neutron. He analyzed the experiment of Cohen,
Corngold and Ramsey (1956) to obtain the limit. Since that time Finkelstein,
Shull and Zulinger have completed an experiment explicitly for this purpose
utilizing deflection effects in crystals of silicon wherein the anomalously
small effective mass of neutrons greatly enhances the sensitivity. They
found that the magnetic pole q_m is limited by

$$q_m < 2 \times 10^{-21} \ e/2\alpha \qquad (4)$$

An experiment to lower this limit still further is planned by Gähler, et al.
(1982).

5. Neutron Electric Dipole Moment

Although the electric dipole moment of the neutron must vanish for a theory
which is symmetric under either parity (P) or time reversal symmetry (T), a
non-zero value is predicted by most theories which account for the known T
violation in the decay of K_L^o. As a result there is considerable theoretical
interests in the experimental limits on the neutron electric dipole because
of the constraints these limits place on theories that are not symmetric under
T.

Most early measurements of the neutron electric dipole moment were magnetic
resonance experiments with polarized neutron beams in which the electric di-
pole moment was measured by the change in the neutron precession frequency
when an electric field was shifted from parallel to antiparallel the magnetic
field (Dress et al. 1977). Scientists at Leningrad (Altarev et al. 1980) and
Grenoble (Harvard-Sussex-Rutherford-ILL collaboration 1975 and Pendlebury
et al. 1984) are currently making measurements on the neutron electric dipole
moment and both groups are using bottled ultracold neutrons with storage times
greater than 5s for which the resonance is more than 1000 times narrower than
in the earlier beam experiments. The published value by the Grenoble group
(Pendlebury, et al. 1984) is $(+0.3 \pm 4.8) \times 10^{-25}$ e cm while the published
value by the Leningrad Group is $(2.3 \pm 2.3) \times 10^{-25}$ e cm. At meetings the

3

two groups have informally reported later preliminary values of (-3.2 ± 3.5) x 10^{-25} e cm and (-2 ± 1) x 10^{-25} e cm respectively. Although the last preliminary value is outside the experimental error, neither group claims to have observed a non-zero neutron electric dipole moment.

Both the Leningrad and Grenoble Groups expect significantly to improve their experiments in the coming years. In the past, for example, the Grenoble experiment has been limited chiefly by counting statistics. However, with the recently completed upgrading of the ILL reactor, the ultra cold beam intensity for this experiment has already been increased by a factor of 140.

6. Neutron Magnetic Dipole Moment

The most accurate value for the neutron magnetic moment is the one recently obtained at the ILL by Greene, et al. (1979). They used a neutron beam magnetic resonance apparatus previously used to set a limit on the neutron electric dipole moment. They attained high precision by successively passing water and neutrons through the same tube and by calibrating the magnetic field with the separated oscillatory field proton resonance when water passed through the tubes. Their value for μ_n, the neutron magnetic moment, when expressed in various relevant units is

$$\mu_n = -\ 1.04187564(26) \ \text{x} \ 10^{-3} \ \mu_B \qquad (0.25 \ \text{ppm}) \qquad (5)$$

$$=\ 1.04066884(26) \ \text{x} \ 10^{-3} \ \mu_e \qquad (0.25 \ \text{ppm}) \qquad (6)$$

$$=-\ 0.68497935(17) \ \mu_p \qquad (0.25 \ \text{ppm}) \qquad (7)$$

$$=-\ 1.91304308(54) \ \mu_N \qquad (0.28 \ \text{ppm}) \qquad (8)$$

where μ_B is the Bohr magneton, μ_e the magnetic moment of the free electron, μ_p is the magnetic moment of the proton and μ_N is the nuclear magneton.

7. Neutron Decay

The early mass measurements of Chadwick and Goldhaber (1935) showed that the neutron was heavier than the proton and electron combined, with the implication that the free neutron itself was unstable against beta decay; this prediction was confirmed experimentally (Snell and Miller 1948) when high flux neutron beams from nuclear reactors became available. The neutron decay is of particular interest because there are no nuclear structure effects to be taken into account in analyzing the data obtained from the study of the neutron decay into a proton, an electron and an anti-neutrino. This decay is consequently an important source of information on the weak interaction.

Although the lifetime of the neutron is of great importance and interest, it has been a difficulty quantity to measure accurately and many of the measurements disagree well beyond the estimated experimental error. Most of the experiments involve measurements on a neutron beam with consequent difficulties in determining accurately the appropriate normalization and the effective solid angle for which the decay products are intercepted. These problems have been overcome in experiments with bottled ultra cold neutrons. In one case

the neutrons were retained by inhomogeneous magnetic fields acting on the neutron magnetic moment (Kuegler, Paul and Trinks 1978). In other cases (Kosvintsev, Kushnir, Morozov and Terekhov 1980) the ultra cold neutrons were retained by total reflection at the walls of an aluminum container, with the wall absorption being measured by the insertions of aluminum vanes in the container. Neither of these methods, however, has so far claimed an accuracy as good as the best beam measurements.

The measurements that are consistent with each other and have the smallest estimated errors are the neutron beam experiments of Christensen et al. (1972) and of Byrne et al. (1980). In the first of these the decay electrons were detected in approximately 4π solid angle. In the second method, if the neutron decayed within a determined volume, the decay protons were electrically trapped and later counted. The results of these two experiments are in close agreement. On this basis the Particle Data Group in 1982 recommended a value for the neutron mean lifetime τ of (925 ± 11) s but in 1984 the Group recommended

$$\tau = t_{1/2}/\ln 2 = 898 \pm 16 \text{ s.}$$

Subsequent to that evaluation Bopp, et al. (1984) measured a new value for g_A/g_V as discussed below and this value implies a τ of 889 ± 10s. Also subsequent to the last Particle Group evaluation, Byrne (1984) analyzed the restraints on the neutron lifetime from triton β decay and concluded that this data excluded one of the direct measurements of the neutron lifetime. With this value excluded he concluded that the best average of the triton and neutron data gave τ = (914 ± 6) s. J. Robson and S. Freedman at this conference will discuss neutron lifetime measurements. I hope their discussion will throw more light on these difficult measurements.

Although the full array of the studies of the beta ray spectrum of the neutron clearly go beyond the scope of a report on the particle properties of the neutron, it is appropriate to report at least briefly, measurements of the weak interaction coupling constants of the neutron. The ratios of the axial-vector (or Gamow-Teller) coupling constant g_A to the vector (or Fermi) coupling constant g_V can be found by at least three methods: (a) from the observed neutron lifetime in combination with calculations of corrected values for ft and f where f is the phase space factor for the electron in neutron decay (Christensen et al. (1972, Kropf and Paul 1974, Byrne et al. 1980 and 1982 and Wilkinson 1981), (b) from the correlation between the spin of polarized neutrons and the momentum of the emitted electrons (Krohn and Ringo 1975 and Erozolinskii, et al. 1979) and (c) from the shape of the proton recoil spectrum in free neutron decay (Stratowa, Dobrozemsky and Weinzierl 1978). The results are (Particle Data Group 1984)

$$g_a/g_V = g_A/g_V e^{i\phi} \tag{10}$$

$$g_A/g_V = 1.2539 \pm 0.0063 \tag{11}$$

$$\phi = (180.11 \pm 0.17)^{\circ} \tag{12}$$

or

$$g_A/g_V = -1.2539 \pm 0.0063 \qquad (13)$$

Subsequent to the last evaluation by the Particle Data Group (1984), Bopp et al. (1984) have utilized the new superconducting spectrometer PERKEO at the ILL to measure the energy dependence of the beta decay asymmetry. From their measured beta asymmetry parameter they obtain a new value for $|g_A/g_V|$ equal to 1.270(9).

8. Neutron Electric and Magnetic Polarizabilities

So far there have been no accurate measurements of either the electric or the magnetic polarizability of the neutron. There have been numerous theoretical calculations of the neutron electric and magnetic polarizabilities as discussed by Schroeder (1980). The electric and magnetic polarizabilities of the proton have been measured by Baranov et al. (1974) and others but there are few measurements of the magnetic polarizability of the neutron. Aleksandrov, Samosvat, Sereeter and Sor (1966) found by studying the angular distribution of neutrons scattered by lead that they could set an experimental upper limit to the neutron electric polarizability α_n. More recently Aleksandrov (1983) has obtained the value

$$\alpha_n = (11 \pm 1) \times 10^{-3} \ \mathrm{fm}^3 \qquad (14)$$

which is considerably larger than Schroeder's (1980) theroetical estimate

$$\alpha_n = 0.85 \times 10^{-3} \ \mathrm{fm}^3 \qquad (15)$$

9. Neutron Oscillations

Recently, serious consideration has been given to the possibility that the free neutron might be a superposition of neutron (n) and antineutron ($\bar{n}$) states similar to the known superposition of K^0 and $\overline{K^0}$ for the free kaon. These considerations give rise to another measurable property of the free neutron: the period $\tau_{n\bar{n}}$ of the oscillation between the n and $\bar{n}$ states. An approximate limit of $\tau_{n\bar{n}}$ 10^5 sec can be set from observations on the stability of nucleons in matter (Learned et al. 1979), Glashow 1979, Kuzmin 1970, Chetrykin et al. 1980, Marshak and Mohapatra 1980 and Green 1982) but such a limit is subject to considerable uncertainty due to nuclear effects. Several experiments are now in progress to measure $\tau_{n\bar{n}}$ for the free neutron but only one of these experiments has so far given a result. The CERN-ILL-Padua-Rutherford-Sussex experiment at ILL in Grenoble, France (Fidecaro, et al. 1985) has set the limit for the free neutron

$$\tau_{n\bar{n}} > 10^6 \text{ s.} \tag{16}$$

it is expected that with improvements to this and the other experiments the limit or $\tau_{n\bar{n}}$ during the next few years will be progressively raised to 10^7 or 10^8 secs.

10. Quantized Properties of the Neutron

A number of particle properties are quantized, so an extended series of measurements with increasing accuracy is not appropriate.

A quantized property with a long history is the neutron spin. As soon as the neutron was discovered it was apparent that if all nuclei were to consist of neutrons plus protons, the neutron would need to have a half integral spin and that simple nuclei could most easily be explained in terms of the value $J = 1/2$ for the neutron spin. Schwinger (1937) showed that the almost complete interference between singlet and triplet scattering in parahydrogen provides a direct proof that the spin of the neutron (its angular momentum in units of $\hbar$) is given by

$$J = 1/2 \tag{17}$$

A closely related discrete property is the quantum statistics followed by the neutron. Even before the neutron was discovered it had been concluded from the rotational spectra of homonuclear diatomic molecules (Heitler and Herzberg 1929 and Rasetti 1930) that nuclei with an odd mass number A obey Fermi-Dirac statistics while nuclei with even A obey Bose-Einstein statistics. This conclusion was a major difficulty for theories which had nuclei consisting of protons plus electrons but these difficulties immediately disappeared when nuclei were assumed to consist of protons plus neutrons if, and only if, the neutrons were assumed to be fermions.

Other quantized properties of the neutron have been set for the neutron either by convention or by definition and have originated from the need to distinguish the neutron from other particles, most of which were discovered after the neutron. For this reason I shall merely list these properties without further discussion. They include:

Intrinsic parity	$= P$	$= + 1$
Isospin	$= I$	$= 1/2$
Component of isospin	$= I_3$	$= - 1/2$
Baryon number	$= B$	$= 1$
Lepton number	$= L = L_e = L_\mu$	$= 0$
Strangeness	$= S$	$= 0$
[Hypercharge	$= Y$	$= 1$]
Charm	$= c$	$= 0$
Bottomness	$= b$	$= 0$
Topness	$= t$	$= 0$

11. Other Neutron Properties

There is considerable arbitrariness as to what should be called a particle property of the neutron and what should be considered neutron structure or particle scattering -- both of which topics are covered in other reports at this meeting. Therefore, I shall merely list without discussion sonme properties which from one point of view could be considered particle properties of the neutron but which more appropriately fit into other reports. These properties include the neutron-electron interaction, the charge distribution within the neutron and in particular the mean squared charge radius $= <\sum_i e_i r_i^2>$, the form factors and structure functions of the neutron as determined by electron-deuteron scattering experiments, and the neutron-proton interaction as determined from the ground state of the deuteron and from neutron proton scattering experiments.

12. Conclusions

In conclusion I have assembled in Table I the particle properties of the neutron which I have discussed. It is apparent that much has been learned about the neutron in the fifty three years since its discovery. What more will be learned in the next fifty years?

Table I. Particle Properties of the Neutron

$$m_n = 1,008664919(14)u \qquad (0.011 \text{ ppm})$$
$$= 1.6749543(86) \times 10^{-27} \text{ kg} \qquad (5.1 \text{ ppm})$$
$$= 939.5731(27) \text{ MeV} \qquad (2.8 \text{ ppm})$$

$$q_n = - (1.5 \pm 2.2) \times 10^{-10} e$$

$$q_m < (2 \times 10^{-21} e/2\alpha$$

$$d = (2.3 \pm 2.3) \times 10^{-25} e \text{ cm}$$

$$\mu_n = - 1.04187564(26) \times 10^{-3} \mu_B \qquad (0.25 \text{ ppm})$$
$$= - 1.04066884(26) \times 10^{-3} \mu_e \qquad (0.25 \text{ ppm})$$
$$= - 0.68497935(17) \mu_p \qquad (0.25 \text{ ppm})$$
$$= - 1.91304308(54) \mu_N \qquad (0.28 \text{ ppm})$$

$$\tau = t_{1/2}/\ln 2 = 898 \pm 16 \text{ secs}$$

$$g_A/g_V = - 1.2539 \pm 0.0063$$

$$\tau_{n\bar{n}} > 10^6 \text{ secs}$$

J = 1/1	P = + 1
I = 1/2	I_3 = - 1/2
B = 1	L = L_e = L_μ = 0
s = 0	Y = 1
t = 0	b = 0

References

Aleksandrov Y A, Samosvat G S, Sereeter Z and Sor T G 1966 JETP Lett. 4 134
Aleksandrov Y A, 1983 Yad. Fiz 37, 253 (1983) and Sov. J. Nucl. Phys. 37, 149
Altarev I S et al. 1980 Nucl. Phys. A341 269
_____ 1981 Phys. Lett. 102B 13
Altarev I S, Barisov Y V, Borovikova N V, Branden A B, Egorov A I, Porsev G D,
    Ryabov V L, Serebov A P, Taldaev R R 1980 Nucl. Phys. A341 269
            1981 Phys. Lett. 102B 13
Anikin G V and Kotukhov I I 1972 Sov. Journ. of Nucl. PHys. 14 152
Baranov R, et al. 1974 Phys. Lett. 52B 122
Bopp, et al. 1984 J. de Physique Colloque 45, C-3 21
Byrne J 1982 Reports Progress Physics 45 115
Byrne J, Morse J, Smith K F, Shaikh F, Green K, and Greene G L 1980 Phys.
    Lett. 92B 274
Cabrera B 1982 Phys. Rev. Lett. 47 1738
Chadwick J 1932 Nature 129 312 and Proc. Roy. Soc. Lond. A136 692
            1933 Proc. Roy. Soc. Lond. A142 1
Chadwick J and Goldhaber M 1934 Nature 134 237
            1935 Proc. Roy. Soc. Lon. A151 479
Chetrykin K G, Kozamonsky M V, Kuzmin V A and Shaposhnikov 1981 Phys. Lett.
    99B 358
Christensen C J, Nielsen A, Bafasen A, Brown W K and Rustad B M 1972 Phys Rev.
    D5 1628
Cohen E R and Taylor B N 1973 Phys. Chem. Ref. Data 2 663 (CODATA Report)
Deslattes R D, Kessler E G, Sauder W C and Heinins A 1980 Annals of Phys.
    129 378
Dirac P A M 1948 Phys. Rev. 74 817
Dylla H F and King J G 1973 Phys. Rev. Lett. A7 1224
Erozolimskii B G, Franck A I, Mostovoi Y A, Arzumanov A S, Vortski L R 1979
    Yad. Fiz. (USSR) 30 692 [Sov. J. Nucl. Phys. (USA)]
Fidecaro et al. 1985 Phys. Lett. B156 122
Finkelstein K D, Shull C D and Zeilinger A 1985 Intl. Conf. on Neutron Scatt.
    and private communications
Gähler R, Kalus J and Mampe W 1982 Phys. Rev. D25 2887
Gähler R, et al. 1984 J. de Physique C3 17
Glashow S 1979 Harvard Preprints HUTP79/A029, 79/A040 and 79/A059
Green K 1982 Rutherford Laboratory Preprint SP 82-60 (Invited talk at Recontre
    de Moriond, Les Aris March 1982
Greene G L, Ramsey N F, Mampe W, Pendlebury J M, Smith K, Dress W B, Miller
    P D and Perrin P 1979 Phys. Rev. D20 2139
Greene G L, Deslattes R D, et al. 1985 private communication
Greenwood R C, Helmer R G, Gehrk R J and Chrien R E 1979 Atomic Masses and
    Fundamental Constants 6 219
Harvard-Sussex-Rutherford-ILL Collaboration (Baker C, Byrne J, Golub R,
    Green K, Heckel B, Kilvington A, Mampe W, Morse J, Pendlebury J M, Ramsey
    N F, Smith K and Sumner T) 1975
Heitler W and Herzberg G 1929 Naturwiss 17 673
Kessler E G, Deslattes R D, Henins A and Sauder W C 1978 Phys. Rev. Lett. 40
    171
Knowles J W 1962 Can. Journ. Phys. 40 257
Kosvintsev Y Y, Kushnir Y A, Morozov V I and Terekhov G I 1980 Pis' ma Zh.
    Eksp. Teor. Fiz. 31 257 [JETP Lett. 31 237 (1980)]

Krohn V E and Ringo G R 1975 Phys. Lett. 55B 175
Kropf A and Paul H 1974 Z. Physik 267 129
Keugler K J, Paul and W Tinks U 1978 Phys. Lett. 72B 422
Kuzmin V A 1970 pis'ma Zh. Eksp. Teor. Fiz. 13 335
Learned J, Reines F and Soni A 1979 Phys. Rev. Lett. 43 907
Marshak R E and Mohapatra R N 1980 Phys. Rev. Lett. 44 1316 and Phys. Lett. 94B 193
Mattauch J H E, Thiele W E and Wapstra J H Nuclear Phys. 67 1, 32 and 73
Particle Data Group 1982 Phys. Lett. 111B i (Roos M, et al.)
Particle Data Group 1984 Rev. Mod. Phys. 56, 51
Pendlebury J M, et al. 1984 Phys. Lett. 136B 327
Ramsey N F 1982 Inst. of Physics Conf. Series 64-2 5
Rasetti F 1930 Z. Physik 61 598
Schroeder V E 1980 Nucl. Phys. B166 103
Schwinger J S 1937 Phys. Rev. 52 1250
Shapiro I S and Estulin I V 1956 Zh. Eksp. Teor. Fiz. 30 579 [Sov. Phys. JETP 3 626 (1957)]
Shull C G, Billman K W and Wedgewood F A 1967 Phys. Rev. 153 1414
Snell A H and Miller L C 1948 Phys. Rev. 74 1217
Stratowa C, Dobrozemsky R and Weinzierl P 1978 Phys. Rev. D18 3970
Taylor B N 1982 (private communication July 19, 1982)
Vylor T, Gromov K Y, Ivanov A I, Osipenko B P, Frolov E A, Chumin V G, Schus A F and Yudin M F 1978 Sov. J. Nucl. Phys. 28 585
Wilkinson D 1981 Progr. in Part. and Nuclear Phys. 6 325

THE NBS COLD NEUTRON RESEARCH FACILITY

J. M. Rowe
235/A106
Institute for Materials Science and Engineering
National Bureau of Standards
Gaithersburg, MD 20899

The NBS Research Reactor at Gaithersburg, Maryland operates at 20MW, and has 25 experimental facilities available for a wide variety of neutron related measurements. Last year, the reactor served over 250 users from industries, universities, and other Government agencies. At the present time, a large-volume heavy-ice cold moderator to be operated at 25K is being tested for insertion into a reserved space in the reactor early in 1986. This moderator will provide a large increase in available cold neutron ($\lambda > 4$ Å) flux, and can provide access for a large number of neutron guide tubes. NBS has proposed the construction of a large (240' x 130') experimental hall and associated instrumentation, which would be operated as a national facility. The NBS proposal includes funding for 11 experimental facilities, and reserves space for an additional 5 facilities to be developed by Participating Research Teams (PRT's). For the NBS developed stations, 2/3 of the available time would be reserved for use by the general U. S. scientific community (to be scheduled by a Program Advisory Committee), with the remaining time reserved to NBS and collaborators. The stations developed by PRT's would be available to the general community, with 2/3 of the time reserved to the PRT. The PRT's would be responsible for the design, funding, construction, staffing, and maintenance of their stations. Although the majority of the facilities will be aimed at use by the materials science, solid state physics, chemistry and biology communities, at least one large station will be reserved for development and use by the group represented by the present meeting. The current status and future prospects of this project will be discussed.

The Research Reactor at the National Bureau of Standards was designed to accomodate a large volume (36 cm. diameter) cold neutron moderator in a region of high neutron flux. The tip of the penetration is situated at the same distance from the core as the thermal neutron beam tubes, as shown in Fig. 1 below. The D_2O ice cold source will be cooled by recirculating helium gas from which the heat is removed by a refrigerator that provides 1 KW of cooling at 25K. In order to reduce the γ-ray heating in the moderator, a water-cooled shield of radiogenic lead and bismuth will be installed between the moderator cryostat and the end of the penetration. The moderator itself will have the geometry shown, with a re-entrant hole to provide the maximum cold neutron flux. The new vertical cold moderator at the Institut Laue Langevin uses this

geometry, and the measured gain in cold neutron flux over the previous moderator is in agreement with theoretical estimates (gain = 1.5 - 2.0). Although the performance of a D_2O ice cold source has not been measured in the actual geometry of the NBS cold source, previous mockup experiments[1,2] and experience with polyethylene moderators at IPNS[3] indicate that effective moderator temperatures should be in the range of 40 - 60 K, which will provide a total cold neutron gain of order 15 for neutrons with $\lambda > 4$ Å.
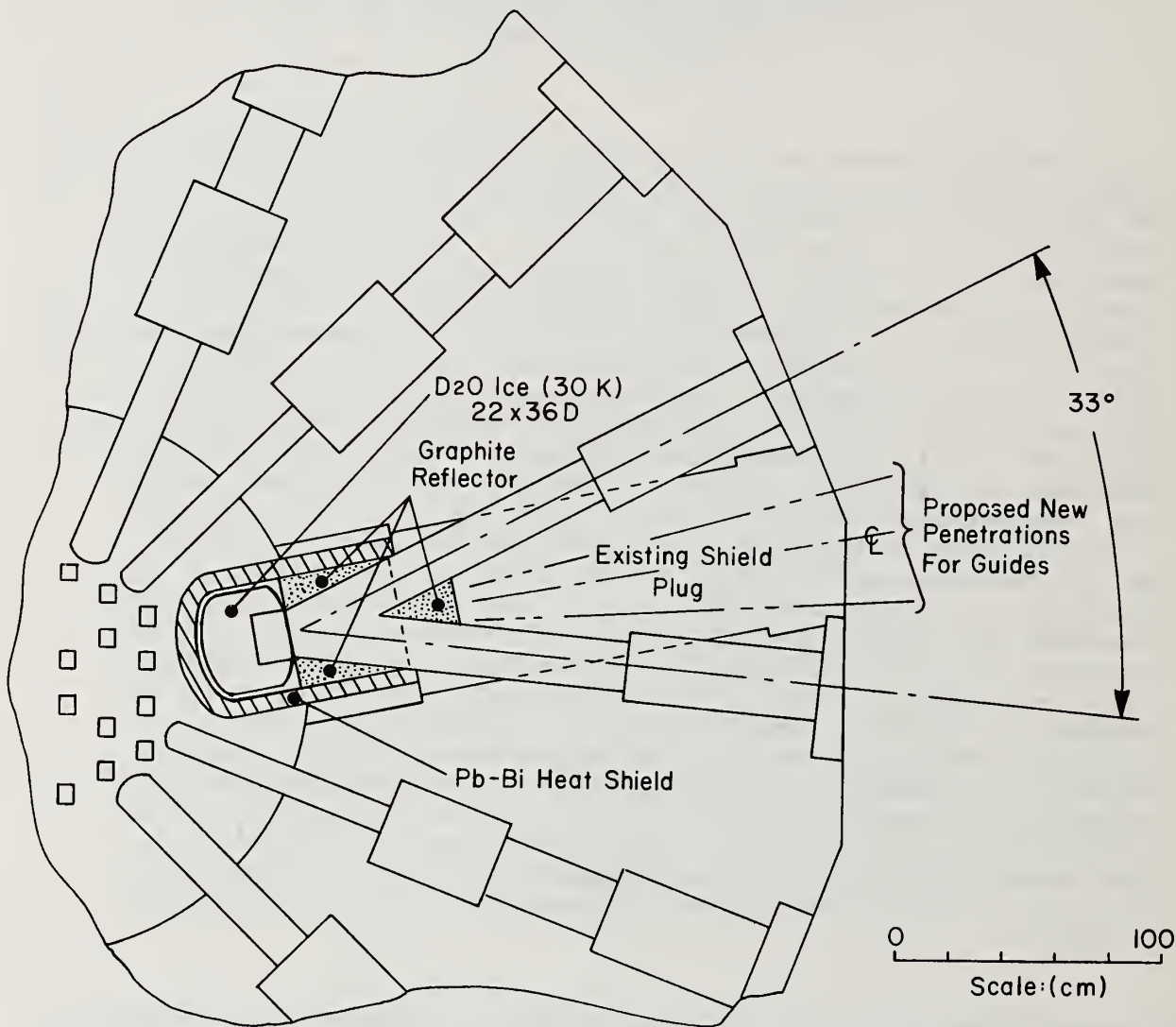
Geometry of Current N.B.S. Cold Source

Figure 1

Funding of $1.5 M per year to install and operate this cold source, and to develop and use two prototype instruments, was obtained beginning in the Fiscal Year 1985 budget. Two cold source cryostats were designed and fabricated, one for immediate use, and the other as a spare. These are now undergoing extensive testing outside the reactor, and installation is

NBS CENTER FOR COLD NEUTRON RESEARCH
EXPERIMENTAL FLOOR

Scale (m)

OFFICE FLOOR

SCALE (m)

13
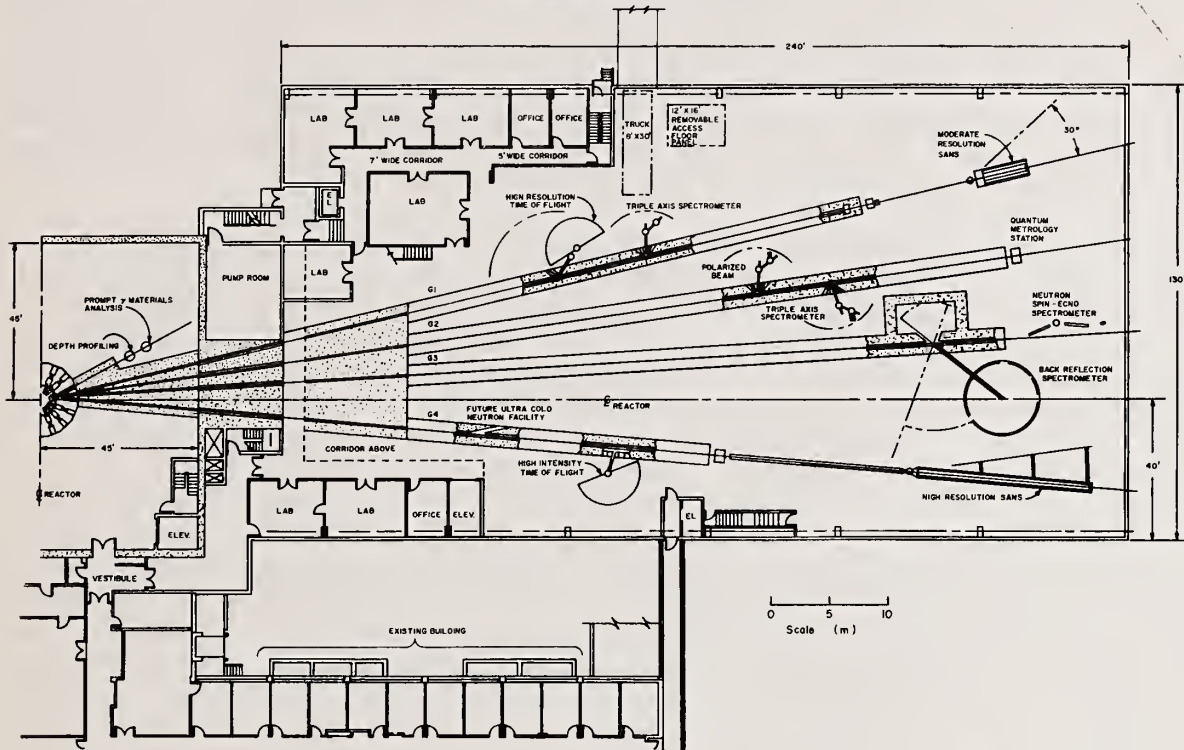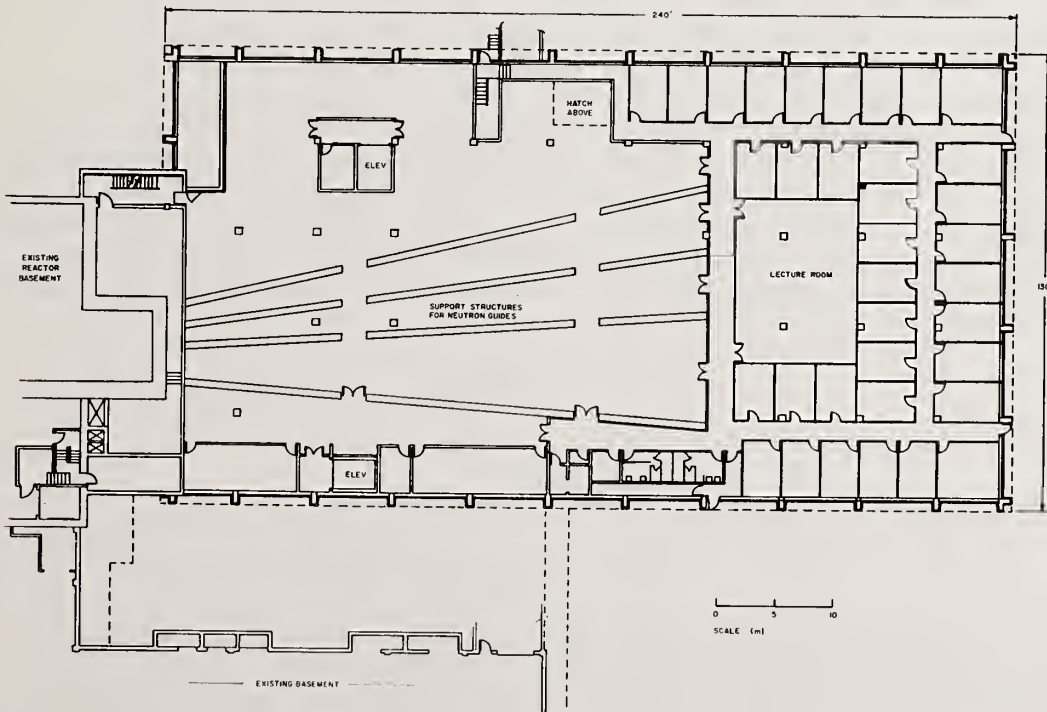
scheduled for early 1986. After installation, testing runs will be required to verify proper operation of the cold source and to determine the performance. After this test period, the cold source will be operated on the same schedule as the reactor, and will provide two beams of cold neutrons for the two new instruments. These instruments are currently being designed and commissioned. More importantly, the cryostat was designed to allow additional penetrations into the cold source for guide tubes.

The geometry of the NBS reactor provides both a large volume for a cold source and ample space in the reactor penetration for extracting large guides well separated in angle (see Fig. 1 and Fig. 2). This provides the basis for a unique opportunity to develop a center for cold neutron research capable of serving the needs of the U. S. scientific community. Such a project has been proposed, and was included in the President's budget for Fiscal Year 1986, but was not approved by Congress as a result of severe budget pressures. A possible layout for this proposed research facility is shown in Fig. 2.
As can be seen from the figure, the proposed facility would be a large experimental hall external to the existing reactor building, served by at least four neutron guides, and including provision for at least fifteen experimental stations. Preliminary design of the guide network is currently underway. From this work, it is clear that we can extract over 500 cm^2 of neutron beams into guides as a result of the cold source and reactor design. The facility would be operated as a national user facility, open to all U. S. scientists. Of the fifteen instruments proposed, NBS requested funding for construction of ten, with the other five reserved for development by other groups, either private or public. The ten to be developed by NBS would be operated so as to provide 2/3 of the time available to the general community, with time scheduled by a Program Advisory Committee, of which the majority of the members and the chairman would be from outside NBS. The instruments would be designed, developed and operated by NBS. The other five stations would be designed, developed and operated by Participating Research Teams (PRT's). In return, the PRT would have 2/3 of the available time to use as they see fit, with the remaining time to be available for general use and scheduled by the Program Advisory Committee. PRT's would be chosen by NBS on the basis of proposals submitted to it, and it is anticipated that one such PRT would be representative of the community attending this workshop. In many cases, NBS would be a partner in PRT's, although this is not a requirement for submission or approval of a proposal. It is intended that PRT's organize themselves, and develop instruments as a group; NBS will not undertake to organize many small groups into a PRT.

Most of the experimental stations presently envisioned would be intended to serve the Materials Science, Solid State Physics, Chemistry, and Biological communities. The proposed instruments are described in the Report[4] of the Major Materials Science Committee of the National Research Council (the "Seitz Committee"). However, as can be seen in Reference 4, we have always envisioned a station dedicated to the "Investigation of fundamental interactions with cold neutrons" in our planning and proposals. Such an effort is entirely within the missions and interests of NBS, and G. Greene is working with us in the facility design to ensure that this need is adequately met. We anticipate that this station will be developed by a PRT in which NBS is a participant, and that the resultant facilities will be operated as a National facility for this type of work. The results of the present workshop will be used to determine the necessary characteristics of the neutron guides and of the building and associated experimental space. As the final architectural design of the building will be undertaken immediately upon funding of the overall NBS facility, it is imperative that any structural requirements be known as soon as possible.

As mentioned earlier, the project has not yet been funded by Congress, but efforts to have the project approved are being vigorously pursued by NBS and The Department of Commerce. The total cost of the proposal is $25 M, which would be spread over four years of construction and development, approximately as shown below.

	FY1	FY2	FY3	FY4
Construction of building	$7.0M	$6.0M		
Fabrication of neutron guides	$0.5M	$1.0M	$0.4M	
Reactor confinement modifications		$0.5M	$1.0M	
Instrument construction	$0.5M	$0.5M	$4.6M	$4.0M

In the Table above, FY1 refers to the first year of approval by Congress.

With this schedule, first beneficial use of the facility could be as soon as 2 1/2 years after approval, subject to some uncertainty because of procurement regulations and other restraints. Of course, not all of the instruments would be in final form, or even ready for installation at initial use. In addition to the construction costs outlined above, the NBS proposal includes a request for the necessary increase in staff and operating expenses associated with a National facility. At the present time, it is impossible to predict the date or probability of final approval of this proposal, but NBS remains committed to the provision of a facility for cold neutron research to meet the needs of the entire U. S. scientific community.

References

1. J. J. Rush, D. W. Connor, and R. S. Carter, Nuclear Science and Engineering 25, 383(1966)
2. R. J. Chin, MSc thesis, MIT, 1971
3. J. M. Carpenter, private communication.
4. Major Facilities for Materials Science and Related Disciplines, Presentations to the Major Materials Facilities Committee of the National Research Council, National Academy Press, Washington, DC (1984).

COLD AND ULTRA COLD NEUTRON BEAMS FOR FUNDAMENTAL
PHYSICS RESEARCH AT THE INSTITUTE LAUE-LANGEVIN

P. Ageron and W. Mampe
Institute Laue-Langevin
156X, 38042 Grenoble, France

All experiments discussed at this workshop need intense beams
of low energy neutrons with low gamma ray and fast neutron back-
grounds. The High Flux Reactor of the ILL, Grenoble offers in connec-
tion with the integrated cold and ultra-cold sources a large variety
of those facilities. The beams, transported in neutron guides, cover
the whole wavelength range from one Angstrom to several thousand
Angstroms.

The neutron is an excellent tool to study fundamental interactions at low
energies. The proceedings of two earlier workshops held at ILL [1,2] as well
as the program of the actual workshop testify the range and importance of the
field. All experiments have in common the design for maximum sensitivity. They
need for this purpose, except for neutron interferometry and high precision
gamma spectrometry, low energy (E_n < 0.005 eV) neutron beams of highest inten-
sity and lowest possible contamination by faster neutrons or other radiations.
Those beams are nowadays readily available at High Flux Reactors with inte-
grated cold sources, like the one at the Institute Laue-Langevin in Grenoble,
France. Information on the reactor itself and the related facilities for solid
state and nuclear physics research can be found in Ref. 1-4. Fig. 1 gives
a general view of the instrument arrangement in the reactor hall, in the main
guide hall and the guide hall for the second cold source. We shall here con-
centrate only on those cold neutron facilities in use for "special beam ex-
periments" in fundamental physics.

Cold neutron sources

The prior condition for this experimental program are the cold sources:
a) a D_2 source operational since 1972 together with the reactor and modified
in 1985. b) a second D_2 source to be installed at the position of an existing
beam tube between 1986 and 87. A detailed technical description of these
sources and their performances can be found in Ref. 5.
a) A large size D_2 moderator instead of a small size H_2 source has been
chosen because it has an overall better thermalisation efficiency (especially
at long wavelength)and its large size allows to feed five 20 cm x 3 cm
neutron guides and one 10 cm $\emptyset$ beam tube. 26 1 of D_2 boil under nuclear
heating at 25 K in an Al sphere of 38 cm diameter and 1.5 mm wall thickness.
The unperturbed flux at the source position is 4.5 x 10^{14} n cm^{-2}s^{-1}. The gain
factor at λ = 6 Å has been measured previously to be 30 and at $\lambda \approx 10$ Å
60 - 70, respectively. In 1985 the source had been replaced by a new, improved
one carrying a cavity filled with D_2 gas of 20cm height, 10 cm width and 25 cm
penetration depth. The gain factor due to this cavity has been measured, in
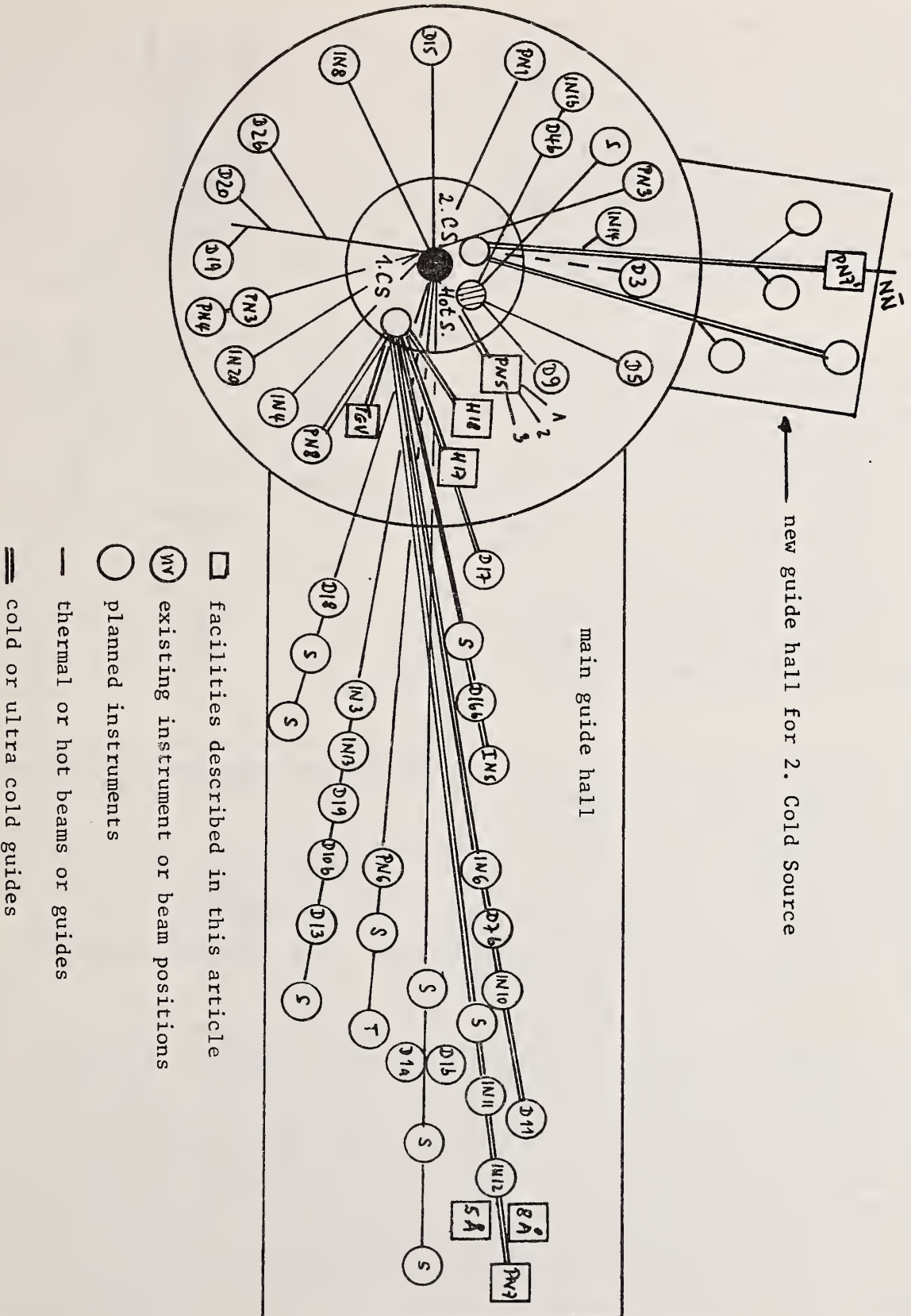
Fig. 1. Schematic view of ILL installations

new guide hall for 2. Cold Source

main guide hall

☐ facilities described in this article

(w) existing instrument or beam positions

◯ planned instruments

| thermal or hot beams or guides

≡ cold or ultra cold guides

qualitative agreement with the calculations, to be 1.6 - 1.7 for wavelength between 3 Å and 6 Å but seems lower at longer wavelength, thus lower for the integrated spectrum (1.2 - 1.4) measured by activation of thin gold foils. Together with the cavity a vertical guide for the extraction of very cold (and ultra cold) neutrons, which will be described later, has been added inside the service tube. The source is shown in fig. 2.

Among the 5 guides, 30 mm in width and 200 mm high and with radii of curvature between 25 m and 2700 m, three are available for fundamental physics experiments: 1) H18, 2) H17 and 3) H14.

1) H18: Has a curvature of 25 m and ends in the reactor hall. The maximum intensity is at 20 Å and the spread $\pm$ 10 Å. The capture flux is $\emptyset_c$ = 5.4 x 10^8 n cm^{-2} s^{-1}. The guide has the total available section of 30 mm x 200 mm. Many long term experiments have been performed on this beam since 1973.

2) H17: A 5 cm high beam section of this guide leaves the reactor hall and is used for a small angle scattering machine. The guide section of the remaining part ends in the reactor hall. Though it is an end position the lateral working area is very limited to one side. The guide curvature is 150 m and the flux maximum at 9 Å. The capture flux has earlier been measured to be 4.5x 10^9 n cm^{-2} s^{-1} and has slightly increased to 5.4 x 10^9 n cm^{-2} s^{-1} due to the gain factor of the modified cold source. This beam has mainly been used for He physics and the superthermal He source.

Fig. 2. Schematic view of the modified vertical ILL cold source with the cavity and the vertical guide.

3) H14: Has a curvature of 2700 m and traverses the whole neutron guide hall. On its way are several inelastic scattering instruments installed. The end position at a distance of about 120 m from the cold source is attributed to fundamental physics experiments. A super-mirror polarizer of the curved soller type is installed together with a spin flipper in a casemate at the end of the guide. The experimental area is still several meters downstream outside the guide hall in an area which allows experiments with hydrogen. The beam area section at the exit of the guide is 30 x 50 mm^2. The polarizer has a transmission of 52% and the polarization has been measured by O. Schaerpf to be 97.4%. The unpolarized and polarized neutron spectra are shown on fig. 3. The absolute numbers are actually higher by 20%. The beam was used for polarized neutron capture experiments and for studies of the neutron decay.

Furthermore, close to the endposition two monochromatic beams are extracted by

crystal monochromators from the main beam: A 20 x 20 mm² beam with 8 Å wavelength and a flux of 5 x 10⁶ n cm⁻² s⁻¹ and a 5 Å beam of 10 x 10 mm² section and 3 x 10⁶ n cm⁻² s⁻¹. The first beam is mainly used for on line tests during the super-mirror and polarizer fabrication by O. Schaerpf's group. Both positions have served as test positions for setting up experiments which later are performed on the full beam of PN7.

b) The second cold source will be as well a D_2 source and housed in a horizontal beam tube of 23 cm $\emptyset$. It will be a cylinder 21 cm in diameter and 21 cm long. The unperturbed flux at this position is 7 x 10¹⁴ n cm⁻² s⁻¹. Heat will be removed from this source as in the existing one by natural convection. 3 guides will be fed by the source, with sections of 6 x 12 cm², 4 x 12 cm² and

Fig. 3. Unpolarized (a) and polarized (b) spectra of the PN7 beam as measured on non modified cold source.

1.5 x 12 cm². The end position of the largest guide (80 m long, 5000 m radius of curvature) will be available for the fundamental physics research program. After a limited period for a new N-N̄ oscillation experiment it will be converted into a large cross section, high intensity polarized beam. The expected capture flux is 1.4 x 10¹⁰ n cm⁻² s⁻¹.

Very cold and ultra cold neutron sources

The very low energy part ($E < E_{max} \ll kT$) of the Maxwell spectrum in the moderator of the reactor at temperature T is

$$\phi(E < E_{max}) = \phi_o/2 \cdot (E_{max}/kT)^2$$

where ϕ_o represents the total neutron flux. For ultra cold neutrons (UCN) with $E_{max} = 1.8 \times 10^{-7}$ eV and for T = 300 K we obtain $\phi = 2.5 \times 10^{-11} \cdot \phi_o$. Though the fraction is small, High Flux Reactors with $\phi_o = 10^{14} - 10^{15}$ n cm⁻² s⁻¹ are capable of producing substantial numbers of very low energy neutrons. The art is to extract those neutrons from the moderator through windows and transport them in a guide to the experimental area without impotant losses. Different ways have been tried at ILL to make beams of very cold neutrons (VCN, between cold and ultra-cold) and ultra-cold neutrons available: 1. PN5 with a converter at room temperature and an inclined guide. 2. TGV extracting neutrons vertically from the 25 k D_2 bath of the cold source which are then decelerated in a Steyerl turbine. 3. Superthermal He source which transforms cold neutrons into ultra-cold neutrons by creation of phonons in Helium. Sources 1. and 3. have been in use since several years whereas 2. is getting ready just now. We present the results from the three facilities in the following section.

1. PN5

The VCN and UCN source PN5 is operational since 1977 and described in detail in Ref. [5]. A schematic view is presented in Fig. 4. The source is installed in an inclined beam tube. The thermal flux at the nose of the beam tube is 6×10^{14} n cm^{-2} s^{-1}. A H$_2$O converter at room temperature, separated by a 0.6 mm zircalloy window, sits at the lower end of an evacuated 5 m long and 67 mm i.d. electropolished stainless steel guide. The out of pile nickel coated glass guide has a cross section of 70 x 70 mm^2 and a radius of curvature of 10 m, thus eliminating the direct radiation together with all neutrons with $\lambda < 20$Å and bending the useful beam into the horizontal plane. A beam switch system allows to direct the beam to 3 different experimental areas. A beam sharing mode is possible if at least one experiment works with stored neutrons. The original in pile guide which had degraded due to an inadequate vacuum systems had been replaced during the 1985 reactor shutdown by the originally ordered exchange source. The UCN density measured in Sept. 85 in a (stainless steel bottle) storage experiment is ~ 1 UCN cm^{-3}. The corresponding UCN flux is under the assumption of a Maxwell spectrum at the source guide exit 120 UCN cm^{-2} s^{-1}. Several experiments described in more detail at this workshop have been performed at this UCN source: EDM experiment, neutron optics, study of the experimental UCN storage time deficiency, a preliminary neutron lifetime experiment and development work in cold neutron technology.
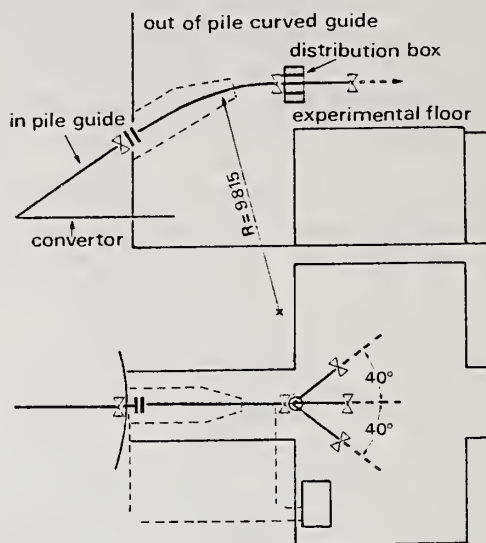
Fig. 4. Schematic view of the very cold and ultra-cold neutron source PN5 at the ILL. (a) side view, (b) top view showing direction of beams.

2. Vertical VCN and UCN neutron source

After the success of PN5 in terms of introducing and perfectioning UCN technologies at ILL and starting a full research program the limitations given by the relatively low UCN density became obvious. In 1978 one of us (P.A.) proposed therefore the installation of a cold guide into the existing D$_2$ cold source of the HFR. The guide was to be connected to a "Steyerl" neutron turbine. The project was accepted by the ILL committee, financed by the Germany Bundesministerium für Forschung und Technologie (except for the inpile part which was paid and contracted by ILL) and designed and realized by H. Nagel from A. Steyerl's group in Garching in collaboration with the ILL. A 5 m long guide section penetrating into the liquid D$_2$ moderator connects the cold source with a neutron shutter on top of the D$_2$O tank of the HFR. This inpile guide section consists of a 70 mm diameter Ni liner of only 0.15 mm wall thickness

(in order to minimize nuclear heating) in an Al vacuum tube. The ensemble is housed in the vertical service channel of the cold source. The neutron guide has an excellent reflectivity for cold neutrons (99% per reflection). It is made, as well as the upper guide section, by a new technique which produces metallic copies of high quality glass surfaces. The technique has been developed by H. Nagel in Garching in collaboration with ILL and is described in more detail in a contribution by A. Steyerl on the occasion of C. Shull's 75. anniversary. The inpile straight guide is separated from the curved guide, passing through the light water of the swimming pool, by two 0.2 mm zircalloy membranes. The inpile section is filled with 1 mbar of He to increase the heat conduction. The installation above the neutron shutter is shown in fig. 5. The curved (r = 13 m) nickel guide with 70 x 70 mm² cross section feeds the turbine. Except for the 1.5 m section in the turbine itself the total guide has been installed in summer 1985 and is called TGV (tube guide vertical). The turbine vacuum vessel with its pumping and vacuum security system has been installed at ILL in Oct. 85 by the Garching group. The installation will be completed with the turbine wheel, the guide sections within the turbine and the beam distribution system before the end of 1985. The turbine wheel has been operated at Garching since April 1985 and has a two times better reflectivity than the first Garching turbine. The turbine wheel has 690 blades, 150 mm high on a radius of 80 cm. It will Doppler shift ∿ 60 Å neutrons into the UCN region. The continuous flux VCN and UCN source will make improved use of the given thermal flux of the HFR by several means: a) the connection to the 25 K D_2 moderator. b) A new low loss guide system. These two improvements by themselves already allow to obtain UCN densities of 30-50 cm⁻³ (v < 6 m s⁻¹). c) The turbine is expected to increase further the UCN density. d) The original 30 x 70 mm² beam at the

Fig. 5. Vertical cold guide (TGV) with Steyerl turbine at ILL.

entrance of the turbine will be increased to a useful section of 200x100 mm² at the exit, thus capable to feed several experiments simultaneously (fig. 6). A beam distribution system similar to the PN5 one will optimize the use of the available UCN.
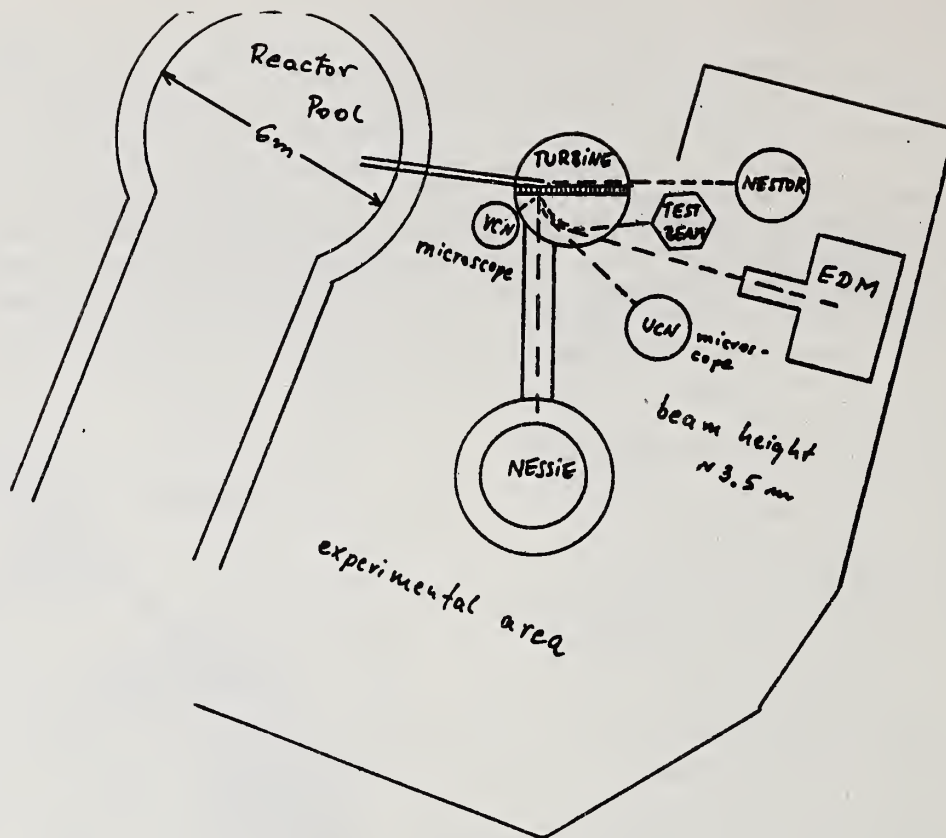
Fig. 6. Beam positions and first generation of experiments on
the new vertical VCN-UCN source.

The remaining part of the TGV beam bypasses the turbine wheel in a bent guide.
It will be available for experiments using very cold neutrons from 6 m s^{-1} to
100 m s^{-1}.

The performance of the TGV before the installation of the turbine has been
investigated by the following methods: a) density measurement of storable
(UCN) neutrons. b) time of flight spectrum of very cold neutrons (VCN)
c) total capture flux by gold foil activation.

a) UCN were stored for different time intervals in a 170 cm long, 67 mm i.d.
electropolished stainless steel tube (V $\sim$ 6000 cm^3). The extrapolated number
of UCN at zero storage time (fig. 7) gives a measured density on PN5 of
0.6 UCN/cm^3 and on the exit of the TGV of 41 UCN/cm^3. Taking into account an
overall efficiency of the bottle system of 0.88 (entrance ellbow) x 0.85
(exit ellbow) x 0.8 (detector) = 0.6 we obtain actual UCN densities
(for v < 6.2 m s^{-1}): 1 UCN/cm^3 for PN5 and 68 UCN/cm^3 for the TGV.

b) The time of flight system consists of: A fixed vertical slit (70 mm high,
1.5 mm wide) at the TGV exit, a chopper disc and a 1.5 m long flight path in
form of two spare TGV guide sections. A detector with a horizontal (20 mm),
1.5 mm wide entrance slit could be moved across the far end of this guide. The

shapes of the spectra as a function of height are similar to those obtained at PN5 with a maximum at v = 60 m s^{-1} corresponding to the design entrance velocity of the turbine. The gain factor in intensity compared to PN5 is about 100.

c) The gold foil activation results as a function of height across the beam are shown on fig. 8. They confirm the gain factor as given in b) over the whole spectrum of the TGV compared to PN5.

3. Superthermal UCN source

In 1975 and in more detail in 1977 R. Golub and M. Pendlebury proposed a new UCN production mechanism based on downscattering of 10 Å neutrons in suprafluid He-4 [7]. Rather than using such a source on an external beam in a continuous flow mode it is especially well adapted for a pulsed mode if connected to UCN storage type experiments: The UCN density ρ [cm^{-3}] achievable in the source is then given by the product of the UCN production rate p [cm^{-3} s^{-1}] per second and the lifetime τ [s] of UCN in the production volume ρ [cm^{-3}] = p · τ. Results from test experiments performed at ILL were in agreement with theoretical predictions [8]. As a consequence of these results one of us (P.A.) proposed and designed a real seize UCN source of this new type (active volume: 67 mm ϕ and 300 cm long in the beam axis). To 85% financed by the ILL and 15% by RAL the proposed cryostat was ordered from industry. The source served to study the production- and loss mechanism of UCN in pure He-4 as a function of temperature (T < 1.2 K) more precisely [9]. A production rate of p $\sim$ 1 UCN cm^{-3} and an UCN lifetime of 150 s have been measured after coating the inner walls of the source with Beryllium. Further experiments on low temperature He-4 physics have been proposed. In order to make full use of the potential of this source for the EDM experiment a low temperature exit system has been designed and built at RAL. This should permit the replacement of the actual cryogenic windows (Al) by a system with acceptable low UCN losses. More details of this source type will be presented in a contribution to this workshop by R. Golub.
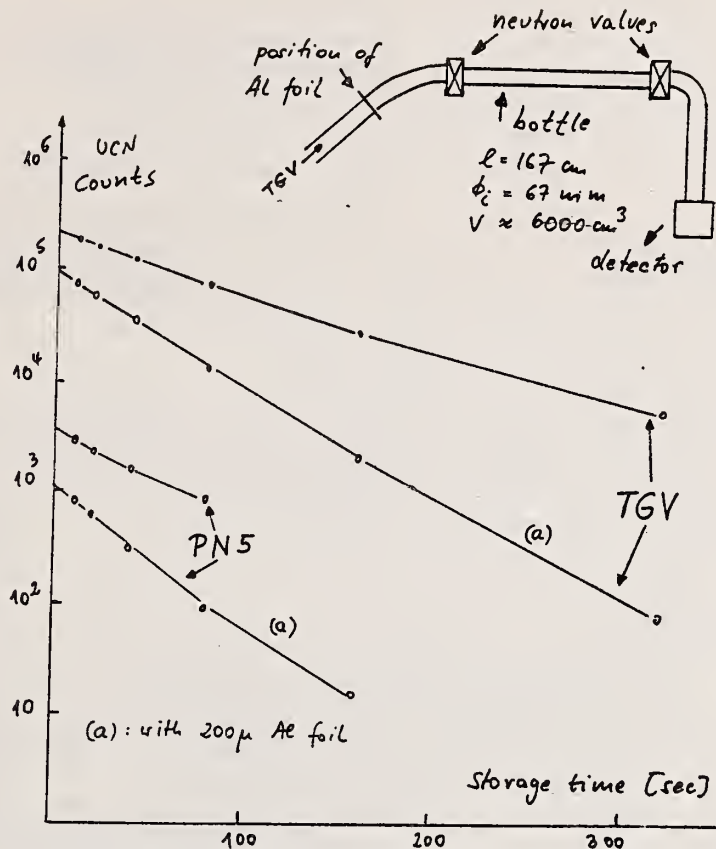
Fig. 7. UCN storage measurements with a 67 mm i.d., 1670 mm long electropolished stainless steel tube at the exit of the TGV and on PN5. Measurements (a) are made with a 200 μm Al foil at the bottle entrance.

We conclude that the existing facilities
are well suited for a rich research program
in fundamental neutron physics and that espe-
cially the new vertical VCN and UCN source,
planned and constructed by A. Steyerl and his
group in Garching, can open a new dimension.

References

[1] W. Mampe and P. Ageron, Inst. of Phys.
Conf. Ser. (1978) 42, 148.

[2] P. Ageron and W. Mampe, Journ. de Phys.
C3-1984, 279.

[3] Commissariat à 1(Energie Atomique 1971
BiST No. 165 and 1972 BiST No. 166.

[4] Inst. Laue-Langevin (1983), Neutron
Beam Facilities at the High Flux Reactor
available for users. ILL, internal re-
port.

[5] P. Ageron, Proceedings of the Conference:
"Neutron Scattering in the Nineties",
Jülich 14-18 Jan. 1985, IAEA-CN-46/16, p. 135.

[6] P. Ageron, M. Hetzelt, W. Mampe, R. Golub, J.M. Pendlebury, K. Smith and
J. Robson, IAEA-SM-219/58 (1978) 53.

[7] R. Golub and J.M. Pendlebury, Phys. Lett. 53A (1975), 133.
R. Golub and J.M. Pendlebury, Phys. Lett. 62A (1977), 337.

[8] P. Ageron, W. Mampe, R. Golub and J.M. Pendlebury, Phys. Lett. 66A (1978),
469.
C. Jewell, B. Heckel, P. Ageron, R. Golub, W. Mampe and P.V.E. McClintock,
Proceed. XVI Int. Conf. on Low Temp. Phys., Los Angeles 1981.

[9] R. Golub, C. Jewell, P. Ageron, W. Mampe, B. Heckel and I. Kilvington,
Z. Phys. B51 (1983) 187.
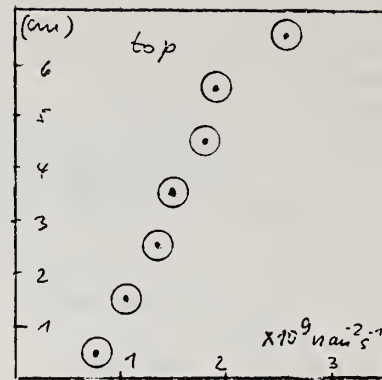
Fig. 8. Capture flux
(2200 m s^{-1}) measured by gold
foil activation at the TGV exit
as a function of height across
the beam.

THE IMPLICATIONS OF NEUTRON BETA-DECAY

J. Byrne

School of Mathematical and Physical Sciences
University of Sussex
Brighton, Sussex, BN1 9QH, U.K.

We analyse the implications of results derived from the
experimental study of neutron β-decay within the context of weak
interaction theory, and comment on their significance in cosmology
and astrophysics.

§1   The weak current

Adopting Pauli's neutrino hypothesis [1] and guided by the analogy with quantum
electrodynamics Fermi described the short range weak interaction in terms of
the contraction of two (polar) vectors representing hadronic and leptonic
currents respectively [2] . Following the discovery of parity violation in weak
processes [3] the theory was subjected to a major modification involving the
introduction of axial vector currents and the resultant theory is a current-
current interaction described by the Lagrangian density

$$L(x) = \frac{G}{\sqrt{2}} J_\mu(x) J_\mu^+(x) \tag{1}$$

wherein the weak current $J_\mu(x)$ couples to itself. Weak decays of which the
prototype is neutron β-decay [4]

$$n \rightarrow p + e^- + \bar{\nu}_e$$
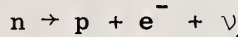
arise as first order terms in the perturbation represented by $L(x)$.

The weak current $J_\mu(x)$ is charged $(Q = \pm 1)$ since it couples states differing
in electric charge by exactly one unit. In the same sense the electromagnetic
current $J_\mu^{EM}(x)$ is a neutral current $(Q = 0)$. Allowing for finer details of
scale associated with the mixing of the down and strange quarks in the hadronic
current, as parameterized by the Cabibbo angle θ_c , a single weak coupling
constant $G \simeq 10^{-5} m_p^{-2}$ is sufficient for the description of all weak processes.

We know now of course that the result (1) is only approximate and the weak
interaction is mediated by exchange of massive vector bosons $W^\pm$ [5] . Weak
processes are therefore second order processes governed by the weak coupling
constant g [6] where

$$\frac{G}{\sqrt{2}} = g^2/8m_w^2$$

Electroweak unification is expressed through the relation (θ_w = Weinberg angle)

$$g = e \sin\theta_w$$

and the apparent weakness of the weak interaction is a consequence of the high

mass of the vector bosons, i.e. $m_W >> m_p$. We also know that there exist weak neutral currents which couple to the massive neutral vector boson Z^0,[7] but, since neither non-locality nor neutral currents play any role in neutron β-decay, we shall continue to work with (1).

§2 Neutron β-decay

The weak current can be divided into a hadronic part $J_\mu^h(x)$ and a leptonic part $J_\mu^\ell(x)$ and we know from study of nuclear β-decay, and from muon decay, that the leptonic current has the form

$$J_\mu^\ell(x) = \bar\psi_\ell(x) \gamma_\mu (1 + \gamma_5)\psi_{\nu_\ell}(x) \tag{2}$$

which is an equal mixture of vector (Fermi) $\bar\psi_e \gamma_\mu \psi_\nu$ and axial vector (Gamow-Teller) $\bar\psi_e \gamma_\mu \gamma_5 \psi_\nu$ currents. The matrix element for neutron β-decay is

$$\langle e^- \tilde\nu_e | J_\mu^\ell(o) | o \rangle = \langle \bar u_e | \gamma_\mu (1 + \gamma_5) | u_{\nu_e} \rangle \tag{3}$$

Since we have no field theoretic description of strongly interacting nucleons we cannot represent the hadronic current in the simple form (2) although it is useful to consider the symmetry properties of the 'bare' nucleonic vector $\bar\psi_p \gamma_\mu \psi_n$ and axial vector $\bar\psi_p \gamma_\mu \gamma_5 \psi_n$ currents. To stress the connection with isospin it is also convenient to represent the nucleonic currents in the form $\bar\psi \gamma_\mu \tau^+ \psi$ and $\bar\psi \gamma_\mu \gamma_5 \tau^+ \psi$ where τ_i are the usual isospin operators and ψ represents the nucleon field.

What we can do is write down the most general form of the matrix elements of the true vector $V_\mu(x)$ and axial vector $A_\mu(x)$ hadronic currents, consistent with Lorentz invariance, and we find for neutron β-decay in particular[8]

$$\langle p | V_\mu | n \rangle = \langle \bar u_p | g_V \gamma_\mu - (g_m - g_V)\frac{\sigma_{\mu\nu}q_\nu}{2m} - ig_s \frac{q_\mu}{2m} | u_n \rangle$$

$$\langle p | A_\mu | n \rangle = \langle \bar u_p | g_A \gamma_\mu \gamma_5 - \frac{g_{II}}{2m}\sigma_{\mu\nu}q_\nu\gamma_5 - ig_p \frac{q_\mu}{2m}\gamma_5 | u_n \rangle \tag{4}$$

where $m = \frac{1}{2}(m_n + m_p)$ and the invariant form factors $g_i(q)$ describe vector (g_V), axial vector (g_A) and induced weak magnetism (g_m), tensor (g_{II}) scalar (g_s) and pseudo-scalar g_p respectively.

Since for neutron decay $|q/m| << 1$, the most significant contribution comes from the vector and axial vector form factors associated with the 'bare' nucleonic currents. Concerning these quantities the most significant information is derived from measuring the differential probability that a polarized neutron should decay with emission of leptons into specified momentum states[9]

$$d^3W(\underline{p}_e, \underline{p}_\nu \underline{J}) = dW(\underline{p}_e)d\Omega_e d\Omega_\nu \{1 + a\, \underline{p}_e \cdot \underline{p}_\nu / E_e E_\nu + \langle \underline{J}/J \rangle \cdot (A\, \underline{p}_e / E_e + B\, \underline{p}_\nu / E_\nu +$$

$$D\, \underline{p}_e \times \underline{p}_\nu / E_e E_\nu)\}$$

where, to lowest order in momentum transfer q,

$$\begin{aligned}
a &= (1 - |\lambda|^2)/(1 + 3|\lambda|) \\
A &= -2(|\lambda|^2 + |\lambda|\cos\phi)/(1 + 3|\lambda|^2) \\
B &= -2(|\lambda|^2 - |\lambda|\cos\phi)/(1 + 3|\lambda|^2) \\
D &= 2(|\lambda|)\sin\phi/(1 + 3|\lambda|^2)
\end{aligned} \tag{6}$$

$V_\mu(x)$ is conserved because $J_\mu^{EM}(x)$ is conserved. Further, we may invoke the Wigner-Eckart theorem to deduce that the matrix elements of the two currents are the same to within a factor given by the relevant Clebsch-Gordon coefficient. We find then that

$$g_s = o \qquad g_m(o) - g_V(o) = g_V(o)(\mu_p - \mu_n) \qquad (11)$$

§5 First and second class currents

The CVC hypothesis predicts a simple relationship between the weak vector form-factors and their electromagnetic analogues. In particular it says that $g_s = 0$ which raises the question why there is no induced scalar in the electromagnetic matrix element. The reason is that C-invariance of the strong interactions rules out the corresponding current $\partial_\mu(\bar\psi\psi)$ which has opposite transformation properties to the bare current $\bar\psi\gamma_\mu\psi^\mu$. A similar analysis may be applied to the induced weak form factors with this minor change that, since the weak current is charged, an additional $n \rightleftharpoons p$ interchange is required. The relevant symmetry is the G parity, where $G = Ce^{-i\pi I_2}$ and I_2 generates a rotation about the 2-axis in isospin space. It turns out that, under the G-parity transformation the bare currents $V_\mu^b \rightarrow V_\mu^b$, $A_\mu^b \rightarrow -A_\mu^b$ and these currents are termed first class; currents with the opposite transformation rule are termed second class [12]. Second class currents are ruled out on the grounds that G parity is conserved in the strong interaction, and we find that

$$g_s = g_{II} = 0 \qquad (12)$$

There are two important addenda to the above argument (i) it fails if the 'bare' current contains second class contributions (ii) if the lepton and antilepton currents couple to hadronic currents which, like the 'bare' hadronic currents, are members of the same isospin multiplet, then $g_i = g_i^*$ for first class and $g_i = -g_i^*$ for second class form factors [13]. It follows that observation of T-violation in neutron β-decay would imply, either the presence of second class currents, or a breakdown of charge symmetry, or both.

§6 Induced weak magnetism and tensor interaction

CVC theory and strong-interaction G parity conservation predicts the values (11) and (12) for weak magnetism (induced pseudo-tensor) and induced tensor form factors respectively. To the question: 'is it possible to test these predictions?', the answer is that a complete separation of $(g_m - g_V)$ and g_{II} may be brought about by measuring the energy dependence of the correlation coefficients $a(E_e)$ and $A(E_e)$ whose zero-momentum transfer values are given in (6) [8]. However the relevant terms are only a few per cent of the leading terms in these correlations and no successful experiment has been reported.

§7 The Goldberger Treiman relation

The Goldberger-Treiman (G-T) relation provides a connection between the axial vector coefficient $g_A(o)$ in neutron decay, the pion decay constant $f_\pi(= 93.24 \pm 0.09 \text{MeV})$ and the pion-nucleon coupling constant $g_{\pi NN}(= 13.396 \pm 0.084)$

$$g_A(o) = f_\pi g_{\pi NN}/m \qquad (13)$$

The relation was originally obtained by dispersion techniques [14]

and
$$\lambda = |\lambda| e^{i\phi} = g_A(o)/g_V(o) \tag{7}$$

Integration of (5) over all momenta gives information on the absolute value of $|g_V|^2 + 3|g_A|^2$ in the form of the ft-value where $t\ell n2$ is the neutron lifetime and f is the Fermi phase space factor

$$ft = (2\pi^3 \ell n2/m_e^5)/G^2 g_V^2 \cos^2\theta_c (1 + 3|\lambda|^2) \tag{8}$$

Allowing for outer radiative corrections $f = 1.71408 \pm 0.00015$ [10] .

§3 Discrete symmetries of the weak interaction

Under the discrete symmetry transformations P , C and T we find that the matrix elements (3) and (4) transform according to the rules

P: $g_i \to g_i$, $\gamma_5 \to -\gamma_5$; C: $g_i \to g_i^*$, $\gamma_5 \to -\gamma_5$; T: $g_i \to g_i^*$, $\gamma_5 \to \gamma_5$

We conclude that, because of the mixing of vector and axial terms in the matrix elements, P and C symmetries are each violated in the weak interaction. The (unitary) symmetry CP and the (anti-unitary) symmetry T are violated if any of the g are complex. Thus a non-zero value for the triple correlation coefficient D in (6) would be evidence for time-reversal non-invariance provided final state interactions could be ignored.

§4 The conserved vector current (CVC) hypothesis

If the strong interactions could be switched off the 'bare' nucleonic electro-magnetic current would have the form

$$J_\mu^{b,EM}(x) = \overline{\psi}\gamma_\mu \tfrac{1}{2}(1 + \tau_3)\psi \tag{9}$$

which subdivides into an isoscalar term $\tfrac{1}{2}\overline{\psi}\gamma_\mu\psi$ and an isovector term $\tfrac{1}{2}\overline{\psi}\gamma_\mu\tau_3\psi$. Supplemented by additional terms describing strange particles in virtual states the isoscalar current would be conserved from baryon conservation. In the same way to get a conserved isovector current the 'bare' current would need to be supplemented by mesonic terms etc. On the other hand the matrix element of the true hadronic electromagnetic current between nucleon states is known i.e.

$$\langle N|J_\mu^{EM}|N\rangle = \langle\overline{u}|(\gamma_\mu - \mu_p/2m \; \sigma_{\mu\nu}q_\nu)(1 + \tau_3/2) - \mu_n/2m \; \sigma_{\mu\nu}q_\nu(1 - \tau_3/2)|u\rangle$$

where μ_p and μ_n are the anomalous magnetic moments of proton and neutron. The isovector contribution is

$$\langle N|J_{\mu,3}^{EM}|N\rangle = \langle\overline{u}|\gamma_\mu - (\mu_p - \mu_n)/2m \; \sigma_{\mu\nu}q_\nu|u\rangle \tag{10}$$

That this is indeed a conserved current $\partial_\mu J_{\mu,3}^{EM} = 0$ is shown by the fact that the coefficient of γ_μ in (10) is unity expressing the fact that the electric charge on the physical proton (neutron) is always unity (zero).

Experimentally $g_V \simeq 1$ in (4) which is evidence for the conservation of the vector current $V_\mu(x)$. However since the 'bare' electromagnetic and weak vector currents are evidently members of an isotriplet it has been proposed that this property remains true for $J_\mu^{EM}(x)$ and $V_\mu(x)$ with full allowance for the strong interactions. This is the CVC hypothesis [11] . It implies that, to the extent that isospin is a good symmetry of the strong interactions,

and subsequently re-derived in various forms of partially conserved axial current (PCAC) theory [15]. It is currently viewed as a consequence of an exact chiral invariance of the strong interactions [16].

The argument assumes that the conserved V- and A-currents associated with chiral invariance are those currents which participate in the weak interactions. Although the vacuum is supposed to be isospin invariant giving rise to the observed hadron isomultiplets, the non-existence of parity doubling indicates that the isoaxial symmetry is spontaneously broken and there exists a triplet of massless Goldstone bosons with the quantum numbers of the pion. The pions are not in fact massless and the axial current cannot be exactly conserved since $<0|\partial_\mu A_\mu|\pi> = f_\pi m_\pi^2 \neq 0$. However applying the conservation law $\partial_\mu A_\mu = 0$ in the limit $m_\pi \to 0$ to the axial matrix element (5) gives

$$2mg_A(0) = iq^2 g_p(0)/2m$$

Since $g_A(o) \neq 0$, $ig_p/2m$ must have a pole at $q^2 = 0$ arising from the Goldstone pion with residue $2f_\pi g_{\pi NN}$. This is just the G-T-relation given above. It's principal importance is that, using the value of $g_A(o)$ determined from neutron decay, it provides a measure of departures from exact chiral symmetry through the parameter [17]

$$\Delta = 1 - mg_A(o)/f_\pi g_{\pi NN}$$

One may use the G-T relation to show that, since $|q| \simeq m_e$ in neutron β-decay the effective induced pseudoscalar coupling coefficient $\simeq (2mm_e/m_\pi^2)g_A = 0.05 g_A$ Since pseudo-scalar coupling does not contribute to allowed β-decay, and enters only as a second forbidden correction, its role in neutron β-decay is negligible.

§8 The Cabibbo hypothesis

Because $J_\mu^h(x)$ cannot be explicitly written in terms of physical hadron fields the procedure has been adopted to specify the selection rules of $J_\mu^h(x)$ with respect to quantities conserved in strong interactions. Thus to describe neutron decay $J_\mu^h(x)$ must have a piece with $Q = 1$, $I = 1$ and hypercharge $Y = 0$. Similarly to describe Λ_0 β-decay there must be a piece with $Q = 1$, $I = \frac{1}{2}$ and $Y = 1$. The Cabibbo hypothesis [18], recognizing that flavour SU(3) is an approximate symmetry of the strong interactions, postulates that V_μ and A_μ are members of SU(3) octets. Adopting the view that the u-, d-, and s-quarks are the elementary hadrons, the weak hadron current is taken to have the form

$$J_\mu^h(x) = \bar{u}(x)\gamma_\mu(1 + \gamma_5)[d(x)\cos\theta_c + s(x)\sin\theta_c]$$

Other quark currents exist of course but these play no role in neutron decay.

The Cabibbo scheme is essentially an extension of CVC theory which relates neutron decay to the other weak decays in the $\frac{1}{2}$ + baryon octet, through the SU(3) equivalent of the Wigner-Eckart theorem. There is a complication in that, in place of the single SU(2) reduced matrix element for each piece of the current, there are two reduced matrix elements in SU(3). Thus, omitting second class currents and induced pseudo-scalar terms we can write the matrix elements between initial and final baryon states as

$$<B_f|J_\mu^h|B_i> = <\bar{u}_f|f_1^{F,D}\gamma_\mu - \frac{f_2^{F,D}}{2m}\sigma_{\mu\nu}q_\nu + g_1^{F,D}\gamma_\mu\gamma_5|u_i>$$

The specific SU(3) predictions for the vector $(f_1^{F,D})$, weak magnetism $(f_2^{F,D})$ and axial $(g_1^{F,D})$ form factors for all seven weak decays in the lowest baryon octet are available in the literature [19]. In respect of neutron β-decay the Cabibbo theory predicts a value for θ_c in good agreement with experiments. However the predicted value of $g_A(o) \simeq 1.18$ is substantially lower than the measured values [20].

§9 The Neutron lifetime

From the point of view of weak interaction physics the prime purpose in undertaking a measurement of the neutron lifetime is to determine $\lambda = g_A(o)/g_V(o)$ from (8) in combination with a value for $G\cos\theta_c$ derived from decay rates of $o^+ \to o^+$ superallowed Fermi decays in mirror nuclei. The validity of the theory may be checked by comparing this value of λ with that determined from (5)-(6), also derived from neutron decay, or with the value $\lambda = F+D$ predicted by Cabibbo theory where F and D are the SU(3) reduced axial matrix elements.

Finally one must emphasize the unique importance of the neutron lifetime in astrophysics where it directly affects the rate at which helium is produced in the early universe [21] and the rate at which it is synthesized from hydrogen in the sun. The latter rate is proportional to $\left| g_A(o) \right|^2$ and has direct relevance to the solar neutrino problem [22].

References

1. Pauli, W., 1930 Collected Scientific Papers Vol. II, p. 1316 (Wiley:N.Y.)
2. Fermi, E., 1934 Z. Phys. <u>88</u> 161.
3. Wu, C.S., Ambler, E., Hayward, R.W., Hoppes, D.D. and Hudson, R., 1957 Phys. Rev. <u>105</u>, 1413.
4. Byrne, J., 1982 Rep. Prog. Phys. <u>45</u>, 115.
5. Arnison et al, 1983 Phys. Lett. <u>B122</u>, 103.
6. Weinberg, S., 1967 Phys. Rev. Lett. <u>19</u>, 1264.
7. Arnison et al, 1983 Phys. Lett. <u>B126</u>, 398.
8. Holstein, B.R., 1974 Rev. Mod. Phys. <u>46</u>, 789.
9. Jackson, J.D., Treiman, S.B., and Wyld, H.W., 1957, Phys. Rev. <u>106</u>, 517.
10. Wilkinson, .D.H., 1981 Prog. Part. Nucl. Phys. <u>6</u>, 325.
11. Feynmann, R., and Gell-Mann, M., 1958 Phys. Rev. <u>109</u>, 193.
12. Weinberg, S., 1958, Phys. Rev. <u>112</u>, 1375.
13. Cabibbo, N., 1964 Phys. Lett. <u>12</u>, 137.
14. Goldberger, M.L. and Treiman, S.B. 1958 Phys. Rev. <u>110</u>, 1178, 1478.
15. Gell-Mann, M. and Levy, M., 1960 Nuovo Cim. <u>16</u>, 705.
16. Pagels, H., 1975 Phys. Rep. <u>16</u>, 219.
17. Dominquez, C.A., 1982 Phys. Rev. <u>D25</u>, 1937.
18. Cabibbo, N., 1963 Phys. Rev. Lett. <u>10</u>, 531.
19. Bender, I., Linke, V., Rothe, H.J. 1968 Z. Phys. <u>212</u>, 190.
20. Bourquin, M. et al, 1983 Z. Phys. C. <u>21</u>, 27.
21. Tayler, R.J., 1968 Nature <u>217</u>, 433; 1980 Rep. Prog. Phys. <u>43</u>, 253.
22. Bahcall, J.H., Huebner, W.F., Lubow, S.H., Parker, P.D. and Ulrich, R.K., 1982 Rev. Mod. Phys. <u>54</u>, 767.

REVIEW OF THE MEASUREMENTS OF THE NEUTRON LIFETIME

J.M. Robson
Physics Department, McGill University
Montreal, Canada, H3A 2T8

A brief review is given of experiments which have measured
the neutron lifetime. Some requirements which new experiments
must satisfy are discussed.

During the last forty years at least 12 experiments have attempted to measure
the lifetime of the free neutron. Ten of these produced published values
which are summarised in figure 1.
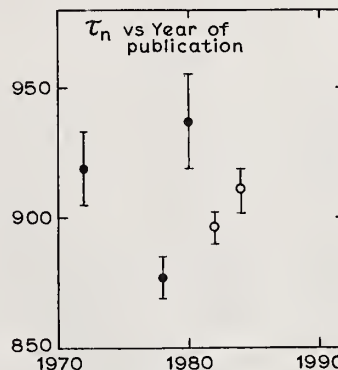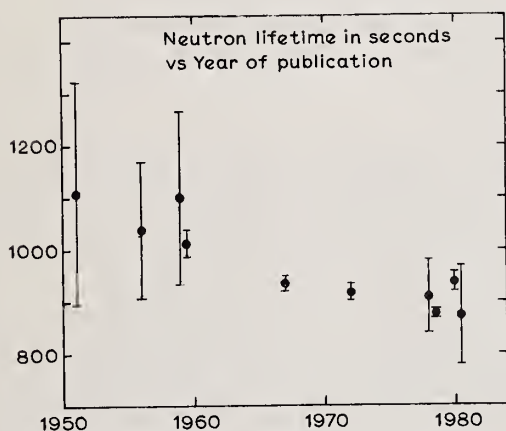
Fig. 1. Measured values of the lifetime
vs date of publication. The experiments
are referenced by number starting with
(1) at the left and going to (10) at the
right.

Fig. 2. The three recent beam
experiment values. The two values
with open circles are derived
values referenced as (11) and (12).

Measurements (7) and (10) used ultra-cold neutrons stored in a magnetic bottle
(7) and a metallic bottle (10) and will be discussed later. All the other
measurements involve the counting of either the electrons or the protons, or
both, resulting from the decays in a supposedly known volume of a neutron
beam. Two features of this series of experiments are apparent from figure 1:

first, the improvement in the claimed precision of the more recent experiments over the earlier ones and secondly the downward trend in the measured values with time. Both are to be expected with the second presumably indicating that the attempts of successive experimenters to improve their collection efficiencies were effective.

Figure 2 shows the three recent beam experiment values plotted on an enlarged scale. Also shown as open circles are the values derived from (a) a combination of polarization and angular correlation coefficients together with the ft values of $0^+ \to 0^+$ superallowed transitions in mirror nuclei (11) and (b) an analysis of the β decay of tritium (12). The three 'precision' experiments claimed individual precisions in the range between 1% and 2% and yet they cover a spread of 7%! This essentially means that we only know the neutron lifetime from direct measurements to a precision of about 3%. Why is this so?

Setting aside the bottle experiments for the moment, the beam experiments can be epitomised by three simple equations:

$$\left|\frac{dn}{dt}\right| = \frac{n}{\tau} \; ; \quad c = \Omega\eta \left|\frac{dn}{dt}\right| \; ; \quad n = \rho V$$

where ρ is the density of neutrons in the source volume V, Ω is the effective solid angle from points in the neutron beam volume to the detector and η is the efficiency of the detector for counting the decay products, either protons or electrons. In general Ω varies across the beam and the equations have to be expressed in integral form.

We can very briefly look at the three experimental arrangements from the point of view of the precision of the factors in the above equations. The Christensen experiment, number 6 in fig. 1, is shown in figure 3 and achieves a solid angle Ω approaching 4π; departures from this are due to inhomogeneity in the magnetic field leading to a small magnetic mirror effect which is dealt with in some detail and rather convincingly in their paper. V is measured to 1/2% by using a small Au^{198} source. The counting rate, c, seems to me to be the least reliable part of this experiment since the ratio of true counts to background was only about 0.5. A strength of this experiment was its repeatability with six separate runs being made.

The Bondarenko experiment, number 8 in fig. 1, was an update of an earlier experiment by Sosnovsky et al, number 4 in fig. 1 and shown in figure 4. The solid angle Ω is quite small and a quantity which essentially combined Ω, V and the neutron density distribution across the beam was estimated by a Monte Carlo simulation and quoted by the authors to 0.03%! They claim that their overall error is about 1%, a remarkable achievement for an experiment which uses such a small solid angle for collection of the decay protons.

The Byrne experiment, shown in figure 5, is a departure from the earlier experiments in that it stored the protons in an electromagnetic trap and subsequently dumped them rapidly into a detector for counting. This technique resulted in a solid angle of 4π and a very low background and thus overcame the drawbacks of the two earlier precision experiments. It had some problems, however, which will be referred to in the paper by Dr. Byrne; one of the most significant of these is that the effective neutron beam length was defined by
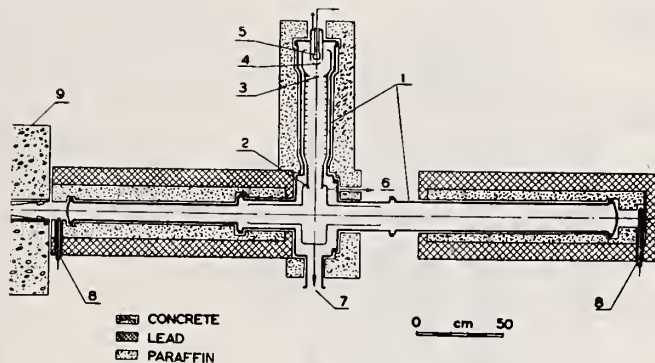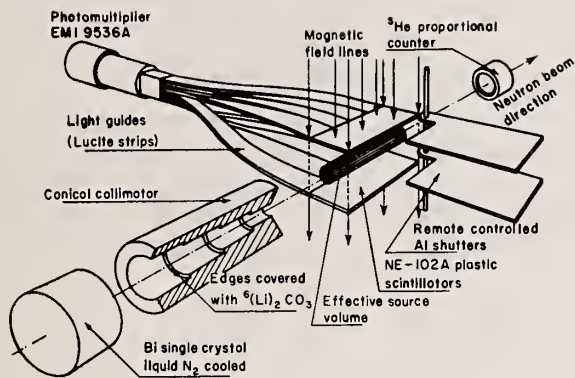
Fig. 3 The Christensen experiment - reference (6)

Fig. 4 The Sosnovsky experiment reference (4)

the magnetic field and had to be estimated by simulation experiments. A notable feature, however, was that the experiment was repeated several times using different magnetic fields, neutron beam diameters and proton collection apertures. The quoted error reflected the degree of consistency between these different tuns and may therefore be more realistic.

Thus all these more precise experiments involved some measurements for which the estimate of the precision was difficult. The Christensen experiment had a large background count, the Bondarenko experiment had a very small solid angle and the Byrne experiment involved an effective beam length defined by a magnetic field configuration. The fact that they disagree is a significant reason for the experiments which are discussed in the following papers.

What are the ideal characteristics of a beam experiment? First, the solid angle for collection of the decay products should be 4π or be measurable with some degree of confidence. Secondly the length of the beam must be either measurable or well defined geometrically. By 'measurable' I include experiments in which the beam length can be varied easily so that the end effects can be eliminated by subtraction between different runs. By well defined geometrically I include experiments in which the beam is in bursts. Thirdly the background must be very small, especially if an experiment is to use a coincidence technique to determine the absolute rate of decay in the neutron beam or neutron burst. Fourth, all corrections for counter windows, grids etc must be quite small. Finally, the system for measuring the neutron density must be demountable and capable of cross calibration with a well established standard. This is the subject of a talk this afternoon which will bring us up
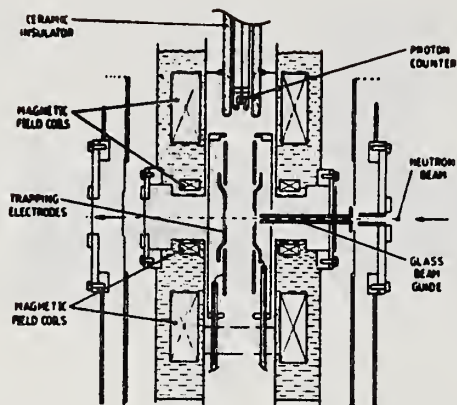
Fig. 5   The Byrne experiment
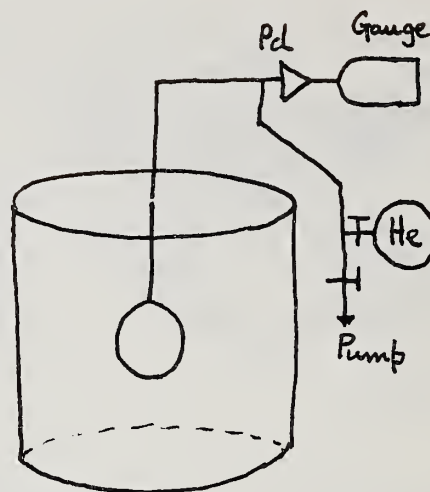
Fig. 6   A bottle inside a nuclear reactor.

to date on this ultimate limitation on the precision of beam type experiments. I expect that the beam experiments which are now planned or in progress will satisfy all these criteria.

Two bottle experiments are recorded in the literature and we may hear about others this afternoon. Ultra cold neutrons are stored in either a magnetic field trap or in a material bottle. At the moment their precision does not rival that claimed by beam type experiemnts but they have the considerable advantage of not requiring precise estimates of volumes, solid angles or neutron densities. On the other hand they have to provide convincing proof that the losses from the bottles, magnetic or material, are well understood and measured. In the long run, however, I expect they will be able to do this and will provide us with a very precise value for the neutron lifetime.

Finally I would like to mention an amusing experiment which I attempted in 1953 but which failed. The idea was to put a bottle inside a nuclear reactor and watch it fill up with hydrogen; see figure 6. A small pressure of helium was introduced in order to convert the recoil protons into hydrogen gas. The experiment failed because of the hydrogen driven out of the wall of the bottle by the intense fast neutron flux and because of the thermal neutron capture in He^3. Perhaps the experiment might now work using modern technology and helium depleted in He^3.

References

1. J.M. Robson, Phys. Rev. <u>83</u> (1951) 349
2. Spivak et al., Proc. Int. Conf. on Peaceful Uses of Atomic Energy. Geneva 1955. U.N. New York Vol. 2, 33
3. N. D'Angelo, Phys. Rev. <u>114</u> (1959) 285
4. Sosnovski et al., Nucl. Phys. <u>10</u> (1959) 395
5. Christensen et al., Phys. Lett. B <u>26</u> (1967) 11
6. Christensen et al., Phys. Rev. D <u>5</u> (1972) 1628
7. W. Paul and U. Trinks, La Techerche <u>9</u> (1978) 1008
8. Bondarenko et al., JETP Lett. <u>28</u> (1978) 303
9. Byrne et al., Phys. Lett. B <u>92</u> (1980) 274
10. Kostvintsev et al., JETP Lett. <u>31</u> (1980) 236
11. D.H. Wilkinson, Nucl. Phys. A <u>377</u> (1982) 474
12. J. Byrne, Nature <u>310</u> (1984) 212.

ABSOLUTE NEUTRON FLUX DETERMINATION-A PROBLEM FOR THE MEASUREMENT OF τ_n

D. M. Gilliam and G. P. Lamaze
National Bureau of Standards
Gaithersburg, Maryland 20899

An accurate measurement of the neutron lifetime requires an accurate determination of the number of neutrons in the counting volume. For measurements in the thermal region, this can be best determined by measuring the neutron flux with thin detectors whose efficiency is inversely proportional to the velocity of the neutron, i.e., $\sigma \propto 1/v$. Three different methods of flux monitoring are presented: (1) the activation foil method, (2) the fission chamber method, and (3) two techniques involving ^{10}B. For each method, experimental problems and expected accuracies are discussed. An intercomparison of the techniques is proposed as well as comparisons with other methods. These intercomparisons are expected to improve the quality of related calibration services offered by NBS.

INTRODUCTION

The neutron lifetime τ_n can be determined by either "bottle" methods or "beam" methods. In "bottle" experiments, ultra-cold neutrons are trapped in a fixed volume of space by total reflection or magnetic confinement. If loss mechanisms other than beta decay can be made sufficiently small, then the neutron lifetime may be determined from the measurement of just the exponential decay constant of the confined neutrons. In "beam" experiments, it is necessary to determine two things: (1) the decay rate within a fixed volume of space through which a beam of neutrons is passing, and (2) the average number of neutrons $\bar{N}$ within that volume during the beta decay counting period. The determination of $\bar{N}$ can be accomplished by several methods, all of which require an absolute determination of either the neutron flux or a closely related neutron density parameter.

Improved measurements of the neutron lifetime will require neutron density or flux determinations at accuracies of better than $\pm$ 0.5%. These accuracy requirements are near or slightly beyond the capabilities of well-established neutron dosimetry techniques routinely employed at NBS.

DEFINITIONS AND NOMENCLATURE

Flux and Density. For the sake of brevity, only the ideal case of the perfectly collimated, steady-state beam will be discussed. The differential (in velocity) neutron density $n(\vec{x},v)$ at a point $\vec{x}$ in space is defined by

$n(\vec{x},v)dvd^3x$ = the expected number of neutrons in the volume
element d^3x about the point $\vec{x}$, whose velocities
lie within dv about v, parallel to the beam axis;
$n(\vec{x},v)$ = 0 for v<0.

The (integral) neutron density $n(\vec{x})$ is given by

$$n(\vec{x}) = \int_{v=0}^{\infty} n(\vec{x},v)dv.$$

The differential (in velocity) neutron flux $\phi(\vec{x},v)$ is related to the differential neutron density by

$$\phi(\vec{x},v) = n(\vec{x},v)v;$$

and the (integral) neutron flux $\phi(\vec{x})$ is

$$\phi(\vec{x}) = \int_{v=0}^{\infty} \phi(\vec{x},v)dv,$$

usually given in units of neutrons/(cm²s). (The quantity $\phi(\vec{x})$, which is called the flux in this paper is also defined as the fluence rate or the flux density in publications of the ASTM and the International Commission on Radiation Units and Measurements.)

Lifetime. Let V, the counting volume, denote that fixed volume in space in which beta decays of the neutrons are counted. Then the quantities of direct experimental interest in a τ_n experiment are A, the beta decay rate (or Activity), and $\bar{N}$, the average number of neutrons within V. The lifetime τ_n is given by

$$\tau_n = \bar{N}/A.$$

(The neutron half-life is $t_{1/2} = \tau_n \ln 2$).

$\bar{N}$ is related to the neutron density by

$$\bar{N} = \int_V n(\vec{x})d^3x.$$

It will be assumed that variation in $n(\vec{x},v)$ along the beam axis (due to neutron decay, scatter off residual gas, etc.) is negligible over the length L of the counting volume V and over the distance from V to any flux or density monitors in the beam. Then, denoting the beam axis as x_3, we may write

$$n(\vec{x},v) = n(x_1,x_2,v),$$
$$n(\vec{x}) = n(x_1,x_2), \text{ and}$$
$$\bar{N} = L \int_S n(x_1,x_2)d^2x,$$

where S is a cross sectional area known to contain all the beam.

Cross Sections and Reaction Rates. If L is known, then $\bar{N}$ can be determined by observing the reaction rate of a thin detector or activation foil in the beam. At a point $\vec{x}$ in the beam, the expected reaction rate per unit area, $r(\vec{x})$, is given by

$$r(\vec{x}) = \rho(\vec{x}) \int_{v=0}^{\infty} \sigma(v) \phi(\vec{x},v)dv$$

where $\rho(\vec{x})$ is the number of target atoms per unit area. The observed reaction rate integrated over the cross sectional area of the beam is

37

$$R = \int_S r(\vec{x})d^2x = \int_S \rho(\vec{x})\left\{ \int_{v=0}^{\infty} \sigma(v)n(\vec{x},v)v\ dv\right\}\ d^2x.$$

It is further assumed that $n(\vec{x},v)$ is a separable function,

$$n(\vec{x},v) = n(\vec{x})p(v),\ \text{with}\ \int_{v=0}^{\infty} p(v)dv = 1;$$

i.e. there are no differences in the velocity profile $p(v)$ from center to edge of the beam. (This assumption is not necessary if $\sigma(v)$ obeys the $1/v$ form exactly.) Then,

$$R = \int_S \rho(\vec{x})n(\vec{x})d^2x \int_{v=0}^{\infty} \sigma(v)p(v)v\ dv.$$

We can now get an expression for $\bar{N}$ in terms of R

$$\bar{N} = \frac{RL}{\displaystyle\int_S \rho(\vec{x})\ \frac{n(\vec{x})}{\bar{n}}\ d^2x \int_{v=0}^{\infty} \sigma(v)p(v)v\ dv}\ ,\ \text{where}\quad \bar{n} = \int_S n(\vec{x})d^2x.$$

The quantity $n(\vec{x})/\bar{n}$ is the relative neutron density distribution over the cross section of the beam. Since the integral over S must include all the beam, $n(\vec{x})/\bar{n}$ would need to be known to the extreme edges of the beam and would be difficult to determine experimentally with sufficient accuracy. Thus it is important that $\rho(\vec{x})$ be as uniform as possible. If $\rho(\vec{x})$ is exactly constant, i.e., $\rho(\vec{x}) = \bar{\rho}$ over all of S, then the integral over S reduces to just $\bar{\rho}$. The deviations of $\rho(\vec{x})$ from uniformity are major considerations in corrections and error assessments. The integral over v also simplifies drastically if the detector cross section $\sigma(v)$ conforms to the $1/v$ shape exactly. If

$$\sigma(v) = \sigma_o\ \frac{v_o}{v},\ \text{then}\quad \int_{v=0}^{\infty} \sigma(v)p(v)vdv = v_o\sigma_o.$$

Again, one may note that deviations from the $1/v$ form are major considerations in corrections and error assessments.

In the ideal case, with both $\rho(\vec{x}) = \bar{\rho}$ and $\sigma(v) = \sigma_o\ \dfrac{v_o}{v}$, then one has

$$\bar{N} = RL/\bar{\rho}\sigma_o v_o\ .$$

The accuracy of the determination of $\bar{N}$ then rests on the accuracies in the determinations of R, $\bar{\rho}$, $\sigma_o v_o$, L, and the corrections to the approximations $\rho(\vec{x}) = \bar{\rho}$ and $\sigma(v) = \sigma_o\ \dfrac{v_o}{v}$.

The determination of L will not be discussed in this paper, but the other factors will be discussed for three cases: (1) the activation foil method, (2) the fission chamber method, and (3) techniques involving ^{10}B.

ACTIVATION MEASUREMENTS

Capture Cross Section Standards. There are two well established capture cross

section standards for foil activation measurements: ^{197}Au and ^{59}Co. Both gold and cobalt are mononuclidic and have well known thermal cross sections and resonance integrals. Table I gives values of cross sections, Westcott g-factors, and resonance integrals for several important standard reactions, including gold and cobalt.

The activation cross section for the ^{59}Co(n,γ)^{60}Co reaction to the ground state differs slightly (about 0.14%) from the total absorption cross section for ^{59}Co due to two weak beta decay branches of a short-lived isomeric state (half-life 10.5 min) which is formed in about 55% of the captures. For gold there is no difference in the absorption and activation cross sections for the 2.6956 day half-life activity. Although the gold cross section at 2200 m/s is somewhat better known than that of cobalt, the non-1/v corrections for gold are larger. Because of the lower cross section for cobalt and its longer half life (5.27 y), cobalt has a lower sensitivity than gold (for short irradiations and analysis periods) by a factor of about 1600. However, the gold sensitivity can be much higher than desired for high flux beams, and the cobalt provides a significantly more evenly-weighted time integration of the beam for runs that are of duration comparable to the gold half life or longer.

Activity Measurement. The present accuracy capability at NBS for measurement of either gold or cobalt activity ranges from about ± 0.3% for gamma counting to ± 0.1% for β-γ coincidence counting[1], for suitable foil diameter, thickness, and activity. The β-γ coincidence counting can be done for thin foils (compared to beta ranges) without dissolving the foil.

Foil Thickness and Uniformity. Foil thickness determination is generally not a major uncertainty factor, but limitations may be reached if very thin foils are used to reduce corrections for self-shielding, hardening of the beam, and scattering. Als-Nielsen[2] gives the scattering correction for 60 mg/cm^2 of gold as 0.4%; the same atomic thickness of cobalt would give approximately the same correction. Als-Nielsen reports a much larger correction for the neutron attenuation and hardening of the beam: 1% for 20 mg/cm^2 gold in a bismuth filtered cold neutron beam.

FISSION CHAMBER MEASUREMENTS

Fission Cross Section Standards. Axton has recently published a new evaluation of the thermal neutron constants for several fissile nuclides.[3] These are given in Table I with Westcott g-factor data and resonance integrals as indices of departure from the ideal 1/v cross section form. As can be seen in the table, knowledge of the velocity profile would be much more important for the non-1/v corrections for these detectors, than for gold or cobalt.

Absolute Fission Counting. For deposits of mass thickness less than 90 µg/cm^2, fission ionization chambers of the NBS design have an absolute efficiency for detection of fission events of greater than 0.99, as shown by Grundl et al.[4] The corrections for extrapolation to zero pulse height and for complete fragment absorption within the deposit thickness both decrease linearly as deposit thickness is reduced; the estimated accuracy of these corrections is about 25% of the value of the corrections. However, even for very thin deposits on backings with a mirror-like appearance, surface

39

roughness can cause complete fragment absorption losses of the order of 0.3%. Calculated correction factors for scattering from typical deposit backings of given thickness are:

0.127 mm	platinum	1.019
1.0 mm	quartz	1.055
0.127 mm	aluminum	1.001

The uncertainty in these corrections is of the order of 10% of the deviation from unity.

Deposit Thickness and Uniformity. The deposits in the NBS collection of Fissionable Isotope Mass Standards (FIMS) are certified for total deposit mass rather than mass thickness (mass/unit area). This distinction is not a trivial one, because of edge effects. The more gradual mass thickness variations over the deposit area are generally very small, because the deposits were given a double, planetary sort of rotation during the vapor deposition process. However, the edges of the deposits have a wedge-like thickness profile that affects about 5% of the total area for the smaller deposits (1.27 cm diameter).

The determination of the total deposit mass for the ^{235}U and ^{239}Pu reference deposits has been made primarily by comparison with destructively analyzed deposits, which were analyzed by isotope dilution mass spectrometry (IDMS). Mass assays were also determined by alpha counting. The mass uncertainty of the NBS reference deposits is ±0.5% for ^{235}U and ±0.4% for ^{239}Pu.

Although the uncertainty of the fission chamber measurements is larger than that of the activation measurements for thermal and cold neutron beams, the fission measurement method is available on a more routine and thoroughly established basis with a wide choice of deposit thicknesses and a few choices of diameters. The supply of activation foils currently on hand is somewhat more limited, but procurement of suitable foils should not be difficult.

^{10}B TECHNIQUES

Charged Particle Detection. Because ^{10}B is an ideal 1/v detector with a large thermal cross section (3838 ± 6 barns), it is an attractive reaction for use in this experiment. Byrne[5] has described a system consisting of a thin layer of boron deposited on a mica foil with the reaction particles detected by four silicon surface barrier detectors. A similar system is currently in use at the NBS reactor for depth profiling measurements[6], where a great deal of experience has been gathered in determining boron concentration profiles. If this method is used in the neutron lifetime measurement, the depth profiling setup could provide the measure of $\rho(\vec{x})$, a critical parameter. This method currently yields mass accuracies of ±0.5% and is expected to improve.

Prompt Gamma Detection. Another method of flux monitoring is the direct observation of the 478 keV gamma ray from the ^{10}B(n,$\alpha\gamma$)^{7}Li reaction. This technique has been used[7] at the NBS Linac in the measurement of the ^{10}B(n,$\alpha\gamma$) cross section in the keV region. Also, the prompt gamma facility[8] at the NBS reactor has been employed to determine the boron content of materials. Counting rates of the 478 keV line at that facility are 530 c/s mg for a flux

of 2×10^8 n/cm²s, which should be more than sufficient for this experiment. This technique could also be combined with prompt gamma measurements of $^{59}Co(n,\gamma)$ as a redundant check on the flux. Accuracies on the order of 0.5 to 1.0% should be attainable. The principal draw back to the prompt gamma method is the large amount of shielding needed for the Ge(Li) detector.

SUMMARY AND COMMENTS

Several methods of flux measurement techniques have been discussed for a proposed measure of the neutron lifetime. If time and funding permit, an intercomparison of some of the above techniques will be made. Comparisons with a novel neutron calorimeter[9] being constructed at LANL are also planned.

The high accuracy requirements of the neutron lifetime experiment are stimulating cross checking of existing NBS neutron flux calibration techniques. If the proposed calorimeter proves successful, this instrument could provide a new basis for NBS thermal neutron dosimetry, making possible much improved accuracy in the calibration services offered to the public.

Table I[†]

Target Nuclide	σ_o(2200 m/s) (barns)	g (20.44°C)	Resonance Int./σ_o
ideal 1/v		1.000	0.4499
^{6}Li	941±0.3%	0.9997	0.451
^{10}B	3838±0.15%	0.9997	0.449
^{197}Au	98.65 ± 0.09%	1.0051	15.84
^{59}Co	37.18 ± 0.16%	1.000	2.00
^{235}U	582.8±0.2%	0.9765±0.0012	0.483
^{239}Pu	747.3±0.3%	1.0552±0.0023	0.406

[†]Note: σ_o and g factors for ^{235}U and ^{239}Pu are from ref 3, other σ_o values from ref. 10, other g factors and resonance integrals from ref. 11.

REFERENCES

1. F.J. Schima, private communication.
2. J. Als-Nielson, NIM 50 (1967),pp. 191-196.
3. E.J. Axton, IAEA-TECDOC-335 (1984).
4. J.A. Grundl et al, Nuclear Technology 25 (1975), pp. 237-257.
5. J. Byrne, Inst. Phys. Conf. Ser. No. 42 (1978), pp. 28-37.
6. R.G. Downing et al, NIM 218 (1983), pp. 47-51
7. R.A. Schrack, G.P. Lamaze, and O.A. Wasson, Nucl. Sci. and Eng. 68 (1978), pp. 189-196.
8. D.L. Anderson et al, J. Radioanal. Chem. 63 (1981), pp. 97-119.
9. J. Wilkerson, "The Determination of the Neutron Lifetime Using e-p Coincidence," proceedings of this workshop.
10. J.R. Stehn, M. Divadeenam, and N.E. Holden, Nuclear Data for Science and Technology (1983), pp. 685-688.
11. B.A. Magurno, R.R. Kinsey, and F.M. Scheffel, Guidebook for the ENDF/B-V Nuclear Data Files, BNL-NCS-31451 (1982).

THE DETERMINATION OF THE NEUTRON LIFETIME USING e-p COINCIDENCE

John F. Wilkerson
Physics Division
Los Alamos National Laboratory
Los Alamos, New Mexico 87545

The neutron lifetime is a critical parameter both in electroweak theory and in astrophysical calculations. Unfortunately, present measurements of the free neutron lifetime, all of similar accuracy, disagree. The resulting value for the lifetime is one of the least accurately determined fundamental nuclear constants. We are currently constructing an experiment to measure the neutron lifetime to better than 1 percent accuracy. The measurement will employ a novel experimental technique, a calorimetric measurement of the neutron flux. We are also employing a sophisticated detector system which should yield good signal to background discrimination. A summary of the experiment design will be presented.

The neutron lifetime is one of the primary values used in determining the fundamental coupling constants of the weak interaction. Additionally, it is a key parameter in many astrophysical calculations, including helium abundance in the universe, the number of species of light stable neutrinos, and solar neutrino flux calculations. At present, the accepted value of the neutron lifetime is 898 ± 16 secs (1), derived from three separate experiments (2-4). The fact that these measurements have comparable accuracy but do not agree within expected statistical bounds is somewhat disturbing. Under the assumptions of the standard model it is also possible to obtain a value for the neutron lifetime from beta asymmetry measurements and electron-neutrino correlation experiments. At present these results are more accurate than the existing direct lifetime measurements. A collaboration between Los Alamos National Laboratory, Drexel University, the National Bureau of Standards, and the University of Washington (5) is currently preparing to measure the neutron lifetime directly using several new techniques. A systematically clean measurement to better than 1 percent accuracy should be possible.

Our experiment will observe the coincidences between electrons and protons emitted by in-flight neutron decays from a thermal neutron beam. The measurements will be made on a beam line at the National Bureau of Standards reactor in Gaithersburg, Maryland. The detector system will observe neutron decays in a ~3 cm diameter collimated beam over a 1-meter long region. By measuring the electron singles rate, the proton singles rate, and the electron-proton coincidence rates, the total neutron decay rate can be determined independently of absolute detector efficiencies. The nearly monoenergetic incident neutron beam will be obtained from a focusing pyrolytic graphite monochromator. The flux of neutrons passing through the detector will be precisely measured using the totally new concept of a calorimetric measurement of the thermal neutron flux. This idea, proposed by Robertson (6), should allow a determination of the neutron flux to an accuracy of 0.1% or better. Before discussing the details of the neutron

lifetime measurement, let's first examine this new technique of calorimetric flux determination.

One of the prime limitations of the accuracy of previous neutron lifetime measurements using thermal neutron beams has been the determination of the neutron flux. Of the many different techniques employed, the use of ^{3}He(n,p)^{3}H in proportional counters seems to be the most accurate. The cross section for this reaction has been determined to 0.2%, but using this technique for actual flux measurements results in about a 0.5% accuracy at best in the flux determination (7).

The use of a device which totally absorbs the incident neutron beam (i.e. a black absorber) by means of a precisely known exothermic reaction can allow a calorimetric measurement of incident neutron flux to at least 0.1%. The ideal material should have: 1) a relatively high energy release, 2) efficient absorption of the thermal neutrons, and 3) all secondary particles from the initial reaction stop in the detector material giving up their energy as well. The reaction

$$n + {}^6Li \rightarrow {}^3H + {}^4He + 4.7819(6) \text{ MeV}$$
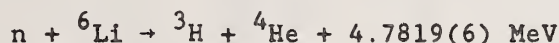
nearly meets these ideal requirements with a Q value known to 130 ppm, a large thermal neutron cross section of 940 barns, and 100% of the cross section in one branch (only the ground-state branch is energetically allowed). However, there are two additional reactions possible for neutrons incident on ^{6}Li:

$$n + {}^6Li \rightarrow {}^7Li + \gamma \quad (\sigma = 0.04 \text{ barns})$$

$$n + {}^6Li \rightarrow n + {}^6Li \quad (\sigma = 0.7 \text{ barns}).$$
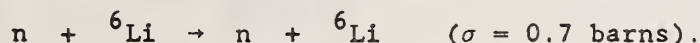
While the radiative capture process is negligible, the elastic scattering process contributes about 0.1% to the total cross section. A calculated correction supported by experiments will establish this small contribution accurately.

The energy deposited via the ^{6}Li(n,α) reaction is $7.6615 * 10^{-13}$ watts/neutron/sec. Typical monochromator scattered neutron fluxes used in reactor based experiments have intensities of 10^6-10^7 neutrons/cm^2/sec, with a corresponding thermal power of 10-100 μW. Measurement of a power this size to an accuracy of 0.1% or better is feasible at a "detector" temperature of about 10K. We note that charged-particle calorimeters based on the general principle outlined above have been constructed to measure beam powers in the 10 mW range to 0.1% accuracy (8).

A prototype double compensated calorimeter using an isotopically-enriched ^{6}Li foil detector has been constructed and is undergoing tests at Los Alamos (6). A schematic view (not to scale) of this calorimeter is shown in Fig. 1. The 5.7 cm diameter by 0.15 cm thick ^{6}Li foil is encapsuled in a 0.013 cm thick Al sheath. The capsule is sealed in an atmosphere of ^{4}He at a pressure of 50 Torr which is used as an exchange gas to insure good thermal contact. Two heaters, H1 and H2, and two silicon diode thermometers, T1c and T1s, are bonded to the capsule assembly. This assembly is suspended inside an

enclosure maintained at a temperature similar to the capsule in order to minimize radiation losses of the capsule. The capsule assembly is maintained at a temperature greater than that of a temperature-stabilized heat sink by supplying electrical power to the assembly's heater. The capsule is connected to the lower temperature heat sink through a thermal link, a material having a small but well defined thermal conductivity. The entire system is cooled using a commercially available closed-cycle He cryogenic refrigerator unit.
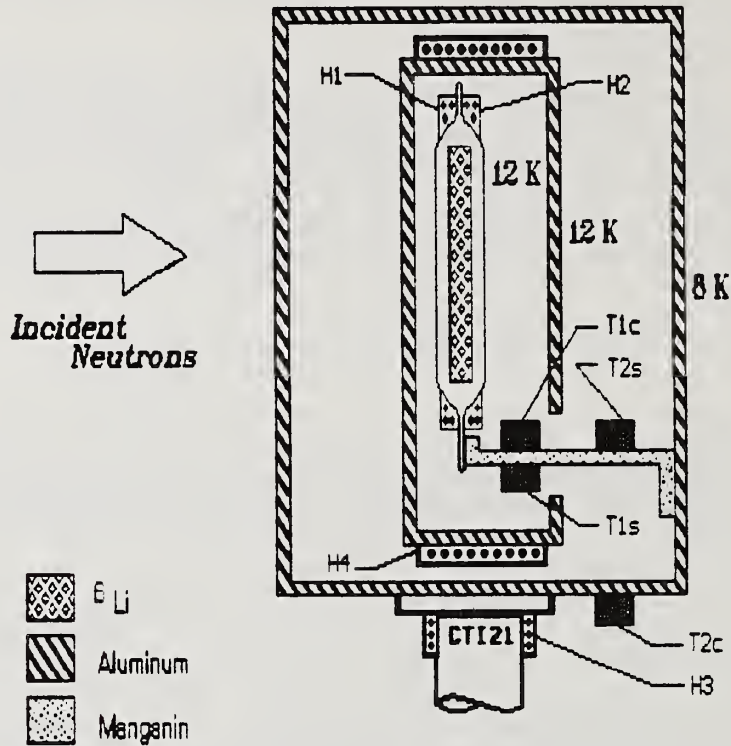
Figure 1. A schematic view of the Los Alamos double compensated calorimeter. (Not to scale)

The double compensation arises because the thermometer T2c attached to the heat sink is used in a closed loop feedback system to stabilize the temperature of the heat sink (and hence the capsule which is attached to the heat sink via the thermal link) by using the heater H3. Additionally, the thermometer T1c regulates, also in a closed loop system, the capsule temperature by using the heater H1 attached directly to the capsule. The thermal link resistance is chosen such that it requires approximately 80 μW of power in heater H1 to generate a temperature difference of 4K between the heat sink (at 8K) and the capsule (at 12K). This power is a little larger than the total neutron power anticipated. Clearly, a fixed amount of power into the capsule is necessary to maintain the fixed temperature desired by the T1c thermometer. Thus, when neutrons are incident on the [6]Li detector, the T1c feedback loop reduces the capsule heater H1's power (electrical heat) by an amount corresponding exactly to the power added by the incident neutrons (exothermic reaction heat) in order to maintain the fixed capsule temperature. Hence, measuring the reduction in the H1 heater power for

incident neutrons is a direct measurement of the neutron flux. This feedback
system can be tested and calibrated by using the second heater H2 attached to
the capsule. While running in feedback mode, a known amount of power can be
put into the heater H2. The amount of power in H1 should decrease by exactly
the amount added to H2.

A detailed and realistic equivalent circuit calculation including an analysis
of frequency response, systematic errors, and noise was performed to optimize
the stability and assist in the construction of the calorimeter (6). The
expected noise per unit bandwidth with the present system is expected to be
about 20 nW peak-to-peak. Thus, with 50 μW neutron power, the noise
fluctuation contributions should only be about 0.06% peak-to-peak in a .01 Hz
bandwidth. Another instability in the system arises from heat sink
temperature fluctuations. This instability is proportional to the
fluctuations divided by the temperature difference between the heat sink and
the capsule. Based on initial measurements, this instability should be at the
0.1% level or less. Figure 2 shows a measurement of the stability of the
calorimeter system. The voltage of the silicon-diode thermometer T2s attached
to the 8K heat sink is plotted as a function of time for a period of 16
hours. Note that a fluctuation of 0.1 mV in voltage corresponds to a
fluctuation of 2 mK in temperature. The results from our initial test lead us
to conclude that a calorimetric measurement of neutron flux is a very
feasible technique and should be a significant improvement over other
methods.
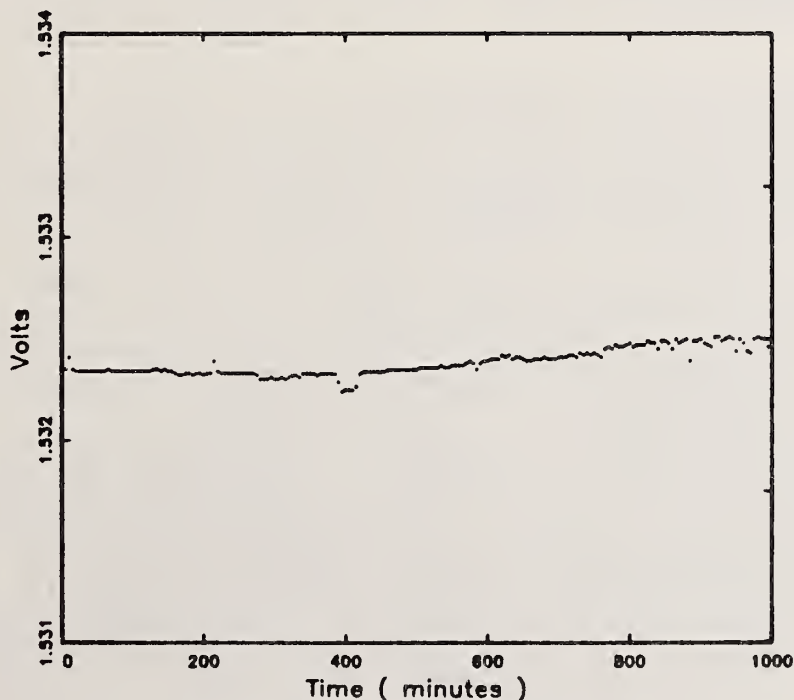
Figure 2. 8-Degree-K Heat-Sink Stability.

Returning to the neutron lifetime measurement itself, cross-sectional views
of the detector system are shown in Fig. 3. The main design goal for this
detector system was to attain the best possible counting rate while

eliminating as much background as possible. Furthermore, we wanted to make the detector system as similar as possible to the detector to be used in our time reversal invariance experiment(9). The detector consists of seven segments to detect electrons. Each 1 meter long segment is composed of 2 pairs of x and y position sensitive detectors and a plastic scintillator. This allows for multiple coincidence requirements for the electrons and also vertex reconstruction. Both of these features should significantly reduce background. The symmetry of the detector also allows automatic vetoing of
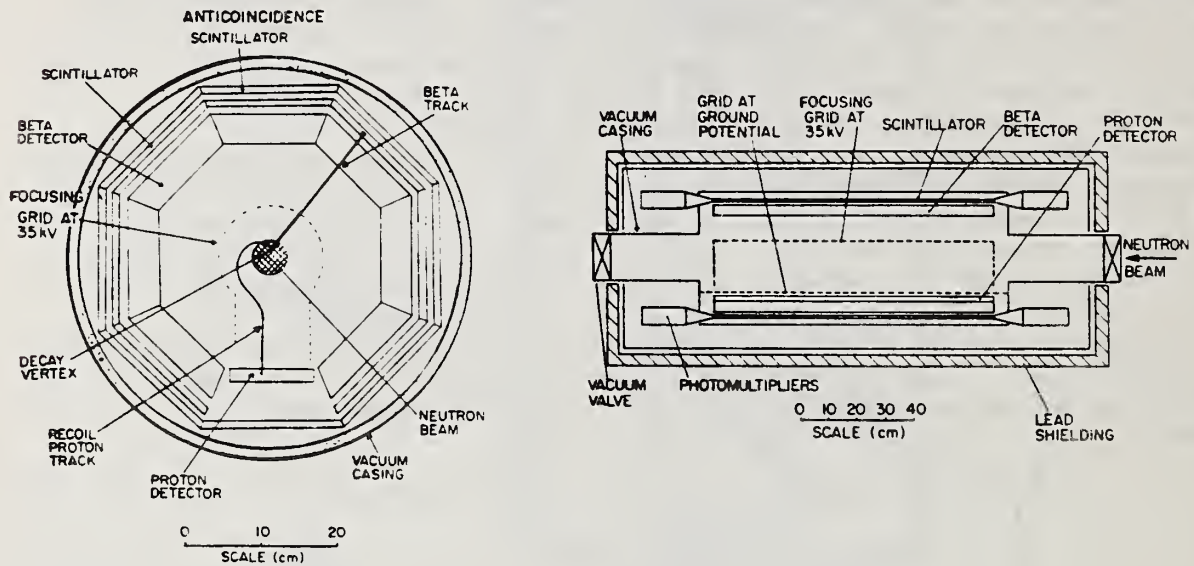
Figure 3. Cross-sectional views of the neutron lifetime detector system.

cosmic ray events in six out of the seven electron detector segments. The focusing grid is used to accelerate the protons to ~35 keV and focus them onto a single multistep avalanche detector. The entire detector system is enclosed in a vacuum chamber. The solid angle for the entire detector will be limited by the electron segments' solid angle and should be about 2π. A preliminary test at NBS using only a single wire counter and scintillator was extremely promising. The single wire chamber in coincidence with the scintillator yielded a room background rate of 5 Hz, compared to a room background rate of 95 Hz in the scintillator. Vertex reconstruction and employing 3 additional wire chambers in the coincidence requirement should reduce this another factor of 10. A neutron flux of 10^8 neutrons/sec should produce an event rate of 40 Hz in the detector. The beam-on background has yet to be measured, but we expect it can be reduced close to the level of room backgrounds.

As mentioned earlier, with our detector design the determination of the lifetime does not require any knowledge of the absolute detector efficiencies. This is the so called 4π beta-gamma coincidence technique. Let

N_e = Number of beta singles detected,

46

N_p = Number of proton singles detected,
N_c^p = Number of beta-proton coincidences detected,
N_t = Total number of neutron decays in the decay volume,
ϵ_e = Efficiency of the beta detectors,
ϵ_p = Efficiency of the proton detector, and
x^p = position in the detector along the neutron beam.

Since ϵ_e, and therefore N_e and N_c are functions of x , then

$$N_e(x) = \epsilon_e(x)N_t \qquad N_p = \epsilon_p N_t \qquad N_c(x) = \epsilon_e(x)\epsilon_p N_t .$$

This reduces to

$$N_t = N_e(x)N_p/N_c(x) .$$

Thus, the neutron decay rate is independent of the detector efficiency. Also note that N_t is also independent of x, because $N_e(x)$ and $N_c(x)$ have the identical x dependence.

To provide a nearly single velocity beam, a new monochromator spectrometer is now being constructed (10). This system is being built and assembled with the goal of reducing gamma ray backgrounds as much as possible. This includes using ^{6}Li shielding to surround the monochromator. The neutron velocity distribution from the monochromator will be calibrated using a narrow slit beam chopper by time of flight methods. The use of a beam chopper will also allow us to accurately measure any higher order velocity harmonics emerging from the crystal monochromator.

In conclusion, we believe that a new measurement of the neutron lifetime is demanded based upon the discrepancies between previous measurements and the importance this constant plays in both electroweak and astrophysics theories. By employing a wholly new technique to determine the neutron flux, and by building a detector system to maximize the signal-to-background ratio an accuracy of 1% or better should be possible.

References

1. Review of Particle Properties, Rev. Mod. Phys. 56, Number 2, Part II, S122 (1984).
2. C.J. Christensen, A. Nielsen, A. Bahnsen, W.K. Brown, and B.M. Rustad, Phys. Rev. D5 1628 (1972).
3. L.N. Bondarenko, V.V. Kurguzov, Yu. A. Prokof'ev, E.V. Rogov, and P.E. Spivak, JETP Lett. 28 303 (1978).
4. J. Byrne, J. Morse, K.F. Smith, F. Shaikh, K. Green, and G.L. Greene, Phys. Lett. 92B 274 (1980).
5. Collaboration members are T.J. Bowles, G.L. Greene, D. Gilliam, B. Heckel, P.W. Koehler, G. Lamaze, P.W. Lisowski, R.G.H. Robertson, R.I. Steinberg, J.W. Sunier, and J.F. Wilkerson.
6. R.G.H. Robertson and P.W. Koehler, To be published.
7. J. Als-Nielsen and O. Dietrich, Phys. Rev. 133 B925 (1964).
8. N. Jarmie, R.E. Brown, R.A. Hardekopf, and R. Martinez, IEEE Tran. on Nucl. Sci. NS-30 1508 (1983).
9. T.J. Bowles, see contribution in these proceedings.
10. J.W. Lynn, private communication.

DETERMINATION OF THE NEUTRON LIFETIME BY COUNTING TRAPPED PROTONS

J. Byrne and P.G. Dawber
School of Mathematical and Physical Sciences
University of Sussex
Brighton, Sussex, BN1 9QH, U.K.

R.D. Scott
Scottish Universities Research and Reactor Centre
University of Glasgow
East Kilbride, Glasgow, G75 0QU, U.K.

J.M. Robson
Department of Physics
McGill University
Montreal, PQ, H3A 2T8, Canada

G.L. Greene
National Bureau of Standards
Gaithersberg, MD. 20899

We describe a proposed new experiment to determine the neutron lifetime by counting decay protons stored in an electromagnetic trap and discuss its novel features in the light of previous experience using the same technique.

§1 Weak decay of the neutron

The free neutron is a β-active nucleus which decays weakly

$$n \rightarrow p + e^- + \tilde{\nu}_e$$

with a lifetime at the level of 10^3 sec. The best estimate of the end point of the kinetic energy spectrum of electrons from neutron β-decay, as derived from the neutron-hydrogen atom mass difference is 782.333±0.017keV [1]. The corresponding maximum kinetic energy of the recoiling protons is 750.7eV .

§2 Measuring the neutron lifetime

If neutrons could be confined in a fixed volume of space either by material barriers or by magnetic fields, then the lifetime τ could be determined by recording the exponential decrease with time of the number of electrons or protons emitted from this source volume. This is the basis of two reported measurements of τ derived from counting ultra-cold neutrons trapped in a magnetic storage ring [2] or in an aluminium bottle of variable geometry [3]. Attractive as these methods sound, in practice they are beset with difficulties since it is virtually impossible to eliminate all loss mechanisms for neutrons

aside from β-decay. In practice, the most successful experiments have been based on the equation

$$dn(t)/dt = -n(t)/\tau$$

where dn(t)/dt is determined by counting decay particles emitted from a given volume of beam and n(t) is found from absolute measurements of neutron density in that volume. The present proposal is to carry out a new measurement of the lifetime by a 'beam' method method as outlined above.

In carrying out this kind of measurement we may identify four distinct problems which must be solved. (i) should electrons or protons be counted and what detectors should be used? (ii) how are the genuine decay events to be distinguished from the background? (iii) how is the neutron density to be determined and (iv) how is the source volume to be defined? In the very first measurement [4] of the neutron lifetime carried out by one of us (J.M.R.) both electrons and protons were counted in coincidence and in this method problems (i) and (ii) were solved simultaneously. The neutron density (iii) was determined by measuring the activity generated by neutron capture in assayed manganese foils. However determination of the neutron source volume (iv) remained a difficulty because the coincidence counting efficiency was a sensitive function of the position of the decaying neutron.

Two of us (J.B. and G.L.G.) have more recently [5] carried out a measurement using a technique, involving the trapping of decay protons as described below. The present proposal is to carry out a very much improved version of this experiment using essentially the same solution to the four problems enumerated above. These solutions are (i) Protons should be counted because, having energies $\leqslant$ 1keV they can easily be accelerated to energies $\simeq$35keV producing a line spectrum which can be counted with 100% efficiency above noise in a silicon surface barrier detector. (ii) The protons emitted in the decay are stored in an electromagnetic potential well for periods up to 200 msec prior to detection. Since electrons and γ-rays are not trapped the background due to these particles is suppressed in the ratio of counting time to trapping time, say $\simeq 10^{-4}$. (iii) The neutron density is determined by counting α-particles from the reaction $^{10}B(n , \alpha)^{7}Li$. (iv) The source volume is that entire volume of neutron beam which traverses the electromagnetic trap.

In the earlier experiments solutions (i) and (ii) worked essentially to perfection. The main problems arose with solution (iv) and to a less marked extent with solution (iii). The operation of the device used to define the source colume and suppress the background in the earlier measurement is shown in Fig. 1. A beam of cold neutrons is projected normal to a 1.2-4.0 tesla magnetic field where electrons and protons from neutron decay move in tight spiral orbits about the field lines with radii $\leqslant$ 3mm . The neutron beam passes transverse to a hollow electrode at ground potential; above and below this central electrode two coaxial cylindrical electrodes are maintained at potentials of about $\simeq$ 1kV . This electrode configuration in combination with the axial magnetic field acts to trap the protons from neutron decay. At the end of the selected trapping period, the protons are released from the trap by a suitable 1kV pulse and accelerated up to a counter maintained at $\simeq$ -25kV .

This system has the following special features (a) the effective source volume is determined solely by the length of beam cut off by the magnetic field lines passing through the bounding edge of the detector aperture, (b) when the neutrons are stored for a period T_s (say 0.1 sec) and the spectrum is sampled for a period T_t following the application of the release pulse (say 10 μsec), the background is reduced in the ratio T_t/T_s. In practice a reduction in background of order 10^{-4} was achieved (cf Fig. 2).

Although the techniques described above worked extremely well the ultimate sensitivity was not reached because of several systematic effects of which the following were the most important (i) Because the neutrons were projected transverse to an inhomogeneous magnetic field it was impossible to assess the effective source volume to better than 2% consistency over a range of experimental conditions. (ii) The second problem was the unreliability of the neutron standards used to make an absolute determination of the neutron density. Because the α-peak observed from the $^{10}B(n,\alpha)^7Li$ reaction is completely resolved from the lithium recoil peak this is an ideal method for neutron counting provided (a) the ^{10}B content and cross-section is known (which it is: $\sigma = 3838\pm6$ barn [6]) and (b) the solid angle for detection of α-particles is known. Experience has shown however that, although ^{10}B α-particle counting can hardly be improved on, the whole neutron counting assembly must be demountable and calibrated against (n,γ) standards which are known to $< 0.2\%$ [6].

§3 Proposed new experiment
The principle of operation of the new experiment will be exactly as in the original version but a number of major changes will be incorporated with the objective of eliminating the main sources of systematic error which were identified in the earlier work. The layout of the new system is sketched in Fig. 3. The neutrons are transported from left to right along an axis which coincides with the axis of the proton trap which itself is positioned at the centre of the superconducting magnet and aligned along the magnetic field at that location. On release the trapped protons exit at the left of the picture where they are accelerated and counted. The detector is necessarily placed outside the path of the incoming neutron beam and the protons are channelled to it by bending the magnetic field through a small (9°) angle away from the symmetry axis near the exit point. In general the physical separation of the proton counter from the neutron counter and from the trap pulse transmission line helps to reduce background from neutron scattering and electrical pickup. The proposed new apparatus has the following detailed features.

(1) The electromagnetic trap for the decay protons is established in a region of space where the magnetic field is uniform at 5 tesla to better than 1%. Within the trap the maximum cyclotron orbit radius of the trapped protons is 0.8 mm. At the exit end of trap the magnetic field slowly reduces to a value of about 4.75 tesla at the position of the detector. Since the magnetic field does not increase between trap and detector there are no 'magnetic mirror' effects to hinder the exit of protons from the trap or to generate background from magnetically trapped decay electrons.

50

(2) The neutron beam from the reactor enters the apparatus through a beryllium window, and is transported by a nickel coated glass guide right up to the trap entrance. After transmission through the trap the neutrons pass through a thin (<50μgm/cm^2) boron foil for α-particle counting as before and are dumped in a lithium beam stop. The principal aims in the design of the neutron beam handling system are (a) to eliminate all scattered neutrons from the apparatus and (b) to eliminate all windows between proton trap and neutron detector.

(3) The neutrons enter the trap parallel to the magnetic field and trapping electrode system rather than in the transverse direction as in the earlier version. Originally, the length of neutron beam from which protons were trapped was determined by the magnetic field strength and was independent of electric field strength. In the proposed arrangement the reverse is true. The net effect of this major modification is (a) to increase the length of the proton trap by an order of magnitude, and the neutron source volume in proportion and (b) to remove all end effects associated with the shape of the magnetic field and the finite size of the proton detector. However, the new configuration introduces end effects which depend on the shape of the potential well near the ends of the trap which in turn may be eliminated as described below.

(4) The trapping electrodes are constructed as a system of coaxial rings each about 0.9cm long and 2cm in diameter. The layout is illustrated schematically in Fig. 4. There are edge effects over a region $\simeq$3cm near the ends of the trap which can be varied in length from 0 to 20cm . The edge effects can be eliminated in their entirety by recording the counting rate differences for a range of traps of different overall length for which the edge effects are the same. This is a very important feature of the new proposal since it eliminates the necessity of carrying out a Monte Carlo type estimate of the edge correction. It's validity has been checked to 0.01% by exact computation of the potential distribution in the proposed electrode configuration.

(5) The protons exit from the trap in the backwards direction as shown in Fig. 3 and are counted in a silicon surface barrier detector maintained at a potential in the range -25kV to -50kV . The proton counter together with its preamplifier, amplifier, power and bias supplies is maintained at a high negative potential (<50kV) and is supplied via an isolating transformer. This is the same system as was employed in the earlier experiment with the proton analogue signal being fed down to ground through a stand-off capacitor.

(6) The proton trapping and detection system is constructed to UHV standards and the whole system is evacuated using vac-ion and sorption pumps. Chambers for servicing the neutron and proton detection systems are coupled to the main cryostat via large (6") gate valves. It is therefore possible (a) to replace the proton counter during operation without disturbing the UHV conditions within the cryostat and (b) to completely decouple the neutron counting system as a

single unit and calibrate it against standard beams and activation foils. This means it is not necessary to rely on 'guaranteed' boron content for neutron target foils or on Monte Carlo calculations of geometrical efficiency factors for α-particle collection.

§5 Statistical and systematic errors

In the original experiment each of five separate measurements was carried out to a statistical accuracy of 0.5% but the ultimate accuracy achieved was dominated by the observed 2% systematic error associated with the proton collection efficiency. This was almost certainly due to the combination of inhomogeneous magnetic field and excessive (4°) divergence in the beam of very cold (25A°) neutrons. In addition neutron counting contributed an error of about 0.5% .

In the new experiment the individual sources of error in neutron counting will be subsumed in a single calibration error which can be reduced to about 0.2% and, in place of the proton collection efficiency error there will be a single trap length error <0.2% . Finally, because of the >>10- fold increase in count rate available from the increased trap length in combination with a high density thermal beam, the statistical error will be reduced by at least a factor of 3 . It therefore seems reasonable to believe that an overall error <0.5% is achievable.

Since the accuracy attainable in this type of experiment is limited by the error on neutron capture cross-sections, in the very long-term one must aim to calibrate against absolute counting of monoenergetic neutrons $(\Delta\lambda/\lambda \approx 10^{-6})$ using a 'black' neutron detector. Assuming the technical problems can be solved in this respect an ultimate accuracy of order 0.1% seems to be within reach.

References
(1) Greenwood, R.C. and Chrien, R.E., 1980 Phys. Rev. C 21, 498.
(2) Kugler, K.J., Paul, W. and Trinks, U., 1978 Phys. Lett. 72B, 421.
(3) Kostvintsev, Yu Yu, Kushnir, Yu A., Morozov, V.I. and Terekhov, G.I., 1980 JETP Lett. 31, 236.
(4) Robson, J.M. 1951 Phys. Rev. 83, 349.
(5) Byrne, J., Morse, J., Smith, K.F., Shaikh, F., Green, K. and Greene, G.L., 1980, Phys. Lett. 92B, 274.
(6) Holden, N.E., 1981 Neutron Capture Cross Section Standards for BNL 325 4th Edition BNL-NCS-51388 UC-346.
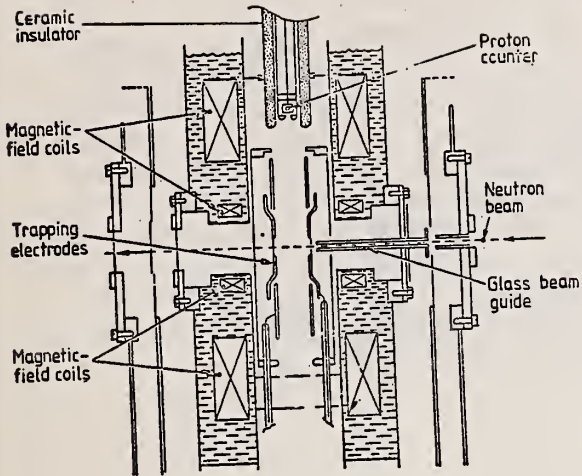
Fig.1 Old apparatus
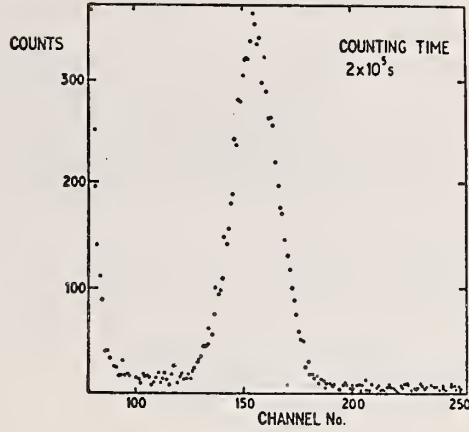
Fig.2 Proton spectrum
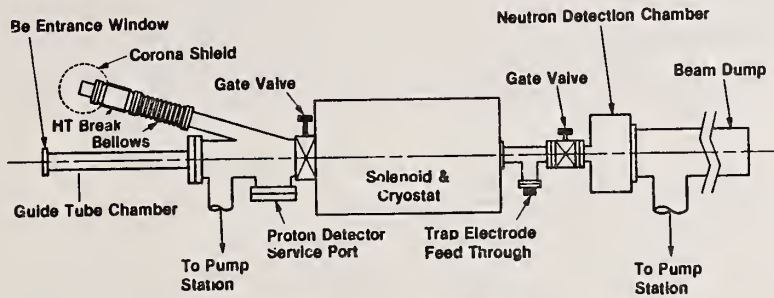
Outline of τ_n Vacuum System

Top View

Fig.3 Layout of proposed new apparatus
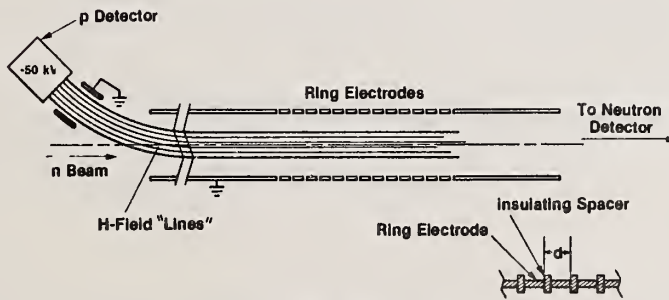
Detail of Trap Electrodes

Fig.4 Proton trap electrode system

IN-BEAM NEUTRON LIFETIME MEASUREMENTS AT THE INSTITUT LAUE-LANGEVIN

D. Dubbers
Institut Max von Laue-Paul Langevin
156X, 38042 Grenoble, France and
Physikalisches Institut der Universität
Philosophenweg 12, D-6900 Heidelberg, Germany

At the ILL there are at present two projects to measure the neutron lifetime "in beam", both using a rather long cold neutron beam volume. Different methods to obtain the neutron lifetime from such measurements are discussed.

1. Introduction

There are two main methods to measure the lifetime of free neutrons:
i) store neutrons in some kind of neutron bottle and measure the exponential decrease of their number as a function of storage time; the advantage of this method is that the absolute number of neutrons stored need not be known; the main problem is the control of the neutron leak rate from the bottle, which may be solved with the methods described in the contribution by W. Mampe.

ii) count the neutron decay products near a beam of (preferentially cold) neutrons; here the main problem is background control (only one out of typically 10^7 neutrons decay within the detector) and the absolute determination of the neutron flux; in this contribution I shall describe current in-beam experiments at the I.L.L., employing some new techniques which may help solve these problems.

2. Principles of in-beam neutron lifetime measurements

The classic method for in-beam neutron lifetime measurements employs a continuous white neutron beam, a detector for electrons and/or protons, and a thin neutron detector which absorbs only a small fraction of the neutrons in the beam. Assuming unity detector efficiencies and 4π detector solid angles, the ratio of number of counts of, say, the decay electrons and neutrons becomes:

$$\frac{N_\beta}{N_n} = \frac{1}{\tau_n} \frac{l_{eff}}{\sigma_o v_o \rho x} \; ; \tag{1}$$

where the effective length l_{eff} of the active neutron beam volume seen by the electron detector, the neutron capture cross-section σ_o at a given neutron velocity v_o, the atomic number density ρ and thickness x of the neutron detector, must all be known with sufficient accuracy to obtain the neutron lifetime τ_n. Eq. (1) does not depend on the neutron velocity spectrum, as the decay probability of a neutron with velocity v within the active beam volume, as well as the

reaction probability in the thin neutron detector, both scale with $1/v$. The validity of the $\sigma \propto 1/v$-law must be assured in order that (1) can be applied.

Some years ago an alternative in-beam method was proposed, by several people independently, which avoids some of the difficulties connected with (1). A rather long decay volume, a chopped neutron beam, and a thick neutron detector are used: while one short bunch of neutrons is well inside and traversing the long spectrometer volume, the gates of the decay electron counters are opened for a short time t_β. Thus the probability of detecting a neutron decay is independent of neutron velocity. The neutrons are then counted absolutely in a thick neutron detector in which all neutrons are stopped. The number of neutrons counted thus is independent of a neutron capture cross-section. Instead of (1) we then simply have:

$$\frac{N_\beta}{N_n} = \frac{t_\beta}{\tau_n} \,, \tag{2}$$

which is less sensitive to systematic errors than (1).

Absolute neutron counting with a thick neutron detector, however, cannot be done directly because neutron count rates would be too high. Instead, one can use one of the following methods:
i) activate a layer of material thick enough to stop all neutrons, and measure afterwards the γ-activity of the material during a time t_γ:

$$\frac{N_\gamma}{N_n} = \frac{t_\gamma}{\tau_\gamma} \,,$$

for $t_\gamma \ll \tau_\gamma$, or from (2):

$$\frac{N_\beta}{N_\gamma} = \frac{\tau_\gamma}{\tau_n} \frac{t_\beta}{t_\gamma} \,; \tag{3}$$

a good absorber is ^{59}Co: the activated ^{60}Co has a well known half-life of about five years and calibrated ^{60}Co sources are available for comparison;

ii) dilute the neutron beam by a known fraction ε, by putting several cadmium sheets into the beam, at different places along the neutron guide, each sheet being randomly perforated by a certain number of small holes; then count the neutrons directly with a fast scintillator, and use:

$$\frac{N_\beta}{N_n} = \frac{1}{\varepsilon} \frac{t_\beta}{\tau_n} \tag{4}$$

At present at I.L.L. there are two in-beam neutron decay instruments operating which have as a common feature a long decay volume and 4π-solid angle loss-free electron detection. There is a one meter long drift chamber run by K. Schreckenbach (I.L.L.), P. Liaud (Chambery), P. de Saintignon (I.S.N.

Grenoble), P. Grivot (I.S.N.) and A. Bussière (Annecy), which works in the chopped beam mode, with neutron detection according to eqs. (3) and (4), and eq. (5) below. The other instrument is the superconducting spectrometer PERKEO, at present run by M. Arnold, J. Döhner, J. Last (Heidelberg), S.J. Freedman (Argonne), and myself, which works both in the continuous beam mode, see eq. (1), and in the chopped beam mode, eq. (3), and also with polarized neutrons, see contribution by S.J. Freedman.

3. The neutron decay drift-chamber detector

This instrument is installed in the neutron guide hall of the I.L.L. (see fig. 1). The neutrons are monochromatized at 8 Å by Bragg reflection from
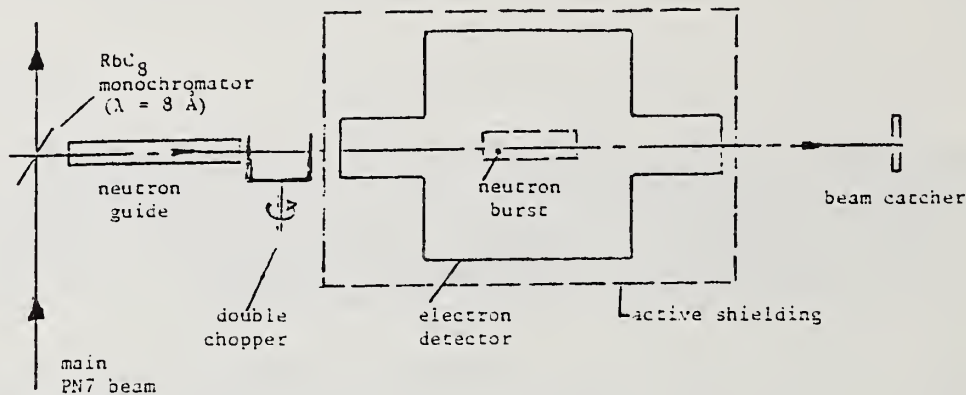
Fig. 1. Scheme of the neutron decay drift-chamber detector

a RbC_8 crystal. The neutrons pass along a $\sim$ 1 m long low background neutron guide and are then chopped by a rotating double chopper in form of a drum, 50 cm ϕ, which also eliminates higher order reflections from the Bragg crystal.

The 15 cm long neutron bunch then enters the 1 m long He-filled position sensitive drift chamber. Neutron decay electrons are registered as a function of time after the closing of the chopper; each neutron burst is completely confined within the detector for 1 msec.

Neutron scattering in the detector gas causes a background arising from radiative neutron capture in the detector material. It can be corrected for by using alternatively CH_4 and CD_4 as quenching gas, thus varying the scattering cross-section by a known amount. The detector is protected against cosmic rays by large plastic scintillators in anti-coincidence.

The neutrons are finally capture in a 3 mm cobalt beam stop. The beam is monitored by a GeLi-detector with calibrated efficiency, which measures the prompt capture gamma lines in ^{60}Co.

For the absolute calibration of the neutron beam a third method has been developed, in addition to the ^{60}Co activation method, eq. (3), and direct neutron counting in a diluted beam, eq. (4): by adding a known amount of ^{3}He gas to the drift chamber, one can also count neutrons in the same drift chamber that counts the electrons, via the ^{3}He$(n,p)^{3}$H reaction. The electron to proton count rate in the detector then is:

$$\frac{n_\beta}{n_p} = \frac{1}{\tau_n} \frac{1}{\sigma_o v_o \rho_{^3He}} \; . \qquad (5)$$

4. The superconducting neutron decay spectrometer PERKEO

PERKEO* is installed outside the far end of the long neutron guide hall of the I.L.L. The neutrons pass through a 1.70 m long multiple collimator made from ^{6}LiF, fly freely through the 2 m long spectrometer and, five meters further downstream, are intercepted by a ^{6}LiF beamstop.
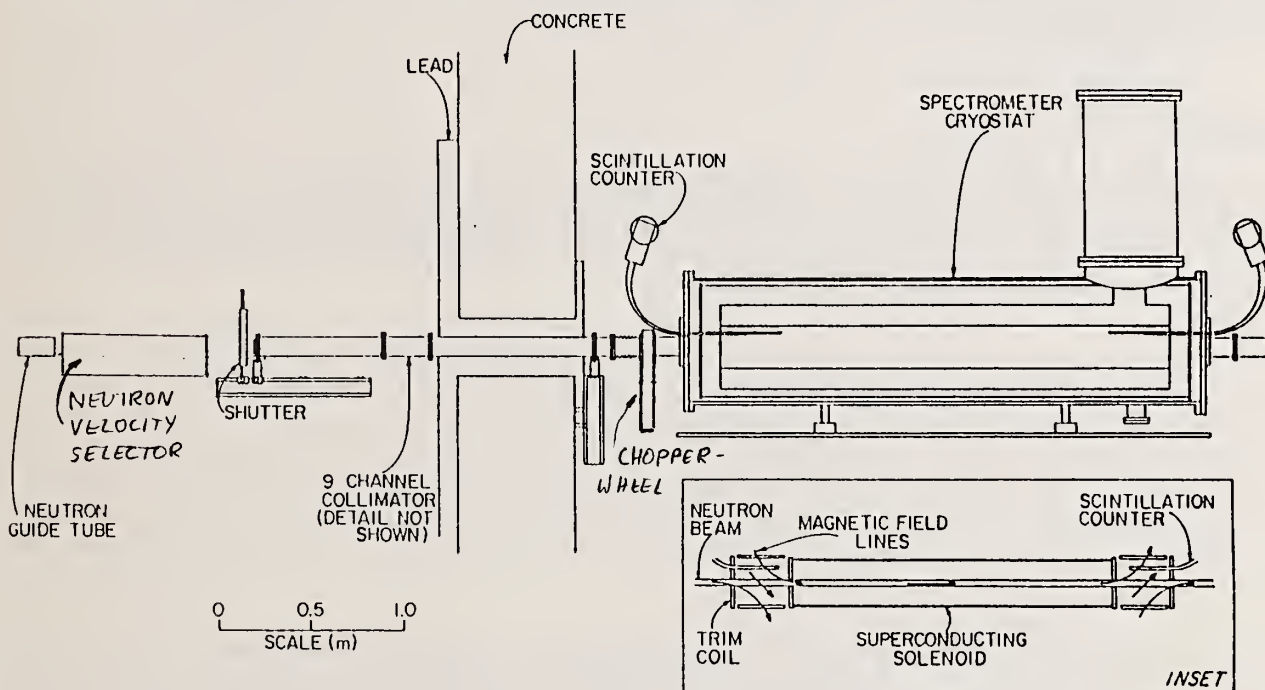
Fig. 2. Arrangement of the PERKEO spectrometer. The inset shows details of the inner region of the superconducting solenoid.

---

*Historical note: The name comes from the famous italian jester at Heidelberg castle, who consumed as much wine ("per que no ?") as the instrument, initially, consumed liquid helium; the big Heidelberg wine barrel had been built for him.

In PERKEO, the decay electrons are confined by a 1.5 Tesla magnetic field parallel to the beam axis, which, at both ends of the spectrometer, bends away from the beam and guides the electrons to plastic scintillators (see fig. 2). In this configuration losses due to electron backscattering at the detector can be completely eliminated. PERKEO produces very clean electron spectra all the way down to 20 keV electron energy. With a continuous beam of unpolarized neutrons the electron count rates are 600/sec, with a deducible background of 30/sec, of which 20/sec are cosmics.

At present we run both in the continuous and in the chopped beam mode. In the continuous mode we are essentially redoing the Christensen et al. measurements of τ_n, with l_{eff} in (1) defined to better than 10^{-3}, and with an excellent signal to background ratio.

In the chopped beam mode we use a 1 m long rotating helical slit neutron velocity selector for a rough monochromatization of the neutron beam, and a 50 Hertz ^{6}LiF chopper-wheel in front of the spectrometer. In this arrangement the count rate is reduced to a few counts per second. The electron spectra are registered as a function of time, after the closing of the chopper, in an event by event mode.

5. Outlook

Both instruments have delivered promising data in all the different data taking modes described above. At present more measurements with these instruments are underway, with continuously improving apparatus, and it will take more time before new results on τ_n will be published.

NEUTRON LIFETIME MEASUREMENTS
WITH BOTTLED NEUTRONS AT ILL

W. Mampe
Institut Laue-Langevin
156X, 38042 Grenoble, France

Two neutron lifetime experiments with storable neutrons are underway at the ILL, Grenoble: one version, prepared at the University of Bonn, will use the improved magnetic storage ring NESTOR on the new vertical guide. A second experiment is based on fluid walled material bottles of different surface to volume ratio.

The beta decay lifetime τ of the neutron is directly related to the axial and polar vector coupling constants g_A and g_V of the weak interaction: $\tau = const \cdot (1+3 \cdot (g_A/g_V)^2)^{-1}$. g_V is known from Fermi mirror transition measurements to a precision of $\sim 5 \cdot 10^{-4}$; g_A, however, derived from correlation coefficient measurements in the system of the decaying neutron has officially still an error of $> 6 \cdot 10^{-3}$. About an improved value of g_A/g_V obtained very recently with Perkeo at ILL we hear for the first time in contributions to this workshop by S. Freedman and D. Dubbers. To this unsatisfactory situation of the relatively poor knowledge of a fundamental constant of nature comes the fact that the directly measured absolute rate of the neutrons beta decay agrees only poorly with the value derived from g_A/g_V as known from angular correlation measurements [1,2].

Several experiments, discussed in more detail at this workshop are underway to improve the value of the neutron lifetime by a direct measurement and extract from it a better value of g_a. One family of experiments measures the decay products in a cold neutron beam, whereas another one tries to measure directly the relative number of remaining neutrons $N(t)/N(0) = e^{-t/\tau}$ as a function of storage time t in a trap. Two experiments of the second family are in preparation at the High Flux Reactor of the Institute Laue-Langevin in Grenoble, after each of them had demonstrated in a first generation version the validity of the method:

Due to their nuclear and magnetic interaction potential $U = \frac{2\pi\hbar^2}{m} \cdot a \cdot N \pm \mu \cdot B$ very low energy (ultra cold $\sim 10^{-7}$ eV) neutrons (mass m and magnetic moment μ) can be trapped in a material container (a = coherent scattering length and N = nuclear density) or in a strong enough closed magnetic field B.

Magnetic storage has been successfully demonstrated at ILL by a group from Bonn University and described in detail elsewhere [3]. Neutrons from the very cold and ultra cold neutron source PN5 at ILL with velocities between 10 and 20 ms^{-1} were injected through a curved guide into a superconducting sextupole field bent into a torus (NESTOR Fig. 1). One spin component remains on a closed orbit R_0 under the influence of the centrifugal force and the magnetic force $F = \mu(\delta B/\delta r) = - const$ (R_0+r). The parameters were $R_0 = 50$ cm, $r_0 = 5$ cm and B = 3.5 T. Neutrons could be detected up to 45 min but their number per filling was very low because of the modest acceptance of the ring.

An increase of the tolerable acceptance by a factor 10 was made possible recently since the resonance losses causing field instabilities in NESTOR could be eliminated.
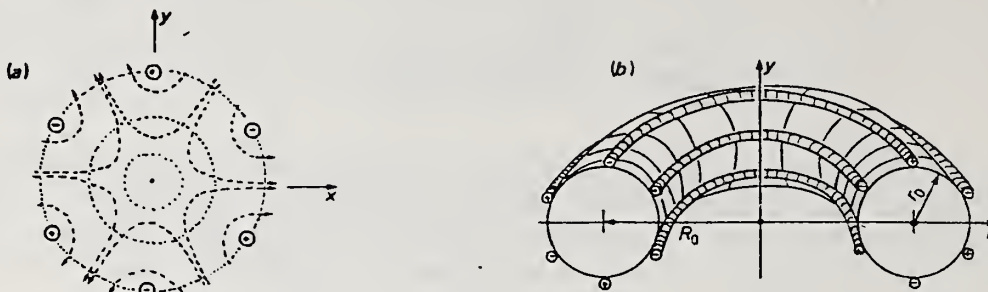

Figure 1. (a) Field lines and field induction B of a linear sextupole and
(b) a sextupole torus.

Secondly the storage ring will be installed at the direct beam section of the new vertical guide (TGV) viewing the cold source. The gain factor in flux compared to PN5 will be about 70. With these improvements an upper limit of the neutron lifetime on the 1 % error level should be obtainable.

A second version of magnetic storage of UCN (produced this time by down scattering of 10 Å neutrons in He-4, see contribution of R. Golub) is a super-conducting hexapole sphere. This very promising project of Bonn University is not followed on for the moment due to the lack of manpower.

A precise n lifetime measurement using storage of UCN in material bottles seemed problematic due to relatively high and unreproducible reflection loss rates. Only recently experiments in Russia [4] and at the ILL [5] could improve the situation by surface cleaning and cooling. A lifetime measurement on the basis of variable bottle surface to volume has been attempted shortly before the reactor shutdown at ILL [6]. The relative number of neutrons $N(t)/N_o$ in a bottle at storage time t is

$$N(t)/N_o = \exp(-(\theta_W + \theta_\beta)t)$$

where $\theta_\beta^{-1} = \tau_\beta$ (s) = beta decay lifetime and θ_W is the velocity dependent wall loss rate $\theta_W = \bar{\mu}(v) \cdot v/l$ ($\bar{\mu}(v)$ = loss rate per bounce averaged over all angles of incidence, l = mean free path). Using two different bottles with mean free path l_1 and l_2 we can for a given velocity v extract θ_β from the measured total loss rates $\theta_m(1,2)$:

$$\theta_\beta = (\theta_m(1) \cdot l_1 - \theta_m(2) \cdot l_2)/(l_2 - l_1) \tag{1}$$

$\bar{\mu}(v) \cdot v$ can only be eliminated in this way if both bottle surfaces have identical loss characteristics. To meet this condition we coated the glass bottle surfaces with a fluid, periodically renewable and being the same for both bottles. The fluid, Perfluoro polyether $PPE(F_3CCF_2OCF_2CF_5)_n$ [7], has a UCN cut off velocity of 4.36 ms^{-1}, low vapour pressure and low reflection losses ($<\bar{\mu}> = 26 \times 10^{-6}$). Both UCN bottles had identical height h = 30 cm in order to keep the energy variation due to gravity the same (max. height for UCN on PPE:h = 96.6 cm) and the lateral dimensions were 30 x 30 cm^2 and 15 x 15 cm^2.

The corresponding mean free paths are l_1 = 20 cm and l_2 = 12 cm. The detected UCN filling density on PN5 was 0.11 UCN cm^{-3} and the measured lifetimes in the interval t_1-t_2 = 320s-640s : $\tau(1)$ = 553 ± 4.5s and for the smaller bottle between 192s - 384s: $\tau(2)$ = 448 ± 9s. The storage time intervals t_1-t_2 are scaled for the bottles as $t_1(1)/t_1(2)$ = $t_2(1)/t_2(2)$ = $(t_1(1)-t_1(2))/(t_2(1)-t_2(2))$ = l_1/l_2 to be able to use (1) for a wider range of velocities. The final result of 6 days of data taking was τ_β = 850 ± 60s. The error is statistical. An error of 1-2 % might have been introduced by UCN not reaching the top of the bottle. The data are shown in fig. 2.

Monte Carlo and analytical calculations have been performed to study the influence of gravity for different velocities and the consequences of the assumption of specular or diffuse reflection on the ratio of the total reflection losses in both bottles.
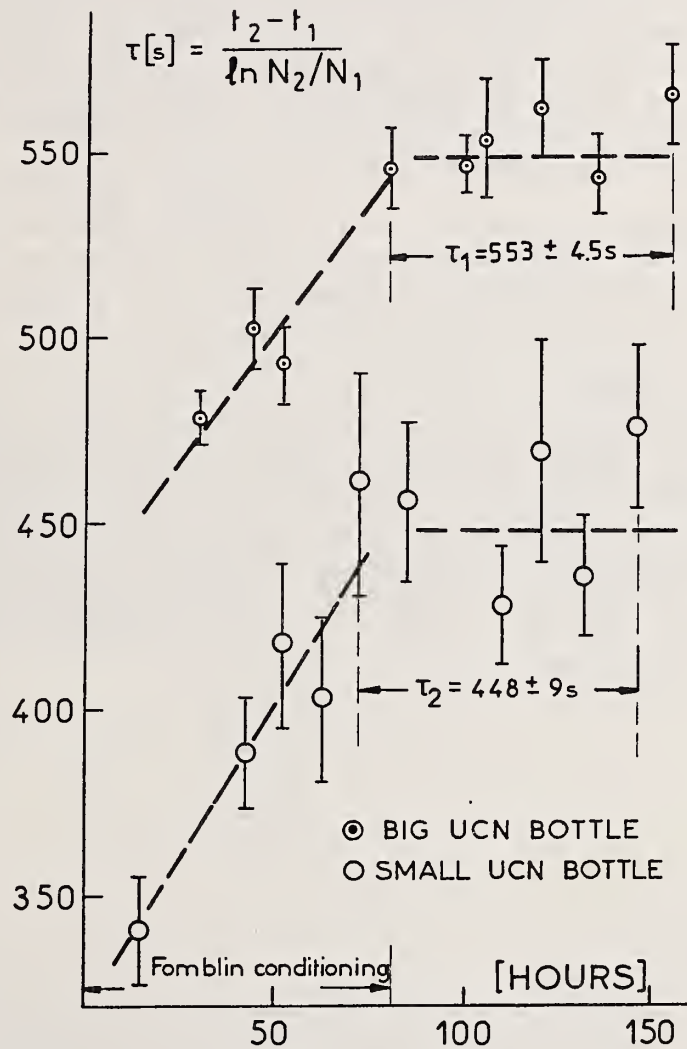
Figure 2. Measured lifetimes in the two bottles as a function of pumping time. The Fomblin outgased during the first 80 hours and did not change its characteristics afterwards.

Though the specular and diffuse reflection calculations gave considerable differences for the mean reflection loss rates in the individual bottles, the ratio of those losses - which enters into the determination of θ_β via (1) - did not change by much: In the case of diffuse reflection the correction is only by 1 % different from the simple model value $l_2/l_1 = 0.6$ obtained from gas kinetic theory.

This method seems promising as an independent approach towards a precise life-time measurement of the neutron. An improved version is in preparation on a stronger UCN source. This together with a longer running time will allow us to reduce the statistical uncertainty to a negligible value. One then can also afford to restrict the accepted velocity range which remarkably reduces the systematic error. By varying the ratio l_1/l_2 and the accepted velocity range we can check the independence of the obtained result from geometry and neutron velocity. Outgasing the PPE in advance will eliminate the in situ conditioning phase.

Neutron confinement, both in magnetic and material bottles, is hoped to produce in 1986 a more precise direct measurement of the absolute value of the neutrons beta decay lifetime.

References

[1] D.H. Wilkinson, Nucl. Phys. A377 (1982) 474.
[2] J. Byrne, Rep. Progr. Phys. 45 (1982) 115.
[3] K.J. Kügler, K. Moritz, W. Paul and U. Trinks, NIM 228 (1985) 240.
[4] Yu. Yu. Kosvintsev, V.I. Morozov and G.I. Tenekhov, JETP 36 (1982) 425.
[5] W. Mampe, P. Ageron and R. Gähler, Z. Phys. B45 (1981) 1.
    P. Ageron, W. Mampe and I.A. Kilvington, Z. Phys. B59 (1985) 261.
[6] P. Ageron, W. Mampe, J.C. Bates and M. Pendlebury, submitted to
    Phys. Lett.
[7] J.C. Bates, NIM 216 (1983) 535.

CORRELATION COEFFICIENTS IN POLARIZED NEUTRON DECAY - EXPERIMENTS WITH PERKEO*

S. J. Freedman
Physics Division, Argonne National Laboratory
Argonne, Illinois 60439

Measurements of the β-asymmetry in neutron β-decay combined with the results of studies of $0^+ \to 0^+$ superallowed nuclear β-decay is now the best way to determine the nucleon vector and axial vector coupling constants. High precision β-asymmetry experiments at the ILL using PERKEO have significantly reduced the error. Unlike the direct neutron lifetime measurements, which formerly claimed the smallest errors in g_A/g_V, the experiments that have measured the β-asymmetry are in good agreement.

The measurement of angular corrections in polarized neutron β-decay was pioneered in the late 50's and early 60's by Burgy, Krohn, Novey, Ringo and Telegdi[1] and by Clark and Robson.[2] In these experiments and those that have followed, no final state spins are observed. By detecting electrons and protons from polarized neutron decay these experiments measured A, the β-asymmetry parameter, B, the ν-asymmetry parameter, and D, a quantity that would indicate a time reversal non-invariant correlation between neutron spin and neutrino and electron momentum of the form $\vec{\sigma} \cdot \vec{p}_e \times \vec{p}_\nu$. Within the allowed approximation in the context of a V-A theory of the weak interaction, the correlation parameters are functions of only the vector and axial vector coupling constants, g_A and g_V. With the notation

$$g_A/g_V = \lambda \, e^{i\phi}, \quad \text{we have} \quad A \approx A_0 = \frac{-2\lambda(\lambda+\cos\phi)}{1+3\lambda^2},$$

$$B \approx B_0 = \frac{2\lambda(\lambda-\cos\phi)}{1+3\lambda^2}, \qquad D \approx D_0 = \frac{2\lambda \, \sin\phi}{1+3\lambda^2},$$

$$\text{and} \quad a \approx a_0 = \frac{1-\lambda^2}{1+3\lambda^2}.$$

Here a_0 is the allowed approximation for the β-ν correlation parameter, a, in unpolarized neutron decay. The neutron has structure and thus its β-decay properties depend on additional "induced" coupling constants. These additional form factors slightly modify the predictions of the allowed approximation. Neutron decay experiments are now nearly sensitive enough to detect deviations

from the allowed approximation but presently recoil effects, induced current effects and radiative effects are included as corrections in determinations of the allowed form factors. Eventually, neutron decay experiments will measure the induced form factors providing tests of the conserved vector current hypothesis and the putting limits on second class currents, free from nuclear physics uncertainties.

Experiments indicate that $D \lesssim 10^{-3}$ and thus g_A and g_V are relatively real to a good approximation. However, the detection of a non-zero D arising from relatively complex g_A and g_V or from complex induced coupling constants remains an important issue for experiment investigation. Measurements of the parity violating correlations proportional to A and B as well as the parity conserving $\beta-\nu$ correlation parameter, a, have been useful for verifying the basic V-A nature of the weak force and as tools for determining the ratio of the vector and axial vector coupling constants.

The weak couplings g_A and g_V are fundamental constants that presently can only be determined from experiment. Vector current conservation preserves the quark vector coupling, and except for radiative corrections the neutron vector coupling is the same as the quark vector coupling. Indeed, current conservation also preserves the vector coupling strength in nuclei; g_V can be inferred from nuclear $0^+ \to 0^+$ superallowed β-decay after accounting for the isospin breaking of the electromagnetic interaction. However, the axial vector current is not conserved and g_A depends on the intricacies of quark interactions inside the nucleon; this manifestly nonperturbative phenomenon is not well understood. Within nuclei, the nucleon axial vector strength should be modified by the nuclear environment and since the process is not understood quantitatively, g_A can only be determined from free neutron β-decay. Apart from their importance in nuclear and particle physics the nucleon weak couplings are critical experimental inputs to theories of astrophysics and cosmology and a great deal of effort goes into determining g_A and g_V experimentally. It turns out that g_A/g_V is close to -1.25 and thus B is rather insensitive to the exact value while A and a are very sensitive. In the past, neutron lifetime measurements have claimed the greatest precision for determining g_A/g_V. However, several of the neutron lifetime measurements are inconsistent and consequently there is a large uncertainty because it is impossible to choose between experiments. As we shall see, the situation has changed and now β-asymmetry measurements provide the most precise g_A/g_V. Except for the most recent experiments with the electron spectrometer PERKEO to be discussed below, all β-asymmetry experiments have followed the general scheme of the pioneering works.

Figure 1 illustrates the apparatus of Clark and Robson.[2] Polarized neutrons were obtained by Bragg reflection off a ferromagnetic crystal of Co-Fe. Other versions of the experiment used small angle reflection from magnetized Co-Fe mirrors to produce polarized neutrons. The β-asymmetry can be measured by simply detecting the electron from polarized neutron decay but to reduce the background it was necessary for Clark and Robson to detect recoil protons in coincidence. In this type of experiment the β-asymmetry is derived from the variation in the β-proton coincidence rate with neutron polarization. Table I shows some important characteristics of β-asymmetry experiments. The early experimenters suffered with the low count rates resulting from the low polarized neutrons fluxes then available and because the experiments had small

ELECTRON DETECTOR

PROTON FOCUSING ELECTRODE

NEUTRON BEAM (INTO PAGE)

PROTON DETECTOR

0   5   10
SCALE (inches)
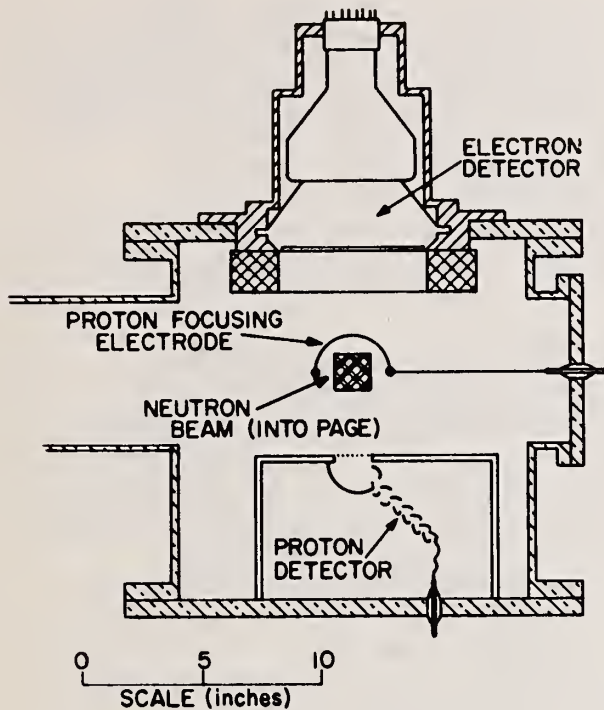
Fig. 1. Experimental arrangement of Clark and Robson.[2] Other β-asymmetry experiments employing coincident electron and proton detection were similar in concept.

source volumes and low detection efficiencies. The earlier experiments were limited both by statistics and systematic error. One type of systematic error resulted from a tendency for biased proton detection efficiences as a consequence of the large v-asymmetry coefficient ($B \approx 1$).

The newest β-asymmetry experiment benefits from several recent technical advances. The experiment employs the PERKEO β-decay spectrometer at the

Table I. Characteristics and Results of β-asymmetry Measurements.

Year	Reference	Polarization (%)	Typical Count Rate (sec^{-1})	Asymmetry	g_A/g_V
1960	Burgy et al.[1]	84±7	0.015	-0.114(19)	-1.257(50)[†]
1961	Clark & Robson[2]	89±5	-	-0.090(50)	-1.20(12)[†]
1969	Christensen et al.[3]	87±3	0.013	-0.115(9)	-1.260(23)[†]
1971	Erozolimskii et al.[4]	77±2	0.055	-0.120(10)	-1.273(27)[†]
1975	Krohn & Ringo[5]	79±1.5	0.117	-0.111(8)	-1.249(22)[†]
1976	Erozolimskii et al.[4]	73.3±2	0.106	-0.112(5)	-1.257(14)[†]
1984	Bopp et al.[6]	96.7±0.7	300	-0.118(3)[*]	-1.270(9)
1985	Bopp et al.[6]	97.4±0.5	300	-0.1146(19)[*]	-1.262(5)

[*] The asymmetries in these experiments are corrected to correspond to the β-asymmetry in the allowed approximation (A_0).

[†] The value of g_A/g_V is obtained by correcting A for induced effects and recoil over the reported energy range by the method described in Ref. 7.

65

Institute Laue-Langevin's 57 MW heavy water reactor at Grenoble, France. PERKEO is located at the end of a cold neutron guide about 120 m from the reactor. Unlike previous experiments, the detectors sit in a low background environment far from the reactor. A supermirror polarizer, another development of the ILL, produces an intense beam with measured polarization > 97%. To further enhance the count rate, the new experiment has 4π detection efficiency over a large region of the neutron beam. Consequently this is the first β-asymmetry measurement accomplished without the need for coincidence proton counting and the count rate is more than three orders of magnitude higher any of the previous experiments.

Figure 2 shows the experimental apparatus. The main component of the experiment is a 1.7 m long 20 cm diameter superconducting solenoid which produces a 15 kgauss magnetic field. After the beam passes the polarizer, guide fields rotate the neutron polarization to be along the axis of the solenoid. The polarization is reversed with a non-adiabatic current sheet spin flipper. A 1.7 m long 9-channel collimator constructed of ^{6}LiF plates produces a neutron beam with a 3x5 cm cross section and a very small divergence. The collimated polarized beam has a capture-flux of 8×10^9 sec^{-1}. Electrons from neutron decay have kinetic energies < 782 keV and they are constrained to move in helical paths with diameters less than 1 cm inside the solenoid. Coils at the ends of the solenoid distort the solenoidal field lines causing electron trajectories to intersect plastic scintillator detectors positioned above the neutron beam. Each scintillator is coupled through light guides to two RCA 8850 photomultipliers operated in coincidence to reduce noise. The detector sensitivity is about 100 photoelectrons/MeV. One novel feature of the experiment is the ability to reconstruct electron backscatter events as coincidences between the two scintillation counters. The electron energy is derived from the sum of both scintillator signals and the detector hit first is determined by timing. About 1% of the events are coincidences. The detectors are easily calibrated with respect to energy with remotely inserting conversion line sources (^{109}Cd, ^{113}Sn and ^{207}Bi) on thin backings. The typical background subtracted neutron decay count rate is about 150 sec^{-1} per detector.
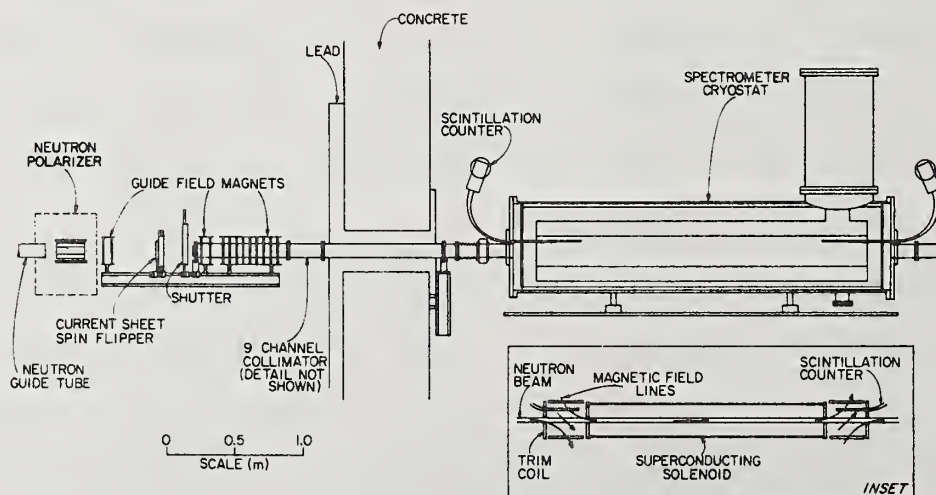

Fig. 2. Eperimental arrangement of PERKEO. The inset shows details of the inner region of the superconducting solenoid.

The experiment measures the β-asymmetry in the simplest way by measuring the count rate asymmetry as a function of β-energy for the two neutron polarization states. To extract the β-asymmetry parameter from the data one considers the following combination of experiment count rates:

$$(N_i^{\uparrow}(E) - N_i^{\downarrow}(E))/(N_i^{\uparrow}(E) + N_i^{\downarrow}(E)) \ ,$$

where the N's are the experimental energy spectra for counter i and polarization state represented by the arrow. Except for a slight complication from finite detector resolution this combination will have the form $\frac{1}{2} \frac{v}{c} PA(E)(1+f)S$. Two correction factors are included: a factor f to account for imperfect spin reversal, and a factor S to account for the magnetic mirror effect. The magnetic field in the spectrometer decreases monotonically from the center of the solenoid to the detectors and thus electrons are never permanently trapped. Nevertheless, a correction in the asymmetry for the magnetic mirror effect of about 10% is necessary to account for events in which the electron is initially directed to a region of increasing magnetic field.
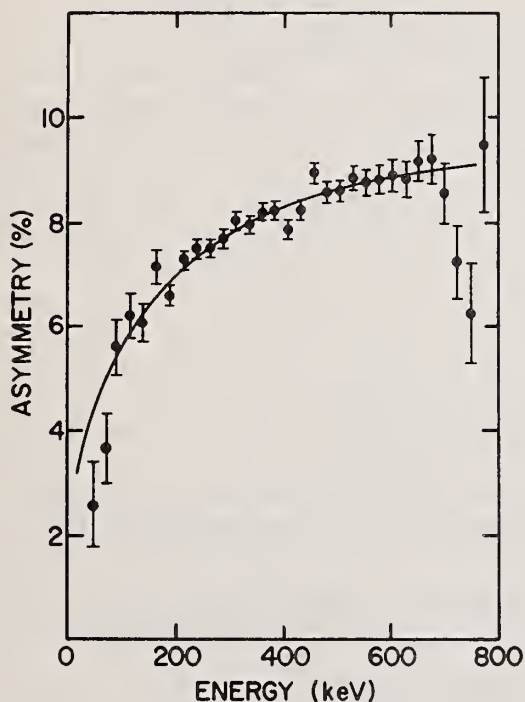
Fig. 3. Experimental β-asymmetry as a function of β-energy from 150 hours of data taken with PERKEO.

Figure 3 is the experimental asymmetry as a function of energy for 150 hours of running. The data is well fit by a function which accounts for the basic v/c energy dependence corrected for weak magnetism, recoil and detector resolution. After accounting for these effects a one-parameter fit determines the combination $\frac{1}{2} PA_0(1+f)S$. The neutron polarization, P, and the spin flip probability, f, is measured periodically during the run. The magnetic mirror correction, S, is straightforward to calculate and the calculation is verified with measurements made with movable conversion line sources.

In the most recent run of the experiment the determined polarization and spin probability are P = (97.4±0.5)% and f = (98.8±0.1)%. The correction for the magnetic mirror effect is slightly different for the two detectors because of the divergence of the neutron beam: S_1 = (88.3±0.5)% and S_2 = (88.7±0.5)%. The data for 150 hours of running gives A_0 = -0.1146(19), implying g_A/g_V = -1.262(5). The error is dominated by systematic uncertainties in the polarization measurement, the background subtraction procedure, the detector response and the energy calibration. The sign of the asymmetry parameter is verified by knowing the sense of the neutron polarization and the sign of the measured asymmetry.
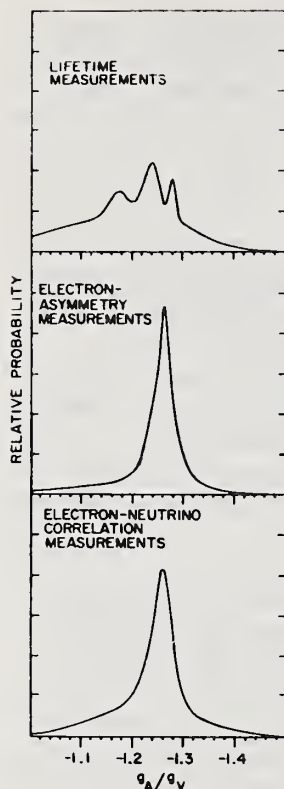
Fig. 4. Ideograms of experiments that determine g_A/g_V. The three ideograms have equal areas.

This value of g_A/g_V can be combined with the value of g_V from superallowed nuclear β-decay to give a prediction for the neutron halflife: $\tau_{1/2} = 622(4)$ sec. This inferred halflife is more precise than any so far obtained from a direct halflife measurement. The value of g_A/g_V determined with PERKEO agrees well with previous correlation measurements.[8]

Figure 4 shows ideograms of the three types of experiments which measure g_A/g_V. It is evident that the lifetime measurements are inconsistent but that the two types of correlation measurements are in good agreement. Indeed the nine lifetime experiments reported since 1951 give a very poor reduced chisquare of about 5. It is interesting to note, however, that the weighted average of g_A/g_V from lifetimes is -1.257 ± 0.005 in good agreement with $g_A/g_V = -1.256\pm0.015$ from the three best e-ν-measurements and with $g_A/g_V = -1.262\pm0.004$ from the eight β-asymmetry measurements done so far.

References

1. M. T. Burgy et al., Phys. Rev. 20, 1829 (1960).

2. M. A. Clark and J. M. Robson, Can. J. Phys. 39, 13 (1961).

3. C. J. Christensen, Phys. Lett. 28B, 411 (1969); this reference combines the result of Ref. 1 in the reported A. Table I includes only the 1969 result.

4. B. G. Erozolimskii et al., Sov. J. Nucl. Phys. 30, 356 (1979); this reference reanalyzes and supercedes earlier papers: B. G. Erozolimskii et al., JETP Lett. B, 252 (1971); JETP Lett. 23, 663 (1976).

5. V. E. Krohn and G. R. Ringo, Phys. Lett. 55B, 175 (1975); this reference combines the results of Refs. 1 and 2 in the reported A. Table I includes only the 1975 result.

6. These results are preliminary, see P. Bopp et al., Journal de Physique C3, 21 (1984); Phys. Rev. Lett. (to be published).

7. D. H. Wilkinson, Nucl. Phys. A377, 424 (1982).

8. For a review of neutron correlation and halflife measurements, see J. Byrne, Rep. Prog. Phys. 45, 115 (1982).

TIME REVERSAL INVARIANCE IN POLARIZED NEUTRON BETA DECAY

Thomas J. Bowles
Physics Division
Los Alamos National Laboratory
Los Alamos, New Mexico 87545

The source of CP violation has been the subject of extensive experimental and theoretical work since its discovery in 1964. Measurements of the triple correlation $\sigma_n \cdot (p_e \times p_\nu)$ in polarized neutron beta decay have been carried out in attempts to define the cause of T (and CP) violation. Recent theoretical work has demonstrated the sensitivity of these measurements to CP violation arising in left-right symmetric models of the weak interaction. The status of previous experiments and theoretical work in polarized neutron beta decay is discussed along with plans for an experiment to substantially improve the sensitivity of the measurement of the triple correlation coefficient.

CP was believed to be a fundamental symmetry of nature until 1964 when this symmetry was shown to be broken in the decay of the neutral kaon system. It was observed (1) that the long lived neutral K-meson (K_L) decayed into two charged pions, a decay made forbidden by CP conservation. This two pion decay mode occurred at a level of $(2.0 \pm 0.4) \times 10^{-3}$ relative to all charged decay modes. Measurements during the last twenty years have improved the accuracy of this observed CP violation to a present accuracy of $\eta_{+-} =$ amplitude ($K_L \rightarrow \pi^+\pi^-$)/amplitude ($K_S \rightarrow \pi^+\pi^-$) = $(2.274 \pm 0.022) \times 10^{-3}$ (2). Several other CP violating decays of the K_L have been observed, eg. $\eta_{oo} =$ amplitude ($K_L \rightarrow \pi^o\pi^o$)/amplitude ($K_S \rightarrow \pi^o\pi^o$) = $(2.33 \pm 0.08) \times 10^{-3}$, but all experimental results can be described by two complex parameters ϵ and ϵ', where $\eta_{+-} = \epsilon + \epsilon'$ and $\eta_{oo} = \epsilon - 2\epsilon'$ (3). Experiments show that ϵ' is small, $\epsilon'/\epsilon = -0.002 \pm 0.005$ (4-5), and thus all the information we have about CP violation is contained in the single complex number ϵ. Since $\epsilon = |Re\epsilon| e^{i\phi_n}$, one can also check to see whether CPT is violated by measuring the phase angle ϕ_n. Measurements of ϕ_n indicate that CPT is conserved and therefore CP violation is equivalent to T violation (3).

Various theoretical explanations for CP violation have been offered, including CP violating phases between six quarks (6), CP violating phases between three or more Higgs doublets (7), existence of a CP violating superweak force (8), CP violating phases in left-right symmetric theories (9-10), etc. (3). A wide range of experiments have been carried out (2-3) to search for CP or T violation. Present limits on the value of ϵ'/ϵ and the electric dipole moment of the neutron (11) are beginning to rule out the Higgs mechanism and the Kobayashi-Maskawa mode (4-5). Thus, considerable attention is presently being given to testing theories which have CP violating phases between V + A admixtures into the usual V-A component of the weak interactions. It has been pointed out that in the most general formalism for CP violation in $SU(2)_L \times SU(2)_R \times U(1)$ theories, there are several CP violating phases which enter (10). The most important experiments (11) which provide information on these phases are measurements of ϵ', the

electric dipole moment of the neutron, the coefficient D of the time reversal odd triple correlation in nuclear beta decay, and the slope asymmetry in $K^{\pm} \to \pi^{\pm}\pi^{+}\pi^{+}$ decays. It is important to note that a nonzero triple correlation coefficient in nuclear beta decay is one feature which distinguishes CP violation arising from mixing in left-right symmetric models from theories in which CP violation arises from Kobayashi-Maskawa phases, or from relative phases between right-handed and left-handed couplings of the S=1 Hamiltonian, or in the Higgs sector (11). Measurements of D provide complementary information to measurements of ϵ' and the slope asymmetry in kaon decay, which measure different combinations of CP violating phases. And while the single-quark contributions to the electric dipole moment of the neutron constrain the same combination of CP violating phases as D, it is estimated that the contributions from two-quark operators are comparable to the contributions from one-quark operators and it is possible that these two contributions may cancel (11). Existing data from all other experiments do not rule out a value of D as large as the present limit on D. Therefore, it is important to improve the sensitivity of the triple correlation measurements in nuclear beta decay at the same time as carrying out experiments with improved sensitivity for ϵ', the electric dipole moment of the neutron, and the slope asymmetry in kaon decay. I will here concentrate on the triple correlation experiments in nuclear beta decay.

The decay probability per unit time for polarized neutrons is given by

$$W(E, \vec{P}_e, \vec{P}_\nu) = F(E) \left\{ 1 + a \frac{\vec{P}_e \cdot \vec{P}_\nu}{E_e E_\nu} + A \frac{\vec{\sigma}_n \cdot \vec{P}_e}{E_e} + B \frac{\vec{\sigma}_n \cdot \vec{P}_\nu}{E_\nu} + D \cdot \frac{\vec{\sigma}_n \cdot (\vec{P}_\nu \times \vec{P}_e)}{E_e E_\nu} \right\}$$

where the Fermi function $F(E)$ is a function of beta energy, P_e and P_ν (E_e and E_ν) are the electron and antineutrino momenta (energy) respectively, σ_n is the neutron spin, and a, A, B, and D are the coefficients of the electron-antineutrino, neutron spin-electron, neutron spin-antineutrino, and triple correlations, respectively. We note that we have neglected recoil order terms (eg. weak magnetism) in the above expression. The triple correlation term is the one we are particularly interested in since it is odd under time reversal. We note that by conservation of energy and momentum, we can rewrite this correlation in terms of observables of the electron and proton:

$$\vec{\sigma}_n \cdot \frac{(\vec{P}_e \times \vec{P}_\nu)}{E_e E_\nu} = -\vec{\sigma}_n \cdot \frac{(\vec{P}_e \times \vec{P}_p)}{E_e (\Delta - E_e - E_p - m_e c^2)}$$

where P_p (E_p) is the recoil proton momentum (energy), Δ is the mass difference between the neutron and proton, and m_e is the electron mass.

In terms of the scalar (S), vector (V), axial vector (A), and tensor (T) coupling constants of the weak interactions, the coefficient D is given by

$$D = \frac{2\ \text{Im}\ (ST* - VA*)}{|V|^2 + |S|^2 + 3|T|^2 + 3|A|^2} \quad .$$

Since any tensor component of the weak interactions is known to be small, the dominant contribution is from the VA* component. Thus, contributions to D from the scalar Higgs sector will be very small. However, as pointed out recently (11), the possibility exists that in the left-right symmetric models of $SU(2)_L \times SU(2)_R \times U(1)$ there can be sizable contributions to D due to T violation. Specifically, D is given by

$$D \approx -(g_R/g_L) \cdot \zeta\ (\cos \theta_R/\cos \theta_L)\ \sin (\alpha + \omega) \quad ,$$

where g_R (g_L) is the coupling constant for the right (left)-handed components of the weak interaction, ζ is the mixing angle between the left-and right-handed fields, θ_R (θ_L) is the mixing angle for the right (left)-handed coupling between quarks, and α and ω are CP violating phases.

Before going on to discuss experimental approaches to measuring D, we must first be sure that a nonzero value of D indicates the existence of T violation. It is well known that final state electromagnetic interactions can produce a nonzero value of D that is not T-violating. However, these final state contributions can be accurately calculated and it has been shown that the dominant contribution to D arises from weak magnetism and produces a value of $D = 2 \times 10^{-5}$ for the triple correlation coefficient in neutron beta decay and a value of $D = 1.6 \times 10^{-4}$ in ^{19}Ne beta decay (12). Thus, an observed value of D larger than this would indicate that the weak interaction is not invariant under T reversal.

Several experiments to measure D have been carried out during the last 25 years. Most recently, experiments have been carried out at the Institute Laue-Langevin (ILL) (13) and at the Kurchatov Institute of Atomic Energy (14) which set limits on D in polarized neutron beta decay and at Princeton University (15) in the beta decay of polarized ^{19}Ne. We note here that the present limit on D in ^{19}Ne is $D = (0.4 \pm 0.8) \times 10^{-3}$ (15) and go on to discuss the experiments on D in neutron beta decay, which have a higher ultimate sensitivity to D than the ^{19}Ne experiments, due to the smaller final state interactions in neutron beta decay.

I will discuss first the ILL experiment. A 100-m-long guide tube transports neutrons from the liquid deuterium moderator in the core of the ILL reactor to an experimental area. The guide tube has a radius of curvature of 2700 m which serves to strongly attenuate fast neutrons and gammas from the reactor core while transporting cold neutrons with high efficiency. At the end of the guide tube the beam passes through a polarizer that produces high transverse polarization of the beam. The beam is then rotated 90° to form a longitudinally polarized beam. The longitudinal polarization is maintained over the length of the detector by a longitudinal magnetic field of a few gauss. The neutron beam then passes into an equipotential region at positive

high voltage by grids that form the decay region. Betas from neutrons
decaying in this region are detected in plastic scintillators above and below
the beam. Recoil protons are accelerated to 20 KeV from the gridded region
into detectors on both sides of the beam. These detectors consist of thin
layers of NaI deposited onto photomultiplier tubes. The neutron beam then
exits the detector and is stopped in a ^{6}LiF beam stop. Timing single channel
analyzers were used to set windows on the beta dn proton energy signals and
to form a time-of-flight spectrum for the protons. In order to minimize
systematic effects, the detector was made as symmetric as possible with two
beta and two proton detectors. With a beta detected in the upper counter,
one than looks for a left-right asymmetry in the number of counts in the two
proton detectors and similarly for betas detected in the lower counter. Data
were collected with the neutron polarization both parallel and antiparallel
to the beam direction. The data were then analyzed in terms of ratios of
events in different detectors. This provides cancellation of most detector
asymmetries. The Kurchatov experiment is similar in overall design, except
that a curved guide tube is not used and that the acceleration gap for the
proton detectors is hemispherical, which allows focusing a larger solid angle
for protons onto a smaller proton detector. The pertinent parameters for the
ILL and Kurchatov experiments are listed in Table I. The final results for
the ILL and Kurchatov experiments are D = (-1.1 ± 1.7)x10^{-3} and D = (+2.2 ±
3.0)x10^{-3} respectively.

Table I
Experimental parameters in measurements of triple
correlation in polarized neutron beta decay.

Experi- ment	Flux (n/s)	Polar- ization	Beam Size	Length of Decay Region	Coincident Decay Rate	Signal to Noise	Number Events
ILL	1 x 10^9	70%	4 x 8 cm	40 cm	1.5 cts/s	4	5.9x10^6
Kurchatov	1 x 10^9	70%	4 x 8 cm	12 cm	0.8 cts/s	2	2.5x10^6
Proposed	2 x 10^9	95%	4 cm	100 cm	100 cts/s	>10	10^9

A collaboration between Los Alamos National Laboratory, the ILL, the
University of Washington, and Drexel University is currently planning to
carry out an improved measurement of D (16).In designing an experiment to
substantially improve on the above results, it was realized that three
things would be essential: 1) much higher event rates with better signal to
noise, 2) the detector geometry must be as symmetrical as possible, and 3)
the neutron beam is circular in cross-section and is relatively small (4 cm
diam), 4) the detector is extremely symmetrical so that betas and protons can
both be detected at all azimuthal angles, 5) noise is reduced by multiple
coincidence requirements for betas and anticoincidence requirements for
protons (A test setup at the National Bureau of Standards reactor by this
collaboration to measure the neutron lifetime has shown that the coincidence
requirement between a scintillator and a proportional drift chamber reduces
the background by an order of magnitude (17).), and 6) every decay can be
kinematically reconstructed. The real key to this experiment is the ability
to kinematically reconstruct each event. This provides the ability to bin
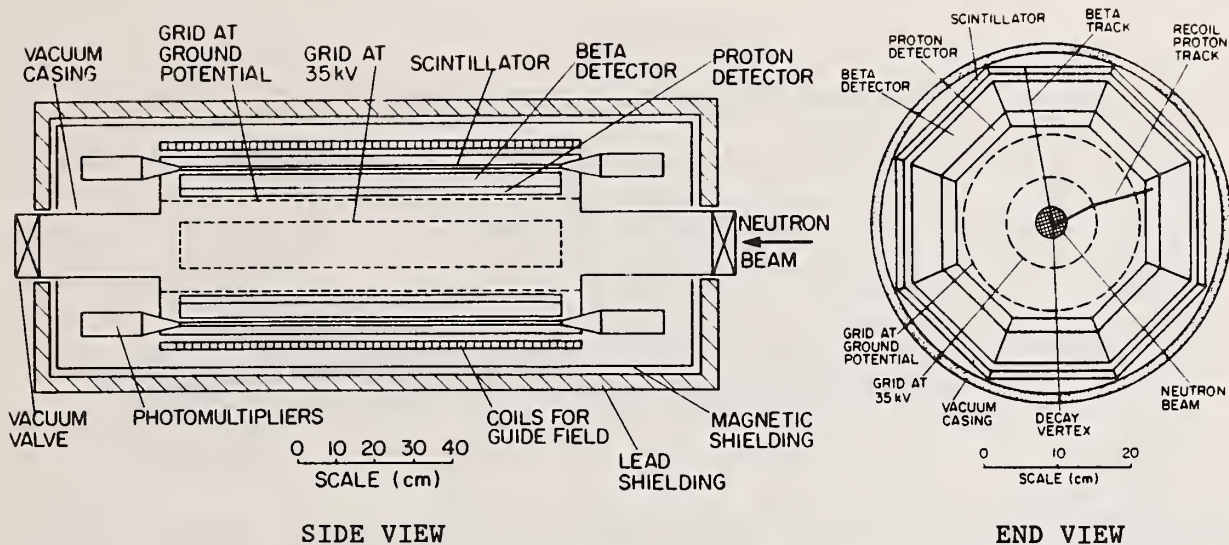
Figure 1.   Cross Sectional View of Spectrometer

the neutron beam to look for systematic effects as a function of radius and position along the beam. It also provides the ability to study the correlation as a function of beta and recoil proton energy and to place computer cuts during analysis on energy spectra and angles between the neutron spin and the electron and proton momenta. The experimental parameters are listed in Table I. The detector is shown in Fig. 1. A decay region at positive high voltage (35KV) is defined by grids. The betas from neutrons decaying in this region pass through two X and two Y proportional drift chambers and are stopped in plastic scintillator which is viewed by photomultiplier tubes at both ends. The recoil protons are accelerated to 35 KeV into multistep avalanche counters (18) where they are stopped. These counters have very thin ($40\mu g/cm^2$) windows and operate at pressures of 5-10 Torr of isobutane. These counters provide two dimensional readout of the proton position, energy, and timing which allows determination of the proton time-of-flight. From these measured quantities and conservation of energy and momentum, it is possible to determine the momenta and energies of the electron, proton, and neutrino as well as the location of the decay vertex. However, the equation giving the decay vertex is quadratic, so that the solution is two-valued. For this particular detector design, this ambiguity can be resolved 30% of the time due to the boundary condition that the decay occurs within the neutron beam.

Sources of possible spurious asymmetries have been discussed in detail in the literature (13-14). The detector response has been studied using Monte Carlo calculations to determine the sensitivity to various systematic effects. It appears that all systematic effects can be kept below the 10^{-4} level, while the statistical accuracy for D should be less than 2×10^{-4}. Thus, this new experiment will provide an order of magnitude greater sensitivity than previous experiments in searching for a finite triple correlation coefficient in polarized neutron beta decay. This will provide a sensitive test of theories in which CP violation is due to CP violating phases in left-right symmetric models of the weak interactions.

References

1. Christenson, J. Jl, J. W. Cronin, V. L. Fitch, and R. Turlay, 1964,
    Phys. Rev. Lett. <u>13</u>, 138.
2. Review of particle properties, 1984, Rev. Mod. Phys. <u>56</u>, Number 2, Part
    II, p. 537.
3. Fitch, V. L. and J. W. Cronin, 1981, Rev. Mod. Phys. <u>53</u>, p. 367.
4. Black, J. K., S. R. Blatt, M. K. Campbell, H. Kasha, M. Mannelli, M. P.
    Schmidt, C. B. Schwarz, R. K. Adair, R. C. Larsen, L. B. Leipuner, W. M.
    Morse, 1985, Phys. Rev. Lett. <u>54</u>, p. 1628.
5. Bernstein, R. H. G. J. Bock, P. Carlsmith, D. Coupal, J. W. Cronin, G.
    D. Gollin, Wen Keling, N. Nishikawa, H. W. M. Norton, B. Winstein, B.
    Peyaud, R. Turlay, A. Zylberstejn, 1985, Phys. Rev. Lett. <u>54</u>, p. 1631.
6. Kobayashi, M. and T. Maskawa, 1973, Prog. Theor. Phys. <u>49</u>, p. 652.
7. Weinberg, S., 1976, Phys. Rev. Lett. <u>37</u>, p. 657.
8. Wolfenstein, L., 1964, Phys. Rev. Lett. <u>13</u>, 569.
9. Mohapatra, R. N. and J. C. Pati, 1975, Phys. Rev. <u>D11</u>, p. 566.
10. Herczeg, P., 1983, Phys. Rev. <u>D28</u>, p. 200.
11. Herczeg, P., 1984, Proceedings of the Third Telemark Miniconference on
    Neutrino Mass and Low Energy Weak Interactions, Oct. 25-27, 1984.
12. Callan, C. G. and S. B. Treiman, 1967, Phys. Rev. D162, p. 1494
13. Steinberg, R. I., P. Liaud, B. Vignon, and V. W. Hughes, 1976, Phys.
    Rev. D13, p. 2469
14. Erozolimskii, B. G., Yu. A. Mostovoi, V. P. Fedunin, A. I. Frank, and
    O. V. Khakhan, 1978, Sov. J. Nucl. Phys. 28, p. 48
15. Hallin, A. L., F. P. Calaprice, D.W. MacArthur, L.E. Piilinen, M.B.
    Schneider, and D. F. Schreiber, 1984, Phys. Rev. Lett. 52, p. 337
16. Bowles, T. J., J. F. Wilkerson (cospokesmen), P. W. Lisowski,
    J. D. Moses, J. Sunier (Los Alamos National Laboratory), R.I. Steinberg
    (Drexel University), B. Heckel (University fo Washington), W. Mampe
    (Institute Laue-Langevin), P. Liaud (University of Chambery)
17. Wilkerson, J. F., see paper in proceedings of this conference
18. Breskin, A., G. Charpak, S. Majewski, G. Melchart, G. Petersen, and F.
    Sauli, 1979, Nucl. Inst. and Meth. 161, p. 19

THE NUCLEON-NUCLEON WEAK INTERACTION

E.G. Adelberger
Physics Department, FM-15
University of Washington
Seattle, WA 98195

The PNC NN interaction provides a unique window on flavor-conserving hadronic weak interactions. The current status of experiment and theory in this area are briefly discussed.

I. Introduction[a]

We can observe the weak interactions between hadrons only when the dominant strong interaction is blocked by a symmetry which is exactly conserved by the strong force. This can be done in two ways:

1) One can observe a flavor (i.e., strangeness or charm) – changing decay process. This is familiar from high-energy physics (for example: $K \to 2\pi$ or $\Lambda \to N\pi$) and is the source of most of our knowledge of hadronic weak interactions.

2) One can observe a parity-violating process. This is a formidable experimental challenge because the observable effects are typically very small. So far experiments have reached interesting level of sensitivity in only one case – the NN interaction. Here one can do scattering experiments (for example, n+p scattering from an s to a p state) or examine parity admixtures in nuclear states.

Clearly experiments of type 2) are very difficult. Therefore, one must ask whether "the game is worth the candle." Now that we have a successful theory of the fundamental electro-weak interaction what motivation is there for undertaking difficult studies of the parity-violating weak NN interaction?

1) First, there is a fundamental distinction between the decay observables (which are flavor-changing) and the parity-nonconserving (PNC) (observables which are flavor-conserving). In the standard model, the GIM mechanism insures that the neutral weak current is flavor-conserving and so cannot be studied in the hadronic decay experiments. The exchange of Z's between quarks can only be "seen" in PNC experiments. Do we expect to see any new fundamental physics in this process considering the success of the standard model? One cannot say. But know that the standard model cannot be complete and that extensions are required. Some proposals for extensions to the standard model posit additional Z bosons which do not couple to leptons, but have "anomalous" couplings to quarks. Probably the only practical way to "see" or set limits on such processes is by PNC NN experiments.

a) because of length limitations references in this paper are minimal. A

complete set of references may be found in Ref. 1.

2) Second, even if we assume that the standard model is an exact theory of the electroweak interactions of point-like fermions (leptons and quarks) there are highly non-trivial problems in applying the theory to composite hadrons. No one yet is able to calculate weak matrix elements of hadronic matrix elements with confidence. But experiments have yielded unexpected dramatic effects which still do not have a satisfactory explanation although the facts have been known for years. A good example is the "$\Delta I=1/2$ rule" observed in strangeness (S) changing weak decays. From the strong isospin (I) properties of the quarks and their currents one would expect that $|\Delta S|=\pm 1$ decays should transform under I rotations as $\Delta I=1/2\times 1=1/2+3/2$. However, one observes that the $\Delta I=1/2$ amplitudes are enhanced over the $\Delta I=3/2$ amplitudes by a factor of ~ 20. This approximate "dynamical" symmetry is not yet understood, because of the theoretical difficulties in computing hadronic weak matrix elements. The problem of calculating hadronic matrix elements, although difficult, is clearly very important. For example, it limits our ability to draw definite conclusion about the source of CP violation from the impressively precise new ϵ'/ϵ measurements in kaon decay. It is worthwhile, therefore, to measure flavor-conserving hadronic matrix elements, to see if there are unexpected results in this sector as were seen in the flavor-changing sector.

II. Isospin Properties of the PNC NN Interaction

The weak NN interaction involves both $W^{\pm}$ and Z^{o} exchange. The $W^{\pm}$ exchange process is dominated by the $(u\to d)\times(d\to u)$ transition whose strength is proportional to $\cos^2\theta_C$ when θ_C is a quark-mixing (i.e., Cabibbo) angle. This transition transforms under I rotations as $\Delta I=1\times 1=0+2$. The $W^{\pm}$ exchange process does receive a contribution from flavor-changing currents [primarily $(u\to s)\times(s\to u)$], but its strength is diminished by a factor of $\sin^2\theta_C$ (when $\tan^2\theta_C\sim 1/2$). Under I-rotation, the flavor-changing currents transform as $\Delta I=1/2\times 1/2=1$. The Z^{o} exchange transition is more complicated under I rotations and does not particularly favor any of the three ($\Delta I=0,1$ or 2) isospin symmetries. As a crude estimate therefore we expect the PNC NN interaction to have roughly comparable $\Delta I=1$ component being dominated by the Z^{o} exchange transition. What does a more elaborate argument predict? We examine this next.

III. The Meson-Exchange Model of the PNC NN Interaction

The most naive model of the weak NN interaction, W and Z exchange between point nucleons, is clearly inadequate because the Compton wavelength of the weak bosons is much smaller than the radius of the nucleon. So far, most analyses of the PNC NN interaction have used a modification of the classical meson (M) exchange model which is quite successful in reproducing the strong NN phase shifts at energies up to nearly 1 GeV. To model the PNC NN interaction, one describes one of the two MNN vertices to the weak interaction. In this picture, all of the physics of W and Z exchange between quarks is hidden inside the PNC MNN vertex, so all the problems of calculating the weak matrix elements have simply been shifted onto computing

76

the PNC MNN vertex. This problem has been studied by a number of investigators. The best known work is probably that of Desplanques, Donoghue, and Holstein (DDH) who used the quark-bag model to compute the PNC MNN vertices in terms of various parameters. Some of these could be fixed from the known s-wave (PNC) hyperon decays B'→B+M, while others could only be estimated within fairly broad uncertainties. From such considerations they estimated "best values" and broad "reasonable ranges" for the strengths of the different terms in the PNC meson-exchange NN potential. I will use the DDH estimates as a benchmark with which to compare the experimental data.

IV. The Low-Energy PNC NN Interaction

Even at low energies, where only s→p transitions are important, the PNC NN interaction is complex. Five s→p transitions are allowed by the Pauli principle. If we neglect CP violation, pion exchange contributes only to one transition, the $^3S_1$→$^3P_1$ $\Delta I=1$ term. This occurs only in the np and not in the pp or nn systems. The exchange of heavier mesons yields a short-range contribution to all five s→p transitions. Therefore, in principle a complete experimental determination of the low-energy PNC NN interaction requires studying at least five observables. One possible set of experiments would be measurements of A_L (the longitudinal analyzing power = $(\sigma_+-\sigma_-)/(\sigma_++\sigma_-)$ where $\sigma_\pm$ are the total cross sections for reactions induced by right or left helicity projectiles respectively) in the $\vec{p}$+p, $\vec{n}$+p and $\vec{n}$+n reactions, measurements of A_γ (the γ-ray asymmetry) in $\vec{n}$+p→d+γ and P_γ (the γ-ray circular polarization) in n+p→d+γ.

So far definite effects have been seen in only one observable - A_L, the longitudinal analyzing power for scattering of polarized protons by hydrogen. The measurements have reached an impressive precision, the quoted errors in A_L are $<10^{-7}$. The results are shown in Fig. 1 along with a prediction based on the DDH "best value" PNC NN interaction. The theory
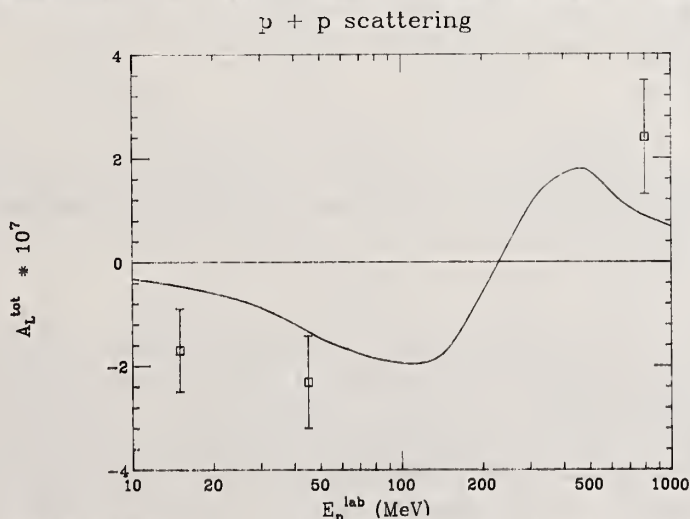
p + p scattering

Fig. 1 A_L measurements in pp scattering along with a DDH "best value" prediction.

77

accounts quite well for the energy dependence of the results, but predictions are about half the measured values. So far, none of the neutron experiments has reached a precision good enough to see the expected effects. Thus there is no data NN data which is sensitive to weak pion exchange. We therefore turn to complex nuclei where the PNC NN interaction induces small parity impurities in nuclear eigenstates.

V. Probing the PNC NN Interaction with Nuclear Parity Mixing

The most interesting cases of parity mixing in complex nuclei are the "parity-doublets" - some examples are shown in Fig. 2. The doublets contain
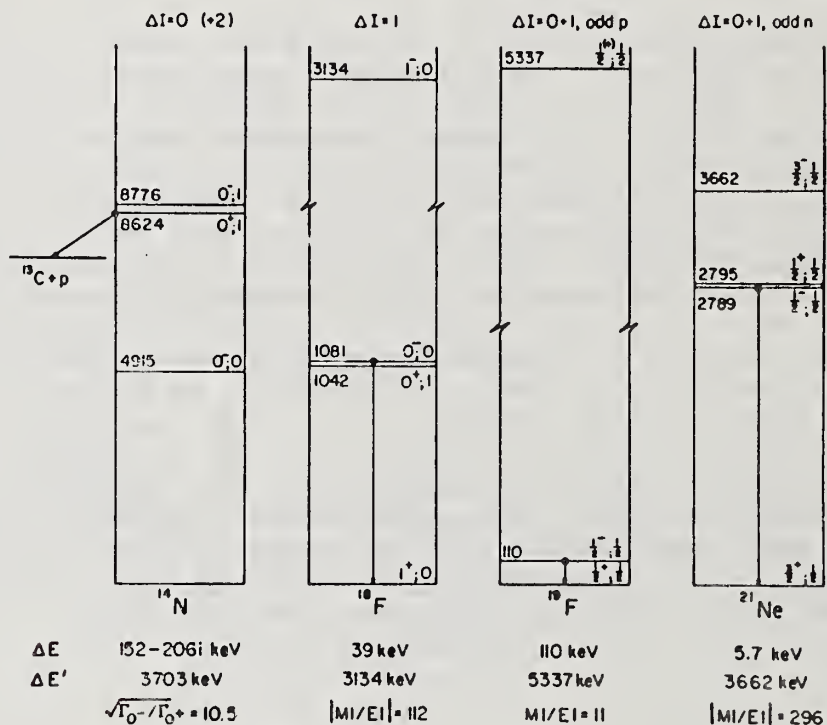
Fig. 2   Parity-mixed doublets in light nuclei. Transitions displaying the amplified effect are indicated. ΔE and ΔE' are the nearest and next nearest energy denominators which govern the parity mixing. The bottom row lists the "amplification factors."

closely spaced pairs of levels of the same spin but opposite parity, and in every case one member of the doublet decays much more slowly than the other. Pseudoscalar observables in the decay of the long-lived state provide a sensitive measure of the PNC matrix element connecting the two members of the doublet. For example, the circular polarization of the 1081 keV γ-ray in ^{18}F is related to the parity mixing of the 0^-;I=0 and 0^+;I=1 doublet by

$$P_\gamma(1081) = \frac{<0^+|V_{PNC}|0^->}{39 \text{ keV}} \frac{<\text{g.s.}|M1|0^+>}{<\text{g.s.}|E1|0^->}.$$

From the measured γ-ray lifetimes of the 0^- and 0^+ states we know that $|<\text{g.s.}|M1|0^+>/<\text{g.s.}|E1|0^->| = 112\pm8$. Thus a measurement of $P_\gamma(1081)$ determines a well defined matrix element of V_{PNC}. Because the members of the doublet have I=0 and I=1 respectively, only the $\Delta I=1$ component of V_{PNC} contributes to the matrix element. So $P_\gamma(1081)$ is sensitive to exactly the same physics – weak pion exchange – as is $A_\gamma(\text{np}\rightarrow\text{d}\gamma)$. One can get a good idea of the "gain" of the nuclear amplifier by noting that the predicted $|P_\gamma(1081)|$ is approximately 3×10^4 times larger than the predicted $A_\gamma(\text{np}\rightarrow\text{d}\gamma)$. This is a considerable advantage to the experimentalist. However, we must consider the "noise" in this amplifier – i.e., theoretical uncertainties in extracting the matrix element of V_{PNC} between NN states from the measured matrix element of V_{PNC} between the 0^- and 0^+ states of ^{18}F. The shell model calculation of the many body matrix element is quite a formidable problem because very large model spaces are needed, and the matrix elements are suppressed by the strong pairing force, the nuclear deformation and shape of the nuclear surface. Fortunately in the case of ^{18}F and ^{19}F one can "calibrate" the necessary matrix elements from experiment. In both the ^{18}F and ^{19}F doublets, one state (or its isospin analog) is a ground state. Therefore, there exists a first-forbidden β-decay transition which connects the two states of the doublet. Since the β-decay operator is known the measured β-decay rates can be used to calibrate the matrix elements.

The four "parity doublets" shown in Fig. 2 have particularly useful isospin properties. The I=0, I=1 doublet in ^{18}F probes the $\Delta I=1$ component of V_{PNC}, the I=1, I=1 doublet in ^{14}N probes the $\Delta I=0$ component (there is a very small contribution from the $\Delta I=2$ interaction) while the I=1/2, I=1/2 doublets in ^{19}F and ^{21}Ne are sensitive to both the $\Delta I=0$ and $\Delta I=1$ interactions. However, because ^{19}F and ^{21}Ne are odd-proton and odd-neutron nuclei respectively, the $\Delta I=0$ and $\Delta I=1$ matrix elements have opposite signs in these two cases.

Results have been reported for ^{19}F (see Ref. 1), ^{18}F (see Refs. 1, 2, and 3), ^{21}Ne (Ref. 1) and an experiment is in progress in ^{14}N (Ref. 4). The mass 18, 19 and 21 observables provide constraints on the $\Delta I=0$ and $\Delta I=1$ PNC NN interactions which are dominated by ρ exchange (F_ρ) and π exchange (F_π) respectively. These $\pm1\sigma$ constraints, along with one from A_L in $\vec{p}+\alpha$, are shown in Fig. 3. At the 1σ level the four constraints do not overlap. However the ^{21}Ne constraint depends on the validity of the shell model isoscalar matrix element. The ^{21}Ne calculations are less reliable than those in ^{18}F and ^{19}F because one cannot do the "β-decay calibration" for ^{21}Ne. Thus the data favor an F_π which is considerably smaller than the DDH "best value" and an F_ρ which is ~ 2 times larger than the "best value." [The increase in F_ρ will improve the agreement between theory and experiment for $A_L(\vec{p}+p)$ also.]

TWO PARAMETER ANALYSIS OF PARITY DOUBLETS
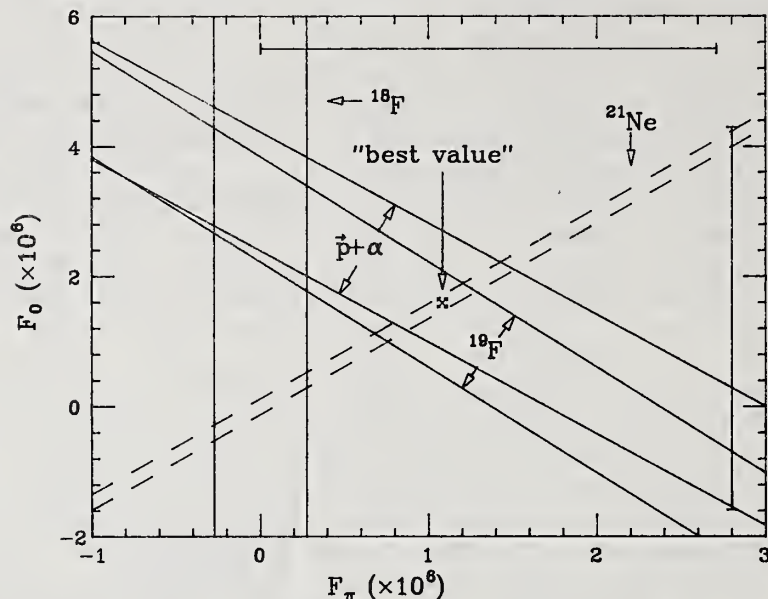
Fig. 3 Constraints (±1σ) on F_π and F_0 from parity mixed doublets. The DDH "reasonable ranges" are shown on the sides.

VI. Conclusions

1) There are no outstanding large discrepancies between nuclear PNC data and the somewhat ill-defined predictions of the standard model. Therefore their is no evidence for funny Z^0's. Previously claimed anomalies were due to wrong experiments or invalid analyses.

2) Data from $\vec{p}+p$, $\vec{p}+\alpha$ and "parity doublets" in light nuclei have restricted several of the parameters of the PNC NN interaction to a small fraction of the DDH "reasonable range."

3) There is evidence that F_π is considerably smaller than the DDH "best value." PNC experiments in the n+p system could be very useful in improving our knowledge of F_π. If the smallness of F_π is confirmed it could be a new dynamical symmetry (the "$\Delta I=0$ rule") in flavor-conserving hadronic weak interactions.

References

1.   E.G. Adelberger and W.C. Haxton, Ann. Rev. Nucl. and Particle Sci., (to be published)
2.   H.C. Evans et al., Phys. Rev. Lett. 55, 791 (1985).
3.   M. Bini et al., Phys. Rev. Lett. 55, 795 (1985).
4.   E.G. Adelberger et al., 1985 Annual Report of University of Washington Nuclear Physics Laboratory, p. 36.

TESTS OF T-INVARIANCE
WITH SLOW NEUTRONS

P. K. Kabir
Beams Physics Laboratory
University of Virginia
Charlottesville, VA 22901

The polarization of neutrons propagating through a medium with spin-polarization $\vec{S}$ may undergo precession about and towards $[\vec{k} \times \vec{S}]$. Either effect is an unambiguous indicator of T-noninvariance. For $S \geq 1$, a similar effect, requiring target spin-alignment only, occurs if there are suitable T-nonvariant interactions even if these conserve parity exactly.

Under rather plausible assumptions[1], one may infer that T-invariance is not a symmetry of all interactions, as expected from the demonstrated[2,3] CP nonconservation in neutral K meson decays, under the theoretical premise of TCP invariance. Nevertheless, despite the prediction of a corresponding T-noninvariant effect[4], the fact remains that there has not yet been any direct demonstration of a T-noninvariant effect in _any_ phenomenon. Therefore, it would be of considerable interest, and provide important information on the origin of the broken symmetry, to find some other phenomenon which shows departure from T-symmetry. A nonvanishing electric dipole moment of the neutron, discussed by Professor Ramsey, would be incontrovertible proof of T-noninvariance. We describe a related effect which, if seen, would be equally unambiguous evidence of lack of T-symmetry.

If the forward scattering amplitude for neutrons from a target with spin $\vec{S}$ contains a term of the form

$$f_T \; \vec{\sigma}_n \cdot [\vec{k} \times \vec{S}] \qquad (1)$$

it would cause the polarization of a neutron beam to precess about $[\vec{k} \times \vec{S}]$ at a rate

$$\chi = 4 \pi k^{-1} N\ \text{Re} f_T \qquad\qquad (2)$$

per unit distance, when passing through matter containing a number density N of such scatterers. In addition, the component of neutron polarization along $[\vec{k} \times \vec{S}]$ would change at a rate

$$\delta = 4 \pi k^{-1} N\ \text{Im} f_T \qquad\qquad (3)$$

per unit distance. Observation of either effect[5,6] would be unambiguous proof of T-noninvariance. Setting $f_T = \gamma_T / m_n^2$ and using current limits on the neutron electric dipole moment as a measure of the obtainable sensitivity in detecting changes of neutron polarization, we estimate that values of γ of the order of 10^{-4} or greater should be detectable. Apart from other problems in searching for this effect, Dr. Heckel has pointed out that the P-nonconserving, but T-invariant, terms in the forward scattering amplitude proportional to $f_k (\vec{\sigma}_n \cdot \vec{k})$ which are known[7,8] to be three or four orders of magnitude greater than this limit, would greatly suppress the effect since the principal precession would then be about $\vec{k}$. This may be obviated by introducing, if necessary, admixtures of other substances such that the average value of f_k for the medium is small compared to the magnitude of f_T being sought.

An interesting question, raised by Professor Ramsey, is whether one could devise tests of T-invariance which, unlike the dipole moment search, do not require the simultaneous violation of

parity. Such a test is also possible[9] with a polarized neutron beam. If we consider targets with spin $S \geq 1$, it is possible to have, apart from a term of the form (1), an additional term of the form

$$g_T (\vec{\sigma}_n \cdot [\vec{k} \times \vec{S}])(\vec{k} \cdot \vec{S}) \tag{4}$$

Such a term is odd under T but even under P, and is therefore sensitive to T-noninvariant effects which do not require parity nonconservation. The effect of a term like (4) is similar to that of (1) except that it depends only on target _alignment_ instead of polarization and vanishes for alignment axis perpendicular to the beam direction; it is maximum for an alignment axis of 45° from the beam axis. Since we need target spin alignment and not polarization, magnetic fields (which could directly affect the neutron spin) are not required and the necessary alignment could be produced by internal quadrupole fields[10]. Another feature of the polarization precession induced by (4) is that it is quadratic in $\vec{k}$, viz. is unchanged under $\vec{k}$ going to $-\vec{k}$, and the effect could be magnified by multiple passages, e.g. in a neutron bottle. Unfortunately, the quadratic dependence on k may also be the main problem in searching for effects due to a term of the form (4). Unless η_T varies rapidly with neutron energy, the expected precession, analogous to (2) and (3), will be proportional to k and therefore vanish for zero energy neutrons. The only hope seems to be if there are p-wave neutron resonances at threshold, or significant s-d mixing associated with a low energy resonance.

References and Footnotes

1. Viz. that CP conconservation in possible unknown channels of neutral kaon decay, is not relatively much larger than in the known channels.

2. J. H. Christenson et al. Phys. Rev. Lett. 13, 138 (1964).

3. V. L. Fitch et al. Phys. Rev. Lett. 15, 73 (1965).

4. P. K. Kabir, Phys. Rev. D2, 540 (1970).

5. L. Stodolsky, Nucl. Phys. B197, 431 (1982).

6. P. K. Kabir, Phys. Rev. D25, 2013 (1982).

7. M. Forte et al. Phys. Rev. Lett. 45, 115 (1978).

8. For a recent review, see J. Byrne, Repts. Prog. Phys. 45, 115 (1982).

9. P. K. Kabir and H. S. Mani, to be published.

10. R. V. Pound, Phys. Rev. 79, 685 (1950).

PARITY VIOLATION IN CAPTURE OF
POLARIZED NEUTRONS

Richard Wilson, M. Avenier, G. Bagieu,
R. Hart, D.H. Koang, M.A. Idrissi, B. Vignon
Harvard University
Cambridge, MA 02138
and
Institut des Sciences Nucleaires
Grenoble, France

The work of the last five years on capture of polarized nuclei is briefly summarized. The accuracy in H and D is limited by statistical accuracy and therefore the beam intensity. It is shown A_γ^{np} to be measured to $\pm 3 \times 10^{-9}$ where a significant effects is expected.

Introduction and Theory

This experimental program had its origins in a conversation with Herman Feshbach while circling for three hours over Boston in the fog. Blinstoyle and Feshbach (1961) had calculated an enhancement factor for the polarization of the γ ray in nd capture (P_γ^{nd}) over that in np capture (P_γ^{up}) of $\sqrt{\sigma_c(H)/\sigma_c(D)} \simeq 25$. Feshbach predicted $P_\gamma^{nd} = 10^{-5}$. This is 20 times present predictions. Lobashov, et al. in Leningrad measured $P_\gamma^{np} = (1.5 \pm 0.3) \times 10^{-6}$. At the time this seemed large, but not unreasonable.

The first proposal to ILL was to study P_γ^{nd} and P_γ^{up}. However it soon became clear that the asymmetry of the γ ray in capture of transversely polarized neutrons is simpler and has fewer systematic errors. Cavaignac, et al. (1977) published a value $A_\gamma^{np} = (-0.6 \pm 2.1) \times 10^{-7}$, $2\frac{1}{2}$ times better than that proposed to ILL. A recent redoing of this by Idrissi (1985) gives $(-4.7 \pm 4.7) \times 10^{-8}$. In the meantime the Leningrad group have remeasured P_γ^{np} and find $(1.8 \pm 1.8) \times 10^{-7}$ (Kaniazkov, 1983). An experiment on A_γ^{nd} gives $(4.2 \pm 3.8) \times 10^{-6}$ (Avenier, et al., 1985) correcting an earlier value.

The errors on these experiments are believed to be entirely statistical. There are a number of ways in which systematic errors can creep in. They are controlled in two ways. Firstly an upper limit on the magnitude is shown to be small. Secondly data are acquired in several beam configurations. For each possible source of error the difference between two configurations is the error; the average cancels the error to first order. By these means we correct for (i) beam fluctuations; (ii) dependence of scintillator efficiency or multiplier gain on magnetic field; and (iii) bending of the neutron in inhomogeneous magnetic fields.

The theoretical predictions have fallen. Here I compare with experiments in light nuclei using the parameters of Desplanques, Donahue and Holstein (1980). It has been found that the experimentally measured quantities depend primarily on two quantities:

$$A_\gamma^{np} = -0.107 \ f\pi$$

$$P_\gamma^{np} = -0.25 \ h$$

$$= -0.25 \ (h_\rho^0 + 0.6 \ h_\omega^0)$$

In the figure are plotted values from a number of experiments on light nuclei P_γ (F^{18}, Ne^{21}, F^{19}); A_{LL} (pp, pα) (Lang, et al., 1985; Evans, et al., 1985) with the np values superposed. A reduction in error by a factor of 3 is needed to get a statistically significant result. For light nuclei the wavefunctions are uncertain--especially for Ne^{21}; for pp and pα experiments, bending of the charged particles produces complicated systematic errors.
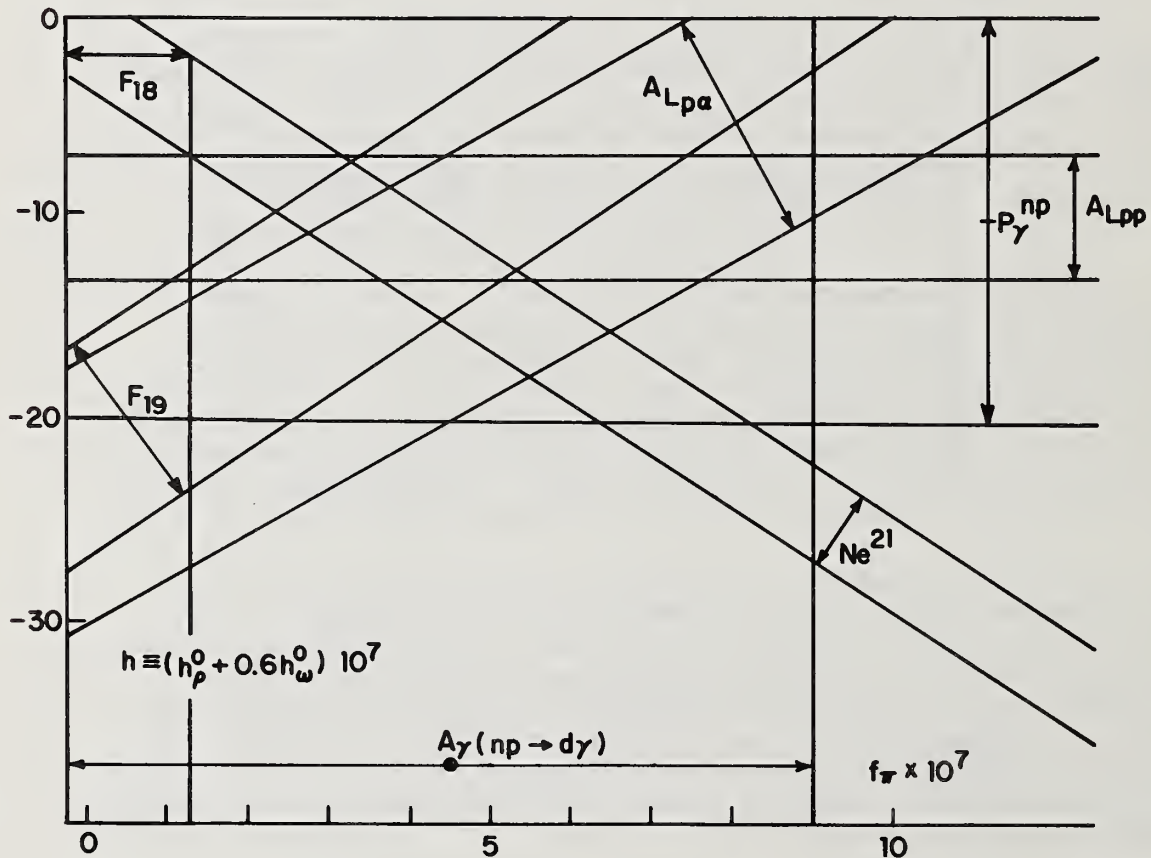
The theoretical value for A_γ^{nd} cannot be put into this form, because small terms are important. This adds to the interest--once the large terms are understood. The enhancement factor varies from term to term, but is always smaller than the 25 of Blinstoyle and Feshbach.

We published a value for A_γ^{nd} of $(8 \pm 4.5) \times 10^{-6}$ (Avenier, et al., 1985). This we must now withdraw and correct, because Guy Bagieu pointed out a systematic error.

In earlier experiments we had measured a ratio

$$R = \frac{\overset{\rightarrow}{N_L} \; \overset{\leftarrow}{N_R}}{\overset{\rightarrow}{N_L} \; \overset{\leftarrow}{N_R}}$$

and noted the value every 30 minutes. For the nd experiment, we "improved" the experiment and sent the value to the computer every minute, averaged the values of R and used this average value.

But we really want the quantity

$$\frac{\overline{\overset{\rightarrow}{N_L}} \; \overline{\overset{\leftarrow}{N_R}}}{\overline{\overset{\rightarrow}{N_L}} \; \overline{\overset{\leftarrow}{N_R}}} = \overline{R} + \tfrac{1}{2}(\text{variance of single measure of } R)$$

By measuring R every minute instead of every 30 minutes, we increased the second term until it became more important. After correcting the data

$$A_\gamma^{nd} = (4.5 \pm 3.8) \times 10^{-6}$$

The theory depends critically upon the "small" terms, but for nd gives A_γ^{nd} (theory) $\approx (0.05 - 1.0) \times 10^{-6}$. The enhancement factor is not as large as 25, and varies for each term.

Scope for Improvement

I now discuss possible improvements of the flux--and therefore of the experiment for three possible beams: (a) H14 at ILL; (b) new cold source at ILL; and (c) proposed source at NBS

The total fluz at the start of the H14 tube, according to ILL catalogues, was, before the 1984-85 shutdown, 2×10^9 $n/cm^2sec.$, over an area of 3 cm x 15 cms, leading to a total flux of $10''$ n/sec. At the end of the H14 guide, about 80 meters away, this is reduced. Firstly, the useable area is only 3 cm x 5 cm; secondly, other experiments intercept and scatter half the beam; and thirdly, the guides are calculated to have an attentuation of 1%/cm, or $e^{-0.8}$. In practice the attentuation seems a little greater--a factor of 5. This gives a total flux at the end of H14 of 3×10^9 n/sec. After the 1984-85 shutdown, improvements in the cold source increased this by a factor of 1.7 to 5×10^9 n/sec (according to P. Ageron of ILL).

At NBS, the plan is to have a large cold source and a guide 17 cm x 6 cm. The intensity expected is about 70% of _previous_ ILL cold sources. This is at the start of the 17 cm x 6 cm guide. This gives about 1.5×10^{11} n/sec total. A neutron will be reflected from the walls half as much in a 6 cm wide guide as in a 3 cm guide so we expect the attentuation to be 1/2%/m. With a 30 m distance, this gives a 10% loss to 10^{11} n/sec total, or 30 times the present intensity at Grenoble.

At ILL, the new cold source will have an intensity of about 8×10^9 per sec over an area of 6 cm x 15 cm or 7.2×10^{11} or 5 times more again than the present H14 guide tube. At the end of a 40 m guide, there would be a 20% reduction to 6×10^{11} n/sec.

The expected accuracy with about 60 days running becomes:

$$
\begin{aligned}
\text{Existing} &\pm 4.5 \times 10^{-8} \\
\text{Present H14} &\pm 3 \quad \times 10^{-8} \\
\text{NBS} &\pm 8 \quad \times 10^{-9} \\
\text{Cold Source ILL} &\pm 3 \quad \times 10^{-9}
\end{aligned}
$$

The new F^{18} experiment suggests that f_π is lower than 5×10^{-7}, and $A_\gamma^{np} < 5 \times 10^{-8}$. Therefore it will be necessary to use all the neutrons possible to have a measureable result. At the higher γ counting rate a simpler detector than the present scintillator can be envisaged.

Another type of experiment can be done with these beams. I have not gotten the precise coefficients for this experiment, but believe it depends upon h more than on f_π. This is to measure the dependence of the cross section on the longitudinal component of the neutron spin A_L^{np}.

We expect that $A_{\gamma L}^{np} \approx 2 \times 10^{-7}$. If so the intensity of any of the present beams is adequate. Modifications to the setup for A_L^{np} would be: (a) to rotate the spin into the direction of motion; (b) to _add_ the counts in the 2 γ counters; or (c) to count the disappearance of a neutron in a counter behind the apparatus. We no longer have automatic cancellation of beam intensity fluctuations so this must be corrected by (d) either using a high rate monitor counter for the beam before capture; or (e) setting up two beams of opposite polarization. I believe that it makes sense to measure $A_{\gamma L}(np)$ the same experimental program as $A_\gamma(np)$.

Other Nuclei

It is worth remembering that parity violation now appears in a number of nuclear systems in which parity violation was definitively observed (by Abov, et al. at ITEP, USSR) was in $Cd^{113}(n\gamma)Cd^{114}$. Other nuclei include $Cl^{35}(n\gamma)Cl^{36}$ (Avenier, et al., 1985a) and $Sn^{117}(n\gamma)SN^{118}$ (Benkoula, et al. 1977). Average violations have been found in uranium and plutonium fission and many other nuclei. The theoretical interpretation of these is not clear, but if the light nuclei are understood, parity violation, which is basically a short range effect, may be used as a probe of the nuclear physics of these heavier nuclei.

References

M. Avenier, G. Bagieu, H. Benkoula, J.F. Cavaignac, A. Idrissie, D.H. Koang, B. Vignon and R. Wilson (1985a), Nucl. Phys. A436, 83.

M. Avenier, J.F. Cavaignac, D.H. Koang, B. Vignon, R. Hart and Richard Wilson (1985b), submitted to Nucl. Phys.

H. Benkoula, et al., (1977), Phys. Rev. Lett. 71B, 287.

R.J. Blinstoyle and H. Feshbach (1961), Nucl. Phys. 27, 398.

J.F. Cavaignac, B. Vignon, Richard Wilson (1977), Phys. Lett. 67B, 148.

B. DesPlanques, J.F. Donahue, and B.R. Holstein (1980), Ann. Phys. (NY) 124, 449.

H.C. Evans, et al. (1985), Phys. Rev. Lett. 55, 791.

E.A. Idrissie (1985), Ph.D. thesis, presented to University of Grenoble.

Lang, et al. (1985), Phys. Rev. Lett. 54, 170.

V.A. Kaniazkov, et al. (1983), Nucl. Phys., A396, 221.

PNC AND TNC ROTATIONS OF THE NEUTRON SPIN

Blayne Heckel
Physics FM-15
University of Washington
Seattle, Washington 98195

Parity (P) non-conserving and time reversal symmetry (T) non-conserving forces can give rise to P-odd and T-odd rotations of the neutron spin as the neutron propogates through a material target. Measurements of polarized neutron transmission through heavy nuclear targets have observed enhanced P-odd rotations due to pnc mixing between compound resonances. Similar resonant enhancements are expected for measurements of T-odd neutron spin rotations. Measurements of the P-odd rotation in light nuclear targets (H,D, and ^{4}He) can provide useful information about the nucleon-nucleon weak interaction.

Experiments using reactor produced neutrons to study the non-conservation of parity and time reversal symmetry have made important contributions to the present understanding of the forces in nature. Many unanswered questions remain, however. Where and how time reversal symmetry non-conservation occurs remains a mystery, and a detailed understanding of the weak interaction between nucleons has not been achieved. Experimental attempts to shed light on these issues are essential for further progress to be made. This paper will discuss measurements of parity non-conserving (pnc) and time reversal symmetry non-conserving (tnc) interactions between a neutron beam and a material target.

In 1964, F.C.Michel /1/ suggested that due to the weak interaction, the coherent forward scattering amplitude, f(0), of a neutron beam passing through material can acquire a pseudo-scalar piece given by:

$$f_{pnc}(0) = G'\vec{\sigma}\cdot\vec{p} \tag{1}$$

where $\vec{\sigma}$ is the Pauli spin and $\vec{p}$ the linear momentum of the neutron, and where G' is a pnc amplitude of order G, the weak coupling constant. For a neutron beam with initial polarization vector perpendicular to the beam momentum, it follows from equation (1) that the two neutron helicity eigenstates will accumulate different phase changes upon passage through the target. The result is a rotation of the polarization vector by an angle, ϕ_{pnc}, in the plane perpendicular to $\vec{p}$:

$$\phi_{pnc} = -4\pi NL \ Re(G') \tag{2}$$

where N is the atomic number density of the target, L the target length, and a positive ϕ corresponds to a right-handed rotation of the neutron spin about its momentum. The imaginary part of equation (1) describes, by the optical theorem, a different total scattering cross section, P, for the two neutron helicity states, similar to circular dichroism in optics /2/:

$$P = \frac{\sigma(+) - \sigma(-)}{\sigma(+) + \sigma(-)} = 4\pi \ Im(G')/\sigma \tag{3}$$

In recent years, several experiments have been performed to measure ϕ_{pnc} and P in medium and heavy nuclear targets. The measurements of ϕ_{pnc} were performed at the Institut Laue-Langevin reactor using cold neutrons for which 97% neutron polarization can be acheived with super-mirror polarizers and for which Bragg scattering in the target can be eliminated. A crossed polarizer neutron polarimeter was constructed that could distinguish between parity conserving rotations of the neutron spin due to magnetic fields and the desired pnc rotation (see ref. 3,4,and 5 for detailed descriptions). Measurements of the transmission asymmetry, P, were performed using thermal neutrons at the Gatchina Reactor /6,7/ and the Kurchatov Reactor /8/, and using resonant energy neutrons in the eV range at the IBR-30 pulsed reactor /9/. A partial list of the results obtained is given below.

$$\phi_{pnc}/L\ (^{117}Sn)\quad = -(37.0 \pm 2.5)\ X\ 10^{-6}\ rad/cm \qquad /4/$$

$$\phi_{pnc}/L\ (^{139}La)\quad = -(\ 219 \pm 29\ )\ X\ 10^{-6}\ rad/cm \qquad /5/$$

$$\phi_{pnc}/L\ (nat.\ Pb) = (2.24 \pm 0.33)\ X\ 10^{-6}\ rad/cm \qquad /4/$$

$$P(E_n=.025\ eV,\ ^{117}Sn) = (\ 6.2 \pm 0.7)\ X\ 10^{-6} \qquad /6/$$

$$P(E_n=.025\ eV,\ ^{139}La) = (\ 9.0 \pm 1.4)\ X\ 10^{-6} \qquad /6/$$

$$P(E_n=1.33\ eV,\ ^{117}Sn) = (\ 4.5 \pm 1.3)\ X\ 10^{-3} \qquad /9/$$

$$P(E_n=0.75\ eV,\ ^{139}La) = (\ 73\ \pm 5\ )\ X\ 10^{-3} \qquad /9/$$

The striking feature about the results above is the large magnitude of the pnc observables (Born approximation estimates for the pnc rotation range from 10^{-7} to 10^{-8} rad/cm). The picture that has emerged to explain these enhanced pnc signals is that the existence of a narrow p-wave neutron resonance near to neutron threshhold can interfere with the predominantly s-wave scattering state and lead to enhanced pnc mixing /10,11,12,13/. In ^{117}Sn and ^{139}La, such p-wave resonances are found at 1.33 eV and 0.75 eV respectively. Similar large pnc signals have been observed in Br and Cd, again accompanied by low energy p-wave resonances /7,8,9/. It was pointed out by Stodolsky /2/ that for P to remain non-zero as the neutron energy goes to zero, an inelastic scattering channel must exist (ie. the elastic scattering contribution to P vanishes). This observation was experimentally confirmed for the cases of ^{117}Sn and ^{139}La /7/ and is important for considerations for future experiments.

The motivation for continued measurements of ϕ_{pnc} and P in heavy nuclear targets has weakened because of the complexity of understanding the nature of the resonant contributions to the neutron scattering state. That is, it has not been possible to extract values for the parameters of the weak nucleon-nucleon interaction through such measurements. Because of the difficulty in general of obtaining direct information about the N-N weak force, it is worthwhile to consider measurements of ϕ_{pnc} and P in systems where such direct information can be obtained: notably in targets of H_2, D_2, ^3He, and ^4He. Each of these cases will be discussed briefly below.

From the standpoint of theory, the cleanest experimental results will come from pnc measurements in the neutron-proton system, for which there are yet no positive results. In this case there are three pnc amplitudes, C, λ_s, and λ_t, all of order 10^{-7} that can contribute at low neutron energies /14/ :

pnc Amplitude	$\vec{S}, \vec{L}, \vec{J}$	ΔT (isospin)
C	$^3S_1 \leftrightarrow {}^3P_1$	$0 \leftrightarrow 1$
λ_s	$^1S_0 \leftrightarrow {}^3P_0$	$1 \leftrightarrow 1$
λ_t	$^3S_1 \leftrightarrow {}^1P_1$	$0 \leftrightarrow 0$

For a measurement of ϕ_{pnc} in a liquid hydrogen target, all three pnc amplitudes contribute /15/:

$$\phi_{pnc}/L \ (H_2) \simeq 6 \times 10^{-3} \ [\ 2C + 4.4\lambda_s - \lambda_t \ ] \ rad/cm \qquad (4)$$

Using cold neutrons and a liquid para-hydrogen target to avoid the large spin incoherent neutron scattering cross section in hydrogen, a target length of ~ 25 cm could be used. A measurement of ϕ_{pnc} to 10^{-7} radians would then result in a sensitivity to the pnc amplitudes at the 10^{-7} level. The measurements of the pnc rotations in heavier nuclear targets, mentioned earlier, approached a sensitivity of 10^{-6} radians with no indication of uncontrollable systematic problems associated with the measurement technique. It is therefore realistic to envision a measurement of ϕ_{pnc} in a para-hydrogen target at the 10^{-7} rad. level ($\sim 4 \times 10^{-9}$ rad/cm).

As mentioned above, the elastic scattering contribution to the transmission asymmetry, P, goes to zero at low neutron energies. In hydrogen, however, there is the neutron capture channel whose pnc observables persist even at zero neutron energy. For the same reasons that the polarized neutron capture onto protons gamma-ray asymmetry, A_γ, depends primarily on the pnc amplitude C (whereas the neutron-proton capture gamma-ray circular polarization is sensitive to λ_s and λ_t) /14/, a measurement of P in a hydrogen target would be primarily sensitive to the isoscalar amplitudes . In this case, the region of interest would be below 10^{-7}, again approximately one order of magnitude lower than the experimental sensitivities already acheived with heavier nuclear targets.

Complete theoretical analyses are also possible for the neutron-deuterium scattering problem /13/. The expected size for ϕ_{pnc}/L in a liquid deuterium target is $\sim 10^{-8}$ rad/cm /16/. Deuterium, however, presents a difficult experimental problem: even in the lowest rotational state of D_2 (ortho-deuterium), both S=0 and S=2 total nuclear spins are present which results in a large spin incoherent neutron scattering cross section. Target lengths would be limited to a few centimeters and the neutron depolarizing mechanism could lead to unforeseen systematic effects. Still, an apparatus to measure ϕ_{pnc} in liquid hydrogen could be easily adapted to a deuterium measurement. Even an upper limit on $\phi_{pnc}(D_2)$ would be of interest as it is one of the few systems sensitive to the neutron-neutron weak interaction in a calculable way. Because of the large neutron spin flip cross section mentioned above and the small neutron capture cross section for deuterium, the transmission asymmetry, P, is suppressed.

The least problematic measurement of ϕ_{pnc} in light nuclear targets would be with a liquid ^{4}He target. The absence of spin incoherent and capture channels allows the use of targets one meter or greater in length, resulting in a sensitivity for ϕ_{pnc}/L at the level of 10^{-9} to 10^{-8} rad/cm. A reactor neutron measurement of P is not reasonable due to the absence of an inelastic

channel. Both T=0 and T=1 (isospin) pnc amplitudes contribute to n-α scattering. The interference between these amplitudes is opposite in the isospin partner p-α system for which pnc results already exist /17/. Positive results in both systems would allow the separate determination of the T=0 and T=1 pnc amplitudes. The n-α measurement may be even more interpretable than the p-α result because of the low neutron energy /13/. Calculated values for the expected magnitude of $\phi_{pnc}(^4He)$ are near 10^{-8} rad/cm /18,19/.

The neutron-^{3}He scattering problem also has simple theoretical features. A strong 0^+ scattering resonance found .5 MeV below neutron threshhold (that is responsible for the large thermal neutron capture cross section in ^{3}He) is accompanied by a 0^- resonance lying .5 MeV above threshhold. Both resonances have large single particle components, and to the extent that pnc mixing between these states dominates the neutron-^{3}He pnc scattering, a measurement would be dominated by the T=0 pnc amplitude /20/. The large neutron capture cross section for ^{3}He makes pnc observables very small for low energy neutrons. However, a measurement of P using .5 MeV neutrons would benefit by the enhancement that comes from sitting on top of a p-wave resonance /11,12,13/, making $P(E_n=.5 \text{ MeV}, ^3He) \sim 10^{-5}$ to 10^{-4}.

The success in observing large pnc effects in neutron scattering experiments raises the question of whether time reversal non-conserving (tnc) forces might be sought in the same manner. Searches for T-odd amplitudes in nuclear transitions often suffer from final state interactions that mimic the effect under investigation. Limits from beta-decay correlations, gamma ray cascades, and tests of detailed balance place the T-odd amplitudes at $\sim 10^{-3}$ times the T-even amplitudes /21/.

Analogous to equation (1), a tnc interaction can give the neutron coherent forward scattering amplitude a tnc component given by /2,22/:

$$f_{tnc}(0) = G_t' \; \vec{\sigma} \cdot (\vec{p} \times \vec{I}) \tag{5}$$

where $\vec{I}$ is the nuclear spin of the target. Equation (5) gives rise to a rotation of the neutron spin, ϕ_{tnc}, about the $\vec{p} \times \vec{I}$ axis and to a different total scattering cross section, P_t, for neutrons polarized parallel to and antiparallel to $\vec{p} \times \vec{I}$. Because the observables are sensitive only to the forward elastic scattering amplitude, there are no amplitudes due to final state interactions that mimic the tnc effects /23/.

With one proviso, there will be the same enhancement factors for the tnc mixing as there are for pnc mixing in a given scattering state /24/. The proviso is that for scattering states labelled by $\vec{L} + \vec{S} = \vec{J}$, the tnc mixing connects only states for which $\Delta S=1$, whereas pnc mixing has no such requirement. Because the enhanced pnc signal in neutron scattering from heavy nuclei is believed to be due to the mixing of nearby s and p-wave resonances, for a study of tnc effects it is important to know S for these resonances as well as L and J.

The experimental situation for measurements of ϕ_{tnc} and P_t is not so simple because of the need for polarized nuclear targets. Brute force polarization via a strong magnetic field is problematic because the Larmor precession of the neutrons greatly reduces the tnc signal amplitude as well as introduces spurious systematic effects /25/. An alternate approach that overcomes these

problems is to achieve the nuclear polarization at low (mG) magnetic field strengths through optical pumping. Nuclear species that may be studied in this way include K, Rb, Cs, Na, ^{129}Xe, ^{199}Hg, and ^{201}Hg. A limitation with optical pumping, apart from its restricted range of applicability, is that with current light sources (lasers) it would be difficult to polarize more than 10^{20} nuclei, whereas it would be desirable to have $\sim 10^{22}$ polarized nuclei per cm^2 of neutron beam. On the other hand, high polarizations that can be easily monitored are possible with optical pumping. Nevertheless, if a nuclear species that can be optically pumped is found to have a large value of ϕ_{pnc} or P, then a search for the corresponding tnc signal should be seriously considered.

Measurements of ϕ_{pnc} and P have proven to be sensitive tests for pnc effects in medium and heavy nuclear targets. Because of the importance to obtain interpretable experimental results regarding the nucleon-nucleon pnc interaction, corresponding measurements should be made in light nuclear targets. The most favorable cases are measurements of ϕ_{pnc} in liquid para-hydrogen and ^{4}He, and of P in para-hydrogen. Advantage can be taken of the enhanced pnc signals in heavy nuclei in searches for the corresponding tnc signals, ϕ_{tnc} and P_t. Progress will be slow until a nucleus that is easy to polarize is found that exhibits the enhanced pnc signals.

References

/1/   F.C.Michel, Phys. Rev. 133, B329 (1964).
/2/   L.Stodolsky, Nucl. Phys. B197, 213 (1982).
/3/   M.Forte, et. al. Phys. Rev. Lett. 45, 2088 (1980).
/4/   B.Heckel, et. al. Phys. Lett. 119B, 298 (1982).
/5/   B.Heckel, et. al. Phys. Rev. C 29, 2389 (1984).
/6/   E.A.Kolomensky, et. al. Phys. Lett. 107B, 272 (1981).
/7/   V.A.Vesna, et. al. JETP Lett. 36, 209 (1982).
/8/   L.N.Bondarenko, et. al. Journal de Phys. C3, 81 (1984).
/9/   V.P.Alfimenkov, et. al. JETP Lett. 35, 51 (1982).
/10/   M.Forte, Inst. Phys. Conf. Ser. Nº 42, 80 (1978).
/11/   V.E.Bunakov and V.P.Gudkov, Z. Phys. A308, 363 (1982).
/12/   O.P.Sushkov and V.V.Flambaum, Sov. Phys. Usp. 25, 1 (1982).
/13/   B.Desplanques, Journal de Phys. C3, 55 (1984).
/14/   G.S.Danilov, Phys. Lett. 18, 40 (1965).
/15/   A.P.Serebrov, Proc. of the XIV Winter School of LIYAF for Nucl. and
            Elem. Part. Phys., USSR Acad. Sci., 28 (1979).
/16/   Y.Avishai, Phys. Rev. Lett. 52, 1389 (1984).
/17/   R.Henneck, et. al. Phys. Rev. Lett. 48, 725 (1982).
/18/   V.F.Dmitriev, et. al. Phys. Lett. 125, 1 (1983).
/19/   Y.Avishai, Phys. Lett. 112B, 311 (1982).
/20/   E.Adelberger, private communication.
/21/   F.Boehm, Comm. Nucl. Part. Phys. 11, 251 (1983).
/22/   P.Kabir, Phys. Rev. D 25, 2013 (1982).
/23/   J.D.Jackson, S.B.Trieman, and H.W.Wyld, Jr., Nucl. Phys. 4, 206 (1957).
/24/   V.E.Bunakov and V.P.Gudkov, LINP preprint 777, Leningrad (1982).
/25/   V.E.Bunakov and V.P.Gudkov, Journal de Phys. C3, 77 (1984).

NEUTRON INTERFEROMETRY: PRESENT STATUS - FUTURE PROSPECTS

S. A. Werner and H. Kaiser
Physics Department and Research Reactor Facility
University of Missouri-Columbia
Columbia, MO 65211

Neutron interferometry, based upon the Bonse-Hart perfect-silicon-crystal x-ray interferometer, was first demonstrated by Rauch, Treimer and Bonse in 1974. Since that time, this single-crystal device has proven to be a marvellous didactive laboratory for probing and elucidating the fundamental quantum mechanical principles of nature. In this paper we enumerate the wide range of experiments carried out to-date, which includes gravitationally-induced quantum interference, the effect of the Earth's rotation on the quantum mechanical phase of the neutron (Sagnac Effect), the observability of 2π-rotation of fermions, spin superposition (Wigner phenomenon), the neutron Fizeau effect, search for quaternions in quantum mechanics, and a search for non-linear terms in the Schrödinger equation. Plans are underway for a neutron Michelson-Morley experiment, various versions of a Wheeler delayed-choice experiment and for the construction of very large-scale interferometers approaching linear dimensions of 1 meter.

Introduction. In this paper we first provide a concise overview of the current status of neutron interferometry, and then we attempt to make some educated guesses and suggestions about the future directions that this field is likely to take. We will also make some comments on the experiments which we are currently pursuing here at the University of Missouri.

As in classical optics, two principal types of interferometers are distinguished, depending on the method used for deriving the two coherent beams from one source; namely division of the wavefront and amplitude division. Both of these methods have been successfully employed using thermal and cold neutrons. In general, wavefront division experiments require long-wavelength neutrons (say 20Å - 200Å), a subject discussed in Anton Zeilinger's paper at this workshop. Amplitude division interferometry, relying on perfect Si crystals, appears to be possible for neutron wavelength of 0.1Å (8.2 ev) up to about 6Å (2.3 mev).[1] Beam splitting of long-wavelength neutrons by mirror reflection/transmission from thin foils is certainly feasible, but it has not yet been incorporated into an interferometer.

Overview. Table I is a list of significant neutron interferometry experiments carried out during the past 10 years. Our intent here is to discuss briefly only a selected number of

these experiments. Fig. 1 is a schematic diagram of a 3-crystal LLL perfect-Si-crystal interferometer; it has been extensively utilized by the MURR and ILL groups. Typical overall dimensions are 5 cm to 10 cm. It is topologically equivalent to a Mach - Zehnder optical interferometer. Fig. 2 is a 2-crystal LL interferometer of the type employed by the MIT group; it is topologicallly similar to a Rayleigh interferometer.
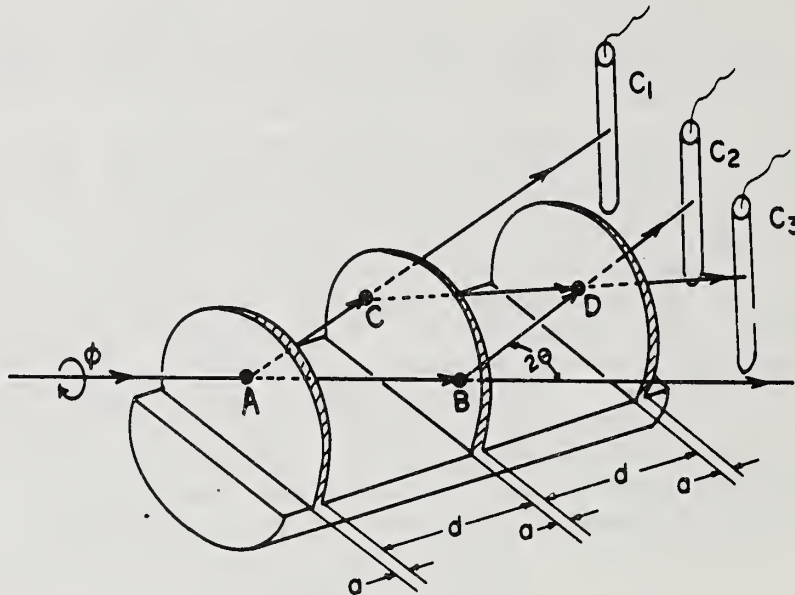

Fig. 1   LLL 3-crystal interferometer.
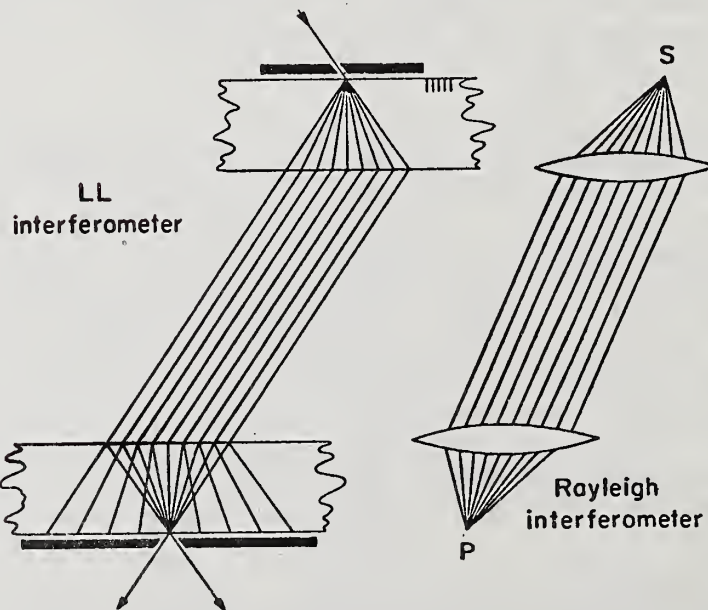
Fig. 2   LL 2-crystal interferometer.

Neutron interferometry has brought a new degree of ease and precision to the measurement of the coherent scattering amplitude, b, of various isotopes. The current level of precision achievable is about 1 part in 10^3 for gases and 1 part in 10^4 for solids. The technique involves measuring the phase shift $\Delta\beta$ due to the passage of one of the coherent neutron beams in the interferometers through a slab of the material being studied of thickness D and atom density N, where

$$\Delta\beta = 2\pi \, (n - 1) \, D/\lambda = -N\lambda Db \quad . \tag{1}$$

Here n is the index of refraction and λ is the neutron wavelength. This phase shift will be energy-dependent for isotopes having a Breit-Wigner resonance in the thermal or epithermal energy range, as is the case for example for ^{149}Sm and ^{239}Pu. Precision values for b can provide new nuclear physics information in certain cases, such as for the charge-dependence of the nuclear forces in the 4-body problem (n-^{3}He, n-^{3}H), and on the parameters characterizing the negative energy resonances in ^{235}U and other heavy nuclei.

In most phenomena of interest in physics, gravity and quantum mechanics due not simultaneously play an active role. However, the neutron interferometer is sufficiently sensitive to detect the small changes in the neutron wavefunction induced by the Earth's gravity, and also the phase shift due to the inertial consequences of its rotation (Neutron Sagnac Effect). The theoretical formulas for the phase shifts in these well-known experiments are

$$\Delta\beta_{grav} = 2\pi \, m_i \, m_g \, (g/h^2) \, \lambda A \sin\phi \tag{2}$$

and

$$\Delta\beta_{sagnac} = 2m_i \, \vec{\omega} \cdot \vec{A}/\hbar \quad , \tag{3}$$

where m_i and m_g are the neutron's inertial and gravitational
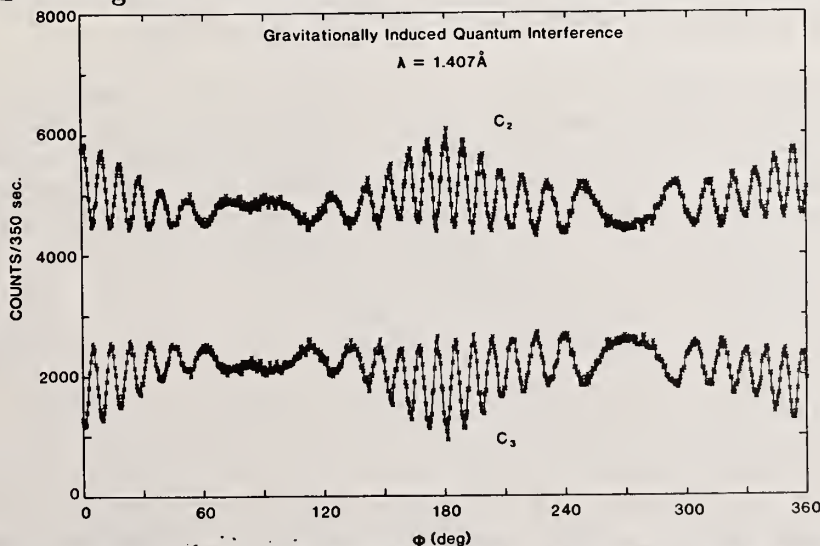
Fig. 3 Full-rotation gravitationally-induced interference.

massses respectively, $\vec{\omega}$ is the angular rotation velocity of the Earth, $\vec{A}$ is the normal area vector of the parallelogram defined by the neutron trajectories in Fig. 1, and ϕ is the angle of "tilting" of the interferometer shown in Fig. 1. A full-rotation interferogram due to gravitationally induced quantum interference, obtained in a recent experiment is shown in Fig. 3.[4c] Fig. 4 is a photograph of the apparatus at Missouri used for these experiments.

The operator for rotation through 2π radians causes a reversal of the sign of the wavefunction of a fermion. Although this effect is well-known in quantum theory, it had not been directly tested experimentally until the advent of neutron interferometry. An extension of the ideas of coherent precession of fermions in an interferometer is the observation of the "Wigner Phenomenon" in which a spin-up wavefunction, $|\alpha\rangle$ is coherently combined with a spin down wavefunction $|\beta\rangle$; the resulting neutron is then polarized in the plane perpendicular to the original axis of quantization. This was nicely demonstrated by the Vienna group in two experiments at the ILL in 1983.[12]

Future Prospects. In a new field such as neutron interferometry it is difficult to predict the future applications. A large number of the classical optics effects and experiments have now also been observed with neutrons.[21] The Michelson-Morley experiment is perhaps the most famous optical interferometer experiment. It is a surprise to most people to learn that pulses of deBroglie waves are just as good as pulses of light in the search for an ether drift. It appears to be the theoretical consensus that one would expect a null-result in a neutron M-M experiment also. However, there may be unexpected effects due to the motion of neutrons relative to the fixed stars. This experiment presents technical challenges to neutron people since a zero-enclosed area interferometer requires back-reflection optical components, and a highly monochromatic device of consequent low intensity. A perfect Si crystal Michelson-type interferometer design has been described by R. Deslattes.

If we bring a massive body up close to the interferometer, is the gravitational potential sufficient to cause a measurable phase shift? To get an idea of the answer to this question, let us suppose that we have an interferometer for which the path lengths are 10 cm, and suppose that we are sensitive to phase shifts of 0.1 deg (0.00174 rad.). For a potential V applied to one of the beams, over a distance S, the phase shift is

$$\Delta\beta = kSV/2E \quad . \tag{4}$$
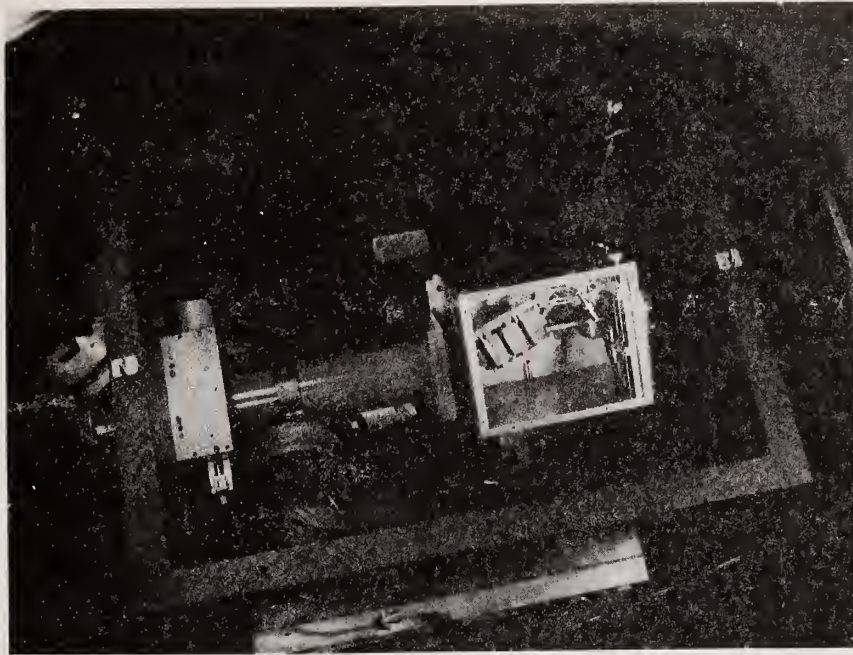
Fig. 4 Apparatus for gravitationally-induced interference.

where k is the neutron wave vector ($2\pi/\lambda$) and E its energy. For $\lambda = 1.4$ Å (E = 0.0472 ev), our sensitivity to a potential is then

$$V = \Delta\beta \ \frac{2E}{kS} = \ 3.7 \times 10^{-14} eV \tag{5}$$

Let us compare this number with the gravitational potential energy of a neutron at the center of a solid sphere of radius Rand density ρ, which is given by the formula

$$V_{sphere} = -2\pi Gm\rho R^2 \ . \tag{6}$$

For a sphere of radius R = 1m and density $\rho = 10$ gm/cm^3, we get

$$V_{sphere} = 4.4 \times 10^{14} ev \ . \tag{7}$$

This potential is therefore of the same order as our current sensitivity in neutron interferometry. The difficulty in performing this "Neutron Cavendish" experiment is one of geometry; one needs the gravitational potential of this sphere (or other massive body) to act preferentially on one beam only. Clearly if we could build a neutron interferometer of linear dimensions of 1m, the necessary beam separation for this experiment would be adequate. Long-base line interferometry (as discussed in R. Deslattes paper) is essential to this and several other experiments. The necessary requirements on thermal and microphonic stability (as discussed by J. Arthur) will be severe. Experiments of this type designed explicitly for a guide hall, far from the noise and pumps of the reactor, have a much higher probability for success. The very-low backgrounds and long-wavelength neutrons inherent in guide-hall/cold source experiments are also important. Other concepts, such as the

Wheeler delayed-choice experiment, higher order gravity experiments, and the measurement of the electric polarizability of the neutron would also most easily be pursued with long-wavelength neutrons in the "quiet" environment obtainable in a neutron guide hall.

Table I (Part 1)   Neutron Interferometry Experiments   (1974-1985)

EXPERIMENT	TECHNIQUE	NEUTRON SOURCE/LOCATION	REFS.
First successful test of the perfect Si crystal neutron interferometer	Thermal, monochromatic neutrons, 3-crystal LLL interferometer	TRIGA, Vienna, Austria (1974)	2.
Observability of 2π-rotations of Fermions	• LLL perfect Si crystal interferometer • Fresnel diffraction of long-λ neutrons at a Bloch Wall	MURR, Columbia, MO, USA HFR, Grenable, France (1975,1976)	3.
Gravitationally - Induced Quantum Interference	LLL perfect Si crystal interferometer	FNR, Ann Arbor, MI, USA MURR, Columbia, MO, USA (1975,1980,1985)	4.
Neutron Sagnac Effect: • Effect of Earth's rotation on Neutron's phase • Laboratory turntable	• LLL perfect Si crystal interferometer • LL-two crystal interferometer	MURR, Columbia, MO, USA (1979) MITR, Cambridge, MA, USA (1984)	5.
Neutron Fizeau Effect: Phase shift of neutrons due to moving matter	• Long-λ, optical bench, interference by division of wave-front • LLL perfect Si-crystal interferometer (a) Moving boundaries (b) Stationary boundaries	HFR, Grenoble, France (1981) HFR, Grenoble, France MURR, Columbia, MO, USA (1985)	6.

101

Table I (Part 2) Neutron Interferometry Experiments (1974-1985)

EXPERIMENT	TECHNIQUE	NEUTRON SOURCE/LOCATION	REF.
Search for non-linear terms in the Schrödinger	• LL-two crystal interferometer • Long-λ Fresnel diffraction	MITR, Cambridge, MA, USA (1980) HFR, Grenoble, France (1981)	7.
Search for an Aharanov-Bohm effect for Neutrons	• LL-two crystal interferometer	MITR, Cambridge, MA, USA (1981)	8.
Focussing of Neutrons with a zone plate	20 Å-neutrons, optical bench	HFR, Grenoble, France (1979)	9.
Precision measurement of the longitudial coherence length of a neutron beam	LLL perfect Si crystal interferometer	MURR, Columbia, MO, USA (1983)	10.
Measurement of the scattering lengths of various isotopes, including the energy dependence. Sm-149, U-238, U-235, Eu, Gd, Dy, etc.	LLL perfect Si-crystal interferometer	HFR, Grenoble, France MURR, Columbia, MO, USA (1975-1985)	11.
Coherent superposition of spin states	RF flipper and DC flipper in LLL-perfect Si interferometer	HFR, Grenoble, France (1983)	12.
4-body nuclear interaction n-^{3}He, n-^{3}H	Gas-cell in LLL-perfect Si crystal interferometer	HFR, Grenoble, France (1979-1985)	13.

102

Table I (Part 3)   Neutron Interferometry Experiments   (1974-1985)

EXPERIMENT	TECHNIQUE	NEUTRON SOURCE/LOCATION	REFS.
Young's double slit experiment with neutrons	20A-neutrons, optical bench Boron-wire slits	HFR, Grenoble, France (1982)	14.
Search for Quaternions in Quantum Mechanics	Ti and Al foils in LLL-perfect Si interferometer	MURR, Columbia, MO, USA (1984)	15.
Quantum Interference in Accelerated Frames	Accelerating/Oscillatin LLL-perfect-Si crystal interferometer	HFR, Grenoble, France (1983)	16.
Search for neutral guage vector boson	Rotating U rod in LL-two crystal interferometer.	MITR, Cambridge, MA, USA (1983)	17.
Static vs. Time-dependent absorption in neutron interferometry	Rotating slotted absorber wheel in LLL-perfect Si interferometer	HFR, Grenoble, France (1984)	18.
First successful operation of a Neutron Microscope: Magnification of x 50	Acromatic two-mirror divice using ultra-cold neutrons	HFR, Grenoble, France (1985)	19.
Diffraction grating interferometer	Thermal Neutrons, small beam separation	IRT, Latvia, SSR (1985)	20.

(REFERENCES)

1. U. Bonse, "Principles and Methods of Neutron Interferometry", in Neutron Interferometry, ed. U. Bonse and H. Rauch, Clarenden Press, Oxford, p.3 (1979).

2. H. Rauch, W. Treimer and U. Bonse, Phys. Lett. 47A, 369 (1974).

3. (a) S. A. Werner, R. Colella, A. W. Overhauser and C. F. Eagen, Phys. Rev. Lett. 35, 1053 (1975).
    (b) H. Rauch, A. Zeilinger, G. Badurek, A. Wilfing, W. Bauspiess and U. Bonse, Phys. Lett. 54A, 425 (1975).
    (c) A. G. Klein and G. I. Opat, Phys. Rev. Lett. 37, 238 (1976).

4. (a) R. Colella, A. W. Overhauser and S. A. Werner, Phys. Rev. Lett. 34, 1472 (1975).
    (b) J.-L. Staudenmann, S. A. Werner, R. Colella and A. W. Overhauser, Phys. Rev. A21, 1419 (1980).
    (c) S. A. Werner, H. Kaiser, M. Arit, R. R. Berliner and H.-C. Hu, International Conference on Neutron Scattering (Santa Fe, Aug. 1985) to be published in Physica.

5. (a) S. A. Werner, J.-L. Staudenmann and R. Colella,, Phys. Rev. Lett. 42, 1103 (1979).
    (b) D. K. Atwood, M. A. Horne, C. G. Shull and J. Arthur, Phys. Rev. Lett. 52, 1673 (1984).

6. (a) A. G. Klein, G. I. Opat, A. Cimmino, A. Zeilinger, W. Treimer and R. Gähler, Phys. Rev. Lett. 46, 1551 (1981).
    (b) M. Arif, H. Kaiser, S. A. Werner, A. Cimmino, W. A. Hamilton, A. G. Klein, and G. I. Opat, Phys. Rev. A. (Rapid Communications) 31, 1203 (1985).
    (c) U. Bonse and A. Rumpf, Acta Cryst. 40A, (1984) and to be published Phys. Rev. Lett. (1985).

7. (a) C. G. Shull, D. K. Atwood, J. Arthur and M. A. Horne, Phys. Rev. Lett. 44, 765 (1980).
    (b) R. Gähler, A. G. Klein and A. Zeilinger, Phys. Rev. A23, 1611 (1981).

8. D. M. Greenberger, D. K. Atwood, J. Arthur, C. G. Shull, M. Schlenker, Phys. Rev. Lett. 47, 751 (1981).

9. A. G. Klein, P. D. Kearney, G. I. Opat, A. Cimmino and R. Gähler, Phys. Rev. Lett. 46, 959 (1981).

10. H. Kaiser, S. A. Werner and E. A. George, Phys. Rev. Lett. 50, 560 (1983).

11. (a) H. Rauch and D. Tuppinger, Z. Phys. A322 (1985).

    (b) H. Kaiser, M. Arif, S. A. Werner, and J. O. Willis,
        Int. Conf. on Neutron Scattering (Santa Fe, Aug.1985) to
        be published in Physica.
    (c) R. E. Word and S. A. Werner, Phys. Rev. B26, 4190 (1982).

12. (a) J. Summhammer, G. Badurek, H. Rauch, U. Kischko, and A.
        Zeilinger, Phys. Rev. A27, 2523 (1983).
    (b) G. Badurek, H. Rauch and J. Summhammer, Phys. Rev.
        Lett. 51, 1015 (1983).

13. (a) H. Kaiser, H. Rauch, G. Badurek, W. Bauspiess and U.
        Bonse, Z. Phys. 291, 231 (1979).
    (b) H. Rauch, D. Tuppinger, H. Wölwitsch and T. Wroblewski,
        to be published in Phys. Lett. B (1985).

14. A. Zeilinger, R. Gähler, C. G. Shull and W. Treimer, Symp. on
    Neutron Scattering, Argonne National Laboratory, AIP Conf.
    Proc. No. 89, p. 93 (1982).

15. H. Kaiser, E. A. George and S. A. Werner, Phys. Rev. A29,
    2276 (1984).

16. U. Bonse and T. Wroblewski, Phys Rev. Lett. 51, 1401 (1983).

17. A. Zeilinger, M. A. Horne and C. G. Shull, Proc. Int. Symp.
    on the Foundations of Quantum Mechanics, Tokyo, p. 289
    (1983).

18. H. Rauch and J. Summhammer, Phys. Lett. 104, 44 (1984).

19. P. Herrmann, K.-A. Steinhauser, R. Gähler, A. Steyerl, and W.
    Mampe, Phys. Rev. Lett. 54, 1969 (1985).

20. A.I. Ioffe, V.S. Zabiyakin, G.M. Drabkin, Phys. Lett. III,
    373 (1985).

21. (a) A. G. Klein and S. A. Werner, "Neutron Optics", Rep.
        Prog. Phys. 46, 259 (1983).
    (b) S. A. Werner and A. G. Klein, "Recent Advances in Neutron
        Optics", to be published as Chap. 4 in Neutron
        Scattering, ed. D.-L. Price and K. Sköld, Academic
        Press. (Dec. 1985).

# PERFECT CRYSTAL SYSTEMS FOR ADVANCED INTERFEROMETER AND RESONATOR DEVICES

H. Rauch
Atominstitut der Österreichischen Universitäten
A 1020 Vienna, Austria

During the last decade perfect crystal interfero-
metry became a new tool for fundamental, nuclear and
solid state physics investigations. A nondispersive
measuring method has proven its capability for increa-
sing the sensitivity of the interferometric method.
Multi-plate interferometry is discussed in respect to
new kinds of phase echo systems and delayed choice ex-
periments. Perfect crystal systems may be useful for
the invention of resonators too. For pulsed sources
various resonators systems using crystals are discussed
which become more powerful by a combination with active
energy shift devices. Resonators for stationary sources
are another primising project.

1. Introduction

The perfect arrangement of the atoms within a perfect crystal
provide the basis for the further development of coherent neutron
optics. Such crystals were used successfully in the past for high
angular resolution nondispersive double crystal arrangements /1/,
for high energy resolution backscattering instruments /2/ and for
perfect crystal interferometry /3/. Monolithicly designed neutron
interferometers were used during the last decade for the realiza-
tion of many basic experiments of quantum mechanics on a macro-
scopic scale with massive particles (e.g./4,5/). Nevertheless,
the status of neutron optics is far
behind the achievements known in
light and electron optics.
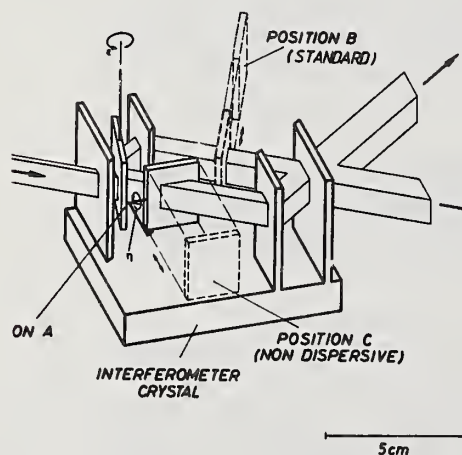
Opticaly active components such as
moving crystals, moving plates, tra-
velling magnetic fields or neutron
magnetic resonance systems may create
new advanced possibilities /6-10/.
The combination of perfect crystal
diffraction with magnetic systems
becomes obvious because the reflec-
tion width of perfect crystals match
well with the Zeman energy shift of
magnetic fields. Various systems
which are in the status of testing
or consideration will be discussed.

Fig.1: Skew symmetricly cut interferometer crystal and indication
of a nondispersive measuring method.

2. Nondispersive Neutron Interferometry

The present status of neutron interferometry has been discussed in the previous contribution by Werner /11/. Recently we have tested a rather large skew symmetricly cut interferometer and nondispersive measuring method (Fig.1 /12/). In the standard measuring method the phase shift and, therefore, the interference pattern depends on the wavelength which causes certain limitations.

$$\chi = (n - 1)kD = - Nb_c \lambda D \qquad (1)$$

$$I = |\psi^I + \psi^{II}|^2 \propto [1 + \cos(Nb_c \lambda D)] \qquad (2)$$

N denotes the particle density, b_c the coherent scattering length and D the thickness of the sample. The contrast of the interference pattern decreases for high orders ($m = Nb_c \lambda D/2\pi$) due to the wavelength spread $\Delta\lambda$ of the beam. For a Gaussian distribution this decrease of the contrast can be written as $B(m) = B(0) \exp [-(1.88\ m\Delta\lambda/\lambda_0)^2]$ /13,14/. Therefore, the number of interference fringes is limited and for precision experiments a separate and accurate measurement of the wavelength distribution is required. This can be omitted when the sample is inserted parallel to the reflecting planes (position C in Fig.1). In this case the beam path in the sample becomes $D_0/\sin\Theta_B$ and in combination with the Bragg-equation one obtains a phase shift $\chi = -Nb_c\lambda D = -2\ d_{hkl} Nb_c D_0$, which is independent from the wavelength and, therefore, also from the wavelength distribution. This feature enables the use of a broad spectrum and provides high intensity which permits phaseshift determinations at an accuracy level better than 10^{-6}.

The reduction of the contrast appears at much higher interference orders and is primarily determined by defocusing effects which
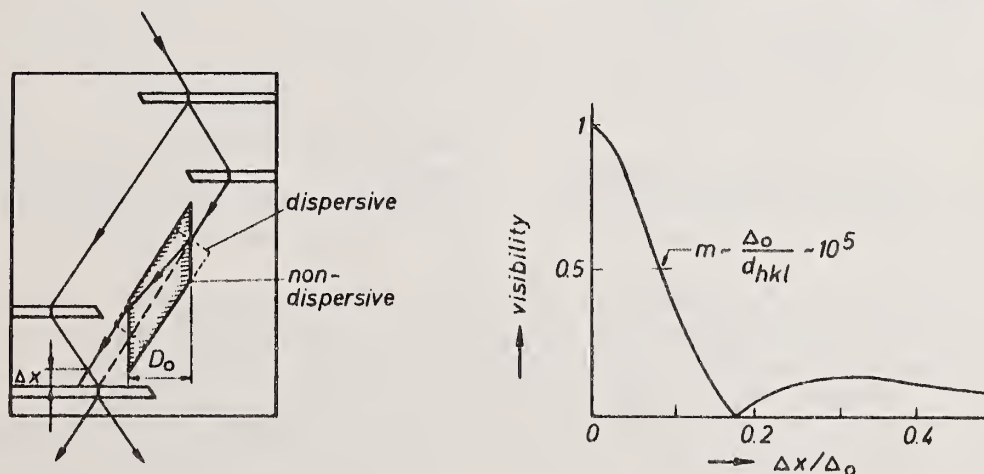

Fig.2: Principle of the nondispensive measuring method and reduction of the visibility of the interference pattern due to defocusing effects.

become visible when the defocusing $\Delta x = d_{hkl} D_0 \, Nb_c \lambda/(2\pi\cos\Theta_B)$ approaches the Pendellösung length Δ_0 of the crystal (e.g./15/). This happens at about the 10^5 th interference order and a residual contrast remains up to even higher orders (Fig.2). This new method has been tested /12/ and very recently we have observed the more than 500th interference order with a 35 mm thick Bi-sample and with a beam monochromacy of only $\Delta\lambda/\lambda = 0.011$. The results are shown on a transparency but they are not included in the proceedings since data evaluation is still in progress.

Another topic we are dealing with is multiplate interferometry where the field of phase echo spectroscopy can be extended /16, 17/ and where new kinds of delayed choice experiments become feasible. A first attempt in this direction was the observation of the different influence on the interference pattern of a static and of a time-dependent absorber /18/. The development of polylithic interferometers - as they exist for X-rays-will follow but will be quite difficult.

3. Gated Crystal Resonators

In the backreflection position the angle of acceptance becomes wide and the plateau of the Darwin reflection curve corresponds to a momentum transfer width of
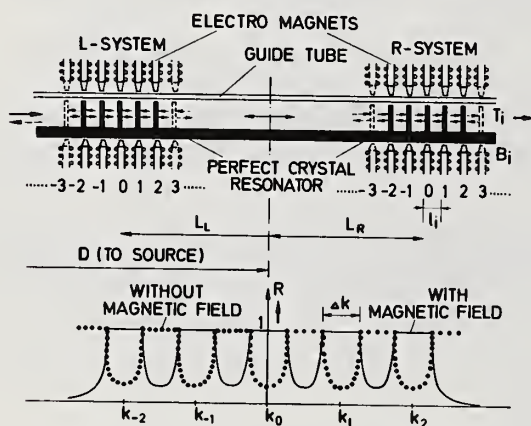
Fig.3: Principle of a multiplate resonator based on magneticly gated crystals.

$$\Delta k \stackrel{\sim}{-} 4 \, k \, N_c b_c \, |F| d^2_{hkl}/\pi \qquad (3)$$

where N_c is the number of unit volumes. On the other hand, the Zeman energy splitting inside a magnetic field B is

$$\Delta k_m = \pm \, \mu Bm/\hbar^2 k \qquad (4)$$

and it can be used to shift the momentum of the neutron beam relative to the Darwin width of the crystal /19,20/. The open and closed position can be controlled by a proper operation of the magnets and neutrons can be caught between the crystals. The efficiency can be increased by a multiplate system maintaining a proper temperature gradient between the crystal plates (Fig.3/10/). For the (111) backreflection from silicon (λ=6.275 Å) the required magnetic field to change from the open to the closed position is 12.6 kG and the necessary temperature difference between the plates is 16°C. The losses within the Darwin width due to crystal reflections are expected to be quite small ($2.2.10^{-5}$) permitting many reflections. The transversal losses have to be minimized by guide tubes.

Fig.4: (x,t) diagram for a multiplate resonator without (left) and with (right) optically active components in between the plates.

The behaviour of the beam in an (x,t)-diagram is shown in Fig.4a. The system can be made even more effective if a neutron magnetic resonance system /21/ or a travelling magnetic wave system /10/ is placed and properly operated between both crystal systems. The additional energy change can be used either for the production of very monochromatic pulses (Fig.4b), or for a time-focusing or for a division of a long pulse into short pulses. For the operation mode shown in Fig.4b the following feasible parameters have to be fulfilled: pulse width of the source 100 μs, distance of the crystal system behind the source 10 m, strength of the guide field of the neutron magnetic resonance system B_0 = 20 kG, distance of the crystals 8.2 cm, temperature difference 8°C and gating field 12.6 kG.

4. Stationary Crystal Resonators

Resonators for ultra-cold neutrons have been developed on the basis of Fabry-Perot interferometers known in light optics /22, 23/. Resonators in the Å-region would be of great interest not only for neutron application. Instead of intensity resonators as discussed in the previous chapter, here the coherence of the beam and the perfectness of the crystal become important. For a two plate resonator as shown in Fig.5, one obtains from the light optics analog for the standing wave between the crystals /24,25/.

$$\Psi_2 = \frac{\Psi_1 \sqrt{1 - v_1^2}(y) \; [1 + e^{-(\Sigma_r - 2ik)(L - x)} v_2(y) e^{i\rho_2(y)}] e^{-(\Sigma_r - ik)x}}{1 - e^{-\Sigma_r L} v_1(y) v_2(y) e^{i(\rho_1 + \rho_2 + 2kL)}} \qquad (5)$$

which shows resonance for

$$\rho_1(y) + \rho_2(y) + \chi(y) + 2kL = 2\pi n \qquad (6)$$

v and ρ characterize the change of the amplitude and of the phase
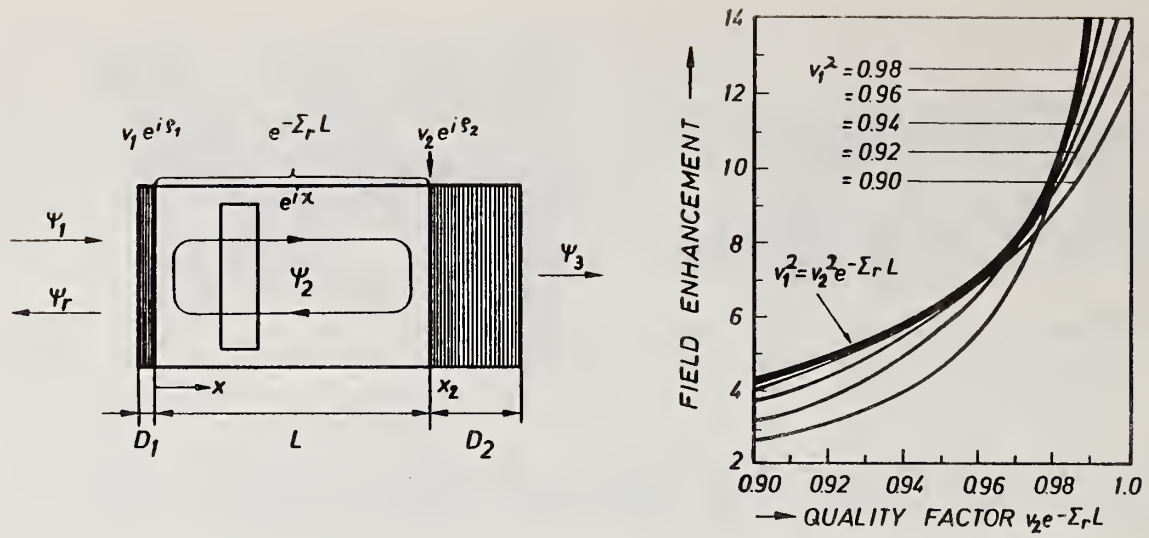
Fig.5: Stationary crystal resonator with a dispersion sensitive compensator $\chi(y)$.

of the wave function during crystal reflection. They can be taken from dynamical diffraction theory and they read for a symmetrical and even backreflection in the standard neutron notation as (e.g. /15/, $A = \pi D/\Delta_0$).

$$\Psi_G = \frac{-i \sin (A\sqrt{y^2 - 1})e^{2\pi i(y + 1)x_2/\Delta_0}}{\sqrt{y^2 - 1} \cos (A\sqrt{y^2 - 1}) - iy \sin (A\sqrt{y^2 - 1})} \, e^{ikx} = ve^{i\rho}e^{ikx} \qquad (7)$$

For a resonant behaviour only the region $|y| < 1$ is of interest and there one gets

$$v = [\, y^2 + (1 - y^2)\, \text{cotgh}^2(A\sqrt{1 - y^2})\,]^{-1/2} \qquad (8)$$

$$\rho = 2\pi(y + 1)x_2/\Delta_0 - \text{arctg} \,[\frac{\sqrt{1 - y^2}}{y} \, \text{cotgh}(A\sqrt{1 - y^2})] \qquad (9)$$

where for thick crystals the second term tends to $\pi/2$. The optimal coupling between the outer and the inner region occurs at

$$v_1{}^2(y) = v_2{}^2(y)e^{-\Sigma_r L} \qquad (10)$$

which can be controled by the thickness of the first crystal. The maximal intensity at the nodes inside the resonator then becomes

$$(\Psi_2{}^*\Psi_2)_{opt} = \frac{1 + e^{-\Sigma_r L/2}v_2}{1 - e^{-\Sigma_r L/2}v_2} \qquad (11)$$

which is also shown in Fig.5. First calculations show promising
results for a reasonable band of y values. Quality factors
($e^{-\Sigma_r L/2}v_2 > 0.99$) seem to be feasible for the neutron case and
related enhancement factors can be expected. The requirements
concerning $\chi(y)$ will be discussed.

References

/ 1/ C.G.Shull, K.W.Billman, F.A.Wedgewood; Phys.Rec.153(1967)1415
/ 2/ B.Alefeld; Sitzungsberichte Bayrische Akademie d. Wissen-
      schaften 11(1966)109
/ 3/ H.Rauch, W.Treimer, U.Bonse; Phys.Lett.A47(1974)369
/ 4/ U.Bonse, H.Rauch (Edr.) "Neutron Interferometry" Clarendon
      Press, Oxford 1979
/ 5/ A.G.Klein, S.A.Werner, Rep.Progr.Phys.46(1983)259
/ 6/ B.N.Brockhouse; Proc.Inel.Scatt.Neutr.Solids a.Liquids,
      p.113, IAEA - Vienna 1969
/ 7/ A.Steyerl; Nucl.Instr.Meth.125(1975)461
/ 8/ B.Alefeld, G.Badurek, H.Rauch; Z.Physik B41(1981)231
/ 9/ H.Rauch; Physica 120B+C(1983)71
/10/ H.Rauch; "Neutron Scatt. in the 90-ties", p.35, IAEA-Vienna
      1985
/11/ S.A.Werner; this Workshop
/12/ H.Rauch, D.Tuppinger; Z.Physik, A322(1985)
/13/ H.Rauch; in /4/ p.161
/14/ H.Kaiser, S.A.Werner, E.A.George; Phys.Rev.Lett.50(1983)560
/15/ U.Bonse, W.Graeff; in "XRay Optics" (Ed.H.J.Oueisser)
      Springer-Verlag, Top.Appl.Phys.22(1977)
/16/ G.Badurek, H.Rauch, A.Zeilinger; in "Neutron Spin Echo"
      (Ed.F.Mezei), Springer Verlag, Lect.Notes in Phys.128(1980)
      136
/17/ D.Petraschek, H.Rauch, D.Tuppinger; in preparation
/18/ H.Rauch, J.Summhammer; Phys.Lett.104(1984)44
/19/ S.Funahaski; Nucl.Instr.Meth.137(1976)99
/20/ B.Alefeld, G.Badurek, H.Rauch; Phys.Lett.83A(1981)32
/21/ B.Alefeld, G.Badurek, H.Rauch; Z.Physik B41(1981)231
/22/ K.A.Steinhauser, A.Steyerl, H.Scheckenhofer, S.S.Malik;
      Phys.Rev.Lett.44(1980)1306
/23/ A.Steyerl, T.Ebisawa, K.A.Steinhauser, M.Utsuro; Z.Physik
      B41(1981)283
/24/ M.Born, E.Wolf, "Principles of Optics", Pergamon Press Ox-
      ford 1980
/25/ H.Kogelnik, T.Li; Proc.IEEE 54(1966)1312

LONG WAVELENGTH NEUTRON INTERFEROMETRY

Anton Zeilinger
Atominstitut der Österreichischen Universitäten
Schüttelstraße 115, A-1020 Wien
Austria
and
Department of Physics
Massachusetts Institute of Technology
Cambridge, MA 02139
U.S.A.

Neutrons in the wavelength range around 20 $\overset{\circ}{A}$ have been used for various optical and interferometric experiments. Some of these experiments concerned precision measurements of the diffraction of neutrons at an absorbing edge and at single and double slit assemblies. The results are in perfect agreement with standard linear wave mechanics and place stringent limits on alternative nonlinear variants of the theory. Another experiment concerned the neutron Fizeau effect which demonstrates the relativistic transformation laws for Schrödinger wave functions. Future experiments with 80 - 100 $\overset{\circ}{A}$ wavelength neutrons will lead to an improvement over the precision of existing experiments. Also, neutron analogs to the Aharonov-Bohm effects and various time-dependent experiments will become realizable with a very long wavelength neutron interferometer using phase gratings as optical elements. Such gratings are based on the earlier successful tests of Fresnel lenses for very cold neutrons.

The successful development of perfect crystal neutron interferometers has led to various most elegant experiments /1,2/. The use of interferometers of this type implies Bragg diffraction and therefore is limited to neutrons in the thermal energy range. An extension to lower energies facilitates the use of time-switched devices and of large-area interferometers.

Concerning the terminology, we note, that cold neutrons are usually understood as those of a few Ångstrom wavelength, while ultracold neutrons are of energy low enough to be totally reflected at all angles of incidence. It is therefore useful, to denominate neutrons in between these two as very cold neutrons. This would then describe neutrons with temperatures between 10^{-2} K and 10K or wavelengths between ca. 10 $\overset{\circ}{A}$ and 300 $\overset{\circ}{A}$ /3/, obviously with some overlap. It is interesting to note, that presently only very little experimentation exists in that energy range. Yet, the advantages of that energy range for neutron optical and interferometric experiments are clear: the refractive

index can already differ from unity enough to facilitate the
operation of more conventional optical elements, and lenses etc.
can still be penetrated by the neutrons. In the following I will
firstly briefly review some of the experiments already performed
with 20 Å neutrons and I will discuss some future possibilities.

The experiments performed hitherto utilized a beam from the cold
source of the ILL High Flux Reactor monochromatized by quartz
prism refraction /4/. With a wavelength of 20 Å detailed
diffraction patterns at macroscopic objects may already be ob-
served. For example, diffraction at a double slit assembly of
100 μm separation between the slits results in a 100 μm spatial
separation between the peaks after a flight path of 5 m length.
Interestingly, at that distance the width of the first Fresnel
zone happens to be of the same magnitude.

Besides its demonstrational value, the study of diffraction at
simple objects also serves as a tool for precision tests of
standard quantum mechanics. For example, it has been conjectured
by various authors, that the linear Schrödinger equation could
be the limit of a higher nonlinear one /5/. In view of the
epistemological relevance of the linearity, experimental tests
are most useful despite the fact, that any possible nonlinear
deviation has to be exceedingly small.

The most basic consequence of the linearity of quantum mechanics
is the unrestricted validity of the superposition principle /6/.
The most direct experimental test of linear quantum superposit-
ion is provided by the double-slit diffraction experiment /7/
(Figure 1). In particular, the experiment tests against any un-
known non-unitary evolution of the two spatially separated
states representing the two partial beams. Such a non-unitary
evolution would result in a reduction of interference contrast
as a function of evolution time. Parametrizing this reduction by
an exponential law $\exp(-t/\tau)$ the excellent agreement between
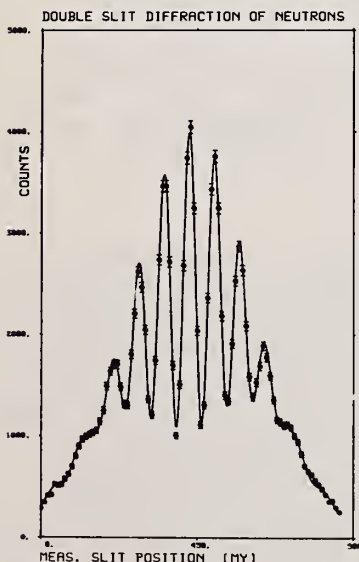
Figure 1: Diffraction of neutrons
with a wavelength of 18.5 Å at a
22-104-23 μm absorbing double slit
assembly. Experimental points shown
with the prediction from standard
linear quantum mechanics. The abscissa
runs from 0 to 100 μm and the ordinate
axis from 0 to 5000 counts.

linear quantum mechanical prediction and experiment (Fig.1)
results in a lower limit of τ = 8sec. Future experiments with
very cold neutrons will improve this limit by at least one
order of magnitude.

Using the same experimental arrangement, diffraction at single
slit assemblies was also studied. Figure 2 shows a typical

SINGLE SLIT DIFFRACTION OF NEUTRONS
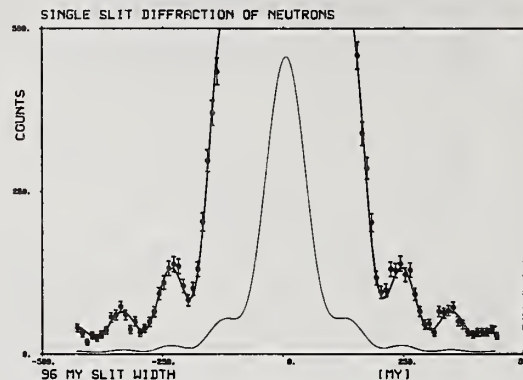
Figure 2: Diffraction pattern of very cold neutrons at a 96 μm
wide absorbing slit. The abscissa is the scanning slit position
and it runs from –500 to +500 μm, the ordinate runs from 0 to
500 counts. The data collecting time was 192 minutes per point.

experimental result. In order to demonstrate in detail the
agreement with theory (solid line), only the wings of the
diffraction pattern amplified by a factor of ten are shown.
The solid line was fitted to the central maximum.

A specific class of possible experiments results, whenever an
alternative nonlinear theory is developed far enough to result
in detailed experimental predictions. This holds for example
for the nonlinear Schrödinger equation proposed by Bialynicki-
Birula and Mycielski who added a term $b.\ln|\psi|^2$ to the linear
Schrödinger equation /5/. Study of the Fresnel diffraction at
an absorbing edge /8/ did provide an upper limit $b=3.3 \times 10^{-15}$eV.
Due to the 1/E dependence of the effect, future experiments with
100Å neutrons should result in an improvement of about two
orders of magnitude.

The low speed of very cold neutrons is of distinct advantage for
experiments studying the effects of time-varying fields or of
moving matter. In the neutron Fizeau experiment, being of the
latter type, a phase shifter plate is moved in the interfero-
meter. It is found, that whenever the neutron optical potential
is wavelength independent, the Fizeau effect depends only on the
motion of the phase shifter surfaces /9/. This result is a con-
sequence of the relativistic transformation properties of the
wavefunction. A most interesting consequence of these conside-
rations is, that the neutron inside a moving plate has a

frequency differing by $\Delta\omega = -(V/\hbar)(v/v_n)$ from that in the vacuum. Here, V is the neutron optical potential and v is the phase shifter's speed parallel to the neutron speed v_n. The resulting phase shift $\varphi_{Fiz.} = -kD(V/2E)(v/v_n)$ for a phase shifter with thickness D is proportional to $1/E$ and was first measured with 20Å neutrons /10/. The prediction of zero phase shift for matter moving parallel to its boundaries, which has also found experimental verification /11/, has recently been shown to be an approximation /12/. Particularly, due to mutiple scattering the neutron optical potential could still be slightly velocity dependent even with a constant scattering length. The predicted effect is largest in the very cold neutron region.

A related experimental situation arises, if some interaction is switched on and off over a larger region of space, such that the neutron does not experience any spatial potential boundaries, i.e. no forces. For the electron, this is the case for the electric Aharonov-Bohm effect /13/ which, due to experimental difficulties has not yet been verified. Specifically, if the potential is V, the Aharonov-Bohm phase shift is $\varphi_{AB} = -\frac{1}{\hbar}\int V(t)\cdot dt$ which is non-dispersive. Thus, no measurement performed on the individual beams could reveal which of the beams was subject to the time-dependent potential.

We note two connections of this to the neutron case. Firstly, that part of the Fizeau phase shift which is due to the frequency change is also dispersion free. Secondly, by using properly switched time-dependent magnetic fields, a neutron analog could be performed /14/. In order to render not even the torque on the neutron detectable either unpolarized neutrons or neutrons polarized in an eigenstate of the magnetic field should be used. A possible experimental setup for very cold neutrons is shown in Figure 3 where the time-dependent magnetic field is
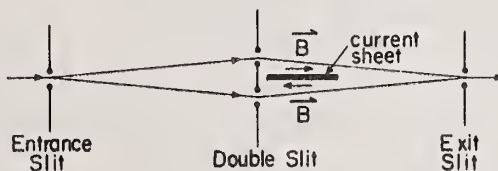
Figure 3: A possible neutron analog to the electric Aharonov-Bohm effect.

generated by a time-dependent current through a current sheet arranged between the beams of a double slit experiment. Such an experiment is clearly feasible since for very cold neutrons and a current sheet of some 10 cm length, magnetic fields in the range of a few Gauß switched with Kilohertz frequencies suffice. It will be interesting to demonstrate the property, that in such an experiment the phase shift is nondispersive. This can be done by contrasting it with a static experiment using the same field strength and demonstrating, that for large enough fields the interference contrast vanishes in the static case only.

Interestingly, there exist also analogs to the static Aharonov-Bohm case. One possible case arises in experiments searching for unknown gauge-type interactions of the neutron. Specific experiments were first proposed by Wu and Yang /15/ in order to search for a possible long-range non-Abelian interaction tied to the conservation of isospin. In analogy to the electron case where an electron current is setup between the arms of an electron interferometer, in the neutron case an **isospin current** has to be set up inside the neutron interferometer (Figure 4).
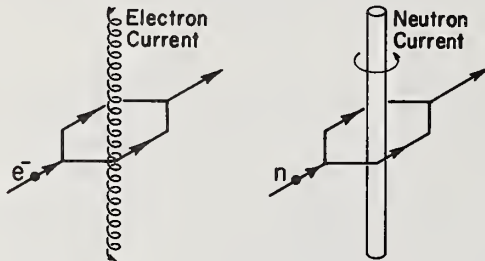

Figure 4: Principle of a neutron Aharonov-Bohm experiment searching for an unknown gauge interaction of the neutron (right) and an electron Aharonov-Bohm setup (left).

This is most easily done by inserting a Uranium rod which has a high net isospin into a neutron interferometer and spinning it rapidly. An experimental search /16/ based on that proposal with a perfect crystal interferometer gave a null result which implies that any non-Abelian gauge interaction connected to isospin is certainly smaller than 5×10^{15} of the electromagnetic one for ranges of millimeters and more. It has been proposed by Shapiro /17/ that this limit could be improved by using a very cold neutron interferometer mainly due to the larger area available then between the beams.

It was pointed out above, that a significant feature of the Aharonov-Bohm effects is the dispersion-free phase shift. We note therefore that the neutron spin-orbit interaction is due to a Hamiltonian $\vec{\mu} \cdot (\vec{k} \times \vec{E})$ which is inversly proportional to the neutron wavelength. This implies again a dispersion-free phase shift for a neutron passing the electric field of a charged wire arranged in the topology of Figure 4. It has been poited out by Aharonov and Casher /18/ that this analogy to the Aharonov-Bohm effect is not coincidental, since a Lagrangian can be constructed which has both effects as its consequence. Due to the non-dispersiveness of this effect the advantage of very cold neutrons does not stem from their speed but from the possibility of having larger area interferometers permitting higher electric charge to be arranged between the interferometer beams.

So far I have not discussed the possible technological developments for very cold neutrons. As an example I point out that a most promising avenue for very cold neutron interferometry is to use sinusoidal phase gratings as the coherent beam splitters. Such gratings would be based on the successful tests of Fresnel

lenses for very cold neutrons /19/. Their usefulness for inter-
ferometry was demonstrated by the development of a Billet-type
split-lens interferometer /20/. Most recently, in a remarkable
achievement, Ioffe, Zabiyakin and Drabkin /21/ could construct
an interferometer for 3.15 Å neutrons based on diffraction
gratings operating in the reflection mode.

I acknowledge useful discussions and a most exiting cooperation
with R.Gähler (Munich), D.Greenberger (New York), M.A.Horne
(M.I.T.), A.G.Klein (Melbourne), G.I.Opat (Melbourne), H.Rauch
(Vienna), C.G.Shull (M.I.T.) and W.Treimer (Berlin).

References

/1/ U.Bonse and H.Rauch (Eds): Neutron Interferometry, Oxford
    University Press, Oxford, 1979.
/2/ H.Rauch in 'Foundations of Quantum Mechanics', S.Kamefuchi et
    al. (Eds), Phys.Soc.Japan, Tokyo, 1984, p. 277.
/3/ A.Steyerl, 'Neutron Physics' p.57, Springer Tracts in Modern
    Physics, Vol. 80, Springer-Verlag, Berlin, 1977.
/4/ R.Gaehler, J.Kalus and W.Mampe, J.Phys.E 13,546(1980).
/5/ P.Pearle, Phys.Rev. D13,857(1976) and D29,235(1984).
/6/ A.Zeilinger in 'Quantum Concepts in Space and Time', R.Pen-
    rose and C.Isham (Eds), Oford University Press (in press).
/7/ A.Zeilinger, R.Gähler, C.G.Shull and W.Treimer, in 'Neutron
    Scattering', Amer.Inst.Phys.Conf.Proc. No. 89, p.93.
/8/ R.Gähler, A.G.Klein and A.Zeilinger, Phys.Rev. A23,1611(1981).
/9/ M.A.Horne, A.Zeilinger, G.I.Opat and A.G.Klein, Phys.Rev.
    A28,1(1983).
/10/A.G.Klein, G.I.Opat, A.Cimmino, A.Zeilinger, W.Treimer and
    R.Gähler, Phys.Rev.Lett. 24, 1551(1981).
/11/M.Arif, H.Kaiser, S.A.Werner, A.Cimmino, W.A.Hamilton,
    A.G.Klein and G.I.Opat, Phys.Rev. A31,1203(1985).
/12/V.F.Sears, Phys.Rev. A32,2524 (1985).
/13/Y.Aharonov and D.Bohm, Phys.Rev. 115,485(1959).
/14/A.Zeilinger, J.physique 45,C3-209(1984).
/15/T.T.Wu and C.N.Yang, Phys.Rev. D12,3845(1975).
/16/A.Zeilinger, M.A.Horne and C.G.Shull in 'Foundations of
    Quantum Mechanics', S.Kamefuchi et al. (Eds), Phys.Soc.Japan,
    Tokyo, 1984, p. 289.
/17/I.S.Shapiro, Pis'ma Zh.Eksp.Teor.Fiz. 35,39(1982).
/18/Y.Aharonov and A.Casher, Phys.Rev.Lett. 53,319(1984).
/19/P.D.Kearney, A.G.Klein, G.I.Opat and R.Gähler, Nature 287,
    313(1980) and A.G.Klein, P.D.Kearney, G.I.Opat and R.Gähler
    Phys.Lett. 83A,71(1981).
/20/A.G.Klein, P.D.Kearney, G.I.Opat, A.Cimmino and R.Gähler,
    Phys.Rev.Lett. 46,959(1981).
/21/A.I.Ioffe, V.S.Zabiyakin and G.M.Drabkin, Phys.Lett. 111,373
    (1985).

LONG BASELINE NEUTRON INTERFEROMETRY

R. D. Deslattes
National Bureau of Standards
Gaithersburg, Maryland 20899

Some potential generalizations of crystal diffraction
interferometers are considered in regard to technical feasi-
bility and application. Emphasis is placed on large scale
systems with characteristic dimensions of the order of 1
meter using laser interferometry to actively stabilize
separated diffraction elements.

1. Background and Motivation

The general status of neutron interferometry was reviewed during this
workshop by S. Werner.[1] Previously, A. Klein and S. Werner had published
a fuller account of the field, to which the interested reader is
referred.[2] Werner sees the past accomplishments as demonstrating that
these modest Si objects provide an excellent laboratory environment for
conducting the **gedanken** experiments of quantum mechanics. I agree with
this point of view but join with many others in admiring the ingenuity of
execution and the clarity of analysis which have characterized the
formation of this sub-field since the earliest demonstrations by Bonse,
Treimer and Rauch.

At the same time many of us are intrigued by the highly delicate tool
offered by coherent deBroglie optics and are searching actively for
applications beyond the range of primarily didactic interest. This type
of interest attaches naturally to both the case of crystal diffraction
interferometers and the longer wavelength systems where nearly conven-
tional optical design is possible. Potential new work in these areas is
discussed elsewhere in this Workshop report by Rauch[3] and by Zeilinger.[4] I
hope that the present modest addendum to their discussions may contribute
toward giving the reader a sense of what the future might see.

I have restricted my attention entirely to cases of interferometry using
diffraction from perfect crystals and addressed the following rather
elementary questions: 1. Are there significant generalizations of
present-day neutron (and x-ray) interferometers which are technically
feasible at the present time? 2. Do any of these appear to be useful as
regards going beyond the laboratory execution of textbook-type **gedanken**
experiments?

The first question is the more easily addressed but the second is the more
significant. The next two sections summarize my sense of how they might
be answered at the present time.

2. Evolution in Interferometry

All, or nearly all, crystal diffraction neutron interferometers to date
have been of monolithic construction with characteristic dimensions of the
order of 10 – 20 cm. The vast majority of these are of the symmetric LLL
geometry (L = Laue). Optical paths in such structures tend to resemble
those in a Mach-Zehnder optical interferometer.

Increased scale in the existing geometries has been widely recognized as a
desirable evolutionary trend. Indeed, for some experiments (e.g., Sagnac
effect), sensitivity varies with the area enclosed by optical paths from
beamsplitter to beam recombinor. In other cases, path lengths are the
more important consideration. As long as we are dealing with interfero-
meter structures carved from single blocks of rather perfect crystal
material, there will be an obvious limitation of scale. Alternatively,
one could realize much larger scale devices if separate crystal optical
units could be used as outlined below.

Similarly, although it is not a major issue, the role of x-ray inter-
ferometry could be changed. In possibly the earliest joint application of
x-ray and neutron interferometry, Collella, Overhouser and Werner (COW)
measured the gravitationally induced crystal distortion. Clearly,
simultaneous, on-line diagnostics offer advantages, although these are not
fundamental in character and should not be expected to yield large gains
in any measure of performance.

On the other hand, the possibility of obtaining neutron and x-ray inter-
ference between entirely separated crystal blocks does hold out promises
of notable gains. Firstly, there are the matters of shape and scale:
Clearly if one had the freedom to place main optical elements at any
distance and in any pattern, several desirable freedoms would emerge,
subject, of course, to essential optical limitations and available flux.

To suggest how these considerations might lead to future experiments, I
turn in the next section to a particular case, namely that of a neutron
Michelson-Morley apparatus. As currently envisioned, it would use active
optical stabilization and be simultaneously viewed by x-rays having the
same wavelength as the neutrons. Experience with some features of the
active stabilization scheme needed in this case supports the surmise that
such an experimental realization is technically feasible at present time.
Granted such feasibility but acknowledging the complexity and effort which
would be required to realize such a system, I turn in the last section (4)
to question what it all might mean.

3. A Neutron (and X-Ray) Michelson-Morely Apparatus

Figure 1 diagrams the essentials of a Michelson-Morley system. Neglecting
the obvious technical problems such a structure has several appealing
aspects. Although one thinks initially of a precisely orthogonal system
as suggested in the figure, small departures from 90° can compensate for
the effect of refractive index in the reflection elements; in fact there
appears to be no reason to restrict the reflection and transmission

elements to being of the same material.
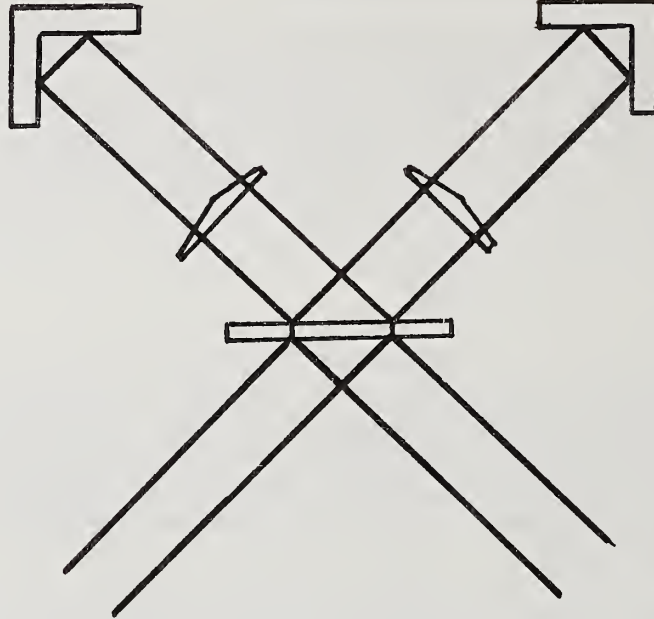
Figure 1. Schematic diagram of a neutron Michelson-Morely
apparatus. X-rays of the same wavelength can satisfy all
diffraction conditions as well with the help of the bi-
prisms indicated. The needed active laser stabilization
system is not shown.

If one wishes to have a simultaneous x-ray probe, then attention is
required to refractive index differences between neutrons and x-rays only
in the retro-reflectors, since the symmetric splitter refractive index
plays no effective external role. Differential effects should be readily
compensated by Fresnel biprisms placed in the arms as indicated.

The remaining purely technical question concerns stabilization of the
indicated optical elements in relative position and angular orientation.
Active optical methods are evidently required since any underlying optical
bench and any method of "fixing" the crystal elements will be subject to
drifts larger than the picometer and nanoradian thresholds of interest.
A reasonable level of experience regarding these questions has been
accumulated in a presently on-going exercise aiming at an optical
determination of an inter-planer spacing in a silicon single-crystal
sample.[5] Both procedures use laser interferometry but for historical
reasons differ significantly in character.

Primary displacements are carried out by servo-locking a Fabry Perot cavity (finesse ~ 1000) to a slaved laser which in turn is frequency-offset-locked to an I_2 stabilized HeNe oscillator (0.6 nm). Short term positioning appears good to ± 1 picometer, while longer term averaging gives another factor of ten. Orientational interferometry has used a 4 probe, two-beam, polarization interferometry to reach nanoradian sensitivity, while giving signals independent (in first order) of the position and orientation of the polarizing beamsplitter. This somewhat complex but rather useful optical element will be described elsewhere. Intrinsic sensitivities available in the individual channels indicate that an average of the four channels should be robust, at least at the level of ± 1 pm. It is thus possible to consider eliminating the displacement channel (Fabry Perot) and by an alternative signal processing of four two-beam outputs acquire both displacement and orientation data from this interferometer cluster alone.

The comments given above are intended to suggest my belief that interferometry of x-rays and neutrons can proceed on a relatively large scale (ca 1 meter), under active interferometric control at a level of 1 picometer or somewhat less. Should such a level of sensitivity become available, we may well ask whether and how it might contribute to obtaining results having more than didactic interest. The concluding section which follows attempts to address this point.

4. Potential Applications of Long Baseline Neutron (and X-Ray) Interferometry

Three possibilities for the technology just described occur very readily to mind. There are likely others, possibly even one which would more adequately motivate this fairly difficult exercise. In any case, the three which I would advance at the moment are: 1. Enhanced sensitivity in experiments of the sort already considered or carried out due to use of a larger scale system. 2. Tests of special relativity (i.e., a preferred frame search) using Michelson-Morely geometry as described above. 3. Measurement of local space curvature as produced by macroscopic inhomogeneous gravitational potentials that might be significant from the point of view of general relativity. I comment briefly on each of these issues in the following paragraphs, referring the reader in each case to a published essay which purports to motivate such an exercise.

The first issue, namely gaining enhanced sensitivity by increasing path lengths, requires little discussion. It is evidently correct; the only questions remaining to be asked are quantitative ones of the form: If it is (conceptually) important to place a smaller upper bound on some property of the neutron or its interaction, does feasible interferometry offer hope of doing so. In general I suspect not owing to the much larger interaction times (over the same length scale) available using ultra-cold neutrons. On the other hand, atomic scale spatial gratings, sub-millisec diffraction patterns and greater fluxes may compensate for the interaction time effect. A quite serious and plausible suggestion in this direction has recently been put forward by Ioffe[6] while others are considered by Werner[1] and by Klein and Werner.[2]

Next I turn to the question of whether or why to do the Michelson-Morely experiment described above. Firstly, it is important to recognize that this (MM) geometry differs in an important and fundamental way from that of the conventional Bonse-Hart (BH) geometry. Because of symmetry, the phase output of a BH geometry device is independent of any "ether wind" type effect. This is easily seen since each optical path has "E-W" and "N-S" components, whereas in the MM geometry one leg could be purely "E-W" while the other would be entirely NS. Of course any such "round-trip" device is first-order insensitive to an additive velocity so that only second and higher order effects survive. Strong advocacy for such an experiment can be found in an essay by Breitenberger[7] who argues that the principle of relativity should hold for deBroglie as well as Maxwell waves.

The matter of space-time curvature and its effect in interferometry has been discussed extensively by Ananden.[8] He shows that with a very large effort, one could hope to detect the presence of the sun and the moon via their tidal effects and possibly even see the earth. There is no question that these effects are calculable and perhaps mildly interesting but G. Greene pointed out[9] that delicate macroscopic instrumentation might be better suited for such a measurement. The problem with the sun and moon and even the earth is that their potentials vary slowly on a scale of even long-baseline neutron interferometry.

A very recent review by Stedman[10] addresses the question of whether or not quantum gravity effects or non-neutonianian effects generally should be seen in B-H type interferometers. His provisional conclusions are not especially favorable for neutron interferometers when compared with optical ring lasers. This is largely because the advantages arising from non-zero mass tend to be overwhelmed by shot noise considerations. However, his analysis has not as yet been carried out of other interferometer geometries where fewer cancellations are sometimes encountered.

I hope in the workshop spirit to have raised more questions than answers, possibly even foolish ones. In any case continued advice and discussion are most welcome.

References

1. S. A. Werner, these proceedings, p.
2. A. G. Klein and S. A. Werner, Reports on Progress in Physics 46, 259 (1983).
3. H. Rauch, these proceedings, p.
4. A. Zeilinger, these proceedings, p.
5. R. D. Deslattes in Precision Measurement and Fundamental Constants - II, B. N. Taylor and W. D. Phillips, ed. NBS Spec. Pub. 617, U.S. G.P.O. (1984) p. 303.
6. A. I. Ioffe, Nucl. Instr. and Meth. 228, 141 (1984).
7. E. Breitenberger, Il Nuovo Cimento 1B, 1 (1971).

8. J. Ananden, Phys. Rev. D <u>30</u>, 1615 (1984).
9. Private communication.
10. G.E. Stedman, Contemp. Phys. <u>26</u>, 311 (1985).

AN EFFECTIVE VIBRATION ISOLATION SYSTEM
FOR PERFECT-CRYSTAL NEUTRON INTERFEROMETRY

J. Arthur
Oak Ridge National Laboratory
P.O. Box X
Oak Ridge, Tennessee 37831

Perfect-crystal neutron interferometers are subject to deg-
radation of their performance caused by vibrational accelerations.
It is shown that the most seriously offending accelerations are
rotational, and an effective and simple vibration isolation sys-
tem that has been developed at the MIT Neutron Diffraction
Laboratory is described.

Introduction

The great sensitivity of a perfect crystal neutron interferometer to small
phase perturbing effects is a consequence of the size of the device relative to
the wavelength of the neutron radiation used -- the separated coherent neutron
paths typically equal 10^9 neutron wavelengths. This sensitivity and the relati-
vely long time required for a neutron to propagate through an interferometer
(~25μs) cause the interferometer to be very sensitive to physical perturbations
of its dimensions which are caused by environmental fluctuations such as vibra-
tions and temperature drifts. This paper summarizes the work that has been done
at MIT on the interferometer vibration problem. The effects on interferometer
performance of vibrational accelerations have been considered by C. G. Shull[1]
and D. K. Atwood[2]. Vibration isolation systems have been constructed and ana-
lyzed by B. E. Takala[3] and J. Arthur[4].

Time-Dependent Phase Perturbations and Interferometer Performance

Figure 1 shows somewhat idealized representations of two common types of
perfect-crystal neutron interferometer. In the Bonse-Hart interferometer, Fig.
1(a), the coherent splitting and recombination of a relatively narrow (~1mm)
neutron beam are accomplished with three thin crystal plates, in symmetric Laue
orientation. In this idealized version with very thin crystals, the beams do
not suffer appreciable spreading as they pass through the device, and can be
thought of as "rays" with negligible width. The two-crystal interferometer
developed at MIT, shown in Fig. 1(b), uses two thick (~1cm) crystal plates for
coherent separation and recombination. A 1mm-wide entrance beam is transformed
into a set of coherent pairs of rays in the region between the crystals. The
coherent ray pairs are symmetrically located about a central ray (two represen-
tative ray pairs are shown in Fig. 1(b)), and taken altogether they form a wide,
continuous beam flowing between the crystals. However, it is emphasized that
coherence exists only between members of ray pairs.

In both types of interferometer, phase perturbations of the separated beams pro-
duce intensity modulations in the radiation exiting from the final crystal sur-
face. Specifically, in an idealized interferometer, the intensity contribution
to either of the exit beams from a coherent ray pair in the interferometer has
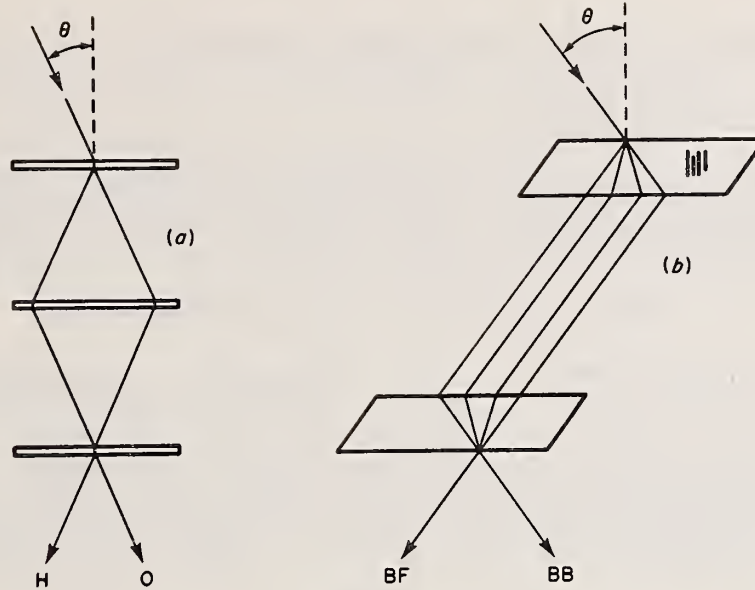
Figure 1

Idealized representations of a Bonse-Hart interferometer (a),
and a two-crystal interferometer (b), showing the coherent
splitting and recombination of neutron rays. Both interfero-
meters are shown using 1.56 Å radiation; because the two-
crystal device relies on diffraction from the (400) crystal
planes while the Bonse-Hart interferometer uses (220) diffrac-
tion planes, the Bragg angles differ.

the form

$$I = 1 + \cos\phi , \qquad\qquad (1)$$

where ϕ is the phase difference developed over the two coherent ray paths.

Following the analysis of Shull[1], consider the effect of a simple sinusoidal
perturbing phase, $\alpha(t)$, with frequency ω and amplitude α_0. It will modify
Eq.(1) to give

$$I(t) = 1 + \cos(\phi + \alpha_0 \sin\omega t) . \qquad\qquad (2)$$

The effect that this perturbing phase has on the contrast, C, which is
defined as

$$C = \frac{I_{max} - I_{min}}{I_{max} + I_{min}} , \qquad\qquad (3)$$

can be found for small α_0 by expanding the cosine function around $\phi = 0$ and
$\phi = \pi$. The ratio of perturbed to unperturbed contrast is the degradation fac-
tor, D, which equals

$$D = 1 - (1/2)(\alpha_0 \sin\omega t)^2 + (1/24)(\alpha_0 \sin\omega t)^4 - \dots (4)$$

If the measuring time is long compared to $1/\omega$, the sinusoidal phase perturbation

125

will be averaged out to give a first order degradation effect of

$$D \approx 1 - (1/4) \, \alpha_0{}^2 \qquad\qquad (5)$$

for each coherent ray pair in the interferometer affected by this perturbation. This result will now be applied to the problem of random vibrational accelerations of an interferometer.

Phase Perturbations Due to Accelerations

Since a crystal interferometer is quite rigid, (such devices are usually carved from a single silicon crystal, with the diffracting crystal plates remaining fixed to the crystal base) the important effects of vibrations are due to linear and rotational accelerations of the interferometer as a whole. The most significant phase effects are caused by translational acceleration perpendicular to the diffracting lattice planes, and by rotation about an axis perpendicular to the scattering plane.[1,2]

The phase effects of transverse linear acceleration can be understood by using the non-inertial reference frame of the interferometer and introducing a fictitious force and potential for the neutrons.[5] An acceleration a will cause a phase shift

$$\Delta\phi_{lin} = A \, \frac{m^2\lambda}{2\pi \, \hbar^2 \cos\Theta} \, a \qquad\qquad (6)$$

in each pair of coherent rays, where A is the area enclosed by the rays, λ is the neutron wavelength, and Θ is the Bragg angle. If the acceleration is sinusoidal with frequency ω, the phase shift becomes

$$\Delta\phi_{lin} = A \, \frac{m^2\lambda}{2\pi\hbar^2\cos\Theta} \, a_{peak} \, \sin\omega t \quad , \qquad\qquad (7)$$

where a_{peak} is the peak linear acceleration.

Rotation of the interferometer causes a phase shift between coherent rays which can be interpreted as a consequence of coriolus forces on the neutrons[6], and which is equal to

$$\Delta\phi_{rot} = A \, \frac{2m}{\hbar} \, \omega_{rot} \quad , \qquad\qquad (8)$$

where ω_{rot} is the angular velocity of the rotation. For the case of periodic rotational acceleration with frequency ω, this becomes

$$\Delta\phi_{rot} = A \, \frac{2m}{\hbar\omega} \, \alpha_{peak} \, \cos\omega t \quad , \qquad\qquad (9)$$

where α_{peak} is the peak angular acceleration.

Each of the phase shifts mentioned above is proportional to the area enclosed by the coherent rays in the interferometer. For the Bonse-Hart interferometer this

presents no problem since all coherent ray pairs enclose the same area. The two-crystal interferometer is a bit more complicated, since different ray pairs enclose different areas. A phase shift which is proportional to enclosed area is equivalent to the phase shift introduced by a wedge of material placed across the beam between the interferometer crystals, so that the outer rays see a greater difference in optical path length than do the central rays. The range of phase shifts must be taken into account when computing the effect on the intensities of the beams leaving the interferometer. For a phase shift that is linearly dependent on enclosed area, the intensity of one of the exit beams can be shown to be[7]

$$I = (\pi/16) + (\pi/8) \frac{J_1(\phi_{Amax})}{\phi_{Amax}} \quad , \tag{10}$$

where ϕ_{Amax} is the phase shift induced in the ray pair enclosing the maximum area. This leads to a modification of the expression for the degradation caused by a small perturbing phase (Eq.(5)). Using a series expansion for the Bessel function J_1, it can be shown[1] that

$$D \approx 1 - (1/16) \alpha^2_{Amax} \quad , \tag{11}$$

when the two-crystal interferometer is subjected to an area-dependent sinusoidal phase perturbation.

Experimental Study Of Vibrational Accelerations and Isolation at MIT

The use of a pair of sensitive pieozoelectric accelerometers and a Fourier spectrum analyzer has greatly facilitated the study of the vibrational environment at the MIT Reactor. The accelerometers are very sensitive to linear accelerations along one axis only. When the pair are mounted with their sensitive axes parallel, in the neutron scattering plane, and perpendicular to the line connecting their centers, they can be used to separately measure linear and rotational accelerations. The sum of the signals from the accelerometers gives the translational acceleration parallel to their axes, while the difference between their signals gives the rotational acceleration. A typical difference signal spectrum is shown in Figure 2(a). The vibration spectrum at the MIT Reactor changes somewhat from day to day, but peak accelerations (for both sum and difference signals) lie between 10^{-6}g and 10^{-4}g, where g is the gravitational acceleration of the earth, 980 cm/s^2. The peak levels tend to occur at harmonics and subharmonics of 120 Hz, the principal vibration frequency of the many transformers and pumps located in the reactor.

To estimate the effect of these environmental vibrations on the performance of an interferometer (for instance, the MIT two-crystal interferometer), it is necessary to adapt Eq.(11) to allow for a range of vibrational frequencies. Since the spectrum features a few prominant peaks, it can be approximated by a limited sum of sinusoidal oscillations, with appropriate amplitudes and frequencies. Equation (11) then becomes

$$D \approx 1 - (1/16) \sum_i \alpha^2_i \quad . \tag{12}$$
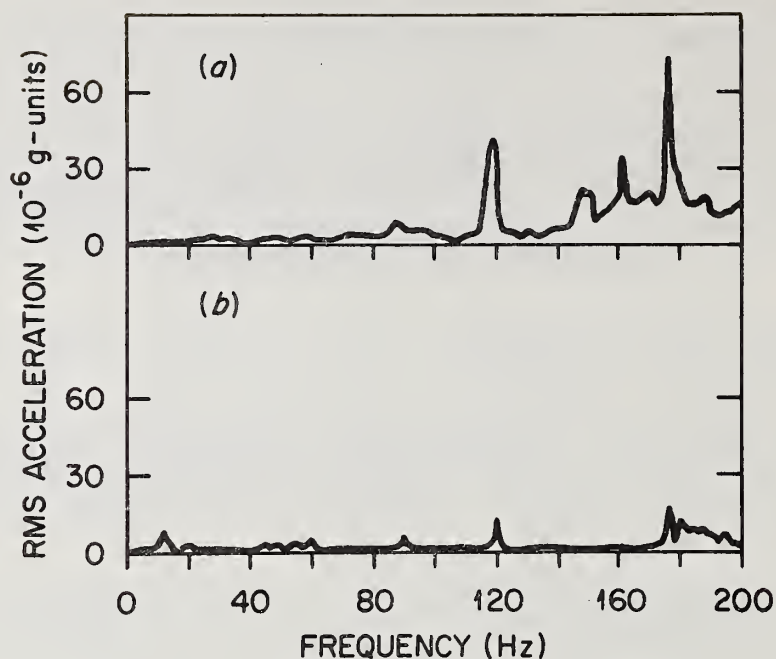
Figure 2
Fourier analysis of the difference signal from two
accelerometers, giving the frequency spectrum of their
rotational acceleration. Spectrum (a) was taken on the
interferometer support table at the MIT reactor without
any vibration isolation system. Spectrum (b) was taken
on top of the vibration isolation system used with the
MIT interferometer.

Now, inserting the constants appropriate for the MIT two-crystal interferometer
into Eq.(7) to find the amplitudes α_i for linear accelerations, one finds

$$\alpha_{lin} = a_{peak} \times 65.3 \frac{rad}{g} \quad , \tag{13}$$

where a_{peak} is determined from a peak in the measured spectrum. It is clear
that for values of a_{peak} in the range $10^{-6}g$ to $10^{-4}g$, α_{lin} will be negligibly
small, and even if several peaks are present in the spectrum, these linear acce-
lerations will not cause a significant deterioration of interferometer perfor-
mace. This will also be true for a Bonse-Hart interferometer. So, at least in
the MIT Reactor environment, one can ignore the effects of linear accelerations.
Unfortunately, rotational accelerations are not so easily neglected. Inserting
the constants appropriate to the MIT interferometer into Eq.(9) gives:

$$\alpha_{rot} = a_{peak} \times \frac{5.98 \cdot 10^6}{2rf} \frac{rad\ cm}{g\ sec} , \tag{14}$$

where a_{peak} is the peak acceleration measured by the accelerometer difference
signal, r is the separation of the accelerometers in cm, and f is the vibration
frequency in Hz. It is apparent that the vibration spectrum shown in Fig. 2(a)
could cause some degradation in interferometer performance; at times when the

128

vibration environment is more severe the degradation could be serious. Thus, vibration isolation schemes for interferometers must be designed to eliminate rotational accelerations.

The interferometer support at MIT was built with these considerations in mind. It consists of a high-quality ball bearing supporting a weighted table on which the interferometer sits. The orientation of the table is maintained by two weak springs connecting two points on its outer edge with an anchor rigidly connected to the base.

If the bearing were perfect, the resonant frequency of this system would be determined by the moment of inertia of the table and the torque constant characteristic of the spring coupling. This was found to be the case for rotational motions with amplitudes large enough to be visible to the eye. However, the ambient vibrational motion is so small that the motion of the table is microscopic. For such motion, the resonant frequency of the system was found to be somewhat higher than expected, and independent of the spring constant. It is believed that the restoring force for such small-amplitude oscillations is provided not by the springs, but by the elasticity of the bearing balls and races. These deform slightly while supporting the load of the table, and microscopic oscillations of the table do not cause the balls to roll, but rather to merely flex a bit. The small-amplitude resonant requency of the final version of this system is 2.5 Hz, whereas the resonant frequency expected from the moment of inertia of the table and the spring constant would be 0.7Hz.

Fortunately, the actual resonant frequency is well below the frequencies of all of the large ambient vibrations. Figure 2(b) shows the rotational acceleration spectrum measured on top of this turntable. The amplitudes are all less than 10^{-5}g, and no appreciable degradation of interferometer performance is expected or observed.

References
1. C. G. Shull, in Physics as Natural Philosophy, edited by A. Shimony and H. Feshbach (MIT Press, Cambridge, 1982).

2. D. K. Atwood, Ph.D. Thesis, MIT, 1982 (unpublished).

3. B. E. Takala, M.S. Thesis, MIT, 1981 (unpublished).

4. J. R. Arthur, Ph.D. Thesis, MIT, 1983 (unpublished).

5. Daniel M. Greenberger, Rev. Mod. Phy. 55, 875 (1983); R. Colella, A. W. Overhauser, and S. A. Werner, Phys. Rev. Lett. 34, 1472 (1975).

6. L. A. Page, Phys. Rev. Lett 35, 543 (1975); D. K. Atwood, M. A. Horne, C. G. Shull, and J. Arthur, Phys. Rev. Lett. 52, 1673 (1984).

7. J. Arthur, C. G. Shull, and A. Zeilinger, Phys. Rev. B32, 1 Nov. 1985.

COLD NEUTRONS AND NEUTRON OSCILLATIONS

Milla Baldo-Ceolin
Dipartimento di Fisica "G.Galilei", Università di Padova, Padova-Italy
Istituto Nazionale di Fisica Nucleare, Sezione di Padova, Padova-Italy

The problem of neutron-antineutron oscillation experimental detection is discussed after a brief presentation of its phenomenology. Experiments deep underground with neutrons bound in nuclear matter are compared with experiments with artificially produced neutron. Thermal, cold and ultracold neutrons are considered. It is concluded that cold neutrons, transported from the reactor to the experimental area through totally reflecting guides, reduce basically the radiation background, and allow, the other conditions being the same, a higher sensitivity. Finally some features of the experiment in preparation at the ILL reactor in Grenoble are summarized.

Physics motivation and experimental status

Baryon number non-conserving interactions may induce neutron-antineutron mixing and consequently neutron-antineutron oscillations, which would occur as a first-order process through a $\Delta B=2$ interaction. The mixing is characterized by a mass splitting between pure baryon states

$$\delta m = <\bar{n}|H|n>,$$

and a corresponding neutron-antineutron oscillation time $\tau_{osc} = 1/\delta m$.

Actually the theoretical models leave a rather large incertitude in the value to be expected for τ_{osc}. The so-called "left-right symmetric" models, however, suggest mainly for the neutron oscillation time a value $\tau_{osc} \sim 10^8 sec$[1].

In the quark-lepton picture the simplest term in the effective Lagrangian that can induce $\Delta B=2$ processes is

$$L_{eff} \simeq M^{-5}(qqq.qqq) + h.c.$$

and therefore, if neutron-oscillation processes are observed, this besides being a manifestation of the baryonic number non conservation will open a new physics in the mass range $M_x \sim 10^4 \div 10^6 GeV$, and provide new experimental input regarding ways to extend the Standard Model.

At present experimental limits for $\Delta B=2$ processes have been obtained in an experiment using free neutrons at the ILL reactor in Grenoble[2], which has set a lower limit to the oscillation time τ_{osc} of $10^6 sec$ corresponding to a $\delta m < 6 \cdot 10^{-28} MeV$. Deep underground experiments, measuring nuclear stability lifetimes[3], give for $\Delta B=2$ processes $T_{ann} > 10^{31} yr$ and this can be interpreted in terms of n-$\bar{n}$ oscillations to give a lower limit to τ_{osc} of $5 \cdot 10^7 sec$[4]

An experiment aiming at $\tau_{osc} \sim 5 \cdot 10^6 sec$, is in progress at the LENA reactor in Pavia[5], and a Padova-Heidelberg-Grenoble-Pavia experiment searching for $n \rightarrow \bar{n}$ transitions up to $2 \cdot 10^8 sec$ level is in preparation at the ILL reactor in Grenoble[6]. Furthermore, a large experiment aiming at τ_{osc} $7 \cdot 10^8 sec$ has been projected at the meson factory in Moscow[7].

In the following I will briefly consider the neutron oscillation phenomenology, discuss the experimental methods for neutron oscillation detection and then present some features of the Grenoble experiment.

As a consequence of a $\Delta B=2$ interaction an initially pure neutron state ($B=+1$) will in time acquire an antineutron ($\bar{n}$) component ($B=-1$) with probability $P(n,t)$[8]

$$P(\bar{n},t) = [\delta m^2/(\delta m^2+\Delta E^2)]\sin^2[(\delta m^2+\Delta E^2)^{\frac{1}{2}} t] \qquad (1)$$

where $2\Delta E$ is the energy difference between the n and $\bar{n}$ states due to external field perturbation. These external interactions may be magnetic, acting through the equal but opposite n and $\bar{n}$ magnetic moments, or nuclear through the differing n and $\bar{n}$ strong interaction properties.

For totally free neutrons $\Delta E=0$ and then

$$P(\bar{n},t) = \sin^2(\delta mt) = (t/\tau_{osc})^2, \quad \text{if } t \ll \tau_{osc} \qquad (2)$$

Although the condition that neutrons are free is never satisfied in nature and ΔE is much larger than δm, neutrons can be considered as free for a time (t) such that $\Delta E \cdot t \ll 1$ ("quasi free neutron" condition). In this case eq.(1) reduces to the free neutron relation of eq.(2). The "quasi free condition", $\Delta E \cdot t \ll 1$, has a basic importance in designing experiments aiming at detecting free neutron oscillations, since it allows the optimization of experimental conditions.

According to the hypothesis of neutron oscillations, a state initially composed of neutrons becomes, after a finite time, a mixture of neutrons and antineutrons. In order to test this hypothesis, one has to detect the antineutron states, which signature is an antineutron-nucleon annihilation, i.e. an energy release of ~ 2 GeV, distributed over several pions, 5 in average, and a total momentum $\bar{p} = 0$.

The sensitivity of an experiment, defined as the maximum value of the oscillation time the measurement can detect, depends on the total number of available neutrons and the effective time along which neutron oscillation can develop. Therefore, in order to attain high sensitivities, first of all very intense neutron sources are required, such as nuclear matter or artificial sources such as nuclear reactors or accelerators.

Depending on the choice between the two possibilities, whether the observed neutrons are bound in nuclear matter or artificially produced, two types of measurements can be made: a static or a dynamical one.

Static measurements. Experiments of the static type take advantage of the fact that a very large number of neutrons are present in nuclear matter. These experiments require very massive set-ups acting as source and detector at the same time, in order that a large amount of matter can be observed over a long period to detect events due to annihilation processes.

The main and unavoidable source of background in this type of experiments, which must be carried out deep underground in order to avoid cosmic ray interactions, are the neutrino interactions (~ 200 events per Kton per year), since when the annihilation process takes place in the core of a heavy or medium heavy nucleus its characteristic signature results practically destroyed due to the high absorption probability in the nucleus of the produced pions.

Moreover, the evaluation of τ_{osc} from measurements of the static type is not straightforward; besides the substantial uncertainties in relating free and bound n-$\bar{n}$ mixing arising from uncertainty in the n optical potential[4], the strength of n $\rightarrow$ $\bar{n}$ transitions needs not to be the same for "quasi free neutrons" isolated or bound in nuclear matter, and consequently τ_{ann} does not constrain the value of the free neutron oscillation time[9].

From proton-decay type experiments it results $\tau_{ann} > 3 \cdot 10^{31}$ years[3].

which, due to background effects, appear to be the experimental limit of the present generation experiments.

Experiments of the dynamical type. Neutron beams from artificial sources provide a more straight-forward way for measuring τ_{osc}. Nuclear fission reactors and accelerators, generating neutrons by spallation, photonuclear or other specific nuclear reactions, are both well suited as a source for this type of experiments.

As auxiliary facilities neutron cooling to liquid hydrogen temperature and neutron beam guide devices can be considered. Beam guides are constant cross-section tubes exploiting neutron total reflexion at their inner surface. By reflection through neutron guides it is possible to take neutron beams at any distance mantaining their current practically constant.

A typical experiment of the dynamical type requires a source of moderated and possibly cooled neutrons, a long drift tube where the neutrons propagate under "quasi free condition", a target at the end of the flight path where antineutron component annihilate and an annihilation products detector.

The constraint which defines the quality of a neutron-oscillation experiment may be deduced from eq. (2) as

$$\tau_{osc} = (N \cdot \varepsilon)^{\frac{1}{2}} \, t = (I \cdot T \cdot \varepsilon)^{\frac{1}{2}} \, L/v \qquad (3)$$

where: I, the neutron current in $n \cdot sec^{-1}$, depends on the power of the neutron source; ε, the fraction of annihilation events which can be unambiguously identified, depends on the properties ("quality") of the detector; $t = L/v$, is the "quasi free propagation" time in sec; v, the neutron velocity in m/sec; T, the data recording time; Nt^2, for a given source, depends upon the neutron energy and the annihilation target area.

Therefore in order to reach high sensitivities, a very intense neutron beam travelling a long distance at low velocity is needed. With $I = 10^{13}n$ sec^{-1}, a drift time $t = L/v \cong 0.1$ sec, a residual gas pressure in the drift vessel 10^{-6} torr, so as to prevent nuclear interactions of the antineutron component with residual gas molecules, and a magnetic field along the propagation region less than 10^{-4} gauss, in one year running time it would be possible to measure τ_{osc} up to $\sim 10^{9}$ sec.

In practice, however, the sensitivity will be limited by the background events which are mainly due to neutral cosmic ray interactions in the annihilation target. Their rate is proportional to the mass of the target[2]. Then, following the fact that antineutron annihilation cross section ($\sigma \propto 1/v$) is very large, thin annihilation target can be used and the background considerably reduced.

A dynamical experiment important feature lays in the fact that the background can be directly measured by changing the intensity of the magnetic field in the propagation region. A magnetic field of ~ 0.1 gauss is sufficient to reduce the neutron-antineutron transition probability practically to zero, since $P(n) \propto (1/B)^2$.

In these experiments gamma rays and fast neutrons from the neutron source and gamma rays from neutron capture along the drift vessel and at the annihilation target can give a large radiation flux on the detector and reduce the detection efficiency.

The radiation effect can be conveniently reduced by means of neutron beam guides slightly bent so as to switch off the radiation coming along with the neutron beam.

In the following we will discuss and compare experiments with thermal and cold neutrons, assuming the "quasi free condition" satisfied. We will

later consider ultra cold neutrons.

Thermal neutrons. A typical experiment would take neutrons directly near the reactor core from a neutron port. Then, since the sensitivity increases as $N^{\frac{1}{2}}$, the largest available port should be used, with the consequence that large fluxes of fast neutrons and γ rays accompany the beam. Since the neutron flux at the source is isotropic, the entire length of the propagation tube has to be lined with neutron absorbing material, and surrounded by a biological shield; furthermore, an elaborate baffle system has to be foreseen along the vacuum pipe in order to protect the detector from neutron capture γ rays.

Moreover, due to the high level of parasite radiation, the detector trigger requires a rather definite configuration, and therefore there is a reduced acceptance for genuine events.

At meson factories there is the possibility of pulsed neutron beams so that the beam associated radiation can be quite reduced, provided the pulsed structure is not lost through the slowing down process.

The final sensitivity, Eq.(3) depends on the annihilation target area as $\tau_{osc} = (I_0(\theta/2)^2 T)^{\frac{1}{2}}L/v$. In fact $I = I_0 A/4\pi L^2$, where I_0 is the neutron current at the source.

Cold neutrons. The advantage of cold respect to thermal neutrons consists at first in the fact that the the lower neutron velocity contributes directly to the overall sensitivity of the experiment, the measurable limit of τ_{osc} being $\propto 1/v$. In particular it is possible to obtain the same sensitivity as in experiments with thermal neutrons with a reduced neutron intensity (and consequently radiation background) $I_c/I_T = (v_T/v_c)^2 \simeq 10^{-2}$, if the rest of the experimental condition remain the same.

A further and even more essential advantage is obtained from the fact that cold neutrons can be easily transported from a position close to the reactor core to the experimental area by reflection through a curved system of neutron guides thus eliminating all γ's and fast neutrons coming directly from the reactor. Neutrons from the exit of the curved guide are then freely drifted in a vessel with a diverging shape, matching the divergence of the incoming beam, thus avoiding collisions on the walls and conserving the full initial current. Furthermore, although with this method the initial neutron current results dramatically reduced, the final sensitivity in τ_{osc} remains practically the same as in the case of cold neutrons directly propagated through vacuum pipes, provided the "quasi free" drift length, source power and annihilation target area are the same. This is because in both cases neutron crossing the target area are in proportion to the solid angle covered by the target, which at first approximation is equal. In fact, $I = I_0(\theta_L/2)^2$ where $\theta_L \propto \lambda(\overset{\circ}{A})$ is the largest limiting angle for total reflection.

Ultra-cold neutrons. At first sight ultra-cold neutrons look the most attractive because UCN are so slow (a few meters per second, and wavelength of the order of a thousand angstroms) as to see condensed matter as an impassable barrier, being totally reflected at any angle at the surface of most solids. This makes it possible to confine them into a "neutron bottle" for several minutes, so allowing a fantastically long observation time ($t\ 10^2$sec).

However, neutrons and antineutrons behave differently at the reflecting surfaces, so that n–n̄ degeneracy is removed. Theoretical models have been

133

developed in order to take into proper account the disphasing effect. Considering that the antineutron-nuclei annihilation cross-section is so large, $\sigma \propto 1/\bar{v}_n$, while most of the particles when reflected at the walls have to cross several atom layers (total reflection taking place at average depth $\lambda/4$): we assume as useful time for neutron oscillations in "quasi free condition" the time between two subsequent collisions at the walls of the neutron bottle. We have evaluated that the average time, $(<t^2>)^{\frac{1}{2}}$ between two subsequent collisions will be approximately $t \cong 0.23$ L where L in meters is the dimension of a neutron bottle with cubic shape.

If neutron oscillations will be detected and τ_{osc} measured by some other method, experiments using trapped ultra cold neutrons would allow to determine $V_n/V_{\bar{n}}$ with high precision, and to look for effects similar to those characterizing K^o-$\bar{K}^o$ oscillations in a medium.

The Grenoble II experiment

The Grenoble II experiment aims at measuring τ_{osc} up to 10^8. The experimental set-up is sketched in Fig.1. It consists of
a) a cold neutron beam transported to the experimental area by reflection through a curved guide and then propagated in the "quasi free" condition;
b) a thin isolated annihilation target, surrounded by a fine grain detector with high spatial and energy resolution;
c) an efficient cosmic ray shield and a veto system.

Furthermore, in order to keep annihilation target area and experimental apparatus not too large, the neutron reflection properties within a guide are exploited to obtain an optical horn focussing system. It consists of a straigth guide with slightly divergent walls such that if δ is the divergence and θ the angle of a neutron trajectory with the guide axis, a reflection reduces the angle θ by 2δ, and the target area needed to contain the full neutron current in proportion.

In the experimental set-up cold neutrons will be transported to the experimental area by the new guide H 52 (60 m long, R = 5000 m). The neutron current will be $I = 3.3 \cdot 10^{11}$ n sec^{-1} and the average temperature $\cong 15^o$K.

The quasi free propagation region will take place along a straight guide ~ 35 m long, with slightly diverging walls (3 mrad) followed by a 35 m long drift vessel where a residual gas pressure $P < 10^{-6}$ torr and magnetic field B 10^{-4} gauss warrant the "quasi free" condition. The average time interval from the last neutron reflection in the divergent guide to the end of the quasi free propagation region will be $t = 0.1$ sec.

As a target a 100μ m thick Carbon foil will be placed down-stream the magnetically shielded region.

Annihilation detector will be shaped as a box surrounding the target with a solid angle $\Delta\Omega/4\pi \cong 1$. The wall of the box will consist of limited streamer tube[10] planes and scintillation counter plates, immediately outside the propagation vessel. The ensemble will work as vertex detector and calorimeter. It has been estimated that $\sim 80\%$ of the annihilation products are fully contained in this ensemble and that the vertex reconstruction is within few centimeters.

The experiment will be protected by proper material against cosmic ray neutrals and by a veto system against charged penetrating particles.

Since the expected cosmic ray background[2] is less than 1 background event in 10^8 sec, the experiment can be run for a year effective time so to reach a sensitivity in τ_{osc} up to $2 \cdot 10^8$ sec. Thus one expects 3 annihilation events per day if $\tau_{osc} = 10^7$ sec, and 10 events per year if $\tau_{osc} = 10^8$ sec.

References

(1)   R.E. Marshak, Proc. Nat. Sci. $\underline{79}$, (1972), 3371.
(2)   G. Fidecaro et al., Phys. Lett. $\underline{156B}$, No. 1,2, (1985), 122.
(3)   T.W. Jones et al., Phys. Rev. Lett. $\underline{52}$, (1984), 720.
      G. Battistoni et al., Phys. Lett. $\underline{133B}$, (1983), 454.
(4)   W.M. Alberico et al., Nucl. Phys. $\underline{A429}$, (1984), 445.
      C.B. Dover et al., Phys. Rev. $\underline{D27}$, (1983), 1090.
(5)   S. Ratti, Proceedings of the "ICOBAN" Meeting, Bombay 1982, p.197.
(6)   M. Baldo-Ceolin, "Workshop on Reactor Based Fundamental Physics",
      Grenoble 1983, Journal de Physique, Colloque C3, Suppl. n.3, Tome 45,
      C3 - 173-183 (1984).
(7)   V.A. Kuzmin, Proceedings of the "ICOBAN" Meeting, Bombay 1982, p.197.
(8)   M. Baldo-Ceolin, Proceedings of the "Conference on Astrophysics and
      Elementary Particles: Common Problems", Roma (1980), p. 251.
      R.E. Marshak and R.N. Mohapatra, Phys. Lett. $\underline{94B}$, (1980), 183.
(9)   P.K. Kabir, Phys. Rev. Lett. $\underline{51}$, (1983), 231.
      J. Basecq and L. Wolfenstein, Nucl. Phys. $\underline{B224}$, (1983), 21.
(10) G. Battistoni et al., Nucl. Instr. and Methods $\underline{176}$, (1980), 297.
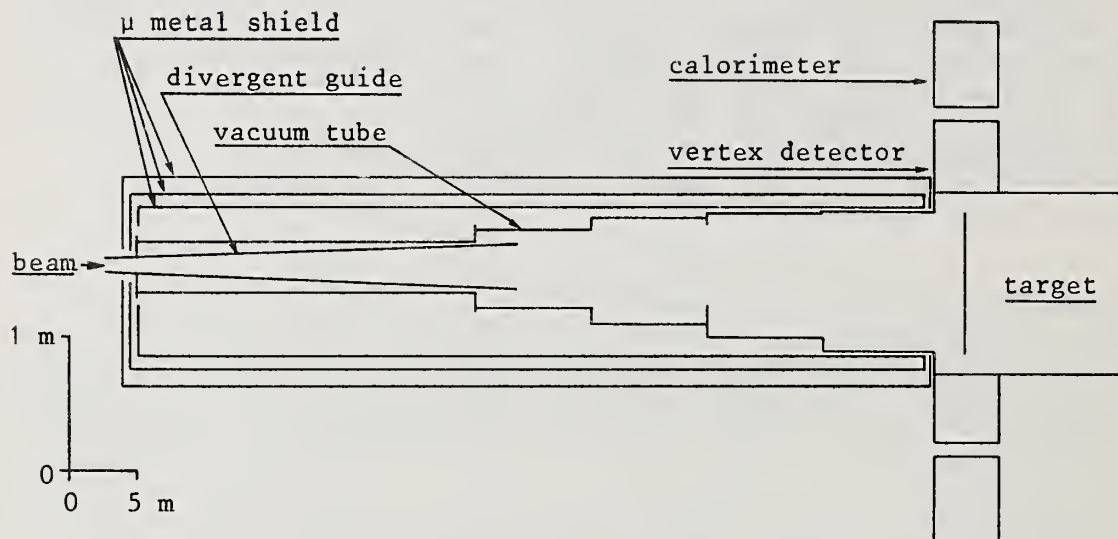
Fig. 1 - Quasi free propagation region and magnetic shielding.

ULTRACOLD NEUTRONS AND THE SEARCH FOR THE ELECTRIC
DIPOLE MOMENT OF THE NEUTRON

J M Pendlebury and K F Smith
University of Sussex
Brighton, BN1 9QH   Sussex UK
on behalf of the Collaboration between the Univerities of Harvard,
Munich, Sussex, and Washington, the Rutherford Appleton Laboratory,
and the Institut Laue Langevin.

The present position on the search for the electric dipole
moment of the neutron is described and likely progress in the
immediate future is discussed with reference to the ultracold
neutron source requirements.

The first experiment to search for a neutron electric dipole moment (EDM)
was that of Smith, Purcell and Ramsey (1951) /1,2/. This new and very
radical experiment set in train a whole series which is still in full spate.
Progress has been intimately tied up with progress in experimental
methods for working with slower and slower neutrons and has culminated in the
present use of ultracold neutrons (UCN). An experiment at the Leningrad
Nuclear Physics Institute /3/ has recently yielded the result that the EDM is
$(-2.0 \pm 1.0) \times 10^{-25}$ e cm employing UCN in a continuous flow mode with an average
dwell time for each neutron of about 6 s. The latest result from the
experiment at ILL, that the EDM is $(-1.8 \pm 2.9) \times 10^{-25}$ e cm has been obtained
with UCN which were completely imprisoned for periods of 80 s /4/. This change
to the use of UCN has been made in order to reduce the so called vxE
systematic error and to give the added convenience of a much smaller resonance
line width with which to look for a very small frequency shift.

The search for the neutron EDM has been reviewed recently by Ramsey /5/. Fig 1
shows the steady improvement in the sensitivity of the measurements as the
years have gone by. Indications from the ILL experiment are, that provided
finance and manpower continue to be available, there is no reason why the
sensitivity should not be improved by a further two or three factors of ten
with at least the same rate of progress as in the past.

Motivation for this long quest comes from the theoretical significance of the
neutron EDM. Any mechanism which gives rise to an EDM in a free particle must
involve the violation of parity P and time reversal symmetry T. It is well
known that parity is violated maximally in the weak interaction. The
expectation that T violation will also be found is prompted, in the first
instance, by the fact that CP violation occurs in the K-meson system.
Accepting the CPT theorem it is then expected that CP violation will
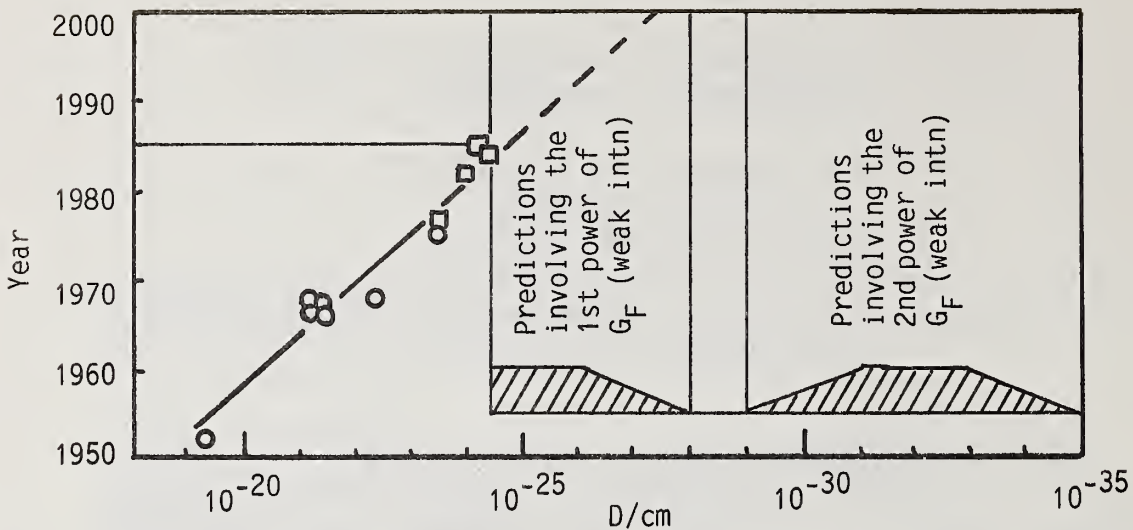
Fig 1   Upper limits from experiments on the neutron electric dipole moment eD, with beams -circles, and with UCN -squares.

be accompanied by T violation. Anticipation of T violating weak forces is reinforced by the fact that the algebraic forms of the operators involved in the Standard Glashow-Salam-Weinberg Model of the weak interaction with six quarks, include naturally some which are T violating and P violating. Calculations on the contribution to the neutron EDM from the Standard Model are now well developed and indicate a natural size of 10^{-32} e cm /6/. There is much faith in the Standard Model, particularly in view of its success in predicting the existence of the W and Z particles and the values of their masses. However, this is not in any way prejudiced by accepting that there may be additional mechanisms which make contributions to the neutron EDM. There is a lot of interest in extending the model to include more particles. In the Standard Model the leading terms in the EDM are second order in the weak interaction. In the models with more particles, there is a greater choice of diagrams and the contributions which are first order in the weak interaction can usually be found with natural sizes of about 10^{-25} e cm. In the Left-Right Symmetric Model, for example, where a further pair of right hand coupled W-particles is introduced as partners for the usual left hand coupled pair, a recent calculation /7/ gives natural EDM sizes of 10^{-25} e cm or 10^{-26} e cm depending on the sign of an unknown phase. Recent calculations with Supersymmetric Models /8,9/ which which introduce boson partners for fermions and vice versa, have indicated sizes in the range 10^{-24} e cm to 10^{-28} e cm. Rather on its own (because there is not much which can be done with it) the superweak ∆S=2 interaction model gives an EDM size of 10^{-29} e cm /4/.

It seems that the discovery of an EDM while searching the next two or three orders of magnitude would be useful evidence in favour of one of the models which are attractive extensions to the Standard Model. If nothing is found then, the constraints on acceptable theories will be tightened again.

Returning now to the experiment, the following is a brief outline of the method used at ILL. It has been described in rather more detail previously /4/. In the present set-up of fig 2, UCN which have passed through a thin polarizing foil of magnetized CoFe fill a 5 litre chamber in about 10 s. A door is then closed to imprison the neutrons for a period T which is currently about 80 seconds. T is essentially the measurement period for this batch of UCN. The chamber is in a uniform B-field of 0.01 gauss where the neutron precession frequency is about 30 Hz. The application of 2 s periods of
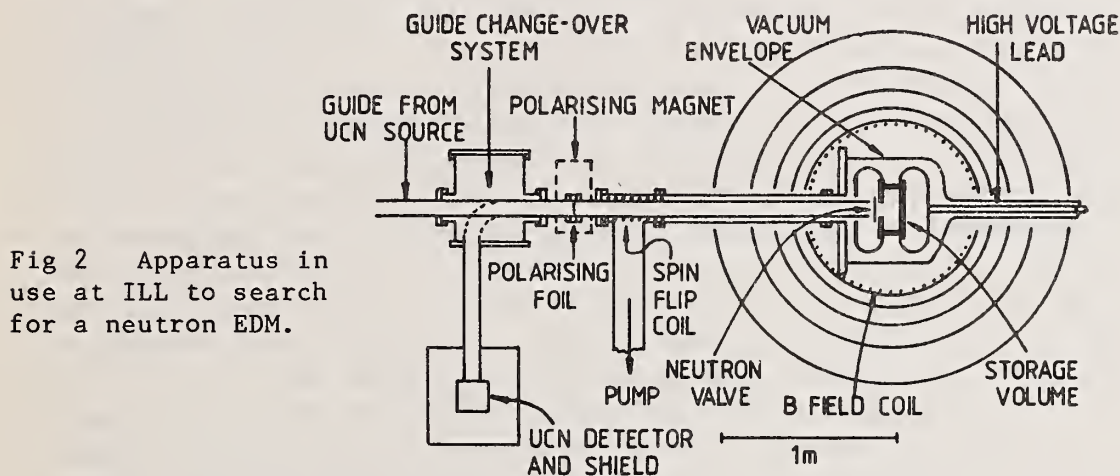

Fig 2   Apparatus in use at ILL to search for a neutron EDM.

resonant oscillating field of frequency 30 Hz at the beginning and end of the imprisonment period, and the need for the neutrons to pass through the same magnetized foil on their way to the detector after their release, provides a way of realizing a Ramsey type magnetic resonance curve in which the number of neutrons counted on emptying varies with small changes in the 30 Hz frequency as shown in fig 3. The line width is close to 1/2T Hz or 0.006 Hz at the current choice of T=80 s. A working point is chosen half way up the central valley and the basic procedure is to look for a change in the UCN counts per
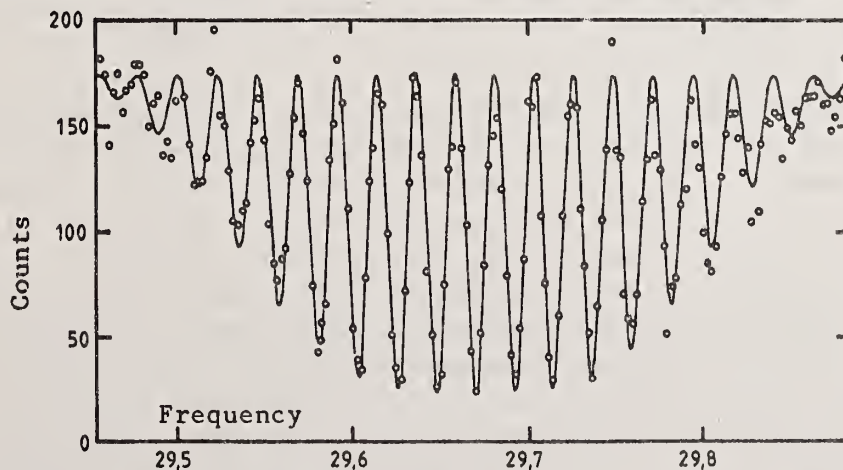

Fig 3   Neutron Magnetic resonance curve for the case T=40 s.

machine cycle on reversing an electric field E which is aligned with the B-field. Such a change could come from the E-field acting on the EDM to alter the UCN precession frequency, thereby slightly shifting the resonance.

If it is assumed that there are no systematic errors and that the dominant source of noise is that due to neutron counting statistics, then after running the experiment for a time t during which N neutrons are counted, one standard deviation σ_D on the measured EDM length D is equal to $\hbar/2e\alpha ET\sqrt{N}$. Here α is the equivalent of the 'visibility' of the resonance pattern as used in optical fringes. Our value of α is about 0.68. Its shortfall from the ideal value of unity is due almost entirely to the imperfect action of the polycrystalline CoFe foil in polarization and analysis. Spin relaxation during imprisonment is too small to be detected under our normal running conditions and the stray neutron background is insignificant at 0.2 counts per machine cycle. We can write $\sigma_D = A/\alpha ET\sqrt{N}$ where A is numerically about 3.2×10^{-14} if everything is in SI units except for D which remains in cm. During the imprisonment the number of contained UCN reduces with characteristic time τ (about 70 s at ILL) due to upscattering and absorption at the walls and to beta-decay. If the filling and emptying time remains short compared with τ, the optimum performance is obtained when T is chosen to be equal to τ. Then $N \simeq f_2 n_a Vt/6\tau$ where V is the volume of the storage chamber and n_a is the observed apparent peak UCN number density in the chamber in the limit $T\rightarrow0$ when running with the polarizer-analyser foil removed. The factor of 6 comprises factors of 2 for the original spin selection and 3 for the loss of neutrons (approximately) in the optimum imprisonment period. Our loss factor f_2 is currently about 0.35 comprising 0.62 from losses in the polarizer and 0.80 from losses in the spin-up neutrons while they are waiting their turn to be counted, and 0.70 for time taken up by the filling and emptying and in changing the electric field. n_a may be expressed as $f_1 n_e$ where n_e is the true number density at the entrance to the apparatus. f_1 is about 0.41 and comprises factors due to finite detector efficiency, 0.80, scattering in the feed guide, 0.80, cutting short the filling, 0.93, cutting short the emptying, 0.93, and wall losses while filling and emptying, 0.75. Finally $\sigma_D = B/\alpha E\sqrt{n_e f_1 f_2 V\tau t}$ where the constant B which replaces A has the numerical value 7.8×10^{-14}. Our current value of the product $f_1 f_2$ is about 0.15. The last expression for σ_D shows that for a given apparatus with a short filling time on a steady state source, the main requirement of the source is that it should produce a high value of n_e. On the other hand, it is also evident that one way to increase the sensitivity is to build a larger apparatus. Scaling all the linear dimensions of the storage volume by a factor of F whilst increasing the high voltage so that E remains constant, reduces σ_D by a factor of F^2. (the time τ will increase with the UCN mean free path until this effect begins to saturate as τ approaches the beta-decay lifetime of about 910 s). What are the limits to this increase in size? One problem is that of the time needed to fill the chamber. Doubling the chamber dimensions at ILL without changing the feed guide would increase the filling period from 10 s to 80 s while τ and T would increase to about 140 s. The sum of filling and emptying periods would then

be dominating the cycle unless it could be reduced by increasing the the area of the feed guide. The large output area of the turbine source being installed at ILL /10,11/ will be an advantage for this kind of development. The liquid helium UCN source mentioned below is also fairly adaptable in this way. An EDM storage chamber of 300 litres would still not be unduly affected by gravity.

The PN5 UCN source at present in use at ILL provides an n_e of about 1400/litre for all UCN up to a maximum speed of 6m/s. The local thermal flux where the UCN are delivered to the guide at the inpile end is about 4×10^{14} $n/cm^2/s$ after allowing for all flux depressions. The UCN density in the moderator (at about 320K) at this point is about 2×10^4 UCN/litre. The loss factor of 1/14 is fairly typical for a UCN extraction system. The source which has been in use for some years at Leningrad provides a value of n_e similar to PN5. It achieves this with a purpose built liquid hydrogen moderator so that there is a gain factor through cooling which compensates for a lower reactor flux. In the main cold source of the ILL reactor it is estimated that there is a UCN density of about 10^6/litre which is almost certainly the highest in existence. The UCN will be extracted using vertical guide and a turbine which are being installed· by a group from the Technical University of Munich in collaboration with the ILL /9,10/. The output n_e is expected to be about 6×10^4 UCN/litre. A second type of new UCN source is also being developed at ILL. It uses the downscattering of cold (9Å) neutrons in liquid helium /12,11/. The use of liquid helium has considerable potential for even stronger sources of UCN and for the EDM search itself /13,14/. This will be discussed in one of the papers which follow. A further device which is being developed at Argonne National Laboratory and Los Alamos /15/ uses the high phase space density in the pulses from a pulsed neutron source to produce UCN. It will also be described in one of the papers which follow.

Usable data with a total collection time $t=2 \times 10^7$ s might reasonably be obtained within the space of one year. For the ILL experiment using an electric field strength of 14kV/cm this would give σ_D a value 7×10^{-26} cm on the PN5 source and about 1.1×10^{-26} cm on the turbine source. If measurements at the latter sensitivity do not reveal an EDM, options for a further big reduction of σ_D will have to be considered. These include (i) cooling the storage chamber to increase τ (ii) building a larger apparatus (which would to some extent replace the gain of the first option) (iii) building a source with a substantially larger UCN density n_e (iv) trying to increase E.

All this of course assumes that the attendant problems of stability and systematic errors can be controlled sufficiently. At ILL conditions for the step to 1×10^{-26} cm on the basis of existing information look encouraging. The atomic rubidium magnetometers already indicate that the B-field stability is good enough to reach 5×10^{-26} cm running as at present. Enough of the remaining field noise can be removed to go the rest of the way by switching the E-field more frequently. At this stage there will still only be a modest 8000 counts to be collected after each cycle of the machine.

Turning now to systematic errors, the first and most obvious is that of direct magnetic field changes which correlate with the E-field sign. The main defence is provided by several atomic rubidium magnetometers stationed round the chamber at distances of about 25 cm. Again, with more rapid reversal of the E-field the magnetometers should detect such spurious interactions down to an equivalent D of 10^{-26} cm. Magnetic fields from the leakage currents of about 10 nA through the storage chamber are of the order 5×10^{-11} G. If the current happened to be very localised and flowed several degrees out of line with the electric field it could produce a spurious D of 10^{-26} cm. Lastly, there is the indirect magnetic $-v \times E$ interaction which has been arguably the most important reason for carrying out the EDM searches with UCN. The spurious D from this cause is given by the space average over the storage volume of the quantity $-m(<\underline{v}> \times \underline{a}).\underline{b}/ec^2$ where $\underline{a}$ and $\underline{b}$ are unit vectors in the direction of the original E and B-fields, m is the neutron magnetic moment and $<\underline{v}>$ is the long time ensemble average of the neutron velocities at any position in the chamber. The largest contribution to $<\underline{v}>$ will almost certainly come from filling transients. However, these transients are known to die out quickly with time constants of only two or three seconds. Delaying the start of the measurement for a few seconds after filling provides a way of detecting such an effect and also a way of reducing it considerably.

Experience also indicates that, for any attempt to reach $\sigma_D = 10^{-27}$ cm some significant apparatus development will be needed, particularly to reduce magnetic field noise and to eliminate systematic effects from leakage currents. It will also need some combination of, even more intense sources of UCN producing $n_e \sim 10^6$/litre, apparatus with a storage chamber volume of the order of 300 litres, and larger E-fields and storage times.

We would like to thank C Hamzaoui for useful discussions.

References
1. Smith J H, Ph D Thesis, Harvard Univ., (1951).
2. Smith J H, Purcell E M, and Ramsey N F, Phys. Rev. 108, (1957) 120.
3. Lobashev V M and Serebrov A P, J. de Physique, C3, suppl. 45, (1984) 11.
4. Pendlebury J M, et al., Phys. Lett. 136B, (1984) 327.
5. Ramsey N F, Rep. Prog. Phys. 45, (1982) 95.
6. Hamzaoui C and Barroso A, Phys. Lett. 154B, (1985) 202.
7. Ecker G and Grimus W, Nucl. Phys. B258 (1985) 328.
8. Kurimoto T, Prog Theo. Phys. 73 (1985) 209.
9. Enqvist et al. Phys. Lett. 151B (1985) 210.
10. Steyerl A, Nuc. Instrum. Meth. 125 (1975) 461.
11. Ageron P and Mampe W, J de Physique C3, Suppl. 45 (1984) 279.
12. Golub R, et al., Z. Phys. B51 (1983) 187.
13. Golub R, J. de Physique-Lettres 44 (1983) L-321.
14. Golub R, J. de Physique C3, Suppl. 45 (1984) 265.
15. Dombeck T W, et al., Nuc. Instrum. Meth. 165 (1979) 139.

SUPERTHERMAL SOURCES OF ULTRA-COLD NEUTRONS (UCN)

R. Golub
Max-Planck-Institut für Physik und Astrophysik
- Werner Heisenberg Institut für Physik
Föhringer Ring 6, D 8000 München 40
Fed.Rep.Germany

UCN are usually produced from a source in which the neutrons are
close to thermal equilibrium with some moderator material. In this
paper we review the principles of two types of sources (superfluid
Helium and surface film sources) in which this is not the case and
which are capable of producing significantly higher UCN intensities
than thermal-equilibrium sources. In addition we discuss a method
for carrying out the search for a neutron edm directly in the Helium
moderator and compare the super-thermal source with a particular type
of thermal equilibrium source (Doppler shifter source). Use of these
sources for producing continuous beams of UCN (e.g. for interferome-
ters) is also described.

When a UCN source is operated far from thermal equilibrium-this is possible if
the relaxation time is long enough - it is possible to produce much higher UCN
densities than in sources with the neutrons close to thermal equilibrium.

For example we can consider a material with only two energy levels separated
by an energy Δ. Then the number of excitations present in the system at tem-
perature T is $\propto e^{-\Delta/T}$ and the ratio of neutron downscattering (production of
an excitation) to neutron upscattering (absorption of an excitation) is $\propto e^{\Delta/T}$
and the steady state UCN density in such a system would be proportional to this
factor in the case when upscattering in the material was the dominant UCN loss
mechanism. Comparison of this exponential factor with the $T^{-3/2}$ dependence of
the UCN density in thermal equilibrium demonstrates the possibility of large
gains in "superthermal" sources [1]. In these sources there is a continuous
flow of energy through the system - from the downscattered neutrons into the
excitations and then into the thermal reservoir which is holding the material
temperature constant.

The above situation can be approximated by superfluid He^4 at a sufficiently
low temperature [2]. In this material the neutron scattering is completely co-
herent so that only neutrons with energy (E_c) and momentum (hk_c) given by the
intersection of the well known He^4 dispersion curve with $E_c = P^2/2m_n$ can come
to rest with the creation of a single excitation (see Fig. 1). Neutrons in a
small band of energies around this point can be scattered into the UCN energy
region. For low temperatures the upscattering is suppressed by the Boltzmann
factor corresponding to E_c which plays the role of the Δ in the above discus-
sion) so that as far as the UCN are concerned we have an approximation to the
idealized 2 level system above. In practice the temperature can be reduced
to the point where the upscattering is negligible and the total storage time
in the source is given by wall losses and neutron ß decay. For a Helium
source totally immersed in a thermal flux at 300 K we calculate [2] a UCN
density

$$\rho_{UCN} = 4 \times 10^{-9} \, \phi_o \quad cm^{-3} \quad (\tau = 200 \; sec) \tag{1}$$

where ϕ_o is the total thermal flux. Cooling the neutrons to liquid Nitrogen temperature should give a gain of approximately 10 over this value. Note that a Maxwellian flux at 300 K contains

$$\rho_{UCN} = 10^{-13} \, \phi_o \quad cm^{-3} \tag{2}$$

In an experimental test of the above ideas [3] a 3 m long 7 cm diameter tube filled with isotopically purified He^4 [4] was exposed to a neutron beam containing a flux at k_c (~ 10 Å wavelength) at the Institut Laue-Langevin in Grenoble. The apparatus was capable of cooling the liquid Helium to below 0.5 K and allowed the study of the dynamics of the neutron build-up and decay in the liquid Helium. A photograph of the apparatus is shown below (courtesy of Oxford Instruments).
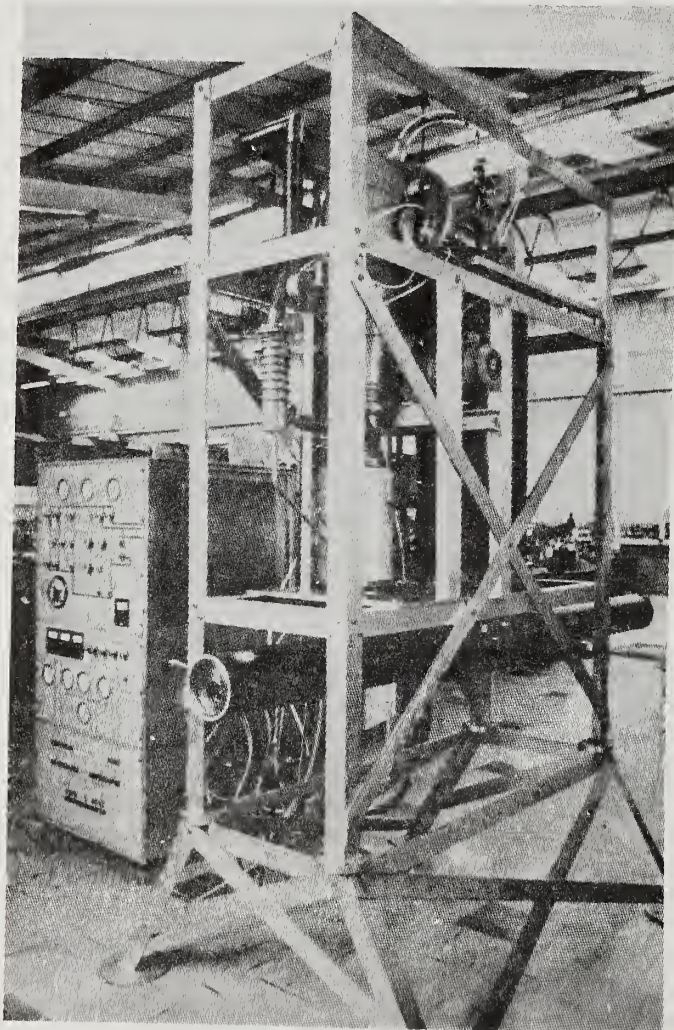
Later experiments (unpublished) obtained a storage time of 150 seconds in a Helium filled Beryllium coated bottle at T = .775 K. By studying the temperature dependence of the measured storage times it was possible to extract values for the upscattering rates (i.e. total cross-sections) for the UCN upscattering in liquid Helium [3]. The results were in reasonable agreement both as to magnitude and temperature dependence with theoretical estimates [5], but further study of the discrepancies is expected to yield important information concerning the 3 phonon interaction in the superfluid. We also hope to gain further insight into this interaction - which plays a major role in determining the shape of the observed dispersion curve - by measuring the energy spectrum of the upscattered UCN using a time of flight technique.

A study of the possibilities of using the Helium source at a spallation neutron source [6]

has shown that the density of UCN expected with a Helium source compared to that expected with a Doppler-shiftler rotating crystal source [7] is given by

$$\zeta_{He}/\zeta_{Dop} \approx 100\,\eta \tag{3}$$

where η is the duty cycle of the pulsed spallation source. The calculation assumed losses of a factor of 6 for the restricted volume of velocity space used by the Doppler source as well as a factor of 10 for crystal reflectivity, pulse broadening and related effects. For the Helium source a storage time of 200 seconds was assumed and no losses were taken into account. However the comparison was made with both sources exposed to an equal incident neutron flux restricted to the same solid angle. While the acceptable solid angle is fixed by total reflection for the Doppler source, in the case of the Helium source there is no such restriction, other than the limits on the source position imposed by keeping the heat input to the Helium within acceptable limits [8]. Thus it was estimated that the ratio - solid angle Helium source : solid angle Doppler source could be as large as 350:1.

Another type of UCN source with a long relaxation time and where the UCN accumulate gradually in the source can be called a "thin film" UCN source [9]. In this source the inner walls of a good UCN container are coated with a thin film of moderator material. The temperature is low enough so that absorption in the moderator is much greater than the upscattering and the film is thick enough so that absorption in the film dominates all other losses. Under these conditions the steady state UCN density is independent of the geometry as well as the density and thickness of the film, depending only on the ratio of downscattering to absorption cross sections of the film material. Calculations based on a Debye model [9] and   later work using a representation of measured excitation spectra [10] show that one expects

$$\zeta_{UCN} \sim 3 \times 10^{-12}\,\phi_0 \qquad \text{- solid Hydrogen film, } T < 10\text{ K}$$

$$\zeta_{UCN} \sim 1.2 \times 10^{-10}\,\phi_0 \qquad \text{- solid Deuterium film, } T \quad 2\text{K} \tag{4}$$

for an incident neutron spectrum at 300 K. This is to be compared to equ. (1) for the Helium source and equ. (2) for the room temperature equilibrium distribution.

Although the discussion so far has been confined to the UCN density that can be accumulated in a closed source, these sources can also produce steady-state UCN beams, providing equally large gains for UCN current density as for number density [9].

If the storage chamber is provided with a permanently open exit hole of area A, then the time for the chamber (of volume V) to empty of UCN (velocity v) is given by

$$\tau_e = 4V/vA \tag{5}$$

If $\tau_e > \tau_o$ (the storage time in the absence of the exit) the steady state UCN

145

density in the source will be greater than 1/2 of its value in the absence of the exit hole. For a 30 liter Helium UCN source with $\tau_\nu = 10^2$ sec this implies an exit area A < 2cm^2. Although this area is rather small there will be many applications of UCN scattering where samples are only available in small sizes so this restriction will not be a problem, considering that the current density will be determined by the extraordinarily large UCN densities available in the Helium source.

Since the thin film source provides a UCN intensity which is independent of the film thickness and hence of τ_o, we see that the ability to shorten τ_o without loss of UCN intensity, will allow either smaller source volumes or larger beam areas. This, together with the higher operating temperatures of the thin film source, make this type of source exceedingly attractive for a UCN scattering installation where world class intensities could be produced even on a small TRIGA reactor [8b]. The UCN could be transported from the source to the scattering sample by means of a focussing, magnetic monochromator [11] or by means of a curved, inclined beam tube forming a monochromatic beam by "reach analysis [12] in the Earth's gravitational field.

The use of a super-thermal UCN source in conjunction with a storage experiment such as the search for a neutron electric dipole moment (edm) was originally envisaged as a more or less straightforward replacement of a conventional source. After an accumulation period a valve in the source would be opened allowing the equalization of densities in the source and measuring apparatus, after which the source and apparatus would again be isolated so that UCN for the next cycle would accumulate in the source while the measurement would proceed in the apparatus.

However, by making use of the fact that the absorption of neutrons by He^3 is almost entirely due to absorption into the J = 0 excited state of He^4, it is possible to create a situation where the two UCN spin states will have radically different storage times in the liquid Helium. This could be brought about by mixing a small amount of polarized He^3 into the He^4. Thus the UCN accumulating in the source would be strongly polarized parallel to the He^3 spins. If during the accumulation period the vessel was subject to a D.C. magnetic field parallel to the He^3 spins and a perpendicular rotating magnetic field as in the usual magnetic resonance apparatus, the steady state total number of UCN in the vessel will be a function of the resonance condition and hence can serve as a detector for a neutron edm if an electric field is applied alternately parallel and anti-parallel to the steady magnetic field [13]. Comparison with the "conventional" use of a superthermal source shows that the sensitivity parameter - the slope of the number of neutrons counted vs. frequency of the rotating magnetic field - is about the same if one assumes a volume dilution factor of 3-4 for the conventional case. The method using the polarized He^3 will eliminate all losses associated with transmission through pipes, windows and polarizing foils. The production of the polarized He^3, low temperature detectors for UCN and other technical problems have been discussed elsewhere [13]. The greatest uncertainty is associated with the effect of the incident radiation fluxes on the normally excellent electrical insulating properties of the liquid Helium.

In this paper we have presented a brief review of a research program which has been worked on at various degrees of intensity for more than a decade. It should by now be obvious that, except for an increase in our knowledge of the physics involved and an improvement in our understanding of the necessary technologies, very little has been accomplished. The question as to whether this is due to unsuitability of the basic ideas, the inability of the present physics research establishment to make room for innovations, or the ability of a single individual to block a meritricious research program for personal reasons, is left for the reader to decide.

In any event we can continue to hope for improved results during the coming decade - work in Japan seems to be continuing at a steady pace [14].

References

[1] R. Golub and J.M. Pendlebury, Phys.Lett. 53A, 133 (1975).

[2] R. Golub and J.M. Pendlebury, Phys.Lett. 62A, 337 (1977).

[3] R. Golub, C. Jewell, P. Ageron, W. Mampe, B. Heckel and I. Kilvington, Z.Phys. B51, 187 (1983).

[4] C. Jewell, R. Golub, P.V.E. McClintock, Cryogenics, July 1982, 373.

[5] R. Golub, Phys.Lett. 72A, 387 (1979).

[6] R. Golub and K. Böning, Proc. of ICANS-V, International Collaboration on Advanced Neutron Sources, Jülich , BRD, June 1981.

[7] Brun et al., Phys.Letts. 75A, 223 (1980).

[8] a) R. Golub, K. Böning, H. Weber in "Realisierungsstudie zur Spallations Neutronenquelle" Teil III, Annex C. G.S. Bauer et al. eds. KFA (Jülich), KFZ (Karlsruhe) June 1981.
See also b) R. Golub, Nuc.Inst.Meth. in Phys.Res. 226, 558 (1984).

[9] R. Golub and K. Böning, Z.Phys. B51, 95 (1983).

[10] Z-Ch. Yu, S.S. Malik and R. Golub (Z.Phys. B, to be published).

[11] R. Golub and P. Carter, Nuc.Inst.Meth. 91, 205 (1971).

[12] A. Steyerl, B. Gmal, K.-A. Steinhauser, N. Achiwa and D. Richter, Z.Phys. B50, 281 (1983).

[13] R. Golub, J. de Physique Lettres 44, L-321 (1983);
J. de Physique - Coll. C3, Supp. No. 3, 45, C3-625 (1984).

[14] H. Yoshiki, in Y. Ishikawa, N. Niimura and M. Misawa eds. KENS Report-V (1984), National Laboratory for High Energy Physics, KEK Report 84-2 Ibaraki-Ken, Japan.
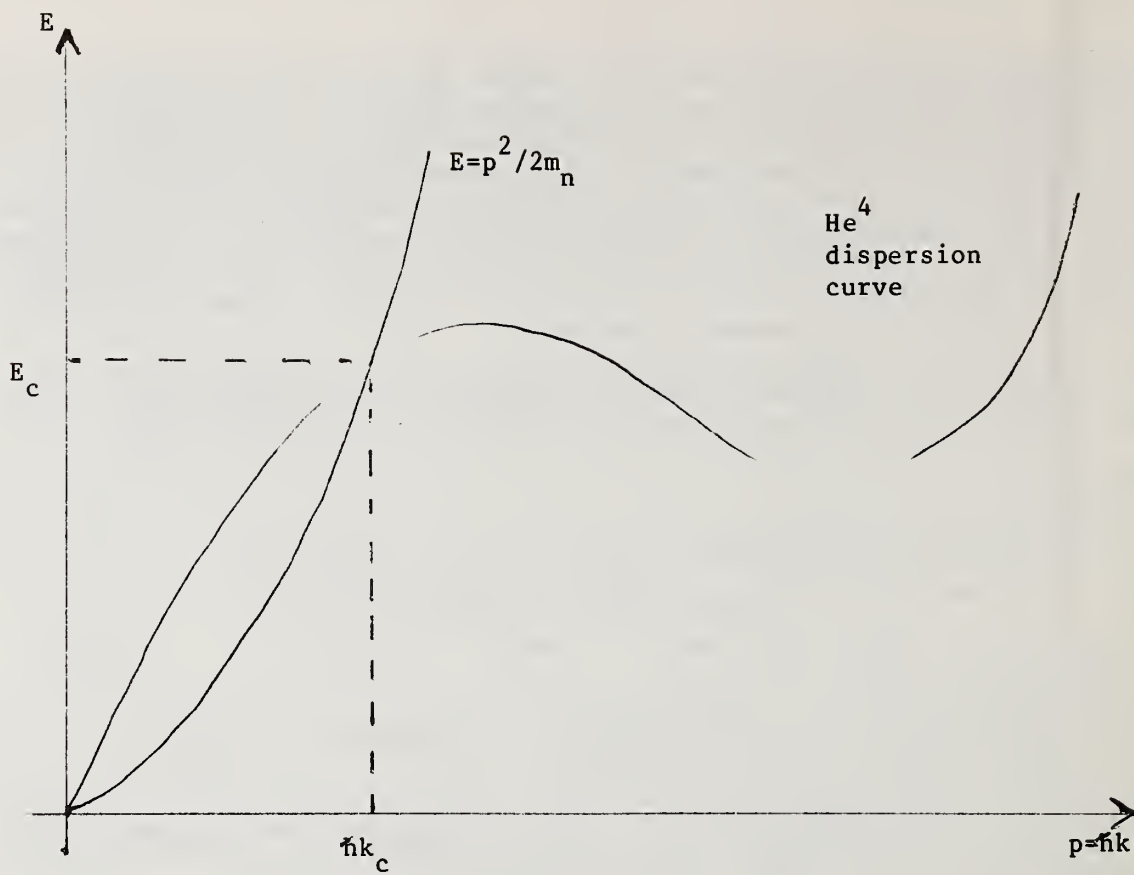
Figure 1

The Production of Slow Neutrons Using Doppler-Shifting From a High-Speed Rotor and Their Application in Fundamental Research

Thomas Dombeck
Los Alamos National Laboratory
Los Alamos, NM 87545

A high-speed rotor with a Bragg scattering crystal in operation at a pulsed spallation source has produced cold (v<30m/s) and ultracold neutrons (v<7m/s) with spatial densities near to those observed at the highest flux reactors. Prospects are discussed for even higher fluxes at the LANSCE facility being commissioned at Los Alamos. Though the rotor is naturally matched to pulsed sources, prospects for producing short bursts, or on the other hand, continuous beams of slow neutrons may have application at reactors as well.

I. Introduction

The uses for cold and ultracold neutrons (UCN) in fundamental and applied research have been pointed out by many authors. The most prominent applications have been the electric dipole moment search[1] (EDM), neutron anti-neutron oscillations[2], neutron polarizability[3], neutron interferometry[4], neutron optics[5] and high resolution spectroscopy[6,7]. With this impressive list of experiments, it is no wonder that much effort has been expended on the development of beams of slow neutrons at reactors and pulsed spallation sources. In this talk I wish to describe the development of the Doppler-shifting rotor which has been put in operation using pulsed sources at Argonne and Los Alamos. Though naturally applicable to pulsed sources, there are certain advantages which this method provides that may be of value at reactors as well.

Extracting UCN from either a steady state or pulsed source is hampered by their high inelastic scattering cross section which diminishes their flux over long distances. Furthermore, pulsed sources have the additional problem where dispersion in velocity leads to a large spreading of the pulse and a consequent loss of density. The solution is to transport higher velocity neutrons nearer to the experiment and convert them to UCN velocities using mechanical means such as a turbine[8] or Bragg reflecting rotor[9]. These conversion schemes lead in principle to about the same density of UCN as is available in the source moderator. This happens because in a Maxwellian the density in velocity space is roughly constant from zero out to the velocity corresponding to the peak of the Maxwellian. In the case of a reactor if the converter is reasonably efficient, one can use any convenient velocity below the Maxwellian peak. For a pulsed source, the pulse spreading is inversely proportional to the transported velocity which dictates as high a transport velocity as practical to retain the density in the source.

II. Operation of the Bragg-Scattering Rotor

In the experiments carried out at Argonne and Los Alamos the neutrons are slowed by overtaking, then Bragg reflecting from a crystal moving at half the neutron velocity, thus leaving them at "zero" velocity in the laboratory. The crystal is thermica (mica with the water replaced by fluorine) which Bragg reflects 400 m/s neutrons. Since the density of neutrons in velocity space in a moderator is proportional to $T^{-3/2}$ where T is the absolute temperature of the moderator, it is desirable to have a moderator of about 20°K. The neutrons are carried to the converter by a guide tube with a polished nickel lining. A nickel mirror reflects neutrons with a normal component of velocity less than 6.6 m/sec, thus preserving the useful density in phase space of the beam. The general arrangement is shown schematically in Fig. 1.

In the converter the neutrons strike the thermica crystals whose reflecting planes are horizontal but the crystals are moving at 30° from vertical. This deviation from vertical is to obtain a larger range in the velocity of the reflected neutrons from a given set of incident neutrons. To see how this works consider the Bragg equation $\lambda = 2d \sin \theta$ (d is the lattice spacing of the relevant crystal planes). Differentiating we get $\Delta\lambda \cong \Delta\theta \cos\theta$. At normal incidence, $\theta = 90^{\circ}$, $\Delta\lambda$ which is a measure of the range of velocities of the reflected neutrons, is zero. This would in turn mean that the vertical component of the UCN velocities would be zero and we would get only a disk of UCN in velocity space instead of a sphere. This would certainly reduce the flow of UCN and would in practice constrain the asymptotic density attainable in a bottle. For even if the density were high in a very small volume in phase space filled by the UCN, it would take impossibly long to fill a bottle. If nothing else the neutron lifetime, 1000 seconds, is a limit to the time available. To avoid this trap we arrange the kinematics as shown in Fig. 1B so that the incident beam is about 30° from normal in the moving crystal system. This kinematics yields a velocity of zero in the laboratory system for the average reflected neutron. There is a considerable dispersion around the average particularly in the horizontal direction where components as large as $\pm$ 14 m/sec are seen.

Even this does not give us the full range of possible UCN velocities ($|v|$ <7 m/sec) in the vertical direction. In effect the velocities in the laboratory system are concentrated in a slab roughly parallel to the rotor arm. Because the velocities are somewhat concentrated in velocity space, Liouville's theorem allows us to concentrate the neutrons in real space by spreading their velocities. This has been demonstrated at Argonne introducing the UCN into a guide via small funnels put just after the scattering crystal.

This system has been shown to work at Argonne[9] and the major component, the rotor, was put in operation at Los Alamos in 1984. The density of UCN produced in the converter system is however substantially lower than the phase space density in the source. A number of measurements on the components of the system, particularly a measurement of crystal reflectivity, and a straightforward Monte Carlo calculation of the system efficiency have
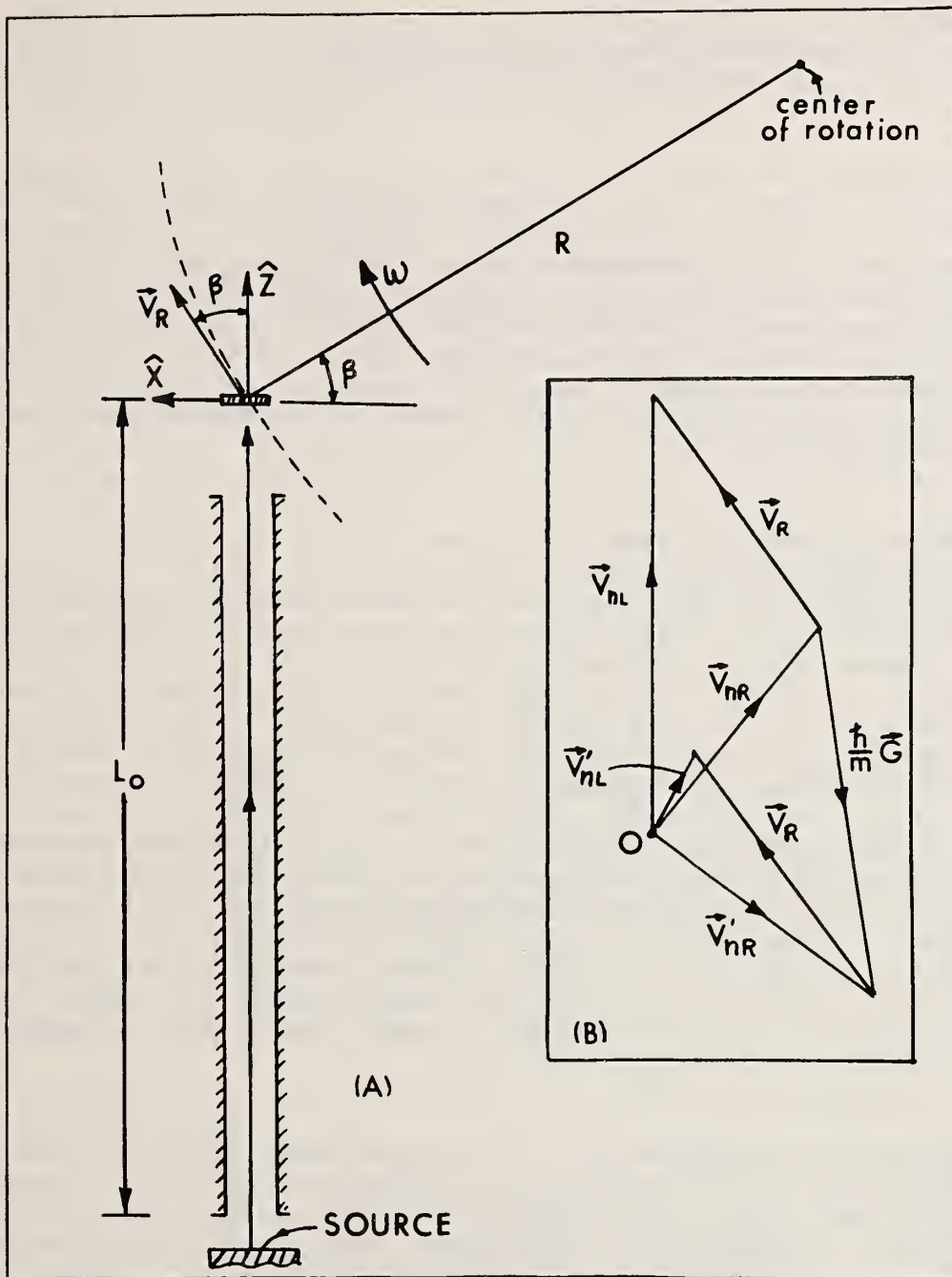
Fig. 1 This schematic describes the principle of operation of the Bragg-scattering rotor for the production of ultracold neutrons. Neutrons from the source scatter off the crystal moving at velocity V_R away from the source. In fig B, the scattering kinematics shows how the neutron velocity V_{nL} can be cancelled upon reflection (see Ref. 10), yielding a zero velocity in the laboratory.

at ILL, Grenoble. shown that the loss of phase space density is due principally to two problems. The most important is the crystal reflectivity which is only about 20%. This could be remedied by a multilayer mirror[11],

which might yield a 75% reflectivity. The second difficulty is the guide
tube from the moderator. Ours gives only one-half the neutrons it should as
demonstrated by more successful guides

The LANSCE spallation source in conjunction with the Proton Storage Ring
(PSR) at Los Alamos[12] will provide the highest peak thermal fluxes of
neutrons available in the near future. Extrapolating from our previous
experience, we believe that densities near 7200 UCN/cc can be produced in a
cloud around the reflecting crystal. Collecting these neutrons and leading
them to a measurement chamber will clearly involve significant losses which,
on the basis of ILL experience we estimate to be near a factor of 10,
yielding 500 to 700 UCN/cc stored in a bottle. This may be an order of
magnitude higher than anticipated at the new cold source put in operation
recently at ILL.[13]

III. Continuous Beams of UCN Using a Rotor

Many applications of UCN, such as the EDM measurement, make use of their
storage capabilities in bottles to increase measurement times. For the rotor
described above with a reflecting crystal area of 2 x 5 cm^2, a continuous
beam of UCN is produced at about 100Hz operation. The maximum rate we have
had available to us at Argonne was 30Hz (LANSCE will be 20Hz) indicating gaps
form in the resulting beam of UCN. To overcome a potential reduction in
stored UCN density as these pulses spread out in a bottle we have provided a
shutter placed a few millimeters from the crystal and before the bottle. The
shutter is a simple rotating disk with a slot in it synchronized with the
crystal and open with the crystal goes by and closed after the 7 m/s neutrons
originating furthest from the shutter pass through it. In practice things
are somewhat more complicated and the overall efficiency due to gaps and
rescattered neutrons is only 50%. It should also be pointed out that the
bottle arrives asymptotically at the peak density using this scheme, that is,
the filling rate is three to five times longer than necessary for a
continuous beam.

It is doubtful that pulsed sources will provide 100Hz operation at anytime in
the conceivable future though of course a reactor could, but at lower peak
densities. However, there are modifications that could provide continuous
beams of UCN. A larger reflecting crystal, 10 x 10 cm^2, would provide this
at LANSCE. It is inconceivable that thermica crystals this large can be
made, but multi-layered crystals may provide an alternative. The major
disadvantage for a larger crystal on the rotor is the velocity differences
along the crystal due to the arc trajectory of the crystal in space. In
fact, a linear crystal motion or at least a constant velocity in the
direction of the incident neutrons at all points along the crystal is
preferred. Schemes have been suggested to accomplish this, such as mounting
the crystal on an axle at the end of the rotor arm and using electromagnets
to induce a counter-rotation at the moment the neutrons are scattered. The
engineering is formidable as the forces approach 10^4g's!

Continuous beams of neutrons are best for interferometry or experiments where counting rates are more important than measurement time. However, the pulsed nature of the rotor-generated neutrons can also be used to advantage in certain applications as discussed in the next section.

IV. Pulsed Beams of Neutrons Using a Rotor

With a narrow reflecting crystal, perhaps narrower than the crystal used at Argonne, a very precise neutron energy determination is possible using time-of-flight (TOF) methods.[7,14] The narrow crystal defines a precise time zero at which the neutrons are produced and sent down a guide toward a target and timed detector. Neutron velocities up to 30 m/s (5 μeV) are available[9] in such a TOF spectrometer. The use of a high resolution spectrometer for long wavelengths has been suggested for macro-molecular systems,[6] and a gravity spectrometer named NESSIE will be put into operation at ILL for such studies. Comparable counting rates and resolutions are possible with the Doppler-shifting rotor. The advantage for the rotor is that all energies can be measured at one setting of the spectrometer. The major disadvantage is the wide divergence of the neutron beam requiring large targets or a transmission geometry.

V. References

1. N. F. Ramsey, Ann. Rev. Nucl. Part. Science $\underline{32}$, 211 (1982).

2. A. Petchek "Neutron Oscillation Experiments Using Ultracold Neutrons," in Proc. of Low-Energy Tests of Conservation Laws in Particle Physics, ed. by M. Blecher and K. Gotow, Blacksburg, VA, 1983.

3. J. Anandan, private communication.

4. A. Steyerl et al., Z. Phys. $\underline{B36}$, 109 (1979).

5. K. A. Steinhauser et al., PRL $\underline{44}$, 1306 (1980); and G. Schultz et al., PRL $\underline{44}$, 1400 (1980).

6. A. Steyerl et al., Z. Phys. $\underline{B50}$, 281 (1983).

7. J. Lynn et al., Physica $\underline{120B}$, 114 (1983).

8. A. Steyerl, NIM $\underline{125}$, 461 (1975).

9. T. Brun et al., PL $\underline{75A}$, 2?3 (1980).

10. T. W. Dombeck et al., Nucl. Inst. Meth. $\underline{165}$, 139 (1979).

11. C. F. Majkrzak and L. Passell, Acta Cryst. (in press).

12. G. J. Russell et al., "LANSCE High Power (200 μA) Target-Moderator Reflector-Shield," in Proc of the Eighth Meeting of the International Collaboration on Advance Neutron Sources (ICANS-VIII), Oxford, England, July 8-12, 1985.

13. A. Steyerl, private communication.

14. T. Dombeck, "A Neutron Spectrometer for Use in the long Wavelength Limit," in Proc. of the Fourth Meeting of the International Collaboration on Advanced Neutron Sources (ICANS-IV), KEK, Tsukuba, Japan, March 1981.

Eric Adelberger
University of Washington
Nuclear Physics Lab GL-10
Seattle, WA 98195
206-543-4080

Muhammad Arif
University of Missouri-Columbia
Physics Department/Research Reactor
Columbia, MO 65211
314-882-3335 or 4211

John Arthur
Oak Ridge National Laboratory
Solid State Division
Oak Ridge, TN 37831
615-574-5241

Milla Baldo-Ceolin
Dipartimento di Fisica "G. Galilei"
Via Marzolo, 8
35131 Padova, Italy
(49) 844221 or 844296

Sean Brennan
National Bureau of Standards
Physics A141
Gaithersburg, MD 20899
301-921-2061

Thomas J. Bowles
Los Alamos National Laboratory
MS 0449
Los alamos, NM 87545
505-667-5005

James Byrne
University of Sussex
Math & Physics Building
Brighton, Sussex, BN19QH, England
0273-606755, ext. 573

Russell C. Casella
National Bureau of Standards
Rm. A106, Bldg. 235
Gaithersburg, MD 20899
301-921-2421

Wayne Cassatt, Jr.
National Bureau of Standards
RADP C225
Gaithersburg, MD 20899
301-921-2551

Chia-Cheh Chang
University of Maryland
Dept. of Physics and Astronomy
College Park, MD 20742
301-454-5341

Chung Y. Chang
University of Maryland
Dept. of Physics
College Park, MD 20742
301-454-3509

Timothy Chupp
Harvard University
Jefferson 261-A
Cambridge, MA
617-495-3257

Kevin Coulter
Princeton University
Physics Dept., Jadwin Hall
P.O. Box 708
Princeton, NJ 08544
609-452-4330

Paul Cowan
National Bureau of Standards
Physics A141
Gaithersburg, MD 20899
301-921-2061

Richard Deslattes
National Bureau of Standards
Physics A141
Gaithersburg, MD 20899
301-921-2061

Thomas Dombeck
Los Alamos National Laboratory
MS D449
Los Alamos, NM 87545
505-667-4685

D. Dubbers
Institut Laue-Langevin
BP 156
38042 Grenoble CEDEX
France

Ken Finkelstein
MIT Neutron Diffraction Lab
138 Albany Street (NW12-119)
Cambridge, MA 02139
617-253-4200

Melvin Freedman
Argonne National Laboratory
Physics Division, Bldg. 203
9700 S. Cass Avenue
Argonne, IL 60439
312-972-4035

Stuart Freedman
Argonne National Laboratory
9700 S. Cass Avenue
Argonne, IL 60439
312-972-4032

David Gilliam
National Bureau of Standards
REACT A106
Gaithersburg, MD 20899
301-921-2767

Robert Golub
Max Planck Institut fur Physics
FohringerRing 6
8000 Munich 40, FRG
(49) 8931893234

Geoffrey L. Greene
National Bureau of Standards
Physics A141
Gaithersburg, MD 20899
301-921-2061

E.E. Gross
Oak Ridge National Lab
Oak Ridge, TN 37830

Blayne Heckel
University of Washington
Physics FM-15
Seattle, WA 98195
206-543-8785

Albert Henins
National Bureau of Standards
Physics A141
Gaithersburg, MD 20899
301-921-2061

P.K. Kabir
University of Virginia
Physics Building
McCormick Road
Charlottesville, VA 22907
804-924-6572

Helmut Kaiser
University of Missouri
Research Reactor
Columbia, MO 65211
314-882-4211

Ernest Kessler
National Bureau of Standards
Physics A141
Gaithersburg, MD 20899
301-921-2061

George P. Lamaze
National Bureau of Standards
REACT A106
Gaithersburg, MD 20899
301-921-2767

Robert LaVilla
National Bureau of Standards
Physics A141
Gaithersburg, MD 20899
301-921-2061

Gabriel Luther
National Bureau of Standards
Physics A141
Gaithersburg, MD 20899
301-921-2061

J.W. Lynn
University of Maryland
Department of Physics
College Park, MD 20742
301-454-7038

Walter Mampe
Institut Laue-Langevin
BP 156 Ave des Martyrs
38042 Grenoble CEDEX
France

Bahram Mashhoon
University of Missouri-Columbia
Department of Physics and Astronomy
Columbia, MO 65211
314-882-6526

Art McDonald
Princeton University
Physics Dept., Jadwin Hall
P.O. Box 708
Princeton, NJ 08544
609-452-4330

James S. O'Connel
National Bureau of Standards
RADP B109
Gaithersburg, MD 20899
301-921-2505

J.M. Pendlebury
University of Sussex
Physics Building
Brighton, Sussex, U.K.

Gabriele Puglierin
Dipartimento di Fisica "G. Galilei"
Via Marzolo, 8
Padova, Italy
(049) 844248

Norman F. Ramsey
Harvard University
Lyman laboratory of Physics
Cambridge, MA 02138
617-495-2864

Helmut Rauch
Atominstitut Schuttelstr. 115
A-1020 Wien
Austria

J.M. Robson
McGill University
Physics Department
3600 University Street
Montreal, Canada H3A 2T8
514-989-9856

J.M. Rowe
National Bureau of Standards
Reactor A106
Gaithersburg, MD 20899
301-921-3634

I.G. Schroder
National Bureau of Standards
Reactor A106
Gaithersburg, MD 20899
301-921-3636

Roger D. Scott
Scottish Universities Research
  and Reactor Centre
East Kilbride
Glasgow G7S OQJ, U.K.
03552-20222, x2471

Richard Steinberg
Drexel University
Department of Physics
Philadelphia, PA 19104

David D. Warner
Brookhaven National Laboratory
Bldg. 510A
Upton, NY 11973
516-282-3823/3908

Samuel A. Werner
University of Missouri-Columbia
Physics Department
Columbia, MO 65211
314-882-7664

Stanley L. Whetstone
Department of Energy
Washington, DC 20545
301-353-3631

John F. Wilkerson
Los Alamos National Laboratory
MS D449
Los Alamos, NM 87545
505-667-9429

Harvey Williard
National Science Foundation
Physics Division
Washington, DC 20550

Richard Wilson
Harvard University
Physics Department
Cambridge, MA 02138

Anton Zeilinger
Atominstitut der Osterreichischen
  Universitaton
Schuttelstr. 115
A-1020 Wien
Austria

U.S. DEPT. OF COMM. **BIBLIOGRAPHIC DATA** **SHEET** (See instructions)	1. PUBLICATION OR REPORT NO. NBS/SP-711	2. Performing Organ. Report No.	3. Publication Date February 1986

4. TITLE AND SUBTITLE

The Investigation of Fundamental Interactions with Cold Neutrons
(Proceedings of a Workshop)

5. AUTHOR(S)
G.L. Greene, editor

6. PERFORMING ORGANIZATION (If joint or other than NBS, see instructions) National Bureau of Standards U.S. Department of Commerce Gaithersburg, MD 20899	7. Contract/Grant No.
	8. Type of Report & Period Covered Final

9. SPONSORING ORGANIZATION NAME AND COMPLETE ADDRESS (Street, City, State, ZIP)

NBS and the U.S. Department of Energy

10. SUPPLEMENTARY NOTES

Library of Congress Catalog Card Number 86-600501

☐ Document describes a computer program; SF-185, FIPS Software Summary, is attached.

11. ABSTRACT (A 200-word or less factual summary of most significant information. If document includes a significant bibliography or literature survey, mention it here)

The National Bureau of Standards is establishing a National Cold Neutron Facility at its 20 MW reactor located in Gaithersburg, Maryland. In order to provide guidance in the development of research plans for the Facility, the Department of Energy and NBS sponsored, on November 14-15, 1985, a workshop on the Investigation of Fundamental Interactions with Cold Neutrons. The 25 papers presented at the workshop are printed in the proceedings.

12. KEY WORDS (Six to twelve entries; alphabetical order; capitalize only proper names; and separate key words by semicolons)

cold neutrons; fundamental interactions; National Cold Neutron Facility; research reactor

13. AVAILABILITY [X] Unlimited ☐ For Official Distribution. Do Not Release to NTIS [X] Order From Superintendent of Documents, U.S. Government Printing Office, Washington, D.C. 20402. ☐ Order From National Technical Information Service (NTIS), Springfield, VA. 22161	14. NO. OF PRINTED PAGES 163
	15. Price

(159) ALL gcg. kdana

NBS Technical Publications

Periodical

Journal of Research—The Journal of Research of the National Bureau of Standards reports NBS research and development in those disciplines of the physical and engineering sciences in which the Bureau is active. These include physics, chemistry, engineering, mathematics, and computer sciences. Papers cover a broad range of subjects, with major emphasis on measurement methodology and the basic technology underlying standardization. Also included from time to time are survey articles on topics closely related to the Bureau's technical and scientific programs. Issued six times a year.

Nonperiodicals

Monographs—Major contributions to the technical literature on various subjects related to the Bureau's scientific and technical activities.

Handbooks—Recommended codes of engineering and industrial practice (including safety codes) developed in cooperation with interested industries, professional organizations, and regulatory bodies.

Special Publications—Include proceedings of conferences sponsored by NBS, NBS annual reports, and other special publications appropriate to this grouping such as wall charts, pocket cards, and bibliographies.

Applied Mathematics Series—Mathematical tables, manuals, and studies of special interest to physicists, engineers, chemists, biologists, mathematicians, computer programmers, and others engaged in scientific and technical work.

National Standard Reference Data Series—Provides quantitative data on the physical and chemical properties of materials, compiled from the world's literature and critically evaluated. Developed under a worldwide program coordinated by NBS under the authority of the National Standard Data Act (Public Law 90-396).
NOTE: The Journal of Physical and Chemical Reference Data (JPCRD) is published quarterly for NBS by the American Chemical Society (ACS) and the American Institute of Physics (AIP). Subscriptions, reprints, and supplements are available from ACS, 1155 Sixteenth St., NW, Washington, DC 20056.

Building Science Series—Disseminates technical information developed at the Bureau on building materials, components, systems, and whole structures. The series presents research results, test methods, and performance criteria related to the structural and environmental functions and the durability and safety characteristics of building elements and systems.

Technical Notes—Studies or reports which are complete in themselves but restrictive in their treatment of a subject. Analogous to monographs but not so comprehensive in scope or definitive in treatment of the subject area. Often serve as a vehicle for final reports of work performed at NBS under the sponsorship of other government agencies.

Voluntary Product Standards—Developed under procedures published by the Department of Commerce in Part 10, Title 15, of the Code of Federal Regulations. The standards establish nationally recognized requirements for products, and provide all concerned interests with a basis for common understanding of the characteristics of the products. NBS administers this program as a supplement to the activities of the private sector standardizing organizations.

Consumer Information Series—Practical information, based on NBS research and experience, covering areas of interest to the consumer. Easily understandable language and illustrations provide useful background knowledge for shopping in today's technological marketplace.
Order the above NBS publications from: Superintendent of Documents, Government Printing Office, Washington, DC 20402.
Order the following NBS publications—FIPS and NBSIR's—from the National Technical Information Service, Springfield, VA 22161.

Federal Information Processing Standards Publications (FIPS PUB)—Publications in this series collectively constitute the Federal Information Processing Standards Register. The Register serves as the official source of information in the Federal Government regarding standards issued by NBS pursuant to the Federal Property and Administrative Services Act of 1949 as amended, Public Law 89-306 (79 Stat. 1127), and as implemented by Executive Order 11717 (38 FR 12315, dated May 11, 1973) and Part 6 of Title 15 CFR (Code of Federal Regulations).

NBS Interagency Reports (NBSIR)—A special series of interim or final reports on work performed by NBS for outside sponsors (both government and non-government). In general, initial distribution is handled by the sponsor; public distribution is by the National Technical Information Service, Springfield, VA 22161, in paper copy or microfiche form.